Leibniz-Institut für Ostseeforschung Warnemünde

Universität Rostock Traditio et Innovatio

Salinity and Temperature Variability in the Baltic Sea under Changing Climate

Kumulative Dissertation
zur Erlangung des akademischen Grades
doctor rerum naturalium (Dr. rer. nat.)
der Mathematisch-Naturwissenschaftlichen Fakultät
der Universität Rostock
vorgelegt von
Leonie Barghorn
geb. am 05.07.1996 in Hamburg
Januar 2025

https://doi.org/10.18453/rosdok_id00005302

Gutachter:innen:

1. Gutachter
Prof. Dr. H. E. Markus Meier
Leibniz-Institut für Ostseeforschung Warnemünde

2. Gutachter
Prof. Dr. Arne Biastoch
Geomar Helmholtz-Zentrum für Ozeanforschung Kiel

3. Gutachterin
Prof. Dr. Anna Rutgersson
Uppsala University

Jahr der Einreichung: 2025
Jahr der Verteidigung: 2025

Thesis advisor: Professor Dr. H. E. Markus Meier Leonie Barghorn

Salinity and Temperature Variability in the Baltic Sea under Changing Climate

Abstract

This thesis analyzes long-term changes in salinity and temperature variability in the Baltic Sea since 1850 using regional hindcast and global climate model ensemble simulations.

The thesis consists of four parts. The first two deal with saltwater inflows that transport highly saline water from the North Sea to the deep layers of the Baltic Sea. They reveal a shift in saltwater inflow seasonality from mainly winter inflows towards more warm summer and early autumn inflows during the model period. Those changes are found across hindcast simulations of three different regional ocean models, despite some fundamental differences in their set up. It is shown that the warm inflows contributed substantially to the exceptional warming observed in deep water layers in the western Baltic Sea. Moreover, the impact of the inflow-driven warming on the concentration of dissolved oxygen in the affected water layers is assessed. A strong connection between warm inflows and oxygen depletion is found. Finally, the causes behind the changes in inflow seasonality are explored. Changes in the seasonality of the freshwater supply (mainly via river runoff) had an impact on the inflow seasonality, but also changes in the wind field.

The last two parts of the thesis broaden the focus to examine the saltwater and sea surface temperature (SST) dynamics in the entire Baltic Sea and its dependence on different drivers. In the third part, the origin of the 30-year variability characterizing the salinity of the Baltic Sea is investigated. It is found to be a combination of two large-scale oceanic and atmospheric patterns: the Atlantic Multidecadal Variability (AMV) and the North Atlantic Oscillation (NAO). Together, they cause the 30-year variability in river discharge. Higher river discharge leads to a lower surface salinity and hence also to a lower salinity of the water flowing out of the Baltic Sea. Since a certain fraction of the outflowing water is mixed into subsequent inflows, higher river runoff leads to less saline saltwater inflows. This feedback mechanism enhances the multidecadal variability in the salinity.

In the fourth part, past and future changes in the SSTs and the drivers behind those changes are examined based on large ensembles of global climate model simulations. It is shown that positive temperature anomalies in the Baltic Sea are not driven directly by the AMV, but by positive NAO phases where the pressure gradient between the Icelandic Low and the Azores High is strong. The direct connection between the AMV and Baltic SSTs found in earlier studies probably results from externally forced contributions to the AMV. As the North Sea and the Mediterranean Sea lie closer to the North Atlantic, they are more directly affected by the temperature variability of the latter. Those relations will probably not change substantially until the end of this century in spite of climate change.

To summarize, this study advances the understanding of the climate variability in the Baltic Sea. It detects for the first time a robust long-term change in the saltwater inflows and identifies a new driver of oxygen depletion in the western Baltic Sea. In addition, it provides new knowledge on the teleconnections between the Baltic Sea and the North Atlantic.

Zusammenfassung

In dieser Arbeit werden Langzeitveränderungen der Salzwasser- und Temperaturdynamik in der Ostsee seit 1850 basierend auf Simulationen mit regionalen Ozeanmodellen und globalen Klimaensembles untersucht.
Die Arbeit besteht aus vier Teilen. Die ersten beiden beschäftigen sich mit Salzwassereinströmen, die salzreiches Wasser aus der Nordsee in tiefe Wasserschichten der Ostsee transportieren. Sie zeigen, dass es seit 1850 eine Verschiebung in der Einstromsaisonalität von hauptsächlich Wintereinströmen hin zu mehr warmen Sommer- und Frühherbsteinströmen gegeben hat. Die Veränderungen sind in drei verschiedenen Ozeanmodellen zu sehen, obwohl diese sich zum Teil deutlich unterscheiden. Die warmen Einströme haben maßgeblich zu den außerordentlichen Temperaturtrends beigetragen, die in tiefen Wasserschichten der westlichen Ostsee beobachtet wurden. Darüber hinaus zeigt sich, dass eine starke Verbindung zwischen warmen Einströmen und Sauerstoffminima besteht. Auch die Ursachen der Veränderungen in den Einströmen werden untersucht. Demnach haben Verschiebungen in der Saisonalität der Süßwassereinträge (vor allem über Flüsse) einen Teil der Trends in der Einstromsaisonalität verursacht. Darüber hinaus haben auch Veränderungen in den Windfeldern eine Rolle gespielt.
Die zweite Hälfte der Arbeit erweitert den Fokus auf die Salzwasser- und Temperaturdynamik der Ostsee im Allgemeinen und ihre Abhängigkeit von anderen Elementen des Klimasystems. Zunächst wird im dritten Teil nach dem Ursprung der 30-Jahres-Variabilität im Salzgehalt der Ostsee gesucht. Es wird gezeigt, dass dieser auf den gemeinsamen Einfluss der multidekadischen atlantischen Variabilität (AMV) und der nordatlantischen Oszillation (NAO) zurückzuführen ist. Zusammen sorgen sie für die 30-Jahres-Variabilität in den Süßwassereinträgen. Stärkere Süßwassereinträge führen zu einem niedrigeren Salzgehalt im Oberflächenwasser der Ostsee und somit auch im aus der Ostsee ausströmenden Wasser. Da ein Teil dieses Wassers in nachfolgende Salzeinströme gemischt wird, sorgen stärkere Süßwassereinträge schlussendlich für weniger salzhaltige Einströme. Dieser Rückkopplungsmechanismus verstärkt die multidekadische Variabilität im Salzgehalt der Ostsee.
Der vierte und letzte Teil behandelt vergangene und zukünftige Veränderungen in der Variabilität der Oberflächentemperatur und die Ursachen dahinter auf der Grundlage von globalen Klimamodellensembles. Er zeigt, dass positive Temperaturanomalien in der Ostsee nicht direkt von der AMV, sondern von positiven NAO-Phasen angetrieben werden, in denen der Druckgradient zwischen dem Islandtief und dem Azorenhoch überdurchschnittlich stark ist. Die direkte Verbindung zwischen der AMV und den Oberflächentemperaturen der Ostsee, die in anderen Studien gezeigt wurde, ist wahrscheinlich eher auf extern angetriebene Anteile der AMV zurückzuführen. Die Nordsee und das Mittelmeer dagegen werden direkter von Temperaturschwankungen des Nordatlantiks beeinflusst. Diese Mechanismen werden sich im Verlauf des Jahrhunderts trotz des Klimawandels voraussichtlich nicht grundlegend verändern.
Insgesamt erweitert diese Studie das Verständnis der Klimavariabilität der Ostsee. Sie zeigt erstmals eine robuste Langzeitveränderung in den Salzwassereinströmen und identifiziert einen neuen Auslöser für Sauerstoffverarmung in der westlichen Ostsee. Außerdem liefert sie neue Erkenntnisse über die Fernwirkungen zwischen der Ostsee und dem Nordatlantik.

Contents

Publications

Publications for the cumulative dissertation

A **Barghorn, L.**, *Meier, H. E. M., and Radtke, H.* (2023). Changes in Seasonality of Saltwater Inflows Caused Exceptional Warming Trends in the Western Baltic Sea. Geophysical Research Letters, 50, e2023GL103853.
https://doi.org/10.1029/2023GL103853

B **Barghorn, L.**, *Meier, H. E. M., Radtke, H., Neumann, T., and Naumov, L.* (2025). Warm saltwater inflows strengthen oxygen depletion in the western Baltic Sea. Climate Dynamics, 63, 29.
https://doi.org/10.1007/s00382-024-07501-x

C *Meier, H. E. M.,* **Barghorn, L.,** *Börgel, F., Gröger, M., Naumov, L., and Radtke, H.* (2023). Multidecadal climate variability dominated past trends in the water balance of the Baltic Sea watershed. npj Climate and Atmospheric Science, 124, 4168– 4187.
https://doi.org/10.1029/2018JC013948

D **Barghorn, L.**, *Börgel, F., Gröger, M., and Meier, H. E. M.* (2025). Atlantic Multidecadal Variability control on European seas is mainly externally forced. Environmental Research Letters (under review)

Other peer-reviewed publications

- *Börgel, F., Neumann, T., Rooze, J., Radtke, H.,* **Barghorn, L.**, *and Meier, H. E. M.* (2023). Deoxygenation of the Baltic Sea during the last millennium. Frontiers in Marine Science. 10:1174039.
https://doi.org/10.3389/fmars.2023.1174039

Conferences

- Exceptional warming and intensified oxygen depletion due to warm saltwater inflows in the western Baltic Sea
Barghorn, L., *Meier, H. E. M., Radtke, H., and Neumann, T.*
Oral presentation (solicited speaker) | 5th Baltic Earth Conference | Jurmala, Latvia | 15.05.2024

- Warm saltwater inflows strengthen oxygen depletion in the western Baltic Sea
  Barghorn, L., *Meier, H. E. M., Radtke, H., and Neumann, T.*
  Oral presentation (highlighted) | EGU 2024 | Vienna, Austria | 15.04.2024

- Seasonality of salinity dynamics in the western Baltic Sea
  Barghorn, L., *Radtke, H., and Meier, H. E. M*
  Oral presentation | IUGG Berlin 2023 | Berlin, Germany | 13.07.2023

- Investigating the properties of small- and medium-size saltwater inflows into the Baltic Sea
  Barghorn, L., *Radtke, H., Väli, G., and Meier, H. E. M.*
  Poster presentation | 4th Baltic Earth Conference | Jastarnia, Poland | 02.06.2022

List of Figures

Abbreviations

AMV	Atlantic Multidecadal Variability
CESM	Community Earth System Model
CMIP	Climate Model Intercomparison Project
CWT	Continuous Wavelet Transform
DO_{min}	Annual minimum of dissolved oxygen
DO_{60}	Annual mean oxygen concentration averaged over depths below 60 m
EOF	Empirical Orthogonal Function
ERGOM	Ecological Regional Ocean Model
fAMV	forced AMV
GAMM	Generalized Additive Mixed Model
GETM	General Estuarine Transport Model
HiResAFF	High Resolution Atmospheric Forcing Fields
ICES	International Council for the Exploration of the Sea
iAMV	internal AMV
JJA	June, July, August
MBI	Major Baltic Inflow
MPI-ESM	Max Planck Institute Earth System Model
MOM	Modular Ocean Model
NAO	North Atlantic Oscillation
N	nitrogen
P	phosphorus
RCO	Rossby Centre Ocean model
S_{17}	salt content in water masses with minimum salinity of 17 g/kg
SCOBI	Swedish Coastal and Ocean Biogeochemical model
SMILE	Single-Model Initial-condition Large Ensemble
SO	September, October
SSP	shared socioeconomic pathway
SST	sea surface temperature
SSTAres	residual sea surface temperature anomaly
T_{max}	maximum temperature below the seasonal thermocline
T_{60}	Annual mean temperature averaged over depths below 60 m

V_{17}	volume of water masses with minimum salinity of 17 g/kg
WCT	Wavelet Coherence Transform

Ente gut, alles gut.

Acknowledgments

A lot of people made this thesis possible. First of all, I have to thank my supervisor Markus for your great support, for always being available, and for enabling experiences like different conferences or the summer school on Askö. I could not have imagined any better supervision. It was a great pleasure to be part of your working group. Speaking of that, I need to thank some group members in particular for their help in programming, paper / thesis editing, and other issues: Hagen, Flo, Matthias, Lev, and Thomas. Thank you also to Joanna and Taavi for being part of my thesis committee together with Markus, Flo and Matthias.

Before starting the PhD, my focus area was solid state physics - quite far away from physical oceanography or climate science. I am quite sure, I would not have gotten this position if I hadn't done an internship at the GEOMAR in 2019, where I also studied the salinity dynamics of the Baltic Sea! Hence, thank you to Andreas, my supervisor at that time. You sparked my interest for the Baltic Sea in the first place.

Pursuing a PhD comes with quite some paper work. Fortunately, whenever bureaucracy hit, Berit would be there to help! Thanks especially for the smooth onboarding despite covid restrictions!

Although it was not really related to my thesis, the 2-weeks cruise with the EMB on the Baltic Sea was a great experience. I am especially thankful to Peter as the cruise-leader that you would let a newbie like I was participate, and to Martin and Jens for sharing the CTD lab with me.

Finally, science is not everything - one also needs a social life. I was lucky to find that even at work thanks to many nice colleagues that became friends over the years: Lloyd (also helped with thesis editing!), Karoline, Kseniia, Anna, Markus, Mira, Erika, Yannik, Sven, Julia, Flo, Lev, Malin... (hopefully, I did not forget anybody), you all made it much easier to get up on gloomy northern German winter mornings and go all the way up to Warnemünde. The next cake time / Baltic Sea swim / climbing session would never be far.

Wie gesagt - Arbeit ist nicht alles. Deswegen möchte ich auch all meinen Freund:innen außerhalb des IOWs danken, insbesondere Gesche, Jasmin und Michelle. Obwohl kaum ein Ort so weit von allem anderen in Deutschland weg ist wie Rostock, haben wir den Kontakt nicht verloren. Danke für alle schönen Gespräche und Treffen. Einen großen Dank an meine Familie - bei euch bin ich immer zuhause, und obwohl ihr alle keine Physiker:innen seid, seid ihr immer total interessiert an dem, was ich mache. Und natürlich danke an dich, Matze. Dass du bei mir bist, ist das größte Geschenk.

1 Introduction

More than 2 billion people live in areas less than 100 km away from the coast (Reimann et al., 2023). Hence, coastal seas have a very high socioeconomic importance. However, they are also strongly impacted by human activities. A prominent example for such coastal seas is the Baltic Sea, a shallow semi-enclosed water basin situated in northern Europe. Some even refer to it as a time-machine showing the future of other coastal seas, since human stressors have become apparent relatively early and their consequences are quite well understood thanks to long-term monitoring programs and several decades of regional modeling (Reusch et al., 2018).

One of the most important stressors is the anthropogenic climate change. The Baltic Sea has been among the fastest warming coastal seas during the last decades (Belkin, 2009) with trends of up to 0.6 °C/decade (Liblik & Lips, 2019, Kniebusch et al., 2019a, Meier et al., 2022b). While the effect of rising temperatures on variables like sea ice is well documented, the implications for the water cycle remain to a large extent unknown (Meier et al., 2022b, Lehmann et al., 2022). Since the circulation of the Baltic Sea is mainly driven by the balance between freshwater from rivers and saline water from the North Sea (Döös et al., 2004), a deeper understanding of how the salinity dynamics react to the changing climate is crucial. In that context, one important variable is the inflow of salt water from the North Sea into the Baltic Sea. Such inflows can only happen sporadically because the connections between the two seas are quite narrow and shallow and hamper the inflowing water. Due to their relatively high salinity, the inflows are denser than the brackish water of the Baltic Sea and therefore propagate into deep water layers (e.g., Wolf, 1972).

In its first part, this work aims to detect long-term changes in the saltwater inflows from the North Sea that are related to climate change. So far, no robust long-term trends have been found in the available inflow time series (Mohrholz, 2018b). However, up to this point there has not been any study looking at seasonal salt import trends, also considering the whole spectrum from the well-known Major Baltic

Inflows (MBIs) down to small inflows. Since summer inflows are in general smaller, warmer and less rich in oxygen than winter inflows (Feistel et al., 2006, Mohrholz, 2018b, Rak et al., 2020), changes in inflow seasonality could have a non-negligible impact on physical and biogeochemical properties of the Baltic Sea. For instance, the impact of warm inflows on the concentration of dissolved oxygen in the affected basins is not yet known and thus the second focus of this study.

A prerequisite for identifying long-term (forced) changes in a time series is a sufficient understanding of the internal variability. The water cycle of the Baltic Sea is characterized by a pronounced multidecadal variability with a period of about 30 years. It is known that the variability in the salinity is strongly connected to the variability in river runoff (Winsor et al., 2001, Meier & Kauker, 2003, Radtke et al., 2020) and that, more generally, the North Atlantic is an important driver of climate variability in the Baltic Sea region (e.g., Börgel et al., 2018, 2020). Still, some open questions remain, also regarding the origin of the 30-year periodicity. They will make up the third part of this work.

Together with salinity, temperature is the most important physical variable characterizing ocean dynamics as their interplay determines the water density. Despite the fact mentioned earlier that the impact of climate change on water temperature is known better than that on the water cycle of the Baltic Sea, some knowledge gaps regarding the temperature variability prevail (Meier et al., 2022b). In particular, it has not yet been studied how the teleconnections between the North Atlantic and the Baltic Sea will develop under future emission scenarios (Meier et al., 2022a). In the last part of this work, ensembles of simulations with state-of-the-art global climate models are employed to separate internal and externally forced temperature changes in the North Atlantic and to analyze how they affect the Baltic Sea.

In the following two chapters, general characteristics of the Baltic Sea, as well as the data sets and methods used in this study are introduced. Chapter 4 then provides an overview of the main findings described in the four publications. At the end, the results are discussed in terms of their significance for Baltic Sea research.

2 Baltic Sea characteristics

The Baltic Sea is a semi-enclosed coastal sea in northern Europe. With a mean depth of about 55 m (The BACC Author Team, 2008), the Baltic Sea is on average rather shallow but its depth varies strongly from the very shallow and narrow Danish straits connecting the Baltic Sea with the North Sea to the deep basins in the central and northern Baltic Sea (see Figure 2.1). The Baltic Sea is characterized by a positive freshwater balance, mainly due to high amounts of river runoff from a catchment area (light grey area in Figure 2.1) about four times as large as the sea itself. The total mean river runoff equals about $14000\,\mathrm{m^3\,s^{-1}}$, compared to $2000\,\mathrm{m^3\,s^{-1}}$ of net precipitation (precipitation minus evaporation) over the sea (Meier & Kauker, 2003). River runoff has an overall maximum in May, although the individual sub-basins have different runoff maxima ranging from March in the Kattegat and Danish straits to July in the Gulf of Finland (Mikulski, 1986, Bergström & Carlsson, 1994).

The freshwater surplus leads to a strong outflow of Baltic Sea water through the Danish straits which is balanced by inflows of highly saline North Sea water (The BACC Author Team, 2008). Since the density of seawater depends on its salinity, the interplay of freshwater supply and saline inflows leads to a pronounced haline stratification: While the surface layer is diluted by the freshwater, the deeper water layers are more saline because of the saltwater inflows from the North Sea. In the central Baltic Sea, the two layers are separated by a halocline at about 50 to 80 m depth (Stigebrandt, 1987, Väli et al., 2013) (see blue curve in Figure 2.2). The northern Baltic Sea (which is not in the focus of this study) is separated from the central basins by a rather shallow sill which strongly restricts the inflow of saline deep water. Hence, there is no permanent halocline (The BACC Author Team, 2008). On average, the salinity in the Baltic Sea amounts to about 7.4 g/kg making it a brackish water body (Meier & Kauker, 2003). Apart from the vertical salinity gradient, there is also a horizontal salinity gradient ranging from high salinities at the connection to the North Sea to almost freshwater conditions in the northernmost part of the Bothnian Bay and the mouth of the river Neva in the eastern tip of the Gulf of Finland (see Figure 2.1 for the location of the different basins). The pronounced salinity gradients strongly shape species distributions

in the Baltic Sea, since many species are only adapted to a narrow range of salinities. In fact, most of them are either marine or freshwater species and only a small number can live under the brackish conditions which prevail in large parts of the Baltic Sea (e.g., Vuorinen et al., 2015).

While the salinity exhibits only a small seasonal variability, the sea surface temperature has a distinct climatology. As a consequence of the surface warming by the incoming shortwave solar radiation and rising air temperature, a thermocline forms in spring at depths of about 25 m (see dashed red curve in Figure 2.2). It is eroded again in autumn due to surface cooling and increased wind-induced mixing (Alenius et al., 1998). Below the summer thermocline, a layer of cold winter water persists, the so-called "Cold Intermediate Layer" (Stepanova, 2017).

The overall circulation of the Baltic Sea, also termed Baltic haline conveyor belt (Döös et al., 2004), is that of an estuary with weakly saline water flowing out at the surface and highly saline water flowing in at the bottom through the consecutive basins of the central Baltic Sea as gravity currents (see Figure 2.3) (The BACC Author Team, 2008, Placke et al., 2018). In the different basins, the water forms cyclonic cells due to the combined effects of Coriolis force and bathymetry (Lehmann & Hinrichsen, 2000, Meier, 2007). Vertical mixing is restricted by the halocline, but depending on the wind direction, up- and downwelling events may occur in certain regions and topographic slopes also act as mixing hotspots (e.g., Holtermann & Umlauf, 2012). The mean residence time of freshwater in the Baltic Sea amounts to roughly 30 years (Winsor et al., 2001, Döös et al., 2004).

2.1 Climate variability

With its location in northern Europe, the Baltic Sea lies at the boundary of two climate zones (The BACC Author Team, 2008). In the southwest, maritime-temperate climate with mild and humid winters prevails while the climate of the northeast is predominantly sub-arctic with cold and dry winters. The northern and eastern gulfs of the Baltic Sea, as well as some shallow coastal zones, are regularly covered by ice in winter (The BACC Author Team, 2008). The exact boundary between the two climate zones may vary depending on the large-scale atmospheric circulation. Especially in winter, the Baltic Sea region is strongly influenced by the North Atlantic Oscillation (NAO). The NAO index is a measure of the pressure difference between the Icelandic Low and the Azores High. During NAO+ phases, this pressure difference is higher than average, leading to stronger westerlies over the Baltic Sea transporting mild and humid air from over the Atlantic. In contrast to that, winters during NAO- phases are rather cold and dry (Kauker & Meier, 2003). The NAO exhibits an interannual to decadal variability (Hurrell, 1995).

Another source of climate variability in the Baltic Sea region is the Atlantic Multidecadal Variability (AMV). It designates fluctuations of the sea surface temperatures in the North Atlantic between colder and warmer states on multidecadal time scales, with periods between 60 and 90 years during the last centuries (Börgel et al., 2018, Wills et al., 2019). Studies have shown that the AMV affects not only temperatures in the Baltic Sea (Kniebusch et al., 2019a, Börgel et al., 2023a), but also the multidecadal variability of precipitation over its catchment area and, hence, also runoff and ultimately salinity (Börgel et al., 2018). Moreover, the AMV modulates the spatial structure of the NAO by shifting the centers of the Icelandic Low and Azores High in zonal direction, thus altering the pathways of westerly winds towards Europe

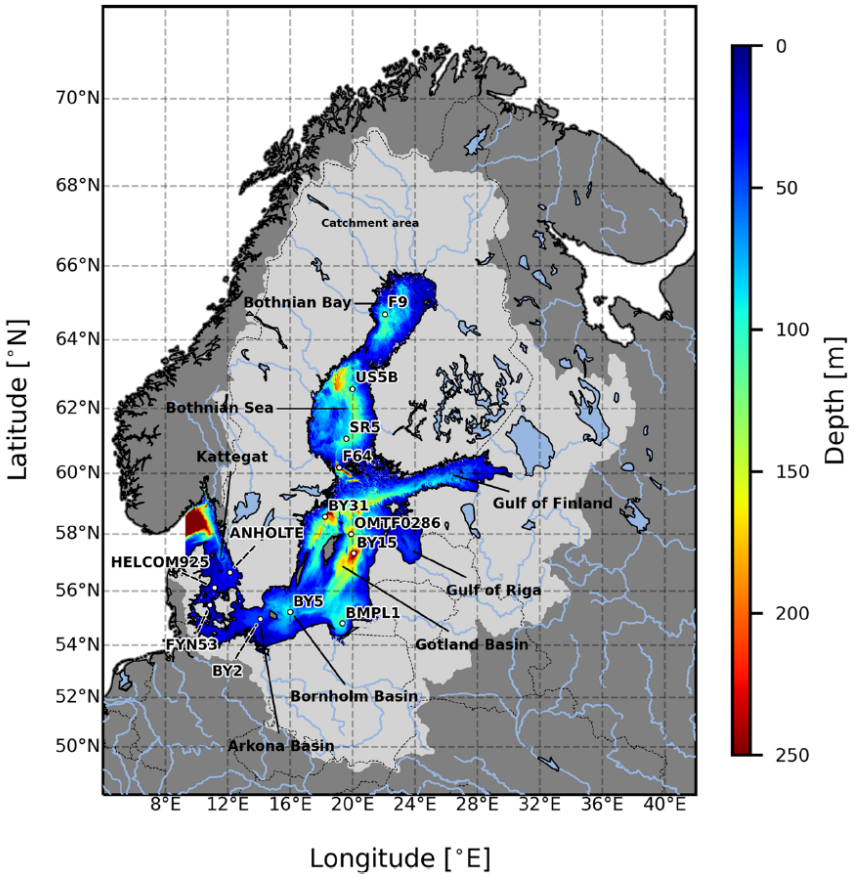

Figure 2.1: Bathymetry of the Baltic Sea and its catchment in light grey (Meier et al., 2023). The different basins and selected monitoring stations are marked.

(Lehmann et al., 2011, Börgel et al., 2020).

The climate of the Baltic Sea itself (including parameters like river runoff, average salinity or sea level) exhibits a multidecadal variability with a period of about 30 years (Winsor et al., 2001, Meier & Kauker, 2003, Kniebusch et al., 2019b, Medvedev & Kulikov, 2019, Radtke et al., 2020, Agha Karimi et al., 2021, Stockmayer & Lehmann, 2023). So far, the origin of this 30-year variability could not be determined, since neither AMV nor NAO show this kind of periodicity (Radtke et al., 2020). It is known, however, that about 50 % of the multidecadal variability in the salinity is caused by the runoff variability (Meier & Kauker, 2003). Of that, one half can be explained directly by the dilution of freshwater into the surface layer of the Baltic Sea (Radtke et al., 2020). For the remaining part, Radtke et al. (2020) reported that periods of higher river runoff coincide with saltwater inflows of a lower average salinity, although it was not clear whether this is a mere correlation or whether a mechanistic explanation exists.

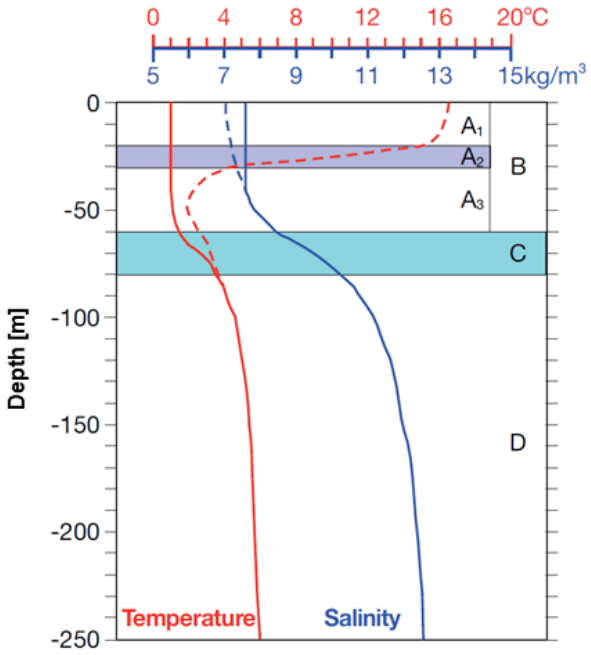

Figure 2.2: Thermal and haline stratification of the central Baltic Sea in winter (solid lines) and summer (partly hatched lines) (taken from The BACC Author Team (2008) and modified). The capital letters stand for saline deep water (D), halocline (C), and surface layer (B). Between spring and autumn, layer B is subdivided into cold intermediate layer (A3), summer thermocline (A2), and warm surface layer (A1).

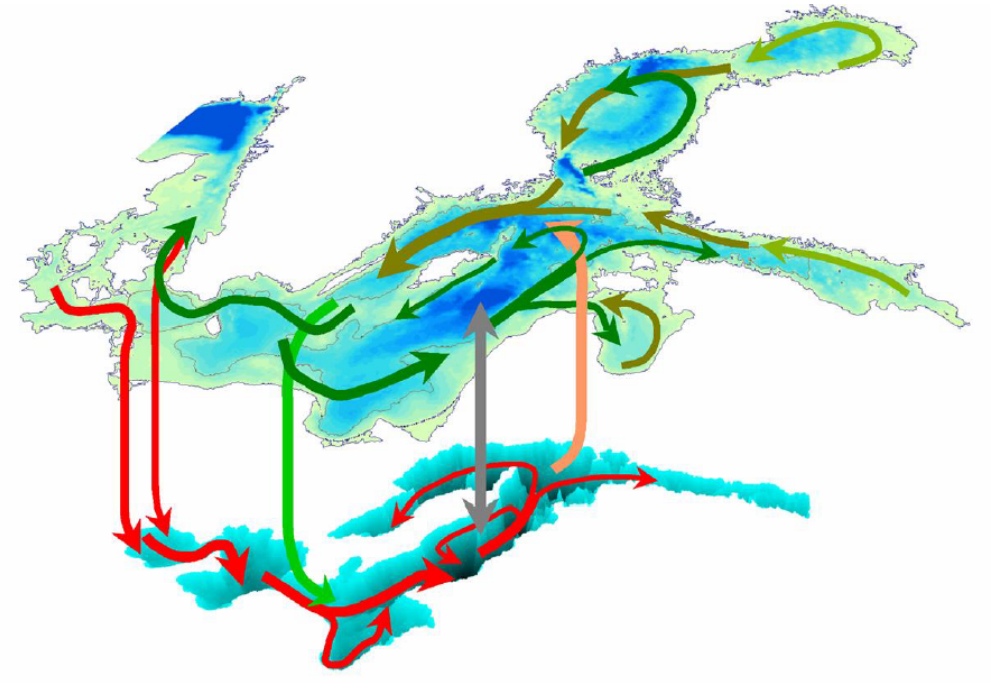

Figure 2.3: Large-scale two-layer circulation scheme of the Baltic Sea with the surface layer circulation marked by green arrows and the sub-halocline circulation marked by red arrows (The BACC Author Team, 2008). Exchange between the two layers happens via diffusion (gray arrow) and entrainment (vertical green and orange arrows).

2.2 Climate change in the Baltic Sea region

The current knowledge of how the anthropogenic climate change affects the Baltic Sea region is summarized in Meier et al. (2022b). Here, only findings most relevant to this thesis are reported. First of all, air temperatures in the Baltic Sea region have been rising with a rate of about 0.1 K per decade since 1878 which is faster than the global average (Meier et al., 2022b). During the last decades, the sea surface temperatures (SSTs) of the Baltic Sea exhibited one of the strongest trends of all coastal seas with a warming of 1.35 °C between 1982 and 2006 (Belkin, 2009). The intensified warming was not entirely attributed to climate change but also partly to a shift of the AMV from a cold to a warm phase (Kniebusch et al., 2019a).

The impact of climate change on the water cycle of the Baltic Sea is less well understood. Neither river runoff nor mean salinity show a systematic long-term trend during the 20th century (Meier et al., 2022b). In the future, river discharge in the northern part of the catchment is expected to increase. Hence, for a long time projection studies modeled a decreasing salinity (e.g., Meier et al., 2012). However, more recent projections including the global mean sea level rise show no significant trend in mean salinity (Meier et al., 2021), as a higher sea level leads to a larger cross section of the Danish straits and therefore to stronger saltwater inflows (Hordoir et al., 2015, Arneborg, 2016, Meier et al., 2017, Saraiva et al., 2019). Some studies report a strengthened stratification (Liblik & Lips, 2019, Stockmayer & Lehmann, 2023), although Liblik & Lips (2019) only considered a time span of 35 years which is comparable to the time scale of multidecadal variability and thus too short to identify long-term changes.

For the large-scale atmospheric circulation and wind patterns, no long-term trends could be found so far, either (Meier et al., 2022b). There are some indications for a more frequent occurrence of blocking patterns in summer (Coumou et al., 2015), possibly related to the decreasing poleward temperature gradient, but it is questionable whether these findings are robust (cf. Woollings et al., 2018).

2.3 Saltwater inflows

As previously mentioned, the overall circulation of the Baltic Sea is estuary-like, with brackish water leaving at the surface and saltwater entering below. However, the inflow of saltwater from the North Sea is not continuous, since the water has to overcome one of the two shallow sills in the Danish straits, namely the Drogden Sill (8 m depth) or the Darss Sill (19 m depth, see Figure 3.1) (Mohrholz, 2018b). There are two types of inflows (Wolf, 1972, Feistel et al., 2006) which are also illustrated in Figure 2.4:

1. Barotropic inflows are driven by barotropic pressure gradients, i.e., sea level inclinations. Usually, the sea level in the Baltic Sea is higher than that of the North Sea due to the strong freshwater input (The BACC Author Team, 2008). However, westerly gales can push North Sea water into the Baltic Sea. This is especially effective if the westerly winds are preceded by easterly gales pushing water out of the Baltic Sea. The largest barotropic inflows importing several Gt of salt into the Baltic Sea occur when about 20 days of easterly winds are followed by about 20 days of westerly winds (Matthäus & Schinke, 1994, Lass & Matthäus, 1996). Large barotropic inflows (MBIs) happen about once a year and mostly between November and January (Matthäus & Franck, 1992, Fischer & Matthäus, 1996, Mohrholz, 2018b). Only they are able to replace the bottom water in

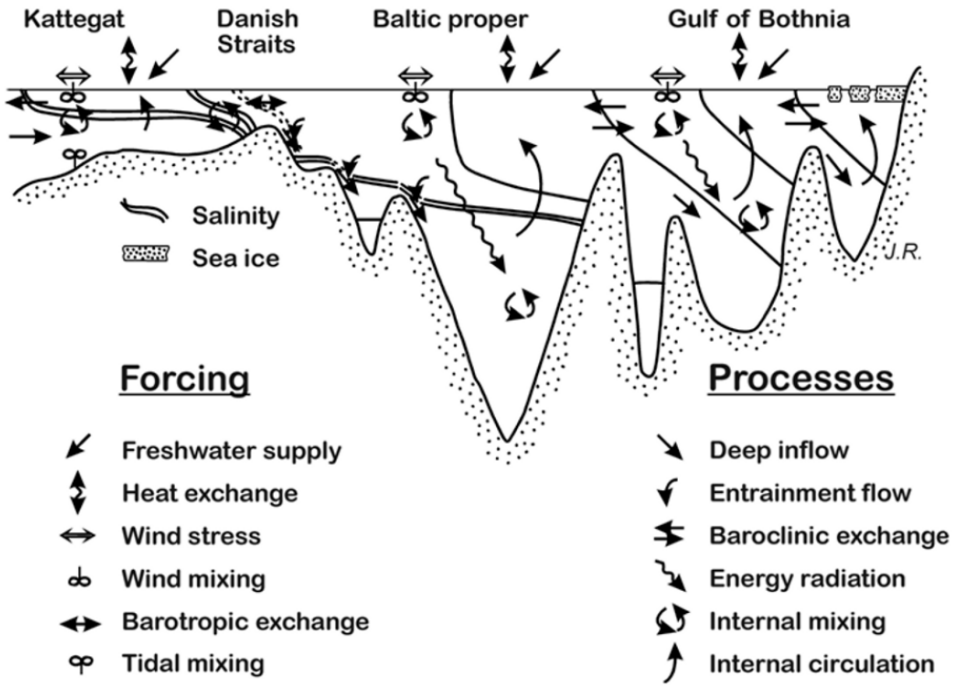

Figure 2.4: Schematic cross section through the basins of the Baltic Sea with isohalines, sea ice, exchange and mixing processes induced by external forcing and internal processes (The BACC Author Team, 2008). Barotropic inflows are visualized as barotropic exchange in the Danish straits and baroclinic inflows as baroclinic exchange in the Kattegat / Danish straits.

the about 250 m deep Eastern Gotland Basin in the central Baltic Sea (Matthäus & Franck, 1992). Smaller barotropic inflows, which can occur throughout the year, rather interleave in or below the halocline (Elken, 1996). Barotropic inflows are characterized by a well-mixed water column over the Darss Sill moving entirely in the same direction (Matthäus & Franck, 1992).

2. Baroclinic inflows are driven by baroclinic pressure gradients. They are evoked by horizontal density gradients, whereby the density is largely determined by the salinity. Hence, baroclinic inflows occur under calm conditions when a stratified water column with a highly saline bottom layer forms in the Danish straits. Such situations can arise throughout the year but are most likely in late summer (Feistel et al., 2006). The first intensively investigated summer inflow happened in 2002 (Feistel et al., 2003). Summer inflows can in theory be both barotropic and baroclinic but are believed to be mainly baroclinic (Feistel et al., 2006). They transport warm surface water from the Kattegat to water layers in or just below the halocline and, in particular, cause distinct temperature maxima in the Bornholm Basin (Mohrholz et al., 2006).

There were no systematic changes in the intensity or frequency of barotropic inflows during the 20th century (Mohrholz, 2018b). Instead, they exhibit the same multidecadal variability as the mean salinity and the runoff and a feedback mechanism between river runoff and inflow variability has been proposed (Radtke et al., 2020). Around 2000, several summer inflows occurred, which led to the hypothesis that their frequency increased lately (Mohrholz et al., 2006, Meier et al., 2006). However, so far, no comprehensive time series of such inflows exists. Data sets like those of Mohrholz (2018a) only consider

barotropic inflows and thus probably miss a large portion of the summer inflows. After all, baroclinic transport accounts for about half of the total salt import throughout the year (Mohrholz, 2018b).

2.4 Oxygen dynamics and hypoxia

While salinity and temperature are essential variables shaping physical processes in the Baltic Sea, oxygen is a key parameter when it comes to biogeochemistry. Oxygen production (in addition to oxygen uptake from the atmosphere) occurs in the euphotic zone via photosynthesis. There are, depending on the availability of the main nutrients nitrogen (N) and phosphorus (P), two large phytoplankton blooms each year; an algal bloom in spring and a cyanobacteria bloom in late summer. Afterwards, the biomass sinks down in the water column and is decomposed by microorganisms under consumption of oxygen. A detailed assessment of the oxygen sources and sinks in the Baltic Sea is provided by Naumov et al. (2023).

Due to the pronounced stratification, the supply of deep water layers with oxygen from above is very limited. Instead, the main source of oxygen are saltwater inflows (MBIs in particular), providing well-oxygenated surface water from the North Sea. On the other hand, inflows lead to a higher bottom salinity and therefore to an increased stratification, hampering the oxygen supply from above (Conley et al., 2009, Väli et al., 2013, Almroth-Rosell et al., 2021).

When the biological or biogeochemical oxygen consumption in a water body exceeds the oxygen supply for a sufficiently long time, hypoxic (less than 2 ml oxygen per l of water) or even anoxic (no oxygen) conditions can establish (Fennel & Testa, 2019). With its permanent stratification, the central Baltic Sea is naturally susceptible to oxygen deficiency. Sediment cores have revealed that periods of low oxygen conditions have occurred during the Holocene Thermal Maximum and the Medieval Climate Anomaly (Zillén et al., 2008, Kabel et al., 2012, Börgel et al., 2023b). As possible drivers of these hypoxic periods, higher bottom salinities (i.e., a stronger stratification), a higher supply of organic matter, and higher water temperatures have been identified. In warmer water, the oxygen solubility is lower and the oxygen consumption higher (Meier et al., 2011, Laufkötter et al., 2017, Börgel et al., 2023b). Krapf et al. (2022) found a positive correlation between bottom temperatures and hypoxic area.

Since the 1950s, hypoxic and anoxic areas in the Baltic Sea have grown larger than ever recorded before (Conley et al., 2009, Carstensen et al., 2014). In 2018, the so far largest extent of anoxia has been reached (Hansson et al., 2019, Almroth-Rosell et al., 2021, Krapf et al., 2022). This deterioration of oxygen conditions has been attributed to eutrophication resulting from a strong increase in anthropogenic nutrient (N and P) loads, mainly from intensified agriculture and urbanization, in the second half of the 20th century (Gustafsson et al., 2012, Meier et al., 2019). Higher nutrient loads fuel a strong production of organic matter and hence cause more detritus (dead organic material) and ultimately a higher oxygen consumption in deep water layers and in the sediments. The interannual variability of the hypoxic area has been related to saltwater inflows due to the previously described reasons (Väli et al., 2013). Moreover, a recent study based on sediment cores revealed that the rather sudden onset of oxygen depletion in the 1950s was likely triggered by the increased stratification after the very strong saltwater inflow in 1951 (Moros et al., 2023).

The nutrient input has decreased since the 1980s, but the hypoxic and anoxic areas did not; in some basins, they even increased (Almroth-Rosell et al., 2021). A main reason are the different types of chemical reactions that unfold under anoxic conditions. In particular, existing phosphorus is re-released from the sediments into the water column, stimulating primary production as soon as it reaches the euphotic zone (Vahtera et al., 2007). This is visualized in Figure 2.5 which shows a schematic comparing nutrient cycling under aerobic and under anaerobic conditions.

Although the previously mentioned impact of higher temperatures on the oxygen concentrations has been shown in several studies, the effect of increasing water temperatures due to global warming on the oxygen conditions still seems to be of minor importance compared to eutrophication (Meier et al., 2019).

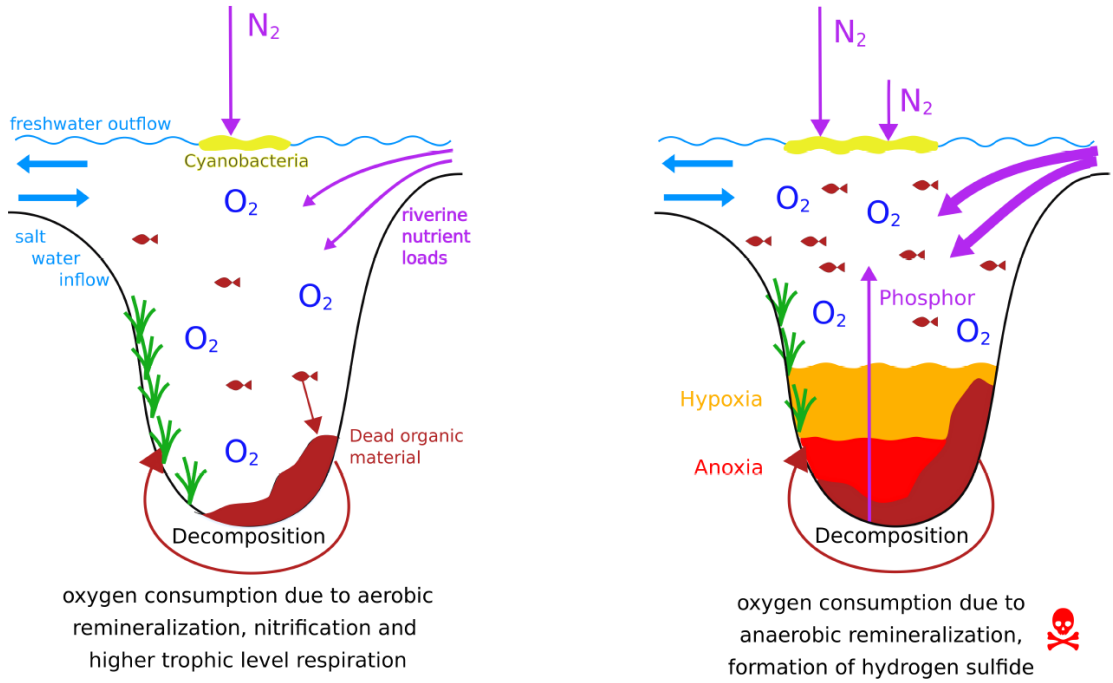

Figure 2.5: Schematic of the nutrient cycling in the Baltic Sea under aerobic conditions (left) and under anaerobic conditions due to eutrophication (right) (Kniebusch, 2019).

3 Data and methods

This chapter will first introduce the regional ocean models (Section 3.1) employed in Barghorn et al. (2023, 2025b) and Meier et al. (2023) and the methods used to analyze their output (Sections 3.2 to 3.5). At the end, data and methods of Barghorn et al. (2025a) are described (Sections 3.6 and 3.7).

3.1 Regional ocean models

3.1.1 Model descriptions

The first three publications in this thesis are based on simulations with three different regional models using similar atmospheric forcing and river runoff. The three ocean models used in this study are the General Estuarine Transport Model (GETM) (IOW, 2023b) in Barghorn et al. (2023, 2025b), the Rossby Centre Ocean (RCO) model (Meier et al., 2003) in Meier et al. (2023) and Barghorn et al. (2025b), and the Modular Ocean Model (MOM) (Griffies, 2004) in Barghorn et al. (2025b). RCO and MOM are both coupled to Hibler-type sea ice models and biogeochemical models. For RCO, the biogeochemistry is modeled by the Swedish Coastal and Ocean Biogeochemical (SCOBI) model (Eilola et al., 2009) and for MOM by the Ecological Regional Ocean Model (ERGOM) (Neumann et al., 2022, IOW, 2023a). In contrast, the GETM setup (Radtke et al., 2020) only includes a basic thermodynamic sea ice model and no biogeochemistry.

The ocean models solve the primitive equations comprising the Reynolds-averaged Navier-Stokes equations with the hydrostatic, shallow, traditional, and Boussinesq approximations, the continuity equation, and tracer equations for temperature and salinity on regular latitude-longitude grids (Meier et al., 1999, Griffies, 2014, IOW, 2023b). Vertical mixing, which cannot be resolved by the model grids, is parameterized by k-ε turbulence models (GETM and RCO) or the K profile parameterization (MOM) (Placke et al., 2018). The biogeochemical models are coupled with the respective ocean model via tracer modules.

They model the oxygen, nitrogen, phosphorus, and, in case of ERGOM, also carbon, and sulfur cycles. For both ERGOM and SCOBI, biological components consist of three types of phytoplankton (i.e., primary producers), zooplankton (which grazes on phytoplankton), and detritus. The models include one sediment layer, where detritus accumulates after sinking in the water column. Oxygen concentration and water temperature control the mineralization of detritus into inorganic phosphorus and nitrogen, both in the sediments and in the water column (Neumann et al., 2022, Eilola et al., 2011).

Basic characteristics of the model setups are summarized in Table 3.1 (Barghorn et al., 2025b), highlighting differences for example in the horizontal and vertical resolution. The former is 1 nm for GETM, 2 nm for RCO and 3 nm for MOM. The bathymetry of the GETM setup is displayed in Figure 3.1. In the vertical domain, GETM uses 50 layers of adaptive coordinates (Gräwe et al., 2019). As the name suggests, the layer thickness is adjusted automatically to allow a higher resolution, e.g., in the vicinity of strong density gradients. Hofmeister et al. (2011) have shown that adaptive vertical coordinates are suitable for the simulation of (small) saltwater inflows. RCO works with 83 vertical layers of 3 m thickness and MOM employs z^* coordinates with 152 vertical layers whose thickness increases gradually with depth from 0.5 m at the surface up to 2 m in the deep basins. The exact depths slightly change with each time step depending on the sea surface elevation.

In the model runs used for this study, daily means of temperature and salinity at selected stations and daily means of salt transport at 8 transects (see Figure 3.1 for the locations) were stored in GETM. In case of 3-d temperature and salinity fields, only 5-day means were stored. In RCO, 3-d snapshots were taken every other day and in MOM, daily means of 3-d fields were stored.

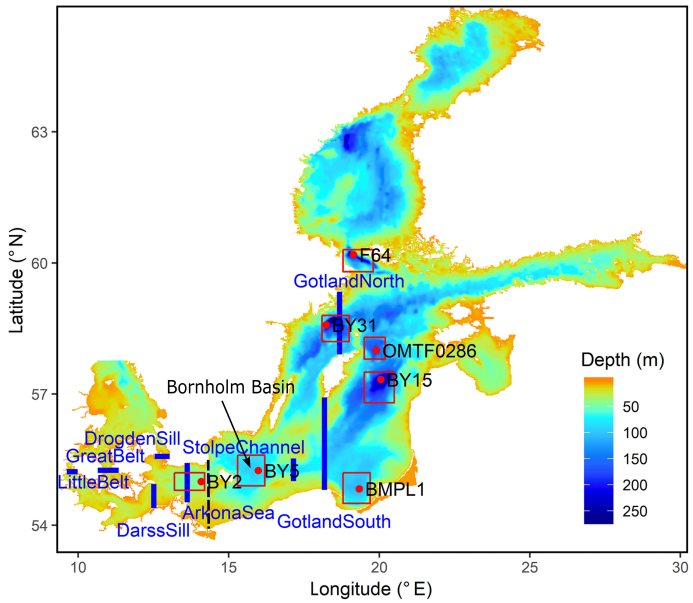

Figure 3.1: Bathymetry of the GETM setup, (taken from Radtke et al. (2020) and modified for Barghorn et al. (2025b)). Red dots indicate stations used for model validation. The observational data for each respective station was assembled over the red boxes. Blue lines denote transects for salt transport calculations. The thin dashed line close to station BY2 shows the eastern border of the volume that is used for calculating the salt content in highly saline water masses of the Arkona Basin.

Table 3.1: Selected characteristics of the model setups (Barghorn et al., 2025b).

	GETM	RCO	MOM
open boundary	Northern Kattegat	Northern Kattegat	Skagerrak
grid	Arakawa-C	Arakawa-B	Arakawa-B
horizontal resolution	1 nm	2 nm	3 nm
vertical resolution	50 layers of adaptive coordinates	83 layers of 3 m thickness	152 layers, thickness increasing towards depth from 0.5 m to 2 m
temporal resolution	daily for transects and stations, 5-daily for 3-d fields	2-daily snapshots	daily
biogeochemical model	None	SCOBI	ERGOM

3.1.2 Details of the reference simulations

All simulations ran from 1850 to 2008 and used the same atmospheric forcing and river runoff. The boundary conditions are slightly different since GETM and RCO have their open boundary in the northern Kattegat while the model domain of MOM also includes the Skagerrak.

Atmospheric forcing

As atmospheric forcing, the High Resolution Atmospheric Forcing Fields (HiResAFF) v2 data set was used (Schenk & Zorita, 2012). Since it had to reach back to the beginning of the instrumental period when measurements were still scarce, the analogue method was used to identify and reconstruct historical states of the atmosphere by finding analogues in a reference period in the more recent past (1958-2007). For GETM and MOM, a correction for strong winds was applied because the comparison with observational data revealed that strong winds are underestimated in the HiResAFF data set. The correction for GETM is given in Radtke et al. (2020). In case of MOM, a gust correction as suggested by Brasseur (2001) was used.

River runoff and boundary conditions

The river runoff time series is a compilation of multiple data sets. It comprises reconstructions by Hansson et al. (2011) for 1850-1900, Cyberski & Wroblewski (2000) for 1901-1920 and Mikulski (1986) for 1921-1949, observations from the BALTEX Hydrological Data Centre for 1950-2004 (Bergström & Carlsson, 1994), and hydrological model results (Graham, 1999) for 2005-2008. Further information can be found in Meier et al. (2019). It should be pointed out that the method used by Hansson et al. (2011) results in a reduced interannual runoff variability compared to the other data sets.

The boundary conditions in GETM and RCO at the open boundary in the northern Kattegat are described by Meier et al. (2019). Daily means of sea surface elevation were derived from a reconstruction of the meridional sea level pressure gradient across the North Sea as in Gustafsson & Andersson (2001).

Other parameters like temperature, salinity, or nutrients were nudged towards observed climatological seasonal means at a station in the southern Skagerrak. More details can be found in Meier et al. (2019). For the MOM run, a statistical model was used to estimate the sea surface elevations from the meteorological forcing. Climatological data at the open boundary were derived from Janssen et al. (1999) for temperature and salinity, and from previous model simulations for the biogeochemical variables.

Initialization

In case of GETM, initial conditions were found by interpolating observational data of 1979 onto the model grid. The first 30 years of the simulation are considered as spin up, since the mean flushing time of the Baltic Sea freshwater amounts to 30 years (Winsor et al., 2001). The initialization of the nutrients in the RCO simulations is based on reconstructions of the pre-industrial Baltic Sea by Savchuk et al. (2008). For the physical fields, present data was used for a spin-up running from 1850 until 1902. The values found at the end of the spin-up were considered as initial values for the simulation starting in 1850. In case of MOM, 30 years of spin-up were run to find the initial conditions.

3.1.3 Observational data for model validation

Observational data for model validation were taken from the ICES data base (ICES, 2023). Data for seven stations in the western and central Baltic Sea (see Figure 3.1) were assembled by Radtke et al. (2020) from the latitude-longitude boxes surrounding the stations to increase the data coverage. For vertical profiles of temperature and salinity, data points were sorted into layers of 10 m thickness as the depths where measurements were taken varied over time. For time series of surface and bottom salinity, the upper 20 m were considered the surface layer and the lowest 10 % of the water column the bottom layer at the respective station. Since the observations were not homogeneously distributed over the year, a seasonal bias correction was performed using the Generalized Additive Mixed Model (GAMM) (Simpson, 2014) as in Radtke et al. (2020). The model splits the time series s into a component $s_{\mathrm{longterm}}(t)$ that varies on decadal time scales and a seasonally varying component $s_{\mathrm{seasonal}}(\tau)$, where τ is the sampling time within a year:

$$s = s_{\mathrm{longterm}}(t) + s_{\mathrm{seasonal}}(\tau) + s_0 + \varepsilon. \tag{3.1}$$

Here, s_0 is a constant offset and ε is the residual. By extracting the seasonal component and subtracting it from s, the time series can be corrected for possible seasonal biases:

$$s_{\mathrm{corr}} = s - s_{\mathrm{seasonal}}(\tau). \tag{3.2}$$

3.1.4 Validation of the reference simulations

Time series of bottom and surface salinity as well as vertical salinity and temperature profiles at the seven selected stations were validated for all three models in Barghorn et al. (2025b). For RCO, salinity time series at three additional stations in the Kattegat / Danish straits and in the northern Baltic Sea, respectively,

were evaluated in Meier et al. (2023). Vertical profiles were averaged over the years 1970-2007, i.e., a period with high coverage of observational data. The same period was used to calculate explained variances of the modeled bottom salinity at stations BY2 and BY5, since these stations are in the focus of this work. Explained variances ρ^2 were computed as in Radtke et al. (2020), following the theoretical framework of Good & Fletcher (1981), by comparing the variance of the observational minus the modeled data σ^2_{res} to the variance of the observational data σ^2_{obs}:

$$\rho^2 = \frac{\sigma^2_{\mathrm{obs}} - \sigma^2_{\mathrm{res}}}{\sigma^2_{\mathrm{obs}}}. \tag{3.3}$$

Further validations of the GETM simulation (including an evaluation of the transport across Darss Sill and Drogden Sill) can be found in Radtke et al. (2020) and of RCO in Meier et al. (2019). Concerning the biogeochemistry, the oxygen content at station BY5 is particularly important for Barghorn et al. (2025b). Other variables and locations were validated for SCOBI in Eilola et al. (2009) and for ERGOM in Naumov et al. (2023).

Validation summary

Figures 3.2 and 3.3 show the validation of vertical profiles and salinity time series at stations BY2 and BY5 (remaining five stations in the reference) for all three models from Barghorn et al. (2025b). Therein, it was concluded that despite some visible model biases, general features like the multidecadal variability or the haline stratification are captured by the models. As already remarked in Radtke et al. (2020), GETM seems to have difficulties in reproducing the bottom salinity time series at BY5 (indicated by the negative explained variance). However, the time series at 60 m depth, important for small and / or warm inflows, is captured much better (Radtke et al., 2020). Another remarkable feature is the drift in MOM over the first 50–60 years. Apparently, the initial values for salinity are too low. Hence, the years before 1920 are not used in MOM. The bottom panels of Figure 3.3 additionally display bottom temperatures and oxygen concentrations at 80 m depth at station BY5. As indicated in the legends, the modeled trends are comparable to the observed trends although both MOM and RCO overestimate the oxygen concentrations.

3.1.5 Sensitivity experiments

The salinity dynamics in the Baltic Sea are mainly driven by the net freshwater supply (primarily through river runoff), wind, and sea level. To investigate how exactly the salinity dynamics depend on these drivers in terms of multidecadal variability and seasonality, sensitivity experiments with manipulated runoff, wind, and mean sea level were conducted. The different experiments are summarized in Table 3.2. Note, that the names used for the GETM experiments in Barghorn et al. (2023) are different from the names of the RCO experiments. This is due to the fact that the original reference simulation in GETM, in contrast to that of RCO, includes the global mean sea level rise. For Barghorn et al. (2025b), the names of the GETM experiments were adjusted to match those of the RCO experiments. In the same publication, an additional RCO sensitivity experiment labeled TAIR was analyzed. In TAIR, global warming was excluded by repeating the atmospheric temperatures and specific humidities of 1904 over the whole model period.

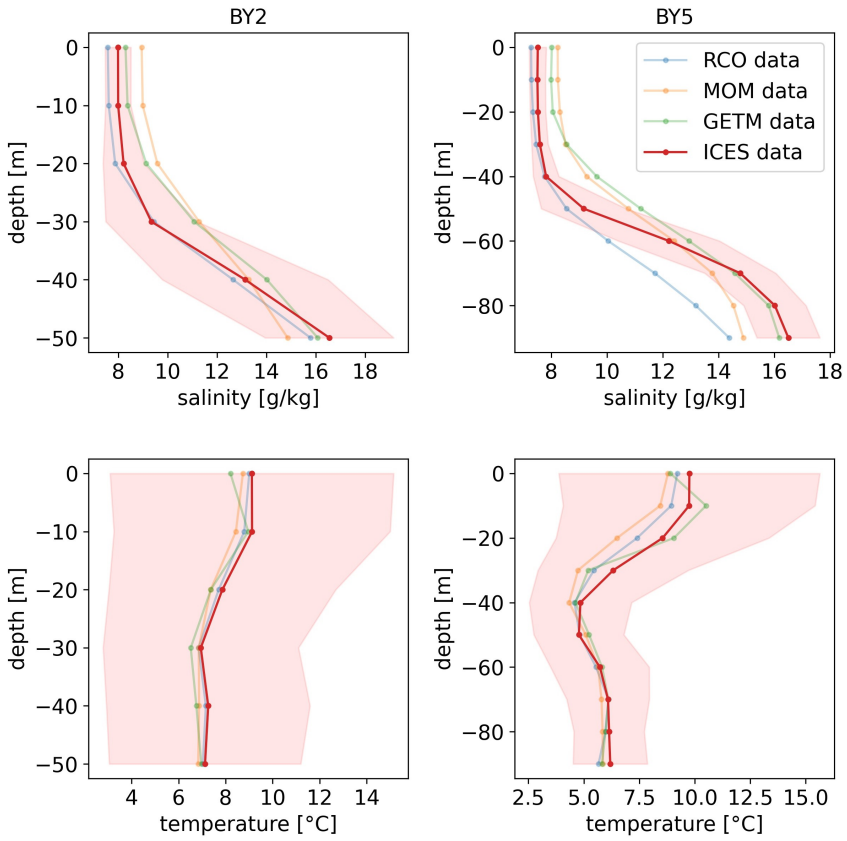

Figure 3.2: Salinity and temperature profiles averaged over the years 1970-2007 at stations BY2 and BY5 from the three models and observational (ICES) data. The red shaded areas denote +/- one standard deviation of the ICES data (full figure with all stations in the Supplements of Barghorn et al. (2025b)).

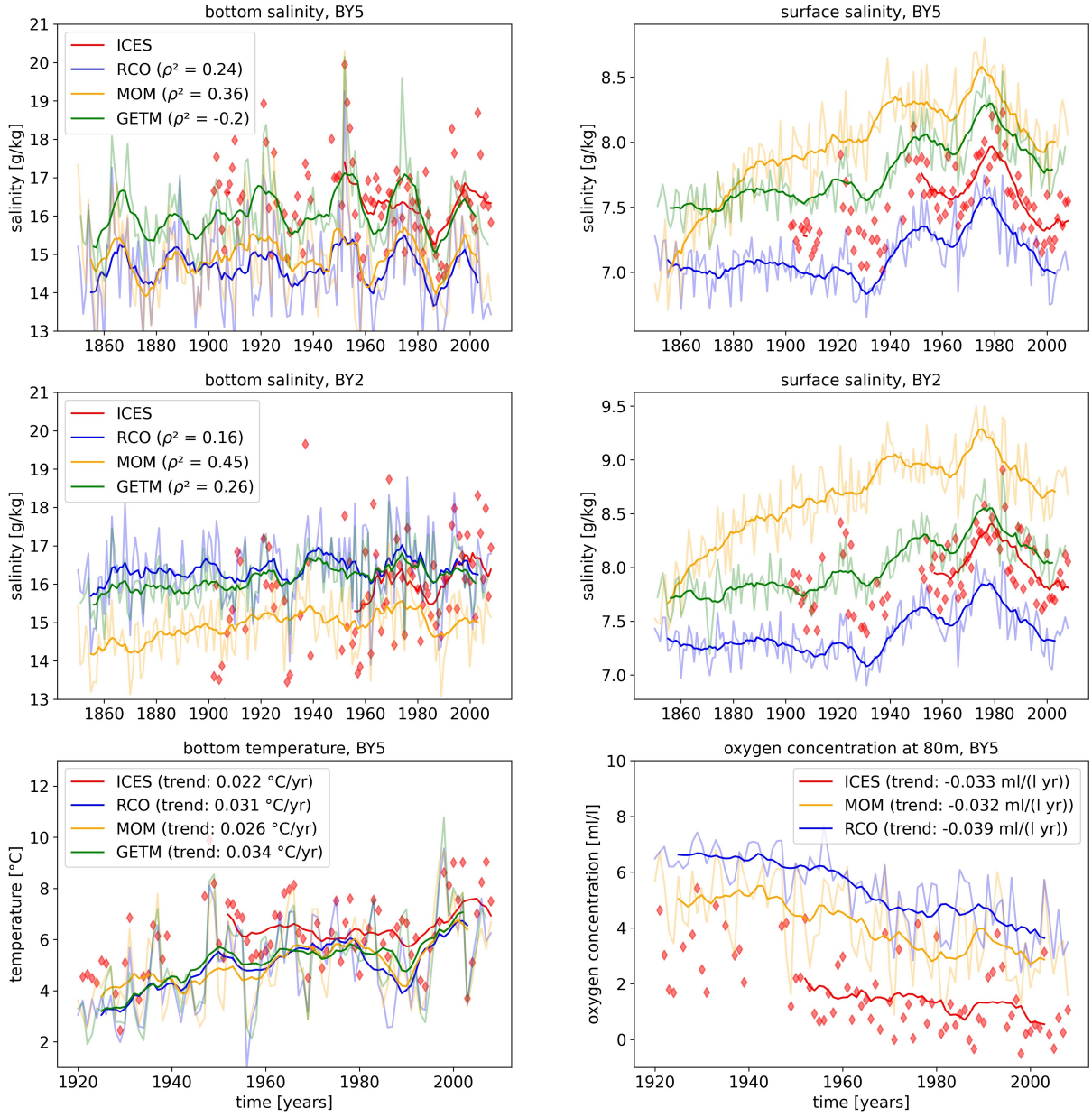

Figure 3.3: Time series of bottom and surface salinity at stations BY5 and BY2 from the three models and ICES data (full figure with all stations in the Supplements of Barghorn et al. (2025b)) plus bottom temperatures and oxygen concentrations at 80 m depth at station BY5 since 1920. Thin and bold lines denote annual and 11-year running means, respectively. ICES data are visualized by red diamonds. Explained variances of the modeled bottom salinity as well as temperature and oxygen trends are given in the legends.

Table 3.2: Sensitivity experiments. Note that the labels for the GETM experiments in Barghorn et al. (2023) (given in brackets) differ from those in Barghorn et al. (2025b), where they were adjusted to match those of the RCO experiments.

Model	Experiment	Description
GETM	REF+ (REF)	reference simulation with global mean sea level rise
	REF (noSLR)	reference simulation without sea level rise
	RUNOFF+ (RUNOFF)	climatological mean runoff repeated for each year, with sea level rise
	(RUNOFF2)	climatological mean runoff repeated for each year, but scaled with original interannual variability, with sea level rise
	(WIND)	multidecadal variability removed from wind and sea level at open boundary
RCO	REF+	reference simulation with sea level rise
	REF	reference simulation without sea level rise
	RUNOFF+	climatological mean runoff repeated for each year, with sea level rise
	TAIR	air temperatures and specific humidities of 1904 repeated for each year, no sea level rise
MOM	REF	reference simulation without sea level rise
	RUNOFF	climatological mean runoff, no sea level rise

3.2 Characterization of saltwater inflows

Two different methods for the detection and quantification of saltwater inflows were used in this work. In Barghorn et al. (2023), the salt import to the Baltic Sea was retrieved from the salt transport over the Darss Sill and Drogden Sill. This method could not be used in Barghorn et al. (2025b) and Meier et al. (2023), since the temporal resolution (2-daily snapshots) of the RCO output is not sufficient to capture the high-frequency variations of the currents going across the sills. Instead, the amount of highly saline water masses in the Arkona Basin was used to parametrize the inflows. A similar strategy was already applied and validated in Meier & Kauker (2003).

3.2.1 Inflow detection in GETM

The output of the GETM simulations contains the daily mean salt transport across the Darss Sill and the Drogden Sill (see Figure 3.1) which are the main bottlenecks for the inflowing water. From the salt transport across the transects, all salt transport directed towards the Baltic Sea with a minimum salinity of 17 g/kg was accumulated. The threshold of 17 g/kg is an empirical value which was introduced by Wolf (1972) and has been proven useful to distinguish inflowing North Sea water from ambient water masses in the Danish straits (e.g., Matthäus & Franck, 1992, Meier & Kauker, 2003, Mohrholz et al., 2015).

Apart from the salinity threshold, two additional criteria were introduced to separate subsequent inflows

from each other and only count inflows from a certain size. Too small inflows are believed to quickly mix with the ambient water in the Arkona Basin, hence not affecting the basins further downstream. To separate individual inflows, days with a salt import of less than 20 Mt were set to zero. As a minimum inflow size, 100 Mt salt import were chosen. It is about the same order of magnitude as the smallest inflows in the DS1 series of Mohrholz (2018a).

The inflow criteria were validated by comparing the resulting salt import time series to the previously mentioned DS1 series (Figure 3.4). Since this work focuses on the multidecadal variability, smoothed time series were compared. As the DS1 series only contains barotropic inflows, the total amount of annual salt import is lower than for the GETM inflow time series, which includes also baroclinic inflows, but the low-frequency variability is very similar.

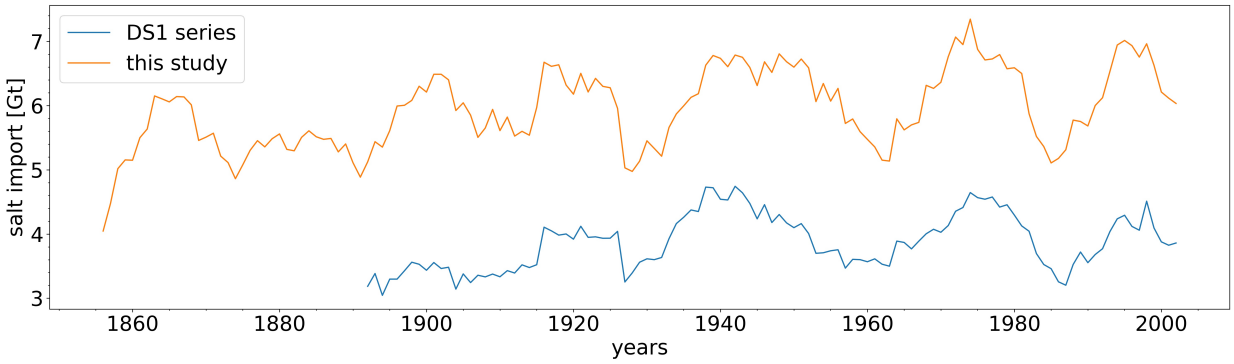

Figure 3.4: 11-year running means of annual salt import from the DS1 series of barotropic inflows by Mohrholz (2018a) and from the GETM inflow series (Barghorn et al., 2023).

3.2.2 Salt import parametrization via salt content in the Arkona Basin

For the determination of the highly saline volume (V_{17}, Meier et al. (2023)) or the salt content in this highly saline volume (S_{17}, Barghorn et al. (2025b)) in the Arkona Basin, the same threshold of 17 g/kg was applied. The volume was bounded by the Darss Sill and Drogden Sill transects in the West and the North, respectively, and by the transect denoted by the thin dashed line in Figure 3.1 in the East. It is situated at the entrance of the Bornholm Gate where the Arkona Basin deepens towards the Bornholm Basin. As previously mentioned, it has been shown that V_{17} (or S_{17}) is a suitable proxy for inflows, at least for MBIs. However, the ability to reproduce the multidecadal or seasonal variability of salt import had not yet been proven. In Barghorn et al. (2025b), this was done by comparing annual and seasonal (June - August and September - October) means of S_{17} to the previously validated salt import time series in the GETM simulation. Figure 3.5 shows this exemplarily for the annual mean S_{17} of GETM. The yellow box displays the Pearson correlation coefficient between the non-smoothed time series from 1920 onward. It is sufficiently high to conclude that S_{17} is able to resolve the annual and seasonal salt import.

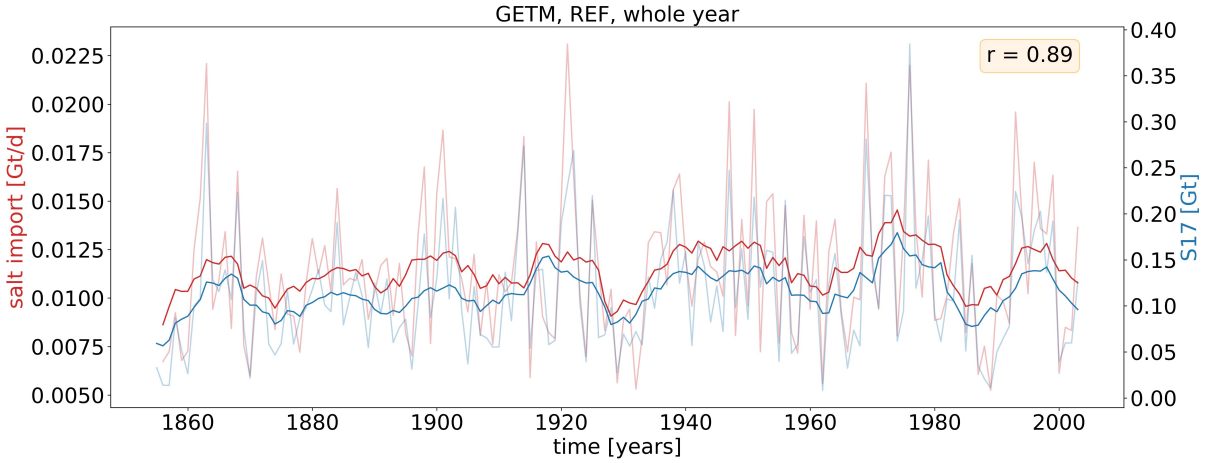

Figure 3.5: Comparison of annual salt import and S_{17} for the reference simulation (REF) of GETM. Bold lines denote 11-year running means. The Pearson correlation coefficient of the non-smoothed time series computed from 1920 onward is given in the yellow box (full figure including summer and early autumn time series in the Supplements of Barghorn et al. (2025b)).

3.3 Oxygen budget

In Barghorn et al. (2025b), the impact of warm saltwater inflows on the oxygen dynamics in the Bornholm Basin is assessed. For that purpose, the oxygen budget in the basin below 60 m water depth was determined following the methodology described in Naumov et al. (2023) for MOM/ERGOM. It includes all biochemical and physical oxygen sources and sinks (see Neumann et al. (2022) for a list of all relevant terms). The main biochemical oxygen source (photosynthesis) as well as oxygen consumption via respiration are negligible in the deep water layers. Instead, the most important oxygen sink is the mineralization of detritus in the sediments (Naumov et al., 2023). Other relevant biochemical oxygen sinks are the oxidation of reduced material, nitrification, and coupled nitrification / denitrification. Physical processes comprise advection and diffusion across the boundaries of the volume.

3.4 NAO index

The winter (December - February) NAO index used in Meier et al. (2023) was compiled from two sources; an Empirical Orthogonal Function (EOF) analysis of the reanalysis product ERA20C (Poli et al., 2016) and long-term observations of the sea level pressure difference between Reykjavik and Gibraltar (Jones et al., 1997).

3.5 Wavelet analysis

Wavelet analysis is a method introduced by Torrence & Compo (1998) to unveil the dominant frequencies in a time series. In contrast to Fourier analysis, it preserves the time information and thus results in a 2-d plot showing the power of individual frequencies and how it changes over the course of the time series. The basic function used for the wavelet transform is called "mother wavelet". In Meier et al. (2023), the Morlet wavelet was used as mother wavelet. It consists of a sine wave modulated by a Gaussian:

$$\psi(t) = \pi^{-1/4}\, e^{i\omega t}\, e^{-t^2/2}, \tag{3.4}$$

where t denotes the time and ω the frequency.

The continuous wavelet transform (CWT) is built by convoluting the (discrete) time series $x(t)$ with a modified version of $\psi(t)$ translated along the time axis by τ and compressed or stretched by s (with the notation of Börgel (2020)):

$$\mathrm{CWT}(\tau, s) = \sum_t \frac{x(t)}{\sqrt{s}} \psi^* \left(\frac{t - \tau}{s} \right), \tag{3.5}$$

where $(^*)$ denotes the complex conjugate. This results in the wavelet power spectrum:

$$\mathrm{Power}(\tau, s) = \frac{1}{s} |\mathrm{CWT}(\tau, s)|^2. \tag{3.6}$$

Apart from CWT, Meier et al. (2023) applied the wavelet coherence transform (WCT), a cross-correlation between two wavelet spectra. It reveals where the two time series have similar frequencies and how their phases are related (Grinsted et al., 2004), indicating whether one of the variables is driving the other.

3.6 CMIP6 Single-Model Initial-condition Large Ensembles

The study of Barghorn et al. (2025a) utilizes so-called Single-Model Initial-condition Large Ensembles (short SMILEs) (e.g., Deser, 2020). As the name suggests, such ensembles consist of model runs that are identical except for the initial conditions. Due to the chaotic nature of the climate system, even tiny changes in the initial conditions will lead to large differences in the internal variability (Lorenz, 1963). If the ensemble is large enough, its members can cover the whole range of possible realizations of internal variability (Olonschek et al., 2023). At the same time, the climate system also responds to external forcing, for instance from anthropogenic greenhouse gas or aerosol emissions or from natural sources like changing solar activity or volcanic eruptions. In contrast to the internal variability, all ensemble members react similarly to the external forcing. Hence, computing the ensemble mean of a certain climate variable will extract its externally forced contribution while the residuals reflect the internal variability. This robust separation of internal variability and externally forced climate response is a large benefit of SMILEs. A number of studies have used them for that purpose, for instance Selten et al. (2004), Branstator & Selten (2009), Deser et al. (2020), Lehner et al. (2020), Wills et al. (2020), Deser & Phillips (2021), and Qin et al. (2022).

Barghorn et al. (2025a) employed two SMILEs with CMIP6 forcing (Eyring et al., 2016) to disentangle internal and externally forced components of the AMV: A 50-member ensemble of the Max Planck Institute Earth System Model (MPI-ESM) (Olonschek et al., 2023) and a 100-member ensemble of the

Community Earth System Model (CESM) (Rodgers et al., 2021). Both models cover the historical period (1850-2014) and one or several shared socioeconomic pathway (SSP) scenarios (2015-2100) (Riahi et al., 2017). In case of MPI-ESM, four scenarios ranging from low to very high emission scenarios were analyzed (SSP126, SSP245, SSP370, and SSP585) while the CESM ensemble was only run for SSP370. For the MPI-ESM ensemble, the low resolution model version 1.2 was used (Mauritsen et al., 2019). It resolves the atmosphere at about 1.8 ° and the ocean on a so-called GR 15 grid with an approximate horizontal resolution of 1.5 ° and 40 vertical levels. The GR 15 grid has a relatively high resolution in the North Atlantic (Jungclaus et al., 2013). In case of the CESM ensemble, CESM version 2 was employed (Danabasoglu et al., 2020). Its atmospheric resolution amounts to 0.9 ° in latitude and 1.25 ° in longitude. In the ocean, the longitudes are resolved at 1.125 ° while the latitudinal resolution increases towards the equator reaching a maximum resolution of 0.25 ° (Rodgers et al., 2021). Both ensembles were constructed by initializing the members with different states from preindustrial control simulations (Olonschek et al., 2023, Rodgers et al., 2021). Although both models underestimate the magnitude of the AMV (Bonnet et al., 2024), they have shown reasonable performance in various studies dealing with the climate variability of the North Atlantic region (Deser et al., 2017, Wills et al., 2019, Mann et al., 2020, Deser & Phillips, 2021, Qin et al., 2022, Coburn & Pryor, 2023, Zanchettin et al., 2023, Palmer et al., 2023, Gu et al., 2024).

3.7 AMV definition

In the literature, several AMV definitions can be found. They mainly differ in the way how the AMV is separated from forced temperature trends. The simplest way would be to compute the area-weighted North Atlantic average of sea surface temperature anomalies (SSTAs) and linearly detrend the resulting time series (Enfield et al., 2001). Börgel et al. (2023a) have shown that simple detrending does not suffice to extract the internal variability. Instead, one could subtract the global mean SSTAs from the North Atlantic SSTAs at each time step as suggested by Trenberth & Shea (2006). This would account for the fact that the forced temperature trends are not necessarily uniform over time. According to Deser & Phillips (2021), the Trenberth and Shea method works well for the historical period, but not under the high emission scenario RCP8.5. There, forced trends get too spatially inhomogeneous to be removed with the global average SSTAs. Instead, Deser & Phillips (2021) used the residual method introduced by Ting et al. (2009) where the local SSTAs are regressed onto the global SSTA (GSSTA) at each time step. The resulting regression pattern p is then scaled with the GSSTA and subtracted from the local SSTAs, such that one is left with temperature residuals SSTAres which are decoupled from the GSSTA:

$$\mathrm{SSTAres}(t, x, y) = \mathrm{SSTA}(t, x, y) - p(x, y)\,\mathrm{GSSTA}(t), \tag{3.7}$$

with t denoting time, x longitudes, and y latitudes. Finally, the area-weighted North Atlantic averages of SSTAres are computed to obtain the AMV index:

$$\mathrm{AMV}(t) = \frac{1}{A}\sum_{i,j} \mathrm{SSTAres}(t, x_i, y_j)\,dA_{ij}, \tag{3.8}$$

where A is the area of the North Atlantic domain as defined below and dA is the weight of the respective grid cell.

Barghorn et al. (2025a) applied the residual method using annual mean SSTAs which were interpolated onto a 1 ° latitude-longitude grid beforehand and smoothed by a Butterworth lowpass filter with a cut-off of 10 years. As described in Robson et al. (2023), the total AMV of a given ensemble member can be expressed as the sum of internal and forced AMV. The total AMV of that ensemble member is retrieved from its SSTAs, the forced AMV (fAMV) from the ensemble mean SSTAs and the internal AMV (iAMV) from the differences between the individual SSTAs and the ensemble mean SSTAs. The global mean SSTAs are computed as the area-weighted averaged SSTAs between 60 °N and 60 °S and the North Atlantic domain (see Figure 4.12) is set between 0 °N and 60 °N and between 80 °W and 0 °W (Trenberth & Shea, 2006). The high latitudes are excluded to avoid possible effects of changes in sea ice (Trenberth & Shea, 2006).

4 Results

4.1 Changes in seasonality of saltwater inflows caused exceptional warming trends in the western Baltic Sea

The Baltic Sea is one of the fastest warming seas in the world (Belkin, 2009). In general, increasing air temperatures due to climate change lead to a heating of the sea surface first, and with time, the heat is transferred downwards (Meier et al., 2022b). However, in some parts of the Baltic Sea, the deep water layers experience a stronger warming trend than the surface (Dutheil et al., 2022). This holds especially for the Bornholm Basin, where the bottom layers have warmed about twice as much as the surface since 1850 (Dutheil et al., 2022, Kniebusch et al., 2019a). Since the temperature in those water layers is largely controlled by lateral advection via saltwater inflows, it was assumed that a shift in inflow seasonality towards more warm summer and early autumn inflows caused this exceptional warming (Mohrholz et al., 2006, Meier et al., 2006). By analyzing a more than 150 years long time series of saltwater inflows from a model hindcast (Radtke et al., 2020), Barghorn et al. (2023) could for the first time prove the existence of a shift in inflow seasonality and its impact on the deep water temperatures in the Bornholm Basin. Based on sensitivity experiments and composites of wind fields, it was proposed that changes in the seasonality of river runoff and wind contributed to the shift in inflow seasonality.

4.1.1 Analyzing saltwater inflow time series

The reference simulation, which runs from 1850 until 2008, was performed by Radtke et al. (2020) using a 1 nm GETM setup (Section 3.1.1). For the inflow time series, the daily salt transport over transects at the Darss and Drogden sills (Figure 3.1) was assembled. Thresholds for minimum salinity and inflow size were defined to distinguish between saltwater inflows and ambient water masses (Section 3.2.1). Summer (June - August; JJA) and early autumn (September - October; SO) averages of salt import were compared to the annual mean salt import to detect shifts in seasonality. The resulting smoothed time series are

displayed in panel (a) of Figure 4.1. Linear trends show that the summer and early autumn salt import increased more strongly over the model period (trends are significant with p-values below 0.05) than the annual salt import. However, due to shortcomings in the model forcing before 1920, the focus was put on the period from 1920 onward. Here, the early autumn salt import increased significantly while the summer salt import decreased slightly.

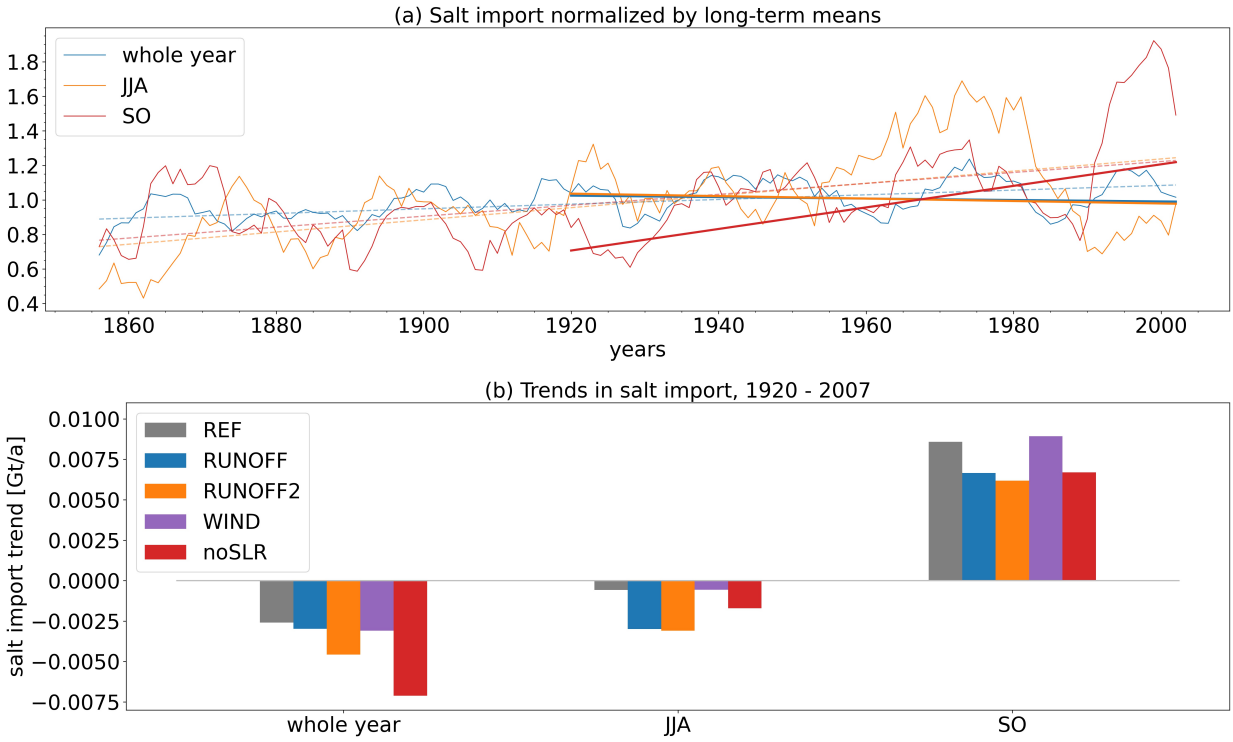

Figure 4.1: (a) Time series of normalized annual, summer (June - August; JJA), and early autumn (September - October; SO) salt import (Barghorn et al., 2023). All curves were smoothed by 11-year running means. Linear trends from 1851 and 1920 onward are denoted by dashed and solid lines, respectively. (b) Trends in annual, JJA, and SO salt import from 1920 onward for the reference simulation (REF) and the sensitivity experiments RUNOFF, RUNOFF2, WIND, and noSLR (see Table 3.2).

4.1.2 Connection to the exceptional warming in the Bornholm Basin

Observational studies indicate that warm inflows cause temperature maxima in or below the halocline in the Bornholm Basin (Feistel et al., 2004, Mohrholz et al., 2006). Hence, the summer and early autumn salt import was compared to the annual temperature maximum (T_{max}) below the seasonal thermocline at station BY5 (see Figure 3.1 for the location) in the Bornholm Basin. Smoothed time series are depicted in Figure 4.2. Both curves exhibit the same multidecadal variability, in particular from about 1920 onward. The Pearson correlation coefficient computed for the annual mean time series since 1920 amounts to 0.55. This implies that the shift in inflow seasonality was a major driver of the exceptional warming in the deep water layers of the Bornholm Basin.

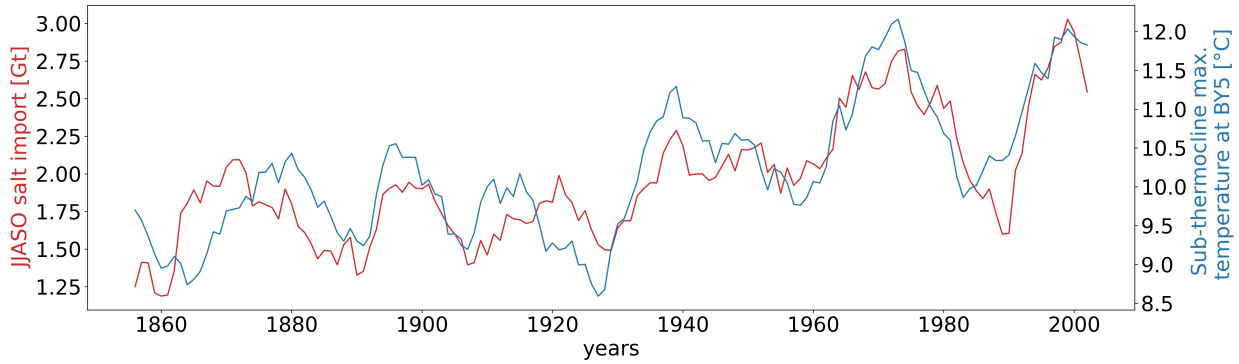

Figure 4.2: 11-year running means of June - October (JJASO) salt import and the annual temperature maximum below the summer thermocline at station BY5 in the Bornholm Basin (see Figure 3.1 for the location) (Barghorn et al., 2023).

4.1.3 Causes of the shift in inflow seasonality

To explore the causes behind the changes in inflow seasonality, sensitivity experiments with manipulated drivers of the salinity dynamics were conducted (Section 3.1.5). Resulting trends of the annual and seasonal salt import are shown in panel (b) in Figure 4.1. It was found that switching off the global mean sea level rise (experiment noSLR) leads to less positive / more negative salt import trends in all seasons. This makes sense since the rising sea level leads to a larger cross section of the Danish straits and thus to larger inflows (Meier et al., 2017, Saraiva et al., 2019, Meier et al., 2021). The experiment with high-pass filtered wind and sea level height at the open boundaries of the model domain (WIND) yielded similar trends as the reference simulation (REF). Finally, both experiments with manipulated runoff showed more negative / less positive seasonal trends while the annual trends are comparable to that of REF. Hence, a shift in runoff seasonality seems to have contributed to the shift in inflow seasonality.

It is known that there has been a shift towards more winter and early spring and less summer runoff during the 20th century due to river regulations and climate-change related shifts in precipitation patterns (Meier & Kauker, 2003, Meier et al., 2022b). Since river runoff alters the sea level of the Baltic Sea, it presumably affects barotropic inflows (Schinke & Matthäus, 1998), although there is no mechanistic explanation for that connection so far. Figure 4.3 shows that the early autumn sea level gradient across the Danish straits is at its minimum roughly when the early autumn salt import reaches its maximum. Thus, there could indeed be a link between runoff and inflow seasonalities.

As previously mentioned, no significant differences were observed between REF and WIND. However, inflows are mainly influenced by high-frequency variations in wind which were still present in WIND. Therefore, the effect of wind changes on the inflow seasonality was reconsidered by computing composites of seasonal averages of the 3rd power of wind speed (a measure of energy input into the ocean) from the model forcing for two 30-year periods, respectively; one with high salt import (1975-2005 for SO and 1960-1990 for JJA) and one with low salt import (1920-1950 for both seasons). Figure 4.4 shows that the 3rd power of wind speed was lower in times of high salt import in case of summer but higher in case of autumn. This indicates that in summer, calm periods favoring baroclinic inflows increased, while in early autumn, gale conditions favoring barotropic inflows increased, although the differences between the

composites are in both cases not significant.

To summarize, the study reveals a shift in saltwater inflow seasonality towards more warm summer and early autumn inflows over the model period. As a consequence, the temperatures in the deep layers of the Bornholm Basin increased more strongly than in the rest of the Baltic Sea. Both runoff and wind changes seem to have contributed to the shift in inflow seasonality, but their role should be further investigated in upcoming studies.

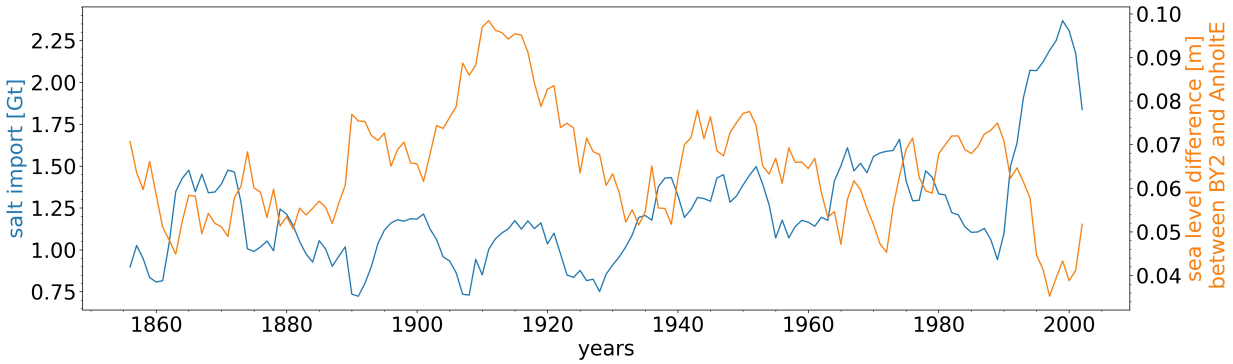

Figure 4.3: 11-year running means of September - October (SO) salt import and sea level difference between the stations BY2 in the Arkona Basin and AnholtE in the Kattegat (see Figure 2.1 for the locations) (Barghorn et al., 2023).

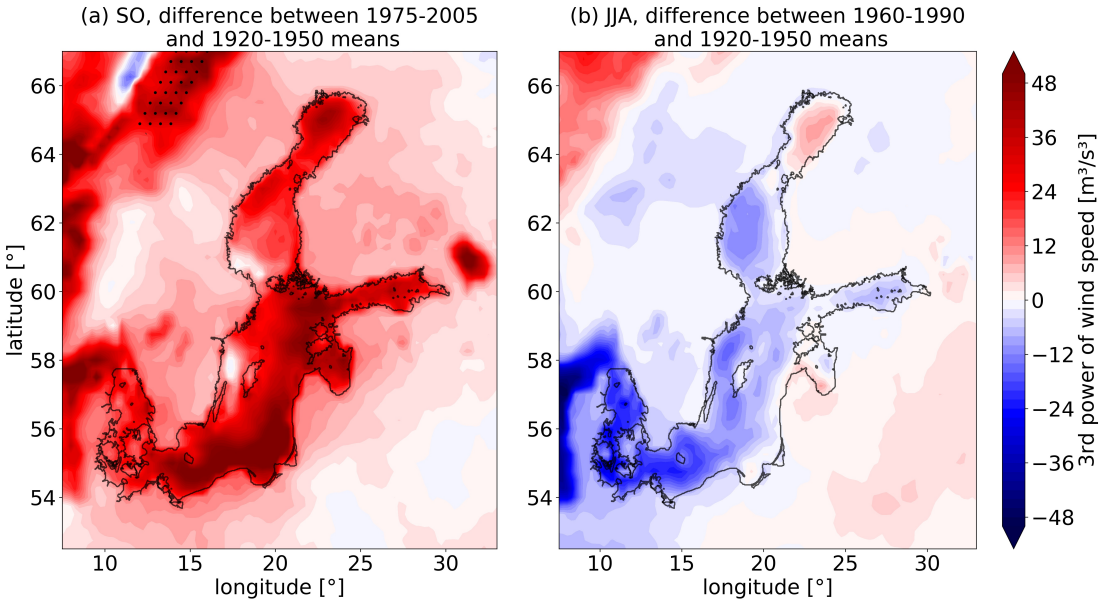

Figure 4.4: Differences in 3rd power of wind speed between 30-year periods with very high (1975-2005 / 1960-1990) and very low (1920-1950) seasonal salt import. Black dots indicate significant differences based on a Student's t test with a significance level of 0.95. (a) for September-October (SO) means, (b) for June - August (JJA) means. Black lines show the GETM domain, i.e., the coastlines and the open boundary in the Kattegat (Barghorn et al., 2023).

4.2 Warm saltwater inflows strengthen oxygen depletion in the western Baltic Sea

The exceptional warming of deep water layers in the Bornholm Basin analyzed in Barghorn et al. (2023) could have severe consequences for the ecosystem, as higher bottom temperatures in the Baltic Sea are in general connected to lower oxygen concentrations via an enhanced mineralization rate (Krapf et al., 2022, Börgel et al., 2023b). In addition, the oxygen solubility in warmer water is lower (e.g., Meier et al., 2011). Since the 1950s, the Baltic Sea received very high nutrient loads from anthropogenic sources and developed one of the largest hypoxic areas worldwide (Gustafsson et al., 2012, Carstensen et al., 2014, Almroth-Rosell et al., 2021, Krapf et al., 2022).

To explore the impact of the inflow-driven warming on the oxygen conditions in the Bornholm Basin, the results of Barghorn et al. (2023), which were obtained with GETM, were compared to similar hindcasts performed with the models RCO and MOM (Barghorn et al., 2025b). Unlike the GETM setup, both models were coupled to biogeochemical models and thus provide information on oxygen concentrations (see Section 3.1.1 for the model descriptions). The study confirms that the temperature maxima caused by warm inflows deteriorated the oxygen conditions in the Bornholm Basin.

4.2.1 Model comparison

Barghorn et al. (2025b) used the salt content in water masses with a minimum salinity of 17 g/kg in the Arkona Basin (S_{17}) as a measure for salt import (see Section 3.2.2). All three models yield very similar time series for annual, summer, and early autumn means of S_{17}. In addition, the trends in S_{17} in the sensitivity experiments confirm the dependency of salt import on river runoff and sea level described in Barghorn et al. (2023). The relation between S_{17} and T_{max} was again comparable for all models. Results are visualized in the Supplements of Barghorn et al. (2025b).

4.2.2 Disentangling the drivers of the exceptional warming

To distinguish the contributions of global warming and the shift in inflow seasonality to the exceptional warming in the Bornholm Basin, an RCO experiment without trends in atmospheric temperatures (TAIR) was compared to the reference simulation (REF). Figure 4.5 shows that the trend in T_{max} in TAIR is almost as high as in REF and that the correlation between T_{max} and summer and early autumn S_{17} is even higher than that of REF (the latter being displayed in Figure 3 of Barghorn et al. (2025b)). Hence, the exceptional warming in the Bornholm Basin was mainly caused by the shift in inflow seasonality, but global warming strengthened it further.

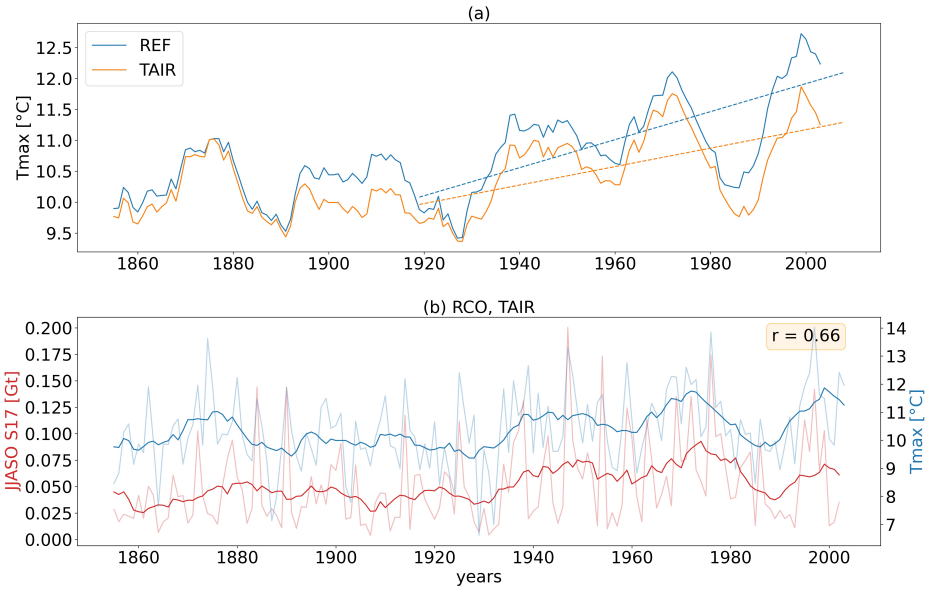

Figure 4.5: (a) 11-year running means of T_{max} for the reference simulation (REF) and the sensitivity experiment (TAIR) of RCO. Linear trends from 1920 onward are indicated by the dashed lines. (b) June - October (JJASO) means of S_{17} versus T_{max} for TAIR. Bold lines depict 11-year running means. The Pearson correlation coefficient, computed from 1920 onward for the non-smoothed time series, is given in the yellow box (Barghorn et al., 2025b).

4.2.3 Consequences of warm inflows for the oxygen concentrations

Since saltwater inflows interleave in or below the halocline in the Bornholm Basin (Mohrholz et al., 2006), averages of temperature and oxygen concentration below 60 m (T_{60} and DO_{60}) were compared to investigate the impact of inflow-driven warming on the oxygen conditions. The resulting time series are highly anticorrelated for both MOM and RCO (not shown). Additionally, a composite plot was produced to extract differences in T_{60} and the annual minimum of dissolved oxygen (DO_{min}) at station BY5 between years with very high ($\geq$ 90th percentile) and very low ($\leq$ 10th percentile) JJASO means of S_{17}. All time series were detrended beforehand. As Figure 4.6 shows, high JJASO means of S_{17} coincide with higher T_{60} and lower DO_{min}, in particular for the lag-1 case where T_{60} and DO_{min} were taken from the year following the extreme value in JJASO mean S_{17}. Those results indicate that the oxygen conditions can be substantially deteriorated due to the inflow-driven warming.

As mentioned earlier, there are two possible explanations for this finding: the lower oxygen solubility of and the higher oxygen consumption in warmer water. Both mechanisms were investigated by analyzing temperatures and oxygen dynamics in the Bornholm Basin below 60 m before, during, and after large warm inflows. For that purpose, oxygen sources and sinks were determined as described in Section 3.3. As an example, the inflow in autumn 1997 is analyzed in Figure 4.7. The upper panel shows that temperatures and oxygen content are highly anticorrelated, indicating that the temperature-dependence of oxygen solubility had a large effect. In the bottom panel, oxygen supply and consumption by physical processes and biochemical processes in the water column and sediments are depicted. Here, oxygen con-

sumption in the sediments increases notably at the onset of the warm inflow. The cumulative effect of elevated sedimentary oxygen consumption during and after the inflow is comparable in terms of magnitude to the effect of the decreased oxygen solubility. Similar results were obtained for other large warm inflows (see Supplements of Barghorn et al. (2025b)).

Several studies have shown that intermittent oxygen deficiency can severely affect benthic organisms and also higher trophic levels (Conley et al., 2009, Carstensen et al., 2014, Casini et al., 2016, Limburg & Casini, 2018). This work identifies a new cause of oxygen deficiency in the Bornholm Basin and therefore highlights the relevance of further studies on the biogeochemistry and ecology in that area.

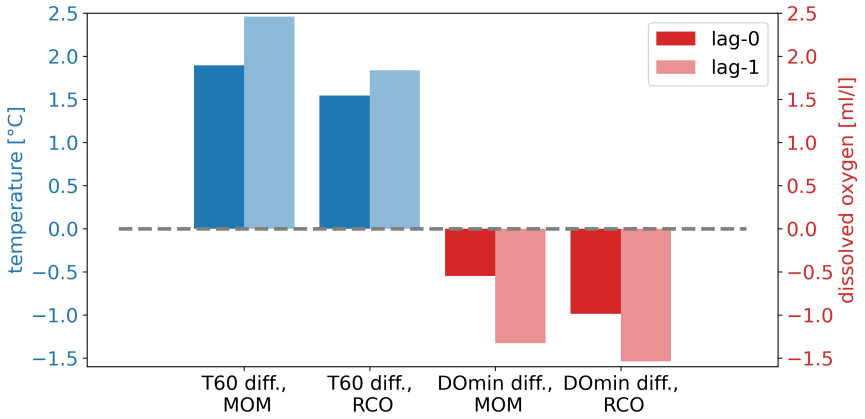

Figure 4.6: Differences in T_{60} and the annual minimum of dissolved oxygen (DO_{min}) at station BY5 between years with very high ($\geq$ 90th percentile) and very low ($\leq$ 10th percentile) JJASO means of S_{17} in the reference simulations of RCO and MOM (Barghorn et al., 2025b). "lag-1" indicates that T_{60} and DO_{min} were taken from the year following the extreme JJASO mean S_{17}.

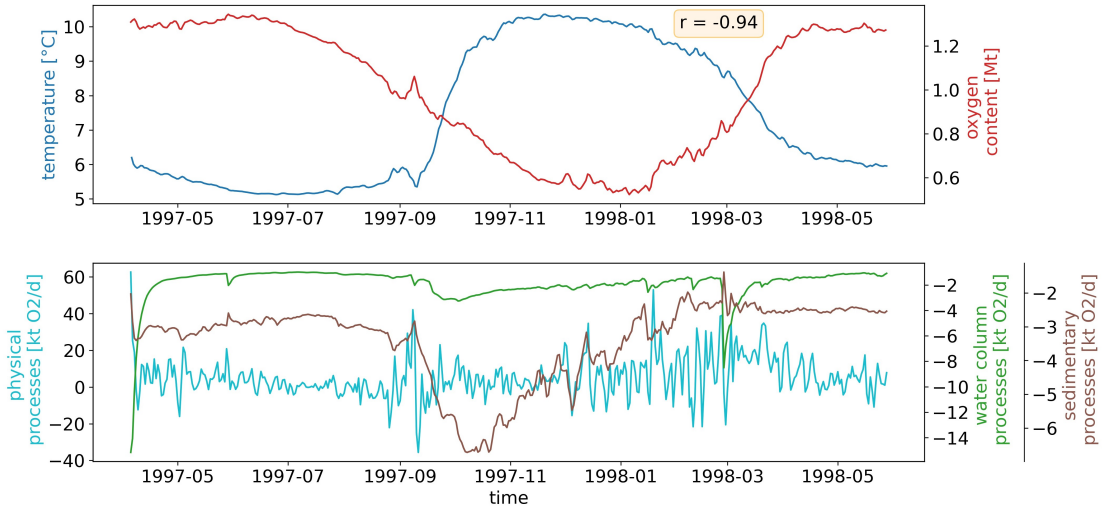

Figure 4.7: Top panel: Oxygen content and temperatures below 60 m in the Bornholm Basin before, during, and after the warm saltwater inflow in autumn 1997. Their Pearson correlation coefficient is given in the yellow box. Bottom panel: Terms of the oxygen budget. Negative values denote oxygen sinks and positive values denote oxygen sources (Barghorn et al., 2025b).

4.3 Multidecadal climate variability dominated past trends in the water balance of the Baltic Sea watershed

The studies described in the previous sections focused on long-term changes in saltwater inflows, rather than their pronounced multidecadal variability. It has been known for some decades already that the water cycle of the Baltic Sea is characterized by such a multidecadal variability with a period length of about 30 years, matching the residence time of freshwater in the Baltic Sea (Winsor et al., 2001, Meier & Kauker, 2003, Schimanke & Meier, 2016, Mohrholz, 2018b, Lehmann et al., 2022). However, there were still open questions regarding the causes of that multidecadal variability and the relations between the salinity of the Baltic Sea and its different drivers. The study by Meier et al. (2023), which is summarized in the following, reveals how an interplay between AMV and NAO (both introduced in Section 2.1) drives multidecadal variations in the water cycle of the Baltic Sea. Moreover, a feedback mechanism between river runoff and salt import is identified.

4.3.1 The origin of the multidecadal variability

Figure 4.8 depicts the results of a wavelet analysis that was applied to a time series of the average salinity of the Baltic Sea retrieved from the previously described RCO hindcast. The local wavelet power spectrum in panel b) shows that the 30-year variability is significant from about 1920 onward and the global wavelet power spectrum in panel c) confirms that it is the only period length with significant power over the course of the time series.

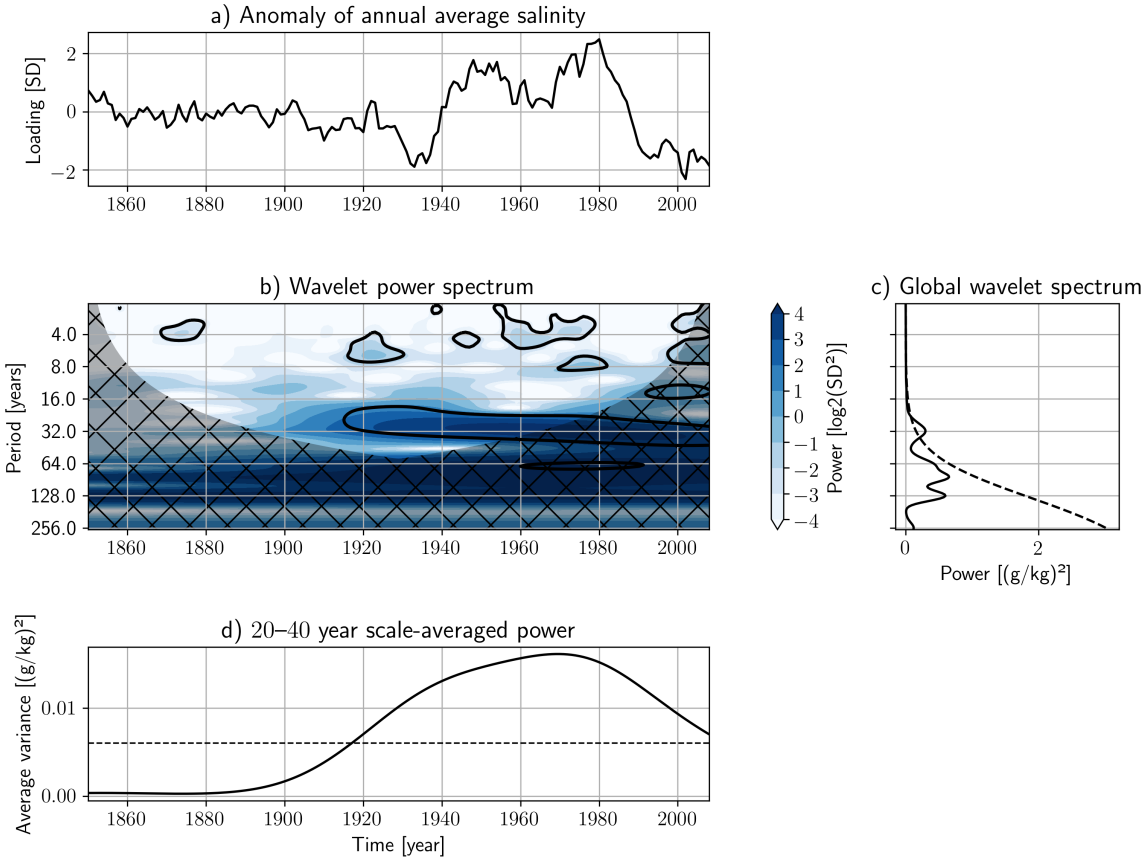

Figure 4.8: Wavelet analysis of annual mean salinity averaged over the Baltic Sea from the RCO reference simulation with sea level rise (REF+, see Table 3.2). a) Detrended and normalized time series, b) local wavelet power spectrum, c) global wavelet power spectrum retrieved by averaging the local spectrum in time, d) wavelet power in the band of 20–40 years. Black contours in b) and dashed lines in c) and d) denote significant power based on a significance level of 0.95 according to Grinsted et al. (2004). The hatched area in b) indicates the cone of influence (Meier et al., 2023).

Earlier studies have already indicated that the water cycle of the Baltic Sea is substantially affected by the North Atlantic, in particular by NAO and AMV (e.g., Börgel et al., 2018, 2020). The AMV has a quite long period length of 60–90 years. The wavelet power spectrum of the NAO index (panels b) and c) in Figure 4.9) reveals that the NAO also shows significant power in that frequency band, although it lies inside the cone of influence which is affected by the edges of the time series. This seems reasonable, as the AMV modulates the location of the centers of action of the NAO (Börgel et al., 2020) and hence also the NAO index. It was argued that the superposition of signals from the AMV itself and the NAO centers' displacement, both with a periodicity of about 60 years, leads to a resulting signal with a period length of about 30 years.

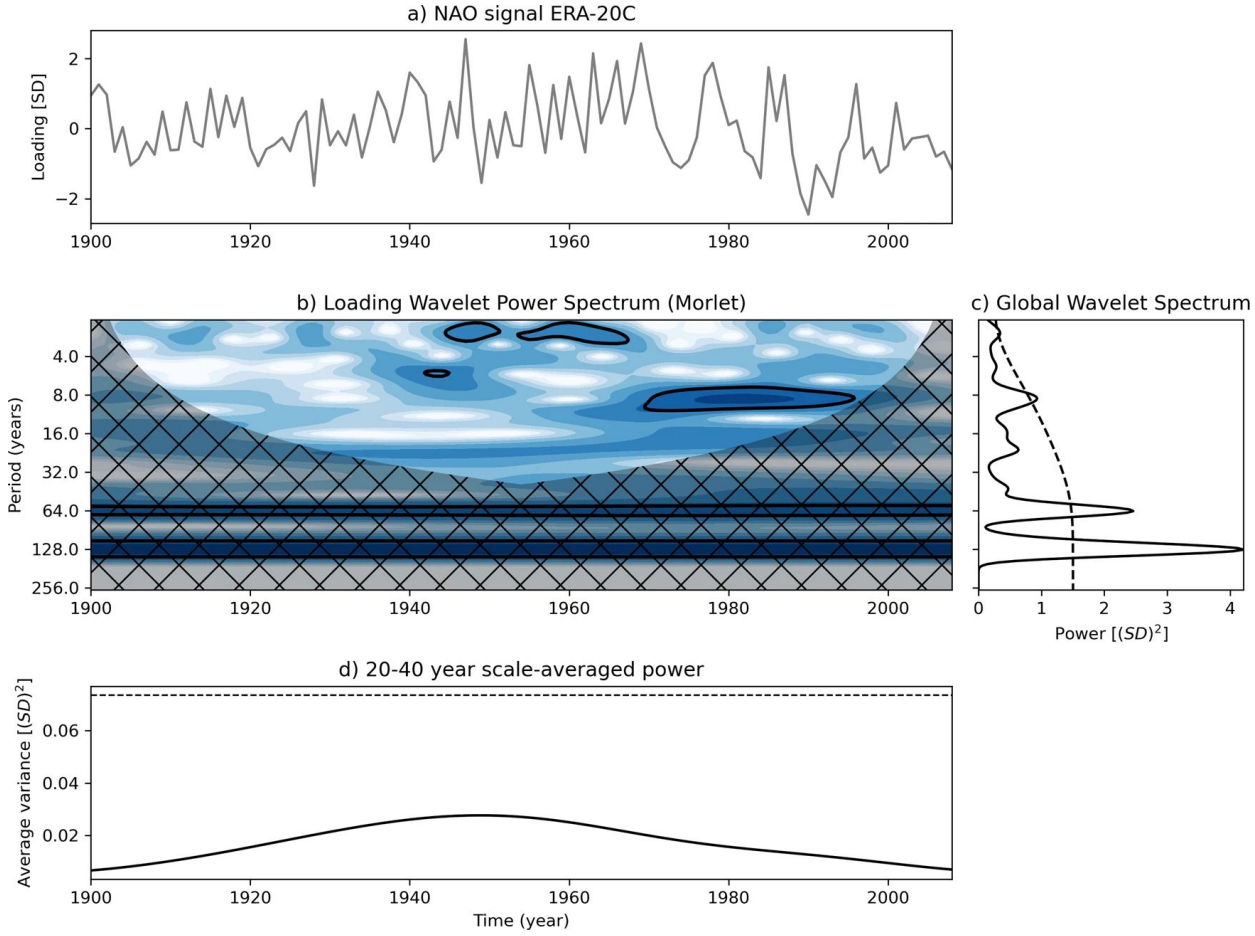

Figure 4.9: Wavelet analysis with similar panels as in Figure 4.8, but for the NAO index (Meier et al., 2023).

4.3.2 Impact of river runoff and wind on the salinity dynamics

It is known that variations in river runoff account for about 50 % of the multidecadal variability in the mean salinity of the Baltic Sea (Meier & Kauker, 2003). Thereof, about half can be explained by the direct dilution of the freshwater (Radtke et al., 2020). So far, there was no sound explanation for the other half. The wavelet coherence spectrum of the annual mean runoff and large inflows (Figure 4.10) shows that not only runoff and salinity, but also runoff and salt import co-vary on a multidecadal time scale, where maxima in river runoff are followed by minima in salt import. Composite plots of surface and bottom salinity differences between the reference simulation (REF+) and the sensitivity experiment with climatological runoff (RUNOFF+) after a freshwater maximum or minimum in REF+ (Figure 4.11, Panels a) - d)) reveal the underlying mechanism: More freshwater input leads to a less saline outflow in the Danish straits. As parts of the outflowing water mix into subsequent saltwater inflows, those inflows also get less saline. This process seems to explain most of the remaining half of the impact of river runoff variations on the multidecadal salinity variability.

In contrast to river runoff, low-frequency variations of wind and sea level only have a minor effect on

the multidecadal variability of mean salinity. This was concluded from a sensitivity experiment where, in addition to climatological runoff, the wind of the year 1904 (and hence also the sea level variation) was repeated for each year of the simulation. Only in longer periods with predominantly westerly winds, the Baltic Sea is filled up to the point that no further inflows can reach the central basins. This is reflected in the panels e) and f) of Figure 4.11, where a period with mostly positive NAO indices (i.e., a lot of westerly winds) is compared to a period of mostly negative NAO indices for the RUNOFF+ experiment.

To conclude, this study advances the understanding of the multidecadal variability in the water cycle of the Baltic Sea. It provides an explanation for the dominance of the 30-year periodicity and new insights concerning the effects of river runoff on the salinity dynamics. Since many species in the Baltic Sea rely on specific salinity ranges (Vuorinen et al., 2015), understanding the long-term development of salinity dynamics is of high importance.

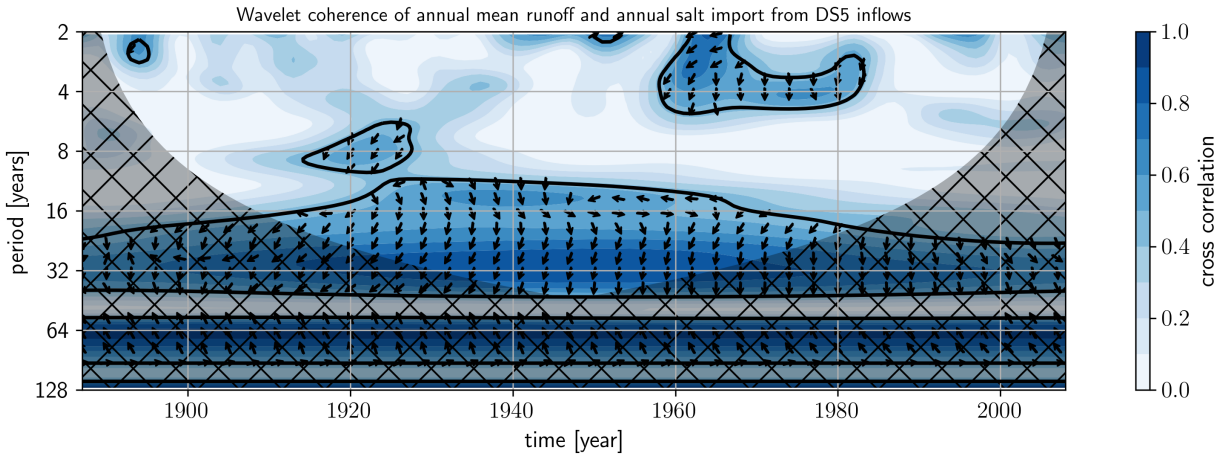

Figure 4.10: Wavelet coherence power spectrum of annual mean river runoff and salt import from the DS5 inflow series by Mohrholz (2018a) (Meier et al., 2023). Again, the black lines denote the 0.95 significance level (Grinsted et al., 2004). The phase relation between the two time series is given by the black arrows: Arrows pointing left stand for anti-phase, and arrows pointing right for in-phase. Arrows pointing up indicate that river runoff is lagging while arrows pointing down indicate that runoff is leading.

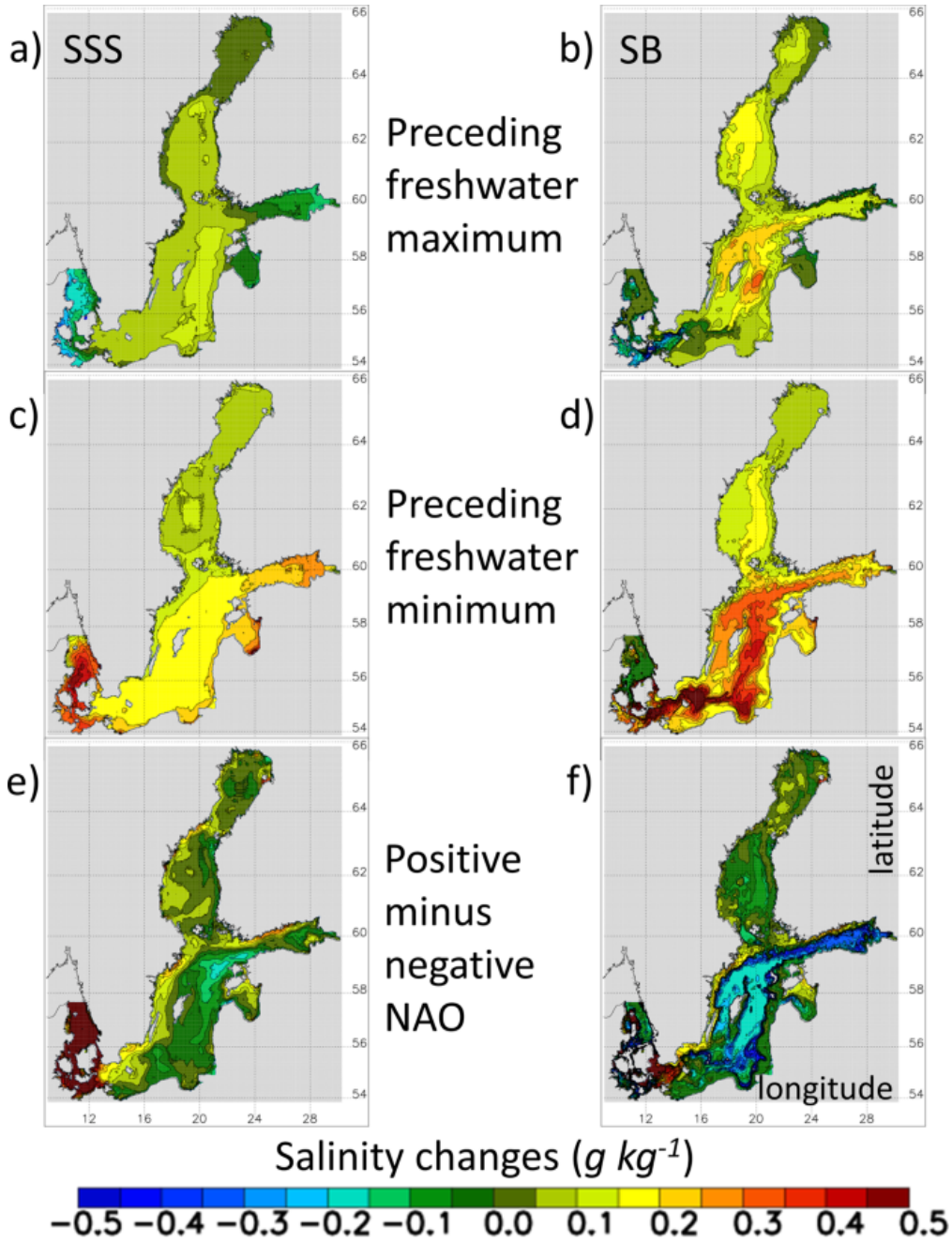

Figure 4.11: Composites of autumn and winter (September - February) average sea surface salinity (SSS, left panel) and bottom salinity (SB, right panel) (Meier et al., 2023). a) and b): Difference in salinity between the experiments REF+ and RUNOFF+ averaged over years with a preceding freshwater maximum (1924–1934, 1951–1962, and 1980–1992). c) and d): As a) and b) but for years with a preceding freshwater minimum (1935–1950 and 1963–1979). e) and f): Winter (December - February) SSS and SB in RUNOFF+; differences between a period with mainly positive NAO indices (1986–1997) and one with mainly negative NAO indices (1957–1982).

4.4 Atlantic Multidecadal Variability control on European seas is mainly externally forced

Like Meier et al. (2023), Barghorn et al. (2025a) examined aspects of the teleconnections between the North Atlantic and the Baltic Sea. This time, the main climate variable was sea surface temperature (SST) and how it is affected by the AMV. There have already been several studies exploring that connection for SSTs (Kniebusch et al., 2019a, Börgel et al., 2020, 2023a), but they focused on the historical period or the last millennium; not on future scenarios. In addition, they relied on single simulations which means they could not distinguish between externally forced and internal contributions to the AMV whose co-existence seems plausible based on a number of studies (e.g., Zhang et al., 2019, Wills et al., 2019, Mann et al., 2020, 2021, Qin et al., 2022, Robson et al., 2023). Barghorn et al. (2025a) instead employed CMIP6 forced historical and scenario simulations of two SMILEs. As described in Section 3.6, members of such ensembles only differ in their initial conditions which allows to separate internal and externally forced contributions to modes of climate variability. Here, SST patterns and time series of internal AMV (iAMV) and forced AMV (fAMV) (see definitions in Section 3.7), as well as forced trends, i.e., trends of ensemble mean SSTs, were computed and analyzed regarding their importance for the Baltic Sea. The same was done for other semi-enclosed European seas, namely the North Sea, Mediterranean Sea, and Black Sea (see Figure 4.12 for the basin boundaries) whose similarities and differences compared to the Baltic Sea will briefly be summarized in the last part of this section. Similarly, only results obtained with the MPI-ESM ensemble are depicted here. A comparison with the CESM2 large ensemble is provided in Barghorn et al. (2025a).

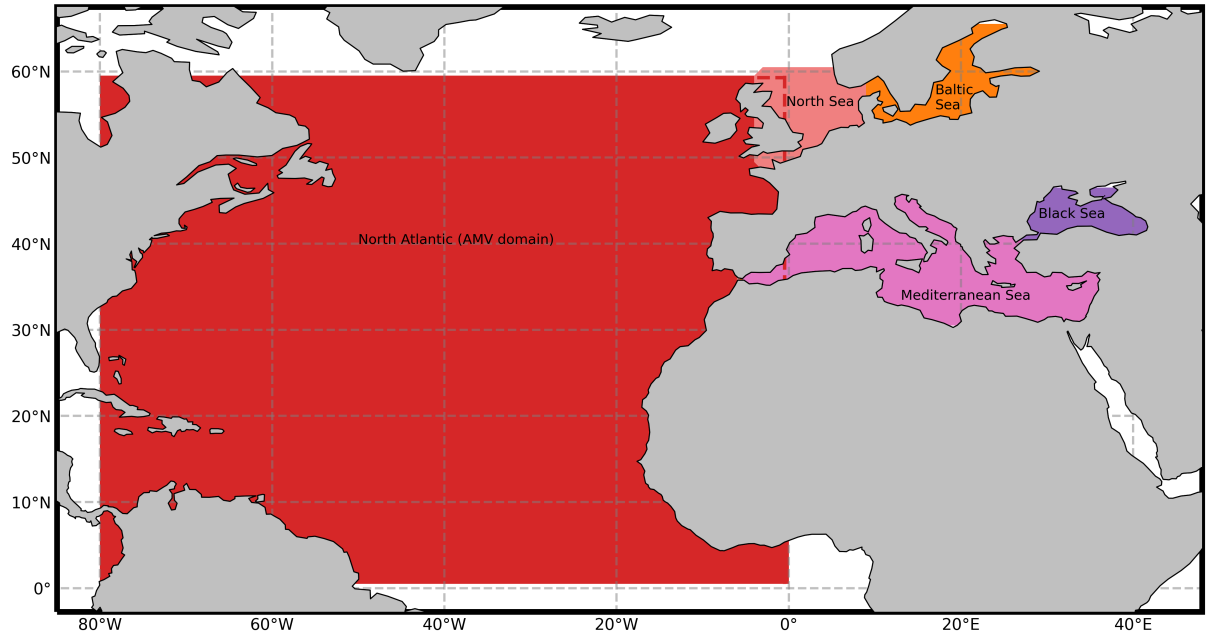

Figure 4.12: Boundaries of the four European seas discussed in Barghorn et al. (2025a) as well as the domain used for the computation of the AMV indices (Barghorn et al., 2025a).

4.4.1 AMV patterns

Figure 4.13 shows the regression patterns of residual SST anomalies (SSTAres) for the different AMV components and the forced local, i.e., local minus global, SST trends. They were computed for the historical period (1880-2020) and the scenario period (1950-2090). The choice of the time ranges is explained in Barghorn et al. (2025a). The iAMV patterns are quite similar for the historical period and all scenarios and comparable to AMV patterns in the literature (e.g., Zhang et al., 2019). In Europe, the effect of the iAMV seems to decrease with increasing distance from the North Atlantic. Hence, the patterns are rather weak in the Baltic Sea. Contrary to that, the fAMV patterns are quite strong in the Baltic Sea and the whole northeastern part of the domain. In that respect, they are comparable to the forced local trends, also concerning the increasing pattern intensity across the scenarios. This agrees with the assumption raised by Qin et al. (2022) and Robson et al. (2023) that the fAMV is a response to the anthropogenic greenhouse gas and aerosol forcing.

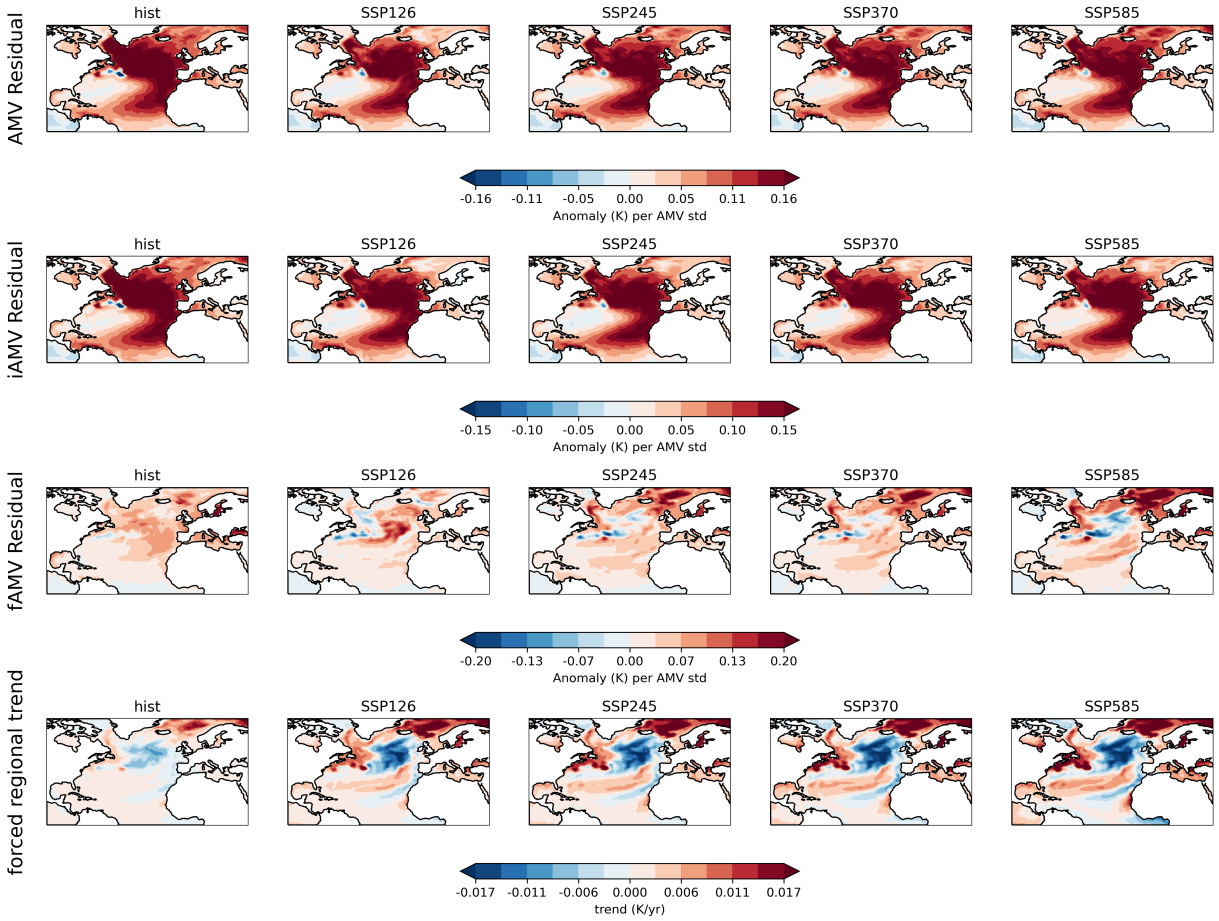

Figure 4.13: SST regression patterns of the total AMV, iAMV, and fAMV plus forced local trends (Barghorn et al., 2025a). All patterns were obtained for the historical period (1880-2020) and the scenarios (1950-2090) with the MPI-ESM ensemble. The AMV patterns were standardized, i.e., multiplied by the standard deviation of the corresponding AMV time series. For total AMV and iAMV, ensemble mean patterns are depicted.

4.4.2 Impact of the AMV on Baltic SSTs

To assess the impact of the AMV on the Baltic SSTs, iAMV-iSSTAres and fAMV-fSSTAres cross correlations were computed (Figure 4.14). The plots show that the maximum correlations with the fAMV are much higher than those with the iAMV (if the ensemble means of the iAMV-iSSTAres cross correlations are considered). In addition, the latter are not at lag-0, but at lag-7, i. e., the Baltic Sea SSTs lead the iAMV by 7 years. Those findings are independent of the time period / scenario considered. The regression patterns of SST, 2m air temperature and sea level pressure at lag-7 (see Figure 6 in Barghorn et al. (2025a)) reveal that an NAO+ phase causes the positive temperature anomalies in the Baltic Sea, as shown in previous studies (Barrier et al., 2014, Wills et al., 2019, Tao et al., 2023, Gröger et al., 2024). At the same time, the NAO drives the AMV and the latter reaches its maximum some years after the NAO maximum (Wills et al., 2019). It seems reasonable that the maximum fAMV-fSSTAres correlation occurs at lag-0 as the fAMV is likely caused by changes in the external forcing which should affect both the North Atlantic and the Baltic Sea at the same time. The implications of these results are remarkable, as they put earlier studies on the AMV and Baltic SSTs, like those by Kniebusch et al. (2019a) and Börgel et al. (2023a), into a new perspective. A substantial part of the supposed impact of the AMV in the historical period was apparently in reality a reaction to external forcing.

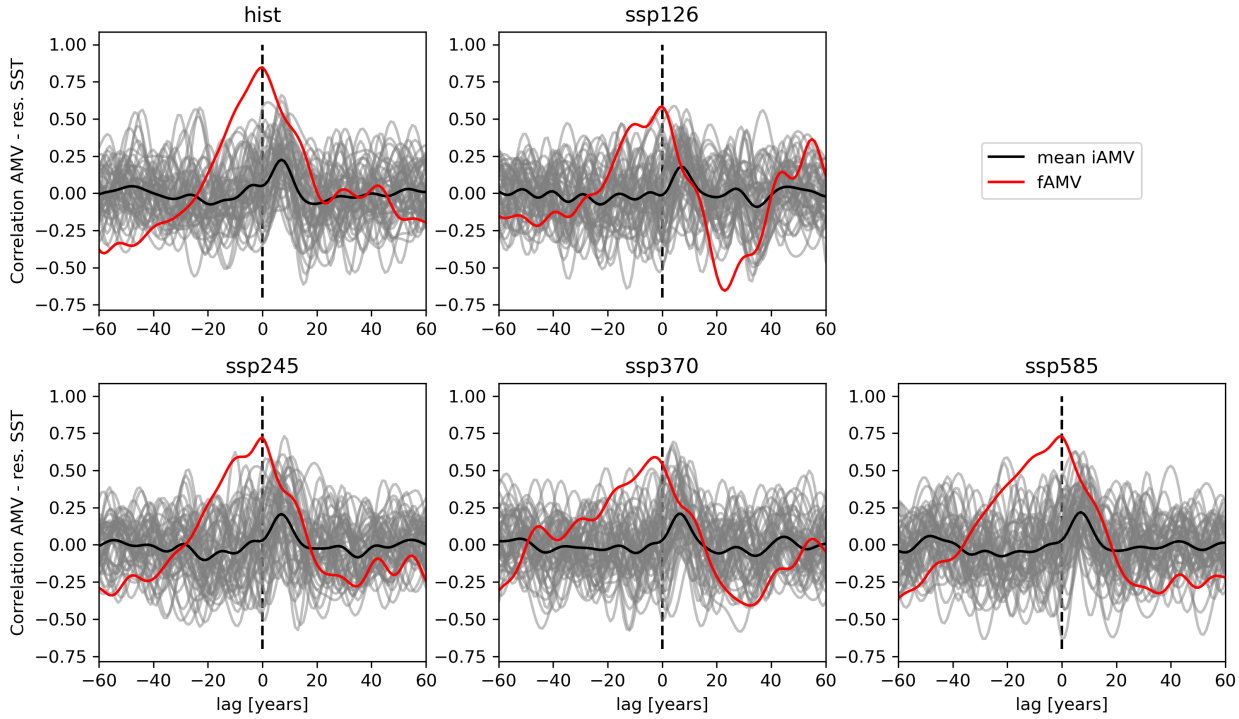

Figure 4.14: Cross correlations between the iAMV / fAMV and the Baltic iSSTAres / fSSTAres for the historical period (1880-2020) and the scenarios (1950-2090) (Barghorn et al., 2025a, mod.). Black lines depict the ensemble means of the iAMV-iSSTAres cross correlations. Positive lags indicate that the local SSTs lead and negative lags indicate a leading AMV.

4.4.3 Comparison with the impact of forced trends

The previous section describes the connections between different AMV components and Baltic SSTs. However, the relative importance of iAMV and fAMV for the Baltic Sea compared to that of forced SST trends still needs to be assessed. Therefore, Barghorn et al. (2025a) constructed time series of "local AMVs" by computing the area-weighted Baltic Sea averages of the non-standardized AMV patterns and multiplying them with the respective AMV time series. Exemplarily for the iAMV:

$$\mathrm{iAMV}_{\mathrm{m}}^{\mathrm{local}}(\mathrm{t}) = \mathrm{iAMV}_{\mathrm{m}}(\mathrm{t}) \cdot \frac{1}{\mathrm{A}} \sum_{\mathrm{i,j}} \mathrm{p}_{\mathrm{m}}(\mathrm{x}_{\mathrm{i}}, \mathrm{y}_{\mathrm{j}})\, \mathrm{dA}_{\mathrm{ij}}, \tag{4.1}$$

where m is the ensemble member (not present in the corresponding fAMV equation), t time, A the area of the Baltic Sea, p the AMV pattern, x longitude, y latitude, and dA the weight of the respective grid cell.

To quantify the importance of the local iAMV and fAMV on an interannual scale, running decadal trends were computed and compared to running decadal trends of the ensemble mean Baltic SSTs, i.e., forced trends (Figure 4.15). For the iAMV, ranges between the 10th and 90th quantiles of the ensemble are displayed. It can be seen that forced trends are mostly larger than AMV trends in the high emission scenarios (SSP370 and SSP585), but not always in the low emission scenarios. Although the ensemble mean iAMV patterns are rather weak in the Baltic Sea (see Figure 4.13), the possible range of decadal local trends evoked by the iAMV is rather large due to the huge spread in the ensemble. This underlines the strength of internal variability in the Baltic Sea.

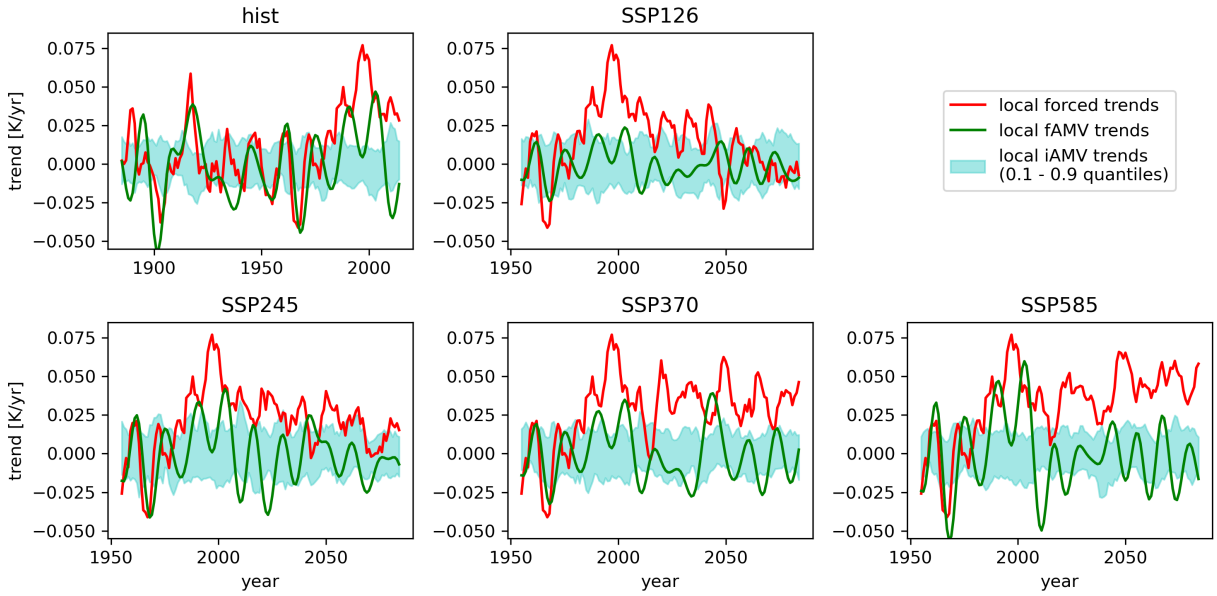

Figure 4.15: Running decadal trends of the "local" fAMV and iAMV compared to running decadal trends of the ensemble mean Baltic SSTs for the historical period (1880-2020) and the scenarios (1950-2090) (Barghorn et al., 2025a, mod.). In case of the iAMV, the ranges between the 10th and 90th quantiles of the ensemble are shown.

4.4.4 Comparison with other semi-enclosed European seas

Barghorn et al. (2025a) found that the fAMV is highly correlated with the basin-averaged fSSTAres at lag-0 also for the other European seas considered in the analysis. However, similar to forced trends, fAMV patterns are slightly less pronounced than in the Baltic in the other European seas, especially in the Mediterranean Sea. In contrast, iAMV patterns are stronger in western than in eastern Europe. The cross correlations in Barghorn et al. (2025a) reveal that both the Mediterranean Sea and the North Sea have the maximum of the ensemble means of the iAMV-iSSTAres correlations at lag-0. Hence, other than the Baltic Sea, they seem to be directly influenced by SST changes in the North Atlantic. Looking at long-term SST trends, they are highest for the Baltic Sea and lowest for the North Sea and the Mediterranean Sea both in the historical period and the scenarios (see Figure 2 in Barghorn et al. (2025a)). Although the ensemble spreads due to internal variability are large, all seas are likely to warm by at least 2 °C in all but the lowest emission scenario (SSP126) until the end of the 21st century compared to 1950. For the Baltic Sea, this also holds in case of SSP126.

5 Discussion and conclusion

This study for the first time identified a long-term change in the seasonal distribution of saltwater inflows into the Baltic Sea and analyzed the consequences of the shift towards more warm summer and early autumn inflows. In that context, it was found that warm inflows contributed substantially to exceptional warming trends and oxygen depletion in the deep layers of the Bornholm Basin (Barghorn et al., 2025b). Both, changes in river runoff and wind seasonality, seem to have contributed to the shift in inflow seasonality (Barghorn et al., 2023). Especially the connection of river runoff and inflow seasonality is novel, as it has been assumed in the past that they cannot be connected due to the decades-long residence time of freshwater in the Baltic Sea (Meier & Kauker, 2003). The third publication in this study (Meier et al., 2023) advances the understanding of Baltic salinity dynamics in general, their connection to large-scale atmospheric and oceanic patterns, and their dependence on the multidecadal variability in runoff, wind and sea level. Finally, the importance of large-scale atmospheric and oceanic patterns was assessed regarding the temperature variability of the Baltic Sea (Barghorn et al., 2025a). For the first time, this was accomplished for different future emission scenarios. In addition, the use of SMILEs allowed for a so far unequaled separation of the internal and externally forced contributions to the teleconnections between the North Atlantic and the Baltic Sea and other European seas. To summarize, this work provides novel insights on possible climate change driven long-term changes on one hand and the natural climate variability of the Baltic Sea on the other hand.

The study has two possible shortcomings. First of all, it is based on model data. Hence, model uncertainties, for example due to limited resolution or model biases, cannot be ruled out. Therefore, several models were used to increase the robustness of the results and the latter were thoroughly validated against observational data and existing literature. Another issue especially in the regional models is the model forcing which reaches far into the past to periods where the available observational data is very scarce. For instance, it is known that the river runoff data for the Baltic Sea is not fully accurate before 1920 (Barghorn et al., 2023). In case of the atmospheric forcing, the years 1958-2007 have served as the refer-

ence period for the analogue method (Schenk & Zorita, 2012). Thus, the forcing of that period is likely to be of higher quality than that of earlier years. However, the results by Barghorn et al. (2023, 2025b) and Meier et al. (2023) are also in general accordance with related earlier (observation-based) studies such as that of Mohrholz et al. (2006) on warm inflows or Winsor et al. (2001) on the connection between outflow and inflow salinity. Similarly, the findings of Barghorn et al. (2025a) are in line with the outcome of other publications (Deser & Phillips, 2021, Qin et al., 2022, Robson et al., 2023).

Unfortunately, the homogeneous atmospheric forcing time series for the regional ocean model runs ends in 2008. Hence, this study does not include the most recent past which has been more and more affected by climate change. Extending the inflow analysis up to the present could be very beneficial as the climate change signal in the investigated variables would probably be more pronounced.

Apart from advancing the understanding of the Baltic Sea climate, this study is also highly relevant for biogeochemical and ecological research because of the essential contribution of warm inflows to increasing deep-water temperatures and oxygen depletion in the Bornholm Basin. Numerous publications deal with the disastrous consequences of hypoxia and anoxia for benthic and pelagic communities in the Baltic Sea (e.g., Conley et al., 2009, Carstensen et al., 2014, Eero et al., 2015, Casini et al., 2016, Limburg & Casini, 2018) and even for species on high trophic levels like the eastern and western Baltic cod (Limburg & Casini, 2019, Receveur et al., 2022). Since hypoxia is a major environmental threat to many coastal seas around the globe, the findings from this study are of interest for other regions as well, in particular for other permanently or seasonally stratified seas with large river runoff like the Chesapeake Bay (Hagy et al., 2004, Ni et al., 2019, Tian et al., 2022).

Future studies should investigate the ecological consequences of the observed changes in the deep layers of the western Baltic Sea due to the shift in inflow seasonality. Further research is also required to quantify the contributions to and to fully understand the underlying mechanisms behind the changes in inflow seasonality. In particular, the role of climate change (as a driver of changes in river runoff and wind fields) for the long-term trends in inflow seasonality is not yet entirely understood. The work presented in Barghorn et al. (2025a) could be greatly advanced by using the global model results to drive a regional ocean model, i.e., by creating regional SMILEs. This would ultimately allow for an in-depth study of past, present, and possible future effects of internal variability and forced trends in the Baltic Sea.

Bibliography

Agha Karimi, A., Bagherbandi, M., & Horemuz, M. (2021). Multidecadal Sea Level Variability in the Baltic Sea and Its Impact on Acceleration Estimations. *Frontiers in Marine Science*, 8, 702512.

Alenius, P., Myrberg, K., & Nekrasov, A. (1998). The physical oceanography of the Gulf of Finland: a review. 3, 97–125.

Almroth-Rosell, E., Wåhlström, I., Hansson, M., Väli, G., Eilola, K., Andersson, P., Viktorsson, L., Hieronymus, M., & Arneborg, L. (2021). A Regime Shift Toward a More Anoxic Environment in a Eutrophic Sea in Northern Europe. *Frontiers in Marine Science*, 8, 799936.

Arneborg, L. (2016). Comment on "Influence of sea level rise on the dynamics of salt inflows in the Baltic Sea" by R. Hordoir, L. Axell, U. Löptien, H. Dietze, and I. Kuznetsov. *Journal of Geophysical Research: Oceans*, 121(3), 2035–2040.

Barghorn, L., Börgel, F., Gröger, M., & Meier, H. E. M. (2025a). Atlantic Multidecadal Variability control on European seas is mainly externally forced. *Environmental Research Letters (under review)*.

Barghorn, L., Meier, H. E. M., & Radtke, H. (2023). Changes in Seasonality of Saltwater Inflows Caused Exceptional Warming Trends in the Western Baltic Sea. *Geophysical Research Letters*, 50(12), e2023GL103853.

Barghorn, L., Meier, H. E. M., Radtke, H., Neumann, T., & Naumov, L. (2025b). Warm saltwater inflows strengthen oxygen depletion in the western Baltic Sea. *Climate Dynamics*, 63, 29.

Barrier, N., Cassou, C., Deshayes, J., & Treguier, A.-M. (2014). Response of North Atlantic Ocean Circulation to Atmospheric Weather Regimes. *Journal of Physical Oceanography*, 44(1), 179–201.

Belkin, I. M. (2009). Rapid warming of Large Marine Ecosystems. *Progress in Oceanography*, 81(1-4), 207–213.

Bergström, S. & Carlsson, B. (1994). River runoff to the Baltic Sea - 1950-1990. *AMBIO*, 23(4-5), 280–287.

Bonnet, R., McKenna, C. M., & Maycock, A. C. (2024). Model spread in multidecadal North Atlantic Oscillation variability connected to stratosphere–troposphere coupling. *Weather and Climate Dynamics*, 5, 913–926.

Branstator, G. & Selten, F. (2009). "Modes of Variability" and Climate Change. *Journal of Climate*, 22(10), 2639–2658.

Brasseur, O. (2001). Development and Application of a Physical Approach to Estimating Wind Gusts. *Monthly Weather Review*, 129(1), 5–25.

Börgel, F. (2020). *Long-term climate variability of the Baltic Sea region*. PhD thesis. Publisher: Universität Rostock.

Börgel, F., Frauen, C., Neumann, T., & Meier, H. E. M. (2020). The Atlantic Multidecadal Oscillation controls the impact of the North Atlantic Oscillation on North European climate. *Environmental Research Letters*, 15(10), 104025.

Börgel, F., Frauen, C., Neumann, T., Schimanke, S., & Meier, H. E. M. (2018). Impact of the Atlantic Multidecadal Oscillation on Baltic Sea Variability. *Geophysical Research Letters*, 45(18), 9880–9888.

Börgel, F., Gröger, M., Meier, H. E. M., Dutheil, C., Radtke, H., & Borchert, L. (2023a). The impact of Atlantic Multidecadal Variability on Baltic Sea temperatures is limited to winter. *npj Climate and Atmospheric Science*, 6(64).

Börgel, F., Neumann, T., Rooze, J., Radtke, H., Barghorn, L., & Meier, H. E. M. (2023b). Deoxygenation of the Baltic Sea during the last millennium. *Frontiers in Marine Science*, 10, 1174039.

Carstensen, J., Conley, D. J., Bonsdorff, E., Gustafsson, B. G., Hietanen, S., Janas, U., Jilbert, T., Maximov, A., Norkko, A., Norkko, J., Reed, D. C., Slomp, C. P., Timmermann, K., & Voss, M. (2014). Hypoxia in the Baltic Sea: Biogeochemical Cycles, Benthic Fauna, and Management. *AMBIO*, 43(1), 26–36.

Casini, M., Käll, F., Hansson, M., Plikshs, M., Baranova, T., Karlsson, O., Lundström, K., Neuenfeldt, S., Gardmark, A., & Hjelm, J. (2016). Hypoxic areas, density-dependence and food limitation drive the body condition of a heavily exploited marine fish predator. *Royal Society Open Science*, 3, 160416.

Coburn, J. & Pryor, S. C. (2023). Evolution of the Internal Climate Modes under Future Warming. *Journal of Climate*, 36(2), 511–529.

Conley, D. J., Björck, S., Bonsdorff, E., Carstensen, J., Destouni, G., Gustafsson, B., Hietanen, S., Kortekaas, M., Kuosa, H., Meier, H. E. M., Müller-Karulis, B., Nordberg, K., Norkko, A., Nürnberg, G., Pitkänen, H., Rabalais, N. N., Slomp, C. P., Voss, M., Wulff, F., & Zillén, L. (2009). Hypoxia-Related Processes in the Baltic Sea. *Environmental Science & Technology*, 43(10).

Coumou, D., Lehmann, J., & Beckmann, J. (2015). The weakening summer circulation in the Northern Hemisphere mid-latitudes. *Science*, 348(6232), 324–327.

Cyberski, J. & Wroblewski, A. (2000). Riverine water inflows and the Baltic Sea water volume 1901-1990. *Hydrol Earth Syst Sci*, 4, 1–11.

Danabasoglu, G., Lamarque, J., Bacmeister, J., Bailey, D. A., DuVivier, A. K., Edwards, J., Emmons, L. K., Fasullo, J., Garcia, R., Gettelman, A., Hannay, C., Holland, M. M., Large, W. G., Lauritzen, P. H., Lawrence, D. M., Lenaerts, J. T. M., Lindsay, K., Lipscomb, W. H., Mills, M. J., Neale, R., Oleson, K. W., Otto-Bliesner, B., Phillips, A. S., Sacks, W., Tilmes, S., Van Kampenhout, L., Vertenstein, M., Bertini, A., Dennis, J., Deser, C., Fischer, C., Fox-Kemper, B., Kay, J. E., Kinnison, D., Kushner, P. J., Larson, V. E., Long, M. C., Mickelson, S., Moore, J. K., Nienhouse, E., Polvani, L., Rasch, P. J., & Strand, W. G. (2020). The Community Earth System Model Version 2 (CESM2). *Journal of Advances in Modeling Earth Systems*, 12(2), e2019MS001916.

Deser, C. (2020). "Certain Uncertainty: The Role of Internal Climate Variability in Projections of Regional Climate Change and Risk Management". *Earth's Future*, 8(12), e2020EF001854.

Deser, C., Hurrell, J. W., & Phillips, A. S. (2017). The role of the North Atlantic Oscillation in European climate projections. *Climate Dynamics*, 49, 3141–3157.

Deser, C., Lehner, F., Rodgers, K. B., Ault, T., Delworth, T. L., DiNezio, P. N., Fiore, A., Frankignoul, C., Fyfe, J. C., Horton, D. E., Kay, J. E., Knutti, R., Lovenduski, N. S., Marotzke, J., McKinnon, K. A., Minobe, S., Randerson, J., Screen, J. A., Simpson, I. R., & Ting, M. (2020). Insights from Earth system model initial-condition large ensembles and future prospects. *Nature Climate Change*, 10(4), 277–286.

Deser, C. & Phillips, A. S. (2021). Defining the Internal Component of Atlantic Multidecadal Variability in a Changing Climate. *Geophysical Research Letters*, 48, e2021GL095023.

Dutheil, C., Meier, H. E. M., Gröger, M., & Börgel, F. (2022). Warming of Baltic Sea water masses since 1850. *Climate Dynamics*, 61, 1311–1331.

Döös, K., Meier, H. E. M., & Döscher, R. (2004). The Baltic haline conveyor belt or the overturning circulation and mixing in the Baltic. *AMBIO: A Journal of the Human Environment*, 33(4-5), 261–266.

Eero, M., Hjelm, J., Behrens, J., Buchmann, K., Cardinale, M., Casini, M., Gasyukov, P., Holmgren, N., Horbowy, J., Hüssy, K., Kirkegaard, E., Kornilovs, G., Krumme, U., Köster, F. W., Oeberst, R., Plikshs, M., Radtke, K., Raid, T., Schmidt, J., Tomczak, M., Vinther, M., Zimmermann, C., & Storr-Paulsen, M. (2015). Eastern Baltic cod in distress: biological changes and challenges for stock assessment. *ICES Journal of Marine Science*, 72, 2180–2186.

Eilola, K., Gustafsson, B., Kuznetsov, I., Meier, H., Neumann, T., & Savchuk, O. (2011). Evaluation of biogeochemical cycles in an ensemble of three state-of-the-art numerical models of the Baltic Sea. *Journal of Marine Systems*, 88(2), 267–284.

Eilola, K., Meier, H. M., & Almroth, E. (2009). On the dynamics of oxygen, phosphorus and cyanobacteria in the Baltic Sea; A model study. *Journal of Marine Systems*, 75(1-2), 163–184.

Elken, J., Ed. (1996). *Deep water overflow, circulation and vertical exange in the Baltic Prober*. Number 6 in Report series //Estonian Marine Institute Tallinn. Tallinn.

Enfield, D. B., Mestas-Nuñez, A. M., & Trimble, P. J. (2001). The Atlantic Multidecadal Oscillation and its relation to rainfall and river flows in the continental U.S. *Geophysical Research Letters*, 28(10), 2077–2080.

Eyring, V., Bony, S., Meehl, G. A., Senior, C. A., Stevens, B., Stouffer, R. J., & Taylor, K. E. (2016). Overview of the Coupled Model Intercomparison Project Phase 6 (CMIP6) experimental design and organization. *Geoscientific Model Development*, 9, 1937–1958.

Feistel, R., Nausch, G., & Hagen, E. (2006). Unusual Baltic inflow activity in 2002–2003 and varying deep-water properties. *Oceanologia*, 48(S), 21–35.

Feistel, R., Nausch, G., Heene, T., Piechura, J., & Hagen, E. (2004). Evidence for a warm water inflow into the Baltic Proper in summer 2003. *Oceanologia*, 46(4), 581–198.

Feistel, R., Nausch, G., Mohrholz, V., Lysiak-Pastuszak, A., Seifert, T., Matthäus, W., Krüger, S., & Hansen, I. S. (2003). Warm waters of summer 2002 in the deep Baltic Proper. *Oceanologia*, 45(4), 571–592.

Fennel, K. & Testa, J. M. (2019). Biogeochemical Controls on Coastal Hypoxia. *Annual Review of Marine Science*, 11, 105–30.

Fischer, H. & Matthäus, W. (1996). The importance of the Drogden Sill in the Sound for major Baltic inflows. *Journal of Marine Systems*, 9(3-4), 137–157.

Good, R. & Fletcher, H. J. (1981). Reporting explained variance. *Journal of Research in Science Teaching*, 18(1), 1–7.

Graham, P. (1999). Modeling runoff to the Baltic Sea. *AMBIO*, 28(4), 328–334.

Griffies, S. M. (2004). *Fundamentals of Ocean Climate Models*. Princeton, N. J.: Princeton Univ. Press.

Griffies, S. M. (2014). *Elements of the Modular Ocean Model (MOM) (2012 release with updates)*. Technical Report 7, NOAA/Geophysical Fluid Dynamics Laboratory.

Grinsted, A., Moore, J. C., & Jevrejeva, S. (2004). Application of the cross wavelet transform and wavelet coherence to geophysical time series. *Nonlinear Processes in Geophysics*, 11(5/6), 561–566.

Gräwe, U., Klingbeil, K., Kelln, J., & Dangendorf, S. (2019). Decomposing Mean Sea Level Rise in a Semi-Enclosed Basin, the Baltic Sea. *Journal of Climate*, 32(11), 3089–3108.

Gröger, M., Dutheil, C., Börgel, F., & Meier, M. H. E. (2024). Drivers of marine heatwaves in a stratified marginal sea. *Climate Dynamics*, 62(5), 3231–3243.

Gu, Q., Gervais, M., Danabasoglu, G., Kim, W. M., Castruccio, F., Maroon, E., & Xie, S.-P. (2024). Wide range of possible trajectories of North Atlantic climate in a warming world. *Nature Communications*, 15, 4221.

Gustafsson, B. & Andersson, H. C. (2001). Modeling the exchange of the Baltic Sea from the meridional atmospheric pressure difference across the North Sea. *J Geophys Res*, 106(C9), 19731–19744.

Gustafsson, B. G., Schenk, F., Blenckner, T., Eilola, K., Meier, H. E. M., Müller-Karulis, B., Neumann, T., Ruoho-Airola, T., Savchuk, O. P., & Zorita, E. (2012). Reconstructing the Development of Baltic Sea Eutrophication 1850–2006. *AMBIO*, 41(6), 534–548.

Hagy, J. D., Boynton, W. R., Keefe, C. W., & Wood, K. V. (2004). Hypoxia in Chesapeake Bay, 1950-2001: Long-term Change in Relation to Nutrient Loading and River Flow. *Estuaries*, 27(4), 634–658.

Hansson, D. C., Eriksson, C., Omstedt, A., & Chen, D. (2011). Reconstruction of river runoff to the Baltic Sea, AD 1500-1995. *Int J Clim*, 31, 696–703.

Hansson, M., Viktorsson, L., & Andersson, L. (2019). *Oxygen Survey in the Baltic Sea 2019 - Extent of Anoxia and Hypoxia, 1960-2019*. Technical Report 67, Swedish Meteorological and Hydrological Institute, Göteborg.

Hofmeister, R., Beckers, J.-M., & Burchard, H. (2011). Realistic modelling of the exceptional inflows into the central Baltic Sea in 2003 using terrain-following coordinates. *Ocean Modelling*, 39, 233–247.

Holtermann, P. L. & Umlauf, L. (2012). The Baltic Sea Tracer Release Experiment: 2. Mixing processes. *Journal of Geophysical Research: Oceans*, 117(C01022).

Hordoir, R., Axell, L., Löptien, U., Dietze, H., & Kuznetsov, I. (2015). Influence of sea level rise on the dynamics of salt inflows in the Baltic Sea. *Journal of Geophysical Research: Oceans*, 120(10), 6653–6668.

Hurrell, J. W. (1995). Decadal trends in the North Atlantic Oscillation: regional temperatures and precipitation. *Science*, 269(5224), 676–679.

ICES (2023). ICES Oceanography [Dataset].

IOW (2023a). Ecological Regional Ocean Model.

IOW (2023b). GETM – A 3D hydrodynamic model for coastal oceans.

Janssen, F., Schrum, C., & Backhaus, J. O. (1999). A Climatological Data Set of Temperature and Salinity for the Baltic Sea and the North Sea. *German Journal of Hydrography*, 51((Suppl 9), 5).

Jones, P., Jonsson, T., & Wheeler, D. (1997). Extension to the North Atlantic oscillation using early instrumental pressure observations from Gibraltar and south-west Iceland. *Int. J. Climatol.*, 17, 1433–1450.

Jungclaus, J. H., Fischer, N., Haak, H., Lohmann, K., Marotzke, J., Matei, D., Mikolajewicz, U., Notz, D., & von Storch, J. S. (2013). Characteristics of the ocean simulations in the Max Planck Institute Ocean Model (MPIOM) the ocean component of the MPI-Earth system model. *Journal of Advances in Modeling Earth Systems*, 5, 422–446.

Kabel, K., Moros, M., Porsche, C., Neumann, T., Adolphi, F., Andersen, T. J., Siegel, H., Gerth, M., Leipe, T., Jansen, E., & Damsté, J. S. S. (2012). Impact of climate change on the Baltic Sea ecosystem over the past 1,000 years. *Nature Climate Change*, 2, 871–874.

Kauker, F. & Meier, H. E. M. (2003). Modeling decadal variability of the Baltic Sea: 1. Reconstructing atmospheric surface data for the period 1902–1998. *Journal of Geophysical Research*, 108(C8), 3267.

Kniebusch, M. (2019). *Detection and attribution studies of climate related changes in the Baltic Sea since 1850*. PhD thesis, Universität Rostock.

Kniebusch, M., Meier, H. E. M., Neumann, T., & Börgel, F. (2019a). Temperature Variability of the Baltic Sea Since 1850 and Attribution to Atmospheric Forcing Variables. *Journal of Geophysical Research: Oceans*, 124(6), 4168–4187.

Kniebusch, M., Meier, H. E. M., & Radtke, H. (2019b). Changing Salinity Gradients in the Baltic Sea As a Consequence of Altered Freshwater Budgets. *Geophysical Research Letters*, 46(16), 9739–9747.

Krapf, K., Naumann, M., Dutheil, C., & Meier, H. E. M. (2022). Investigating Hypoxic and Euxinic Area Changes Based on Various Datasets From the Baltic Sea. *Frontiers in Marine Science*, 9, 823476.

Lass, H. & Matthäus, W. (1996). On temporal wind variations forcing salt water inflows into the Baltic Sea. *Tellus A: Dynamic Meteorology and Oceanography*, 48(5), 663–671.

Laufkötter, C., John, J. G., Stock, C. A., & Dunne, J. P. (2017). Temperature and oxygen dependence of the remineralization of organic matter. *Global Biogeochemical Cycles*, 31(7), 1038–1050.

Lehmann, A., Getzlaff, K., & Harlaß, J. (2011). Detailed assessment of climate variability in the Baltic Sea area for the period 1958 to 2009. *Climate Research*, 46(2), 185–196.

Lehmann, A. & Hinrichsen, H.-H. (2000). On the wind driven and thermohaline circulation of the Baltic Sea. *Physics and Chemistry of the Earth, Part B: Hydrology, Oceans and Atmosphere*, 25(2), 183–189.

Lehmann, A., Myrberg, K., Post, P., Chubarenko, I., Dailidiene, I., Hinrichsen, H.-H., Hüssy, K., Liblik, T., Meier, H. E. M., Lips, U., & Bukanova, T. (2022). Salinity dynamics of the Baltic Sea. *Earth System Dynamics*, 13(1), 373–392.

Lehner, F., Deser, C., Maher, N., Marotzke, J., Fischer, E. M., Brunner, L., Knutti, R., & Hawkins, E. (2020). Partitioning climate projection uncertainty with multiple large ensembles and CMIP5/6. *Earth System Dynamics*, 11(2), 491–508.

Liblik, T. & Lips, U. (2019). Stratification Has Strengthened in the Baltic Sea – An Analysis of 35 Years of Observational Data. *Frontiers in Earth Science*, 7, 174.

Limburg, K. E. & Casini, M. (2018). Effect of Marine Hypoxia on Baltic Sea Cod Gadus morhua: Evidence From Otolith Chemical Proxies. *Frontiers in Marine Science*, 5, 482.

Limburg, K. E. & Casini, M. (2019). Otolith chemistry indicates recent worsened Baltic cod condition is linked to hypoxia exposure. *Biology Letters*, 15, 20190352.

Lorenz, E. N. (1963). Deterministic Nonperiodic Flow. *Journal of the Atmospheric Sciences*, 20(2), 130–141.

Mann, M. E., Steinman, B. A., Brouillette, D. J., & Miller, S. K. (2021). Multidecadal climate oscillations during the past millennium driven by volcanic forcing. *Science*, 371, 1014–1019.

Mann, M. E., Steinman, B. A., & Miller, S. K. (2020). Absence of internal multidecadal and interdecadal oscillations in climate model simulations. *Nature Communications*, 11(49).

Matthäus, W. & Franck, H. (1992). Characteristics of major Baltic inflows—a statistical analysis. *Continental Shelf Research*, 12(12), 1375–1400.

Matthäus, W. & Schinke, H. (1994). Mean atmospheric circulation patterns associated with major Baltic inflows. *Deutsche Hydrographische Zeitschrift*, 46(4), 321–339.

Mauritsen, T., Bader, J., Becker, T., Behrens, J., Bittner, M., Brokopf, R., Brovkin, V., Claussen, M., Crueger, T., Esch, M., Fast, I., Fiedler, S., Fläschner, D., Gayler, V., Giorgetta, M., Goll, D. S., Haak, H., Hagemann, S., Hedemann, C., Hohenegger, C., Ilyina, T., Jahns, T., Jimenéz-de-la Cuesta, D., Jungclaus, J., Kleinen, T., Kloster, S., Kracher, D., Kinne, S., Kleberg, D., Lasslop, G., Kornblueh, L., Marotzke, J., Matei, D., Meraner, K., Mikolajewicz, U., Modali, K., Möbis, B., Müller, W. A., Nabel, J. E. M. S., Nam, C. C. W., Notz, D., Nyawira, S.-S., Paulsen, H., Peters, K., Pincus, R., Pohlmann, H., Pongratz, J., Popp, M., Raddatz, T. J., Rast, S., Redler, R., Reick, C. H., Rohrschneider, T., Schemann, V., Schmidt, H., Schnur, R., Schulzweida, U., Six, K. D., Stein, L., Stemmler, I., Stevens, B., von Storch, J.-S., Tian, F., Voigt, A., Vrese, P., Wieners, K.-H., Wilkenskjeld, S., Winkler, A., & Roeckner, E. (2019). Developments in the MPI-M Earth System Model version 1.2 (MPI-ESM1.2) and Its Response to Increasing CO2. *Journal of Advances in Modeling Earth Systems*, 11, 998–1038.

Medvedev, I. & Kulikov, E. (2019). Low-Frequency Baltic Sea Level Spectrum. *Frontiers in Earth Science*, 7, 284.

Meier, H. E. M. (2007). Modeling the pathways and ages of inflowing salt- and freshwater in the Baltic Sea. *Estuarine, Coastal and Shelf Science*, 74(4), 610–627.

Meier, H. E. M., Andersson, H. C., Arheimer, B., Blenckner, T., Chubarenko, B., Donnelly, C., Eilola, K., Gustafsson, B., Hansson, A., Havenhand, J., Höglund, A., Kuznetsov, I., MacKenzie, B. R., Müller-Karulis, B., Neumann, T., Niiranen, S., Piwowarczyk, J., Raudsepp, U., Reckermann, M., Ruoho-Airola, T., Savchuk, O. P., Schenk, F., Schimanke, S., Väli, G., Weslawski, J.-M., & Zorita, E. (2012). Comparing reconstructed past variations and future projections of the Baltic Sea ecosystem—first results from multi-model ensemble simulations. *Environmental Research Letters*, 7, 034005.

Meier, H. E. M., Andersson, H. C., Eilola, K., Gustafsson, B., Kuznetsov, I., Müller-Karulis, B., Neumann, T., & Savchuk, O. (2011). Hypoxia in future climates: A model ensemble study for the Baltic Sea. *Geophysical Research Letters*, 38, L24608.

Meier, H. E. M., Barghorn, L., Börgel, F., Gröger, M., Naumov, L., & Radtke, H. (2023). Multidecadal climate variability dominated past trends in the water balance of the Baltic Sea watershed. *npj Climate and Atmospheric Science*, 6(1), 58.

Meier, H. E. M., Dieterich, C., & Gröger, M. (2021). Natural variability is a large source of uncertainty in future projections of hypoxia in the Baltic Sea. *Communications Earth & Environment*, 2(1), 50.

Meier, H. E. M., Dieterich, C., Gröger, M., Dutheil, C., Börgel, F., Safonova, K., Christensen, O. B., & Kjellström, E. (2022a). Oceanographic regional climate projections for the Baltic Sea until 2100. *Earth System Dynamics*, 13(1), 159–199.

Meier, H. E. M., Döscher, R., Coward, A., Nycander, J., & Döös, K. (1999). RCO - Rossby Centre regional Ocean climate model: model description (version 1.0) and first results from the hindcast period 1992/93. *SMHI Reports Oceanography*, 26.

Meier, H. E. M., Döscher, R., & Faxén, T. (2003). A multiprocessor coupled ice-ocean model for the Baltic Sea: Application to salt inflow. *Journal of Geophysical Research*, 108(C8), 3273.

Meier, H. E. M., Eilola, K., Almroth-Rosell, E., Schimanke, S., Kniebusch, M., Höglund, A., Pemberton, P., Liu, Y., Väli, G., & Saraiva, S. (2019). Disentangling the impact of nutrient load and climate changes on Baltic Sea hypoxia and eutrophication since 1850. *Climate Dynamics*, 53, 1145–1166.

Meier, H. E. M., Feistel, R., Piechura, J., Arneborg, L., Burchard, H., Fiekas, V., Golenko, N., Kuzmina, N., Mohrholz, V., Nohr, C., Paka, V. T., Sellschopp, J., Stips, A., & Zhurbas, V. (2006). Ventilation of the Baltic Sea deep water: A brief review of present knowledge from observations and models. *Oceanologia*, (48), 133–164.

Meier, H. E. M., Höglund, A., Eilola, K., & Almroth-Rosell, E. (2017). Impact of accelerated future global mean sea level rise on hypoxia in the Baltic Sea. *Climate Dynamics*, 49, 163–172.

Meier, H. E. M. & Kauker, F. (2003). Modeling decadal variability of the Baltic Sea: 2. Role of freshwater inflow and large-scale atmospheric circulation for salinity. *Journal of Geophysical Research*, 108(C11), 3368.

Meier, H. E. M., Kniebusch, M., Dieterich, C., Gröger, M., Zorita, E., Elmgren, R., Myrberg, K., Ahola, M. P., Bartosova, A., Bonsdorff, E., Börgel, F., Capell, R., Carlén, I., Carlund, T., Carstensen, J., Christensen, O. B., Dierschke, V., Frauen, C., Frederiksen, M., Gaget, E., Galatius, A., Haapala, J. J., Halkka, A., Hugelius, G., Hünicke, B., Jaagus, J., Jüssi, M., Käyhkö, J., Kirchner, N., Kjellström, E., Kulinski, K., Lehmann, A., Lindström, G., May, W., Miller, P. A., Mohrholz, V., Müller-Karulis, B., Pavón-Jordán, D., Quante, M., Reckermann, M., Rutgersson, A., Savchuk, O. P., Stendel, M., Tuomi, L., Viitasalo, M., Weisse, R., & Zhang, W. (2022b). Climate change in the Baltic Sea region: a summary. *Earth System Dynamics*, 13(1), 457–593.

Mikulski, Z. (1986). Inflow from drainage basin. In *Water Balance of the Baltic Sea*, volume 16 of *Baltic Sea Environment Proceedings* (pp. 24–34). Helsinki, Finland: Baltic Mar Environ Prot Comm.

Mohrholz, V. (2018a). Baltic saline barotropic inflows (SBI) 1887 - 2018 [Dataset].

Mohrholz, V. (2018b). Major Baltic Inflow Statistics – Revised. *Frontiers in Marine Science*, 5, 384.

Mohrholz, V., Dutz, J., & Kraus, G. (2006). The impact of exceptionally warm summer inflow events on the environmental conditions in the Bornholm Basin. *Journal of Marine Systems*, 60, 285–301.

Mohrholz, V., Naumann, M., Nausch, G., Krüger, S., & Gräwe, U. (2015). Fresh oxygen for the Baltic Sea — An exceptional saline inflow after a decade of stagnation. *Journal of Marine Systems*, 148, 152–166.

Moros, M., Kotilainen, A. T., Snowball, I., Neumann, T., Perner, K., Meier, H. E. M., Papenmeier, S., Kolling, H., Leipe, T., Sinninghe Damsté, J. S., & Schneider, R. (2023). Giant saltwater inflow in AD 1951 triggered Baltic Sea hypoxia. *Boreas*, 53, 125–138.

Naumov, L., Neumann, T., Radtke, H., & Meier, H. E. M. (2023). Limited ventilation of the central Baltic Sea due to elevated oxygen consumption. *Frontiers in Marine Science*, 10, 1175643.

Neumann, T., Radtke, H., Cahill, B., Schmidt, M., & Rehder, G. (2022). Non-Redfieldian carbon model for the Baltic Sea (ERGOM version 1.2) – implementation and budget estimates. *Geoscientific Model Development*, 15(22), 8473–8540.

Ni, W., Li, M., Ross, A. C., & Najjar, R. G. (2019). Large Projected Decline in Dissolved Oxygen in a Eutrophic Estuary Due to Climate Change. *Journal of Geophysical Research: Oceans*, 124(11), 8271–8289.

Olonschek, D., Suarez-Gutierrez, L., Milisnki, S., Beobide-Arsuaga, G., Baehr, J., Fröb, F., Ilyina, T., Kadow, C., Krieger, D., Li, H., Marotzke, J., Plésiat, E., Schupfner, M., Wachsmann, F., Wallberg, L., Wieners, K.-H., & Brune, S. (2023). The New Max Planck Institute Grand Ensemble With CMIP6 Forcing and High-Frequency Model Output. *Journal of Advances in Modeling Earth Systems*, 15, e2023MS003790.

Palmer, T. E., McSweeney, C. F., Booth, B. B. B., Priestley, M. D. K., Davini, P., Brunner, L., Borchert, L., & Menary, M. B. (2023). Performance-based sub-selection of CMIP6 models for impact assessments in Europe. *Earth System Dynamics*, 14, 457–483.

Placke, M., Meier, H. E. M., Gräwe, U., Neumann, T., Frauen, C., & Liu, Y. (2018). Long-Term Mean Circulation of the Baltic Sea as Represented by Various Ocean Circulation Models. *Frontiers in Marine Science*, 5, 287.

Poli, P., Hersbach, H., Dee, D. P., Berrisford, P., Simmons, A. J., Vitart, F., Laloyaux, P., Tan, D. G. H., Peubey, C., Thépaut, J.-N., Trémolet, Y., Hólm, E. V., Bonavita, M., Isaksen, L., & Fisher, M. (2016). ERA-20C: an atmospheric reanalysis of the twentieth century. *Journal of Climate*, 29(11), 4083–4097.

Qin, M., Dai, A., & Hua, W. (2022). Influence of Anthropogenic Warming on the Atlantic Multidecadal Variability and Its Impact on Global Climate in the Twenty-First Century in the MPI-GE Simulations. *Journal of Climate*, 35(9), 2805–2821.

Radtke, H., Brunnabend, S.-E., Gräwe, U., & Meier, H. E. M. (2020). Investigating interdecadal salinity changes in the Baltic Sea in a 1850–2008 hindcast simulation. *Climate of the Past*, 16(4), 1617–1642.

Rak, D., Walczowski, W., Dzierzbicka-Glowacka, L., & Shchuka, S. (2020). Dissolved oxygen variability in the southern Baltic Sea in 2013-2018. *Oceanologia*, 62, 525–537.

Receveur, A., Bleil, M., Funk, S., Stötera, S., Gräwe, U., Naumann, M., Dutheil, C., & Krumme, U. (2022). Western Baltic cod in distress: decline in energy reserves since 1977. *ICES Journal of Marine Science*, 79, 1187–1201.

Reimann, L., Vafeidis, A. T., & Honsel, L. E. (2023). Population development as a driver of coastal risk: Current trends and future pathways. *Cambridge Prisms: Coastal Futures*, 1(e14), 1–12.

Reusch, T. B. H., Dierking, J., Andersson, H. C., Bonsdorff, E., Carstensen, J., Casini, M., Czajkowski, M., Hasler, B., Hinsby, K., Hyytiäinen, K., Johannesson, K., Jomaa, S., Jormalainen, V., Kuosa, H., Kurland, S., Laikre, L., MacKenzie, B. R., Margonski, P., Melzner, F., Oesterwind, D., Ojaveer, H., Refsgaard, J. C., Sandström, A., Schwarz, G., Tonderski, K., Winder, M., & Zandersen, M. (2018). The Baltic Sea as a time machine for the future coastal ocean. *Science Advances*, 4(5), eaar8195.

Riahi, K., Van Vuuren, D. P., Kriegler, E., Edmonds, J., O'Neill, B. C., Fujimori, S., Bauer, N., Calvin, K., Dellink, R., Fricko, O., Lutz, W., Popp, A., Cuaresma, J. C., Kc, S., Leimbach, M., Jiang, L., Kram, T., Rao, S., Emmerling, J., Ebi, K., Hasegawa, T., Havlik, P., Humpenöder, F., Da Silva, L. A., Smith, S., Stehfest, E., Bosetti, V., Eom, J., Gernaat, D., Masui, T., Rogelj, J., Strefler, J., Drouet, L., Krey, V., Luderer, G., Harmsen, M., Takahashi, K., Baumstark, L., Doelman, J. C., Kainuma, M., Klimont, Z., Marangoni, G., Lotze-Campen, H., Obersteiner, M., Tabeau, A., & Tavoni, M. (2017). The Shared Socioeconomic Pathways and their energy, land use, and greenhouse gas emissions implications: An overview. *Global Environmental Change*, 42, 153–168.

Robson, J., Sutton, R., Menary, M. B., & Lai, M. W. K. (2023). Contrasting internally and externally generated Atlantic Multidecadal Variability and the role for AMOC in CMIP6 historical simulations. *Philosophical Transactions A*, 381, 20220194.

Rodgers, K. B., Lee, S.-S., Rosenbloom, N., Timmermann, A., Danabasoglu, G., Deser, C., Edwards, J., Kim, J.-E., Simpson, I. R., Stein, K., Stuecker, M. F., Yamaguchi, R., Bódai, T., Chung, E.-S., Huang, L., Kim, W. M., Lamarque, J.-F., Lombardozzi, D. L., Wieder, W. R., & Yeager, S. G. (2021). Ubiquity of human-induced changes in climate variability. *Earth System Dynamics*, 12(4), 1393–1411.

Saraiva, S., Meier, H. E. M., Andersson, H., Höglund, A., Dieterich, C., Gröger, M., Hordoir, R., & Eilola, K. (2019). Uncertainties in Projections of the Baltic Sea Ecosystem Driven by an Ensemble of Global Climate Models. *Frontiers in Earth Science*, 6, 244.

Savchuk, O., Wulff, F., Hille, S., Humborg, C., & Pollehne, F. (2008). The Baltic Sea a century ago - a reconstruction from model simulations, verified by observations. *J Mar Syst*, 74(1-2), 485–494.

Schenk, F. & Zorita, E. (2012). Reconstruction of high resolution atmospheric fields for Northern Europe using analog-upscaling. *Climate of the Past*, 8(5), 1681–1703.

Schimanke, S. & Meier, H. E. M. (2016). Decadal-to-Centennial Variability of Salinity in the Baltic Sea. *Journal of Climate*, 29(20), 7173–7188.

Schinke, H. & Matthäus, W. (1998). On the causes of major Baltic inflows —an analysis of long time series. *Continental Shelf Research*, 18(1), 67–97.

Selten, F. M., Branstator, G. W., Dijkstra, H. A., & Kliphuis, M. (2004). Tropical origins for recent and future Northern Hemisphere climate change. *Geophysical Research Letters*, 31(21), 2004GL020739.

Simpson, G. (2014). Modelling seasonal data with GAMs.

Stepanova, N. B. (2017). Vertical structure and seasonal evolution of the cold intermediate layer in the baltic proper. *Estuarine, Coastal and Shelf Science*, 195, 34–40.

Stigebrandt, A. (1987). A Model for the Vertial Circulation of the Baltic Deep Water. *Journal of Physical Oceanography*, 17(10), 1772–1785.

Stockmayer, V. & Lehmann, A. (2023). Variations of temperature, salinity and oxygen of the Baltic Sea for the period 1950 to 2020. *Oceanologia*, 65(3), 466–483.

Tao, L., Fang, J., Yang, X., Sun, X., Cai, D., & Wang, Y. (2023). Role of North Atlantic Tripole SST in Mid-Winter Reversal of NAO. *Geophysical Research Letters*, 50(15), e2023GL103502.

The BACC Author Team, Ed. (2008). *Assessment of climate change for the Baltic Sea Basin*. Regional climate studies. Berlin ; London: Springer. OCLC: ocn182664247.

Tian, R., Cerco, C. F., Bhatt, G., Linker, L. C., & Shenk, G. W. (2022). Mechanisms Controlling Climate Warming Impact on the Occurrence of Hypoxia in Chesapeake Bay. *JAWRA Journal of the American Water Resources Association*, 58(6), 855–875.

Ting, M., Kushnir, Y., Seager, R., & Li, C. (2009). Forced and Internal Twentieth-Century SST Trends in the North Atlantic. *Journal of Climate*, 22(6), 1469–1481.

Torrence, C. & Compo, G. P. (1998). A Practical Guide to Wavelet Analysis. *Bulletin of the American Meteorological Society*, 79(1), 61–78.

Trenberth, K. E. & Shea, D. J. (2006). Atlantic hurricanes and natural variability in 2005. *Geophysical Research Letters*, 33, L12704.

Vahtera, E., Conley, D. J., Gustafsson, B. G., Kuosa, H., Pitkänen, H., Savchuk, O. P., Tamminen, T., Viitasalo, M., Voss, M., Wasmund, N., & Wulff, F. (2007). Internal Ecosystem Feedbacks Enhance Nitrogen-fixing Cyanobacteria Blooms and Complicate Management in the Baltic Sea. *AMBIO: A Journal of the Human Environment*, 36(2), 186–194.

Vuorinen, I., Hänninen, J., Rajasilta, M., Laine, P., Eklund, J., Montesino-Pouzols, F., Corona, F., Junker, K., Meier, H. E. M., & Dippner, J. W. (2015). Scenario simulations of future salinity and ecological consequences in the Baltic Sea and adjacent North Sea areas–implications for environmental monitoring. *Ecological Indicators*, 50, 196–205.

Väli, G., Meier, H. E. M., & Elken, J. (2013). Simulated halocline variability in the Baltic Sea and its impact on hypoxia during 1961-2007. *Journal of Geophysical Research: Oceans*, 118(12), 6982–7000.

Wills, R. C. J., Armour, K. C., Battisti, D. S., & Hartmann, D. L. (2019). Ocean–Atmosphere Dynamical Coupling Fundamental to the Atlantic Multidecadal Oscillation. *Journal of Climate*, 32(1), 251–272.

Wills, R. C. J., Battisti, D. S., & Armour, K. C. (2020). Pattern Recognition Methods to Separate Forced Responses from Internal Variability in Climate Model Ensembles and Observations. *Journal of Climate*, 33(20), 8693–8719.

Winsor, P., Rodhe, J., & Omstedt, A. (2001). Baltic Sea ocean climate: an analysis of 100 yr of hydrographic data with focus on the freshwater budget. *Climate Research*, 18, 5–15.

Wolf, G. (1972). Salzwassereinbrüche im Gebiet der westlichen Ostsee. *Beiträge zur Meereskunde*, 29.

Woollings, T., Barriopedro, D., Methven, J., Son, S.-W., Martius, O., Harvey, B., Sillmann, J., Lupo, A. R., & Seneviratne, S. (2018). Blocking and its Response to Climate Change. *Current Climate Change Reports*, 4, 287–300.

Zanchettin, D., Fang, S.-W., Khodri, M., Omrani, N.-E., Rubinetti, S., Rubino, A., Timmreck, C., & Jungclaus, J. H. (2023). Thermohaline patterns of intrinsic Atlantic Multidecadal Variability in MPI-ESM-LR. *Climate Dynamics*, 61, 2371–2393.

Zhang, R., Sutton, R., Danabasoglu, G., Kwon, Y.-O., Marsh, R., Yeager, S. G., Amrhein, D. E., & Little, C. M. (2019). A Review of the Role of the Atlantic Meridional Overturning Circulation in Atlantic Multidecadal Variability and Associated Climate Impacts. *Reviews of Geophysics*, 57, 316–375.

Zillén, L., Conley, D. J., Andrén, T., Andrén, E., & Björck, S. (2008). Past occurrences of hypoxia in the Baltic Sea and the role of climate variability, environmental change and human impact. *Earth-Science Reviews*, 91, 77–92.

A

Curriculum Vitae

Curriculum Vitae

Personal Information

Name Leonie Barghorn

Contact l.barghorn@yahoo.de

Education

Since 2022 PhD candidate for Dr. rer. Nat. in Physical Oceanography at the University of Rostock

Oct. 2018 – Sept. 2021 Physics studies (Physics M. Sc.) at the University of Göttingen (major field of studies: Solid State and Materials Physics, final grade 1.0)

- Selected courses: Lecture "Geophysikalische Strömungsmechanik", lecture "Advanced Statistical Physics", seminar "Klima und Wetter"
- Master thesis: "Macroscopic and Microscopic Electrical Investigations of Gold Schottky Barriers on Nb-doped SrTiO3" (1.1)

Jan. 2019 – May 2019 ERASMUS semester at the Université Claude Bernard Lyon 1 in the masters program "Science des Océans, de l'Atmosphère et du Climat"

- Selected courses: lecture "Physique du climat", lecture "Math pour le climat"

Oct. 2015 – Dec. 2018 Physics studies (B. Sc.) at the University of Göttingen (final grade: 1.3)

- Selected courses: lecture "Physik komplexer Systeme"
- Bachelor thesis: Investigation of a manganite-titanate p-n heterojunction (1.0)

Experience

February 2023 Field work on 12-day Baltic Sea monitoring cruise with RV Elisabeth Mann Borgese

Since January 2022 Research Scientist at the Leibniz Institute for Baltic Sea Research Warnemünde (IOW), Department of Physical Oceanography and Instrumentation

Nov. 2021 – Dec. 2021 Research Assistant at the 4th Physical Institute at the University of Göttingen

Sept. 2019 – Oct. 2019 Internship at GEOMAR (Helmholtz Centre for Ocean Research Kiel)

- Investigation of links between the salinity of the Baltic Sea and the freshwater supply due to river runoff and precipitation

Feb. 2018 – Dec. 2021 Freelance author for Utopia GmbH, since Dec. 2018 also editor (topics including climate change, energy transition)

Scholarships and Awards

June 2024 3rd place in the science communication competition "Rostock's Eleven"

May 2024	Young Scientists Award for the best oral presentation at the 5th Baltic Earth Conference
Oct. 2022 – Jan. 2024	enrolled in the mentoring program "Karrierewegementoring" for female PhD candidates of the University of Rostock
July 2022	Berliner-Ungewitter-Preis for outstanding master theses, University of Göttingen
June 2022	Young Scientists Poster Award at the 4th Baltic Earth Conference
Oct. 2015 – Sept. 2016	Scholarship (Deutschlandstipendium)
2014	School leaving award of the German Physical Society (DPG)

Teaching

Since Nov. 2024	Co-supervision of a master thesis
Sept. 2023 – Oct. 2023	Supervision of a 3-weeks internship
August 2022, 2023	Teacher at the 8th and 9th International Baltic Earth Summer School
Sept. 2016 – Oct. 2016	Tutor at the Institute for Theoretical Physics of the Physics Faculty of the University of Göttingen in the preparatory course for Mathematics

Training Courses

September 2023	2-day training course on moderation, Rostock
May 2023	2-day rhetoric and presence training course, Rostock
March 2023	Baltic Earth PhD Winter School, Rostock
November 2022	2-day media training course, Rostock
August 2022	8th Baltic Earth International Summer School, Askö, Sweden
March 2022	3rd Baltic Earth Winter School, Rostock

Publications in Peer-Reviewed Journals

2025	Barghorn, L., F. Börgel, M. Gröger, and H. E. M. Meier. *Atlantic Multidecadal Variability control on European seas is mainly externally forced*. Environmental Research Letters (under review)
2025	Barghorn, L., H. E. M. Meier, H. Radtke, T. Neumann, and L. Naumov (2025). *Warm saltwater inflows strengthen oxygen depletion in the western Baltic Sea*. Climate Dynamics. 63: 29, doi: 10.1007/s00382-024-07501-x
2023	Barghorn, L., H. E. M. Meier, and H. Radtke (2023). *Changes in seasonality of saltwater inflows caused exceptional warming trends in the western Baltic Sea*. Geophys. Res. Lett. 50: e2023GL103853, doi: 10.1029/2023GL103853
2023	Meier, H. E. M., L. Barghorn, F. Börgel, M. Gröger, L. Naumov, and H. Radtke (2023). *Multidecadal climate variability dominated past trends in the water balance of the Baltic Sea watershed*. npj Clim. Atmos. Sci. 6: 58, doi: 10.1038/s41612-023-00380-9

2023	Börgel F., T. Neumann , J. Rooze, H. Radtke, L. Barghorn, and H. E. M. Meier (2023). *Deoxygenation of the Baltic Sea during the last millennium*. Front. Mar. Sci. 10: 1174039, doi:10.3389/fmars.2023.1174039

Scientific Presentations

May 2024	*Exceptional warming and intensified oxygen depletion due to warm saltwater inflows in the western Baltic Sea.* Oral presentation (solicited speaker) at the 5th Baltic Earth Conference in Jurmala, Latvia
April 2024	*Warm saltwater inflows strengthen oxygen depletion in the western Baltic Sea.* Oral presentation (highlighted) at the EGU General Assembly 2024 in Vienna, Austria
July 2023	*Seasonality of salinity dynamics in the western Baltic Sea.* Oral presentation at the IUGG General Assembly Berlin 2023, Germany
June 2022	*Investigating the properties of small- and medium-size saltwater inflows into the Baltic Sea*. Poster presentation at the 4th Baltic Earth Conference in Jastarnia, Poland

Evaluation activities

2024	peer review for Communications Earth and Environment

Outreach

Since Dec. 2024	co-host of “Wellenlänge Wissenschaft”
November 2024	guest in the radio broadcast “Wellenlänge Wissenschaft“ (LOHRO)
October 2024	participation in “book a scientist” (video chats with interested laymen)
August 2024	Interview in NDR Radio MV
August 2024	Talks for the general public at “Science@Sail” and “Warnemünder Abende”
June 2024	IOW candidate in the science communication competition “Rostock’s Eleven”
May 2024	poster presentation at the “Open Ship Day”
January 2024	presentation at a visit by the regional government of Mecklenburg-Vorpommern (MV)
December 2023	participation in “I’m a scientist” (live chats with pupils)
September 2023	talk at the “Klimatag Bad Doberan”
August 2023	Interview in “Forschung aktuell” by radio channel “Deutschlandfunk”
August 2023	talk at a visit by representatives of the State Chancellery of MV
June 2023	presentation at a visit by the Federal Minister of Environment and the State Minister of Science, Culture, Federal and European Affairs for MV
April 2023	Participation in the “Zeig dich!” initiative of the graduate academy of the University of Rostock
June 2022	poster presentation at the “Ostseetag”

Computer Skills

Advanced: Python, Linux / Unix, Matlab, R, Latex
Basic: bash, C, Climate Data Operators (cdo), nco, Content Management Systems, LabView, ImageJ

Languages

English, French (fluent)

Memberships

Since 2023	European Geosciences Union
Since 2022	Graduate Academy of the University of Rostock
Since 2014	German Physical Society

Voluntary Work

Nov. 2023	Co-organizer of a weekend seminar entitled “Autonome Waffensysteme und Künstliche Intelligenz” for students from different disciplines
Jan. 2023 – Nov. 2023	Member in the working group “Communication” of the Leibniz PhD Network
June 2022 – June 2024	PhD representative of the Physics Department of IOW
Since summer 2019	Coordination of a fund-raising campaign for the St. Mary’s Secondary School in Muzizi, Uganda
May 2019 – Dec. 2021	Member of Slow Food Youth Göttingen
Oct. 2015 – March 2019	Committed in the self-administration of the Physics’ faculty of the University of Göttingen (e. g. head of students’ council, member of faculty council, member of a review committee)
Sept. 2014 – May 2015	Weltwärts voluntary work in Uganda (Organizations: Diocese of Fulda and Diocese of Hoima)
July 2014 – Dec. 2016	Author for the “Hamburg-Geschichtsbuch“ (www.geschichtsbuch.hamburg.de)

Rostock, January 7, 2025

Leonie Barghorn

B

Declaration of my contributions to the publications

B.1 Changes in seasonality of saltwater inflows into the Baltic Sea

I prepared this paper during my first year as a PhD student at the Leibniz Institute for Baltic Sea Research Warnemünde. My work started with the analysis of a model simulation which was set up by Hagen Radtke who also performed two sensitivity experiments. Two other sensitivity experiments were prepared and conducted by me. My co-authors provided helpful ideas to my analysis as well as notes and comments to the paper which they both reviewed but otherwise, I conceptualized and wrote the paper myself. Revisions were also implemented by me.

B.2 Warm saltwater inflows strengthen oxygen depletion in the western Baltic Sea

This paper is the output of the second year of my PhD. The additional model data compared to my first paper was provided by H. E. Markus Meier, Thomas Neumann, and Lev Naumov. I conceptualized the study, conducted the analysis and wrote the manuscript. My co-authors provided ideas to the analysis and helped with editing and revising the manuscript.

B.3 Multidecadal climate variability dominated past trends in the water balance of the Baltic Sea watershed

I calculated and plotted several wavelets, global power spectra and wavelet coherence spectra for the Supporting Information of this paper, including pre-processing of the input data. Moreover, I helped editing the paper.

B.4 Atlantic Multidecadal Variability control on European seas is mainly externally forced

This study was developed in my third year as a PhD student. I conceptualized the study with help from my co-authors and wrote the manuscript which my co-authors edited. The analysis was conducted by me with some support by Florian Börgel.

C
Publications

The following publications are included in the appendix in the order of appearance:

A **Barghorn, L.**, *Meier, H. E. M., and Radtke, H.* (2023). Changes in Seasonality of Saltwater Inflows Caused Exceptional Warming Trends in the Western Baltic Sea. Geophysical Research Letters, 50, e2023GL103853. https://doi.org/10.1029/2023GL103853

B **Barghorn, L.**, *Meier, H. E. M., Radtke, H., Neumann, T., and Naumov, L.* (2025). Warm saltwater inflows strengthen oxygen depletion in the western Baltic Sea. Climate Dynamics, 63, 29. https://doi.org/10.1007/s00382-024-07501-x

C *Meier, H. E. M.,* **Barghorn, L.,** *Börgel, F., Gröger, M., Naumov, L., and Radtke, H.* (2023). Multidecadal climate variability dominated past trends in the water balance of the Baltic Sea watershed. npj Climate and Atmospheric Science, 124, 4168–4187. https://doi.org/10.1029/2018JC013948

D **Barghorn, L.**, *Börgel, F., Gröger, M., and Meier, H. E. M.* (2025). Atlantic Multidecadal Variability control on European seas is mainly externally forced. Environmental Research Letters (under review)

AGU ADVANCING EARTH AND SPACE SCIENCE

Geophysical Research Letters®

RESEARCH LETTER
10.1029/2023GL103853

Changes in Seasonality of Saltwater Inflows Caused Exceptional Warming Trends in the Western Baltic Sea

L. Barghorn[1], H. E. M. Meier[1], and H. Radtke[1]

[1]Leibniz Institute for Baltic Sea Research Warnemünde, Rostock, Germany

Key Points:

- Summer and early autumn salt import into the Baltic Sea increased significantly since 1851 compared to the annual salt import
- Salt import between June and October is highly correlated with the annual sub-thermocline temperature maximum in the western Baltic Sea
- The shift in inflow seasonality was partly caused by seasonal changes in river runoff

Supporting Information:

Supporting Information may be found in the online version of this article.

Correspondence to:

L. Barghorn,
leonie.barghorn@io-warnemuende.de

Citation:

Barghorn, L., Meier, H. E. M., & Radtke, H. (2023). Changes in seasonality of saltwater inflows caused exceptional warming trends in the western Baltic Sea. *Geophysical Research Letters*, *50*, e2023GL103853. https://doi.org/10.1029/2023GL103853

Received 24 MAR 2023
Accepted 16 JUN 2023

Abstract During the last decades, the Baltic Sea has been among the fastest warming seas in the world. The warming is mainly driven by increasing air temperatures but deeper water layers can also be warmed by lateral advection of heat. By analyzing a 159 years long (1850–2008) hindcast simulation of the Baltic Sea, we link the exceptionally strong bottom water warming in the western Baltic Sea to a shift in the seasonality of saltwater inflows from the North Sea to the Baltic Sea. Over the model period, warm summer and early autumn inflows have increased while cold winter inflows have decreased. Sensitivity experiments reveal that these changes were partly driven by a shift in river runoff seasonality. The strong warming could lead to faster oxygen depletion in the affected layers and thus have ecological consequences.

Plain Language Summary The Baltic Sea is home to various marine and freshwater species and an important economic factor for the surrounding countries. Like other seas, the Baltic Sea is getting warmer due to climate change. The water at the surface warms especially fast because it takes up heat from the warming atmosphere. After some time, temperatures also increase in deeper layers. However, some deep parts in the western Baltic Sea are warming even faster than the sea surface. In our study, we investigate if the exceptional warming can be explained by an increase in warm saltwater inflows from the North Sea. Hence, we use a model simulation of the Baltic Sea for over 150 years to compare long time series of warm inflows and the temperatures in the deep layers of the western Baltic Sea. We find a strong correlation. Thus, we can link the exceptional warming in the deep layers of the western Baltic Sea during the last decades to an increase in warm inflows. The warming has ecological consequences since in warmer water, the oxygen is consumed faster and the deep water layers of the Baltic Sea are suffering from low oxygen concentrations.

1. Introduction

According to the Sixth Assessment Report by the Intergovernmental Panel on Climate Change (IPCC), the global mean sea surface temperature has increased by about 0.9°C since 1900 (IPCC, 2021). One of the fastest warming seas is the shallow, semi-enclosed Baltic Sea (Belkin, 2009) with an increase in sea surface temperature of about 0.3–0.6°C per decade since 1980 (Liblik & Lips, 2019; Meier et al., 2022). The surface warming is mainly driven by increasing air temperatures (Dutheil et al., 2022a; Kniebusch, Meier, Neumann, & Börgel, 2019). Since the Baltic Sea is strongly stratified, vertical exchange between the well-mixed surface layer and deep water below the permanent halocline in 50–80 m depth (Väli et al., 2013) is rather limited. Thus, lateral advection of heat plays a major role for the warming of the deep basins in the western and central Baltic Sea (Meier et al., 2022).

An exceptionally strong bottom water warming compared to other basins of the Baltic Sea was detected in the Bornholm Basin (western Baltic Sea, Figure 1) (Dutheil et al., 2022b; Mohrholz et al., 2006). Mohrholz et al. (2006) linked it to increased summer and early autumn saltwater inflows (in the following labeled "summer inflows") which transport warm surface water from the Baltic Sea entrance area to deep layers of the western and central Baltic Sea.

In general, the inflow of saline North Sea water into the Baltic Sea is hampered by shallow sills in the Danish straits, namely the Darss Sill (19 m) and the Drogden Sill (8 m, see Figure 1) (Mohrholz, 2018b). Very large so-called Major Baltic Inflows (MBIs) can only happen if, first, easterly winds push water out of the Baltic Sea for about 3 weeks and, second, westerly winds of a comparable duration push large amounts of saline water back over the sills (Lass & Matthäus, 1996). Such wind patterns occur roughly once per year between autumn and early spring (Matthäus & Franck, 1992; Mohrholz, 2018b). In contrast to that, small- to medium-sized inflows happen throughout the year (Mohrholz, 2018b). Unlike MBIs, they cannot reach the deepest parts of the central Baltic Sea and supply them with fresh oxygen but they mainly interleave in or below the halocline (Elken, 1996;

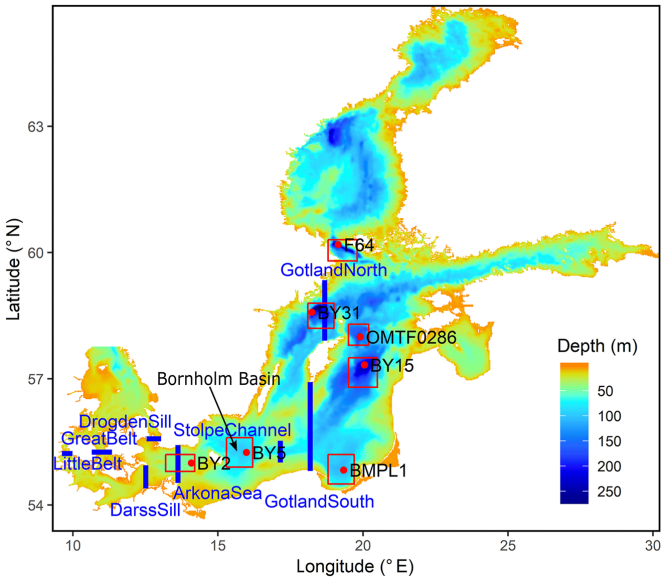

Figure 1. Model topography. Blue lines indicate transects across which salinity-discriminated salt transport is computed. The Bornholm Basin (western Baltic Sea) is marked. Red stations are used for model validation. Red squares show areas from which ICES data for the respective stations are taken. Modified from Radtke et al. (2020).

Matthäus & Franck, 1992; Mohrholz et al., 2006). Small- and medium-sized inflows can be both barotropic (driven by sea level gradients, mainly due to wind) or baroclinic (driven by horizontal salinity gradients during periods of calm weather) (Feistel et al., 2006; Wolf, 1972). Summer inflows are believed to be mainly baroclinic (Feistel et al., 2006).

The first pronounced summer inflow that was intensively investigated occurred in 2002 (Feistel et al., 2003, 2006; Mohrholz et al., 2006). Consequently, there is no long time series of summer inflows derived from observations like the ones that exist for MBIs (Fischer & Matthäus, 1996; Mohrholz, 2018b). However, such a time series would be necessary to detect systematic trends in summer inflows and distinguish it from the multidecadal variability which characterizes the water cycle in the Baltic Sea (Kniebusch, Meier, & Radtke, 2019; Lehmann et al., 2022; Meier & Kauker, 2003a; Mohrholz, 2018b; Radtke et al., 2020; Schimanke & Meier, 2016).

In this study, we investigate systematic changes in the seasonality of saltwater inflows during the last decades and whether those changes contributed to the exceptional temperature trend in the Bornholm Basin. In order to get a continuous and long time series of salt import from small, medium and large inflows, we analyze a long (1850–2008) hindcast simulation of the Baltic Sea. Furthermore, we conduct several sensitivity experiments where we modify different drivers of salinity dynamics, namely river runoff, wind and sea level. With this, we aim to quantify the impact of these drivers on any possible long-term changes in inflow activity.

The strong warming of the Bornholm Basin might have severe consequences for the ecosystem. Like in other basins in the central Baltic Sea, the deep water of the Bornholm Basin is hypoxic or even anoxic most of the time (Almroth-Rosell et al., 2021; Krapf et al., 2022). Higher bottom temperatures speed up mineralization of organic matter in the sediments and cause increased oxygen consumption (Krapf et al., 2022; Laufkötter et al., 2017). Warm saline inflows can also lead to a (temporal) eastward spread of non-indigenous species' habitats (Hinrichsen et al., 2022). Our results provide a more comprehensive understanding of temperature variability in the deep Bornholm Basin and thus help to investigate its ecological consequences. Furthermore, the mechanisms of bottom warming might be applicable to other strongly stratified coastal seas like the Chesapeake Bay which also suffers from (seasonal) hypoxia that is exacerbated by global warming (Ni et al., 2019; Tian et al., 2022, e.g.,).

2. Materials and Methods

2.1. Data and Model Setup

The characteristics of the reference simulation are summarized in Radtke et al. (2020). They performed a simulation of the Baltic Sea (Figure 1) from 1850 to 2008 using the General Estuarine Transport Model (GETM) with 1 nautical mile horizontal resolution and 50 vertical layers with adaptive coordinates (Gräwe et al., 2019). The latter allow to increase the resolution in depths with strong density gradients which leads to a more realistic simulation of inflows (Hofmeister et al., 2011). For the time series of monthly river runoff, different data sets were merged (Meier et al., 2019). At the lateral boundary of the model domain, daily mean sea level elevations were obtained from a reconstruction of the meridional sea level pressure gradient across the North Sea (Meier et al., 2019). Atmospheric forcing was provided by the HiResAFF (High Resolution Atmospheric Forcing Fields) v2 data set which was prepared with the analogue method (Schenk & Zorita, 2012).

2.2. Model Validation

For model validation, mean vertical temperature and salinity profiles from 1970 to 2007 at selected stations are compared to observational data from the ICES oceanographic database (Figure S1 in Supporting Information S1) (ICES, 2023). The ICES data are processed as in Radtke et al. (2020). Modeled and observed profiles exhibit the same qualitative features, namely the seasonal thermocline and the permanent halocline, but the latter tends to be shallower in the model data. This could be due to underestimated mixing or too weak winds. Modeled salinities are generally too high. Most important for an accurate simulation of summer inflows is the reproduction of the salinities in/below the halocline in the western Baltic Sea (stations BY2 in the Arkona Basin and BY5 in the Bornholm Basin). Here, the modeled values lie within 1 standard deviation of the ICES data. Time series of bottom and surface salinities were already validated by Radtke et al. (2020). They found that the multidecadal variability in surface and bottom salinities is in general well represented by the model. In case of the annual mean bottom salinity, the explained variance is highest at the northernmost stations (BY31, OMTF0286, and F64) with more than 50% and lowest at BY5 (17.4%). However, the explained variance at BY5 in 60 m depth, at the relevant height for small and/or warm inflows, is much better with 34%. Radtke et al. (2020) additionally analyzed the transport across the Darss and Drogden sills. They found a correlation of 58.6% for the daily mean volume transport across Drogden Sill and correlations of 43.5% (3 m depth) and 40.5% (17 m depth) for the daily mean eastward velocity at Darss Sill between 1995 and 2008.

2.3. Inflow Classification

In order to detect saltwater inflows into the Baltic Sea, salinity-discriminated transports are computed from the model output for selected transects (see Figure 1) following the Total Exchange Flow framework (Burchard et al., 2018; MacCready, 2011; Walin, 1977) as in Radtke et al. (2020). Afterward, we choose the transects "DarssSill" and "DrogdenSill" for the actual inflow detection since the two sills are the main barriers for the inflowing water. Finally, we introduce salt import thresholds to separate individual inflows from each other and only count inflows from a certain size. Too small inflows might just mix with the ambient water in the Arkona Basin but not reach the other basins further downstream. We follow these steps:

1. From salinity-discriminated salt transport at Darss Sill and Drogden Sill transects, the total inward salt transport by water masses with a salinity larger than 17 g/kg is extracted. This empirical salinity threshold was first introduced by Wolf (1972) to distinguish inflowing saltwater from the ambient water in the Danish straits and is commonly used in the literature to detect MBIs (Matthäus & Franck, 1992; Meier & Kauker, 2003a; Mohrholz et al., 2015).
2. The total salt import per day is calculated.
3. Days with salt import <20 Mt are neglected.
4. Consecutive inflow days are summed up.
5. Inflows with at least 100 Mt salt import are registered.

To justify our inflow criteria, we compare our salt import time series with the DS1 series of barotropic inflows by Mohrholz (2018a) which, in contrast to earlier observation-based inflow reconstructions, is unaffected by inhomogeneities in the salinity observations at Darss Sill (Mohrholz, 2018b). Figure S2 (Supporting Information S1)

shows that the low frequency variability is comparable. Since our time series consists of barotropic and baroclinic inflows, the total annual salt import is higher than in the DS1 series. The smallest inflows from the DS1 series are in the same order of magnitude as our salt import threshold of 100 Mt.

2.4. Sensitivity Experiments

In addition to the reference simulation (REF), the following sensitivity experiments are conducted in order to quantify the impact of drivers affecting the salinity dynamics:

1. RUNOFF: The interannual variability of river runoff is removed by computing the long-term monthly runoff climatology of the respective rivers and repeating it for each year of the modeled time period.
2. WIND: Meteodata and sea level at the open boundary are high-pass filtered with a cut-off period of 11 years. Linear trends are removed before high-pass filtering and afterward added again to the filtered time series.
3. RUNOFF2: We remove changes in runoff seasonality by applying a climatological seasonal cycle but keep the interannual runoff variability.
4. noSLR: We remove the linear trend in the sea level at the open boundary which reflects the global mean sea level rise (SLR).

High-pass filtering in WIND and detrending in noSLR are done for each grid cell separately. It should be noted that we only modify the runoff in RUNOFF and RUNOFF2, that is, the net precipitation (precipitation minus evaporation) over the catchment area of the Baltic Sea, but not the net precipitation over the Baltic Sea itself. Since the latter only contributes roughly 10% of the total freshwater supply (Meier & Kauker, 2003b), its variability is negligible compared to the runoff variability.

3. Results

In order to identify changes in inflow seasonality, we compare the salt import by inflows detected according to the steps described in Section 2.3 for three different periods: Summer (June– August; JJA), early autumn (September–October; SO) and the entire year. Figure 2a shows the three time series. They are smoothed by 11-year running means to extract the previously mentioned multidecadal variability. Linear trends from 1851 show that the normalized salt import in summer and early autumn increased more strongly than the annual salt import. Both trends are significant with p-values below 0.05 (Wald Test). More specifically, summer salt import was highest between 1960 and 1980 and early autumn salt import at the end of the 1990s. The interannual variability of runoff before 1900 is probably underestimated (Meier et al., 2019) and before 1920, the runoff data are not properly resolved for the different basins (not shown). Since this might have affected the salinity dynamics, we also compute trends from 1920. We find that the trend for SO is significantly positive while the one for JJA is slightly negative (Figure 2).

In Figure S3 (Supporting Information S1), we compare the average monthly salt import for three 30-year periods (1865–1895, 1920–1950, and 1975–2005) which are equally distributed over the model period. The strongest increase toward the last period happened in October while the salt import in winter decreased. For the later two periods, we also compare two-dimensional maps of bottom salinity in the western Baltic Sea. The most pronounced change in early autumn is found in the Baltic Sea entrance area where the bottom salinity increased strongly (Figure 3).

As described in Section 1, the exceptionally strong bottom water warming in the Bornholm Basin could have been (partly) caused by increased summer inflows and reduced winter inflows (Dutheil et al., 2022b; Kniebusch, Meier, Neumann, & Börgel, 2019). Figure 4 compares June– October (JJASO) salt import, that is, the whole "warm" inflow season, with the annual sub-thermocline vertical temperature maximum in the Bornholm Basin. Both smoothed time series exhibit a similar multidecadal variability. The time series of annual means are significantly correlated with Pearson correlation coefficients of 0.53 (from 1851) and 0.55 (from 1920). Thus, the previously mentioned attribution is reasonable.

We conducted the sensitivity experiments RUNOFF, RUNOFF2, WIND, and noSLR to find out which of the different drivers of salinity dynamics caused the shift in inflow seasonality. The resulting smoothed salt import time series are shown in Figure S4 in Supporting Information S1 and the respective differences to REF in Figure S5 (Supporting Information S1). For all runs, the multidecadal variability is very similar. The largest deviations exist between REF and RUNOFF, especially in summer (JJA) around 1970. RUNOFF2 is quite similar to RUNOFF in case of JJA salt import (visible in Figure S5 in Supporting Information S1). A comparison of the linear trends

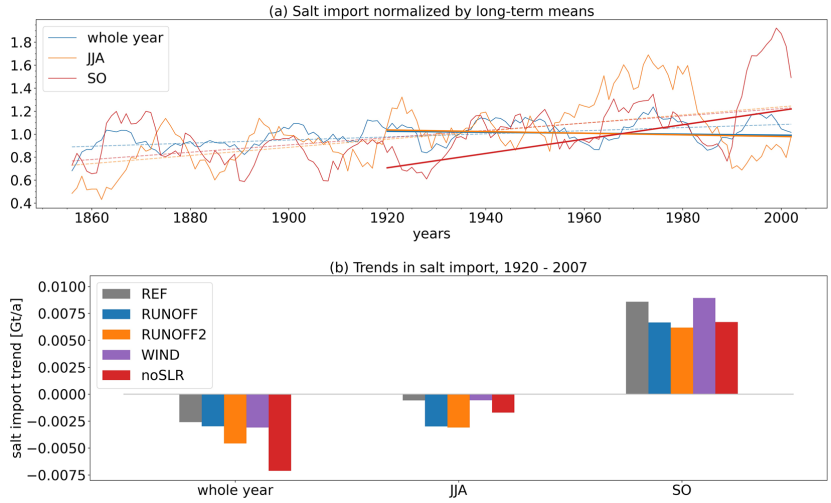

Figure 2. (a) 11-year running means of salt import per year, June– August (JJA) and September– October (SO) with linear trends from 1851 to 1920. All values were normalized by respective long-term means. (b) Trends in salt import from 1920 for the reference simulation REF and sensitivity experiments RUNOFF, RUNOFF2, WIND and noSLR.

in JJA and SO salt import since 1920 shows that the trends in RUNOFF and RUNOFF2 are less positive in SO and more negative in JJA compared to REF and WIND (Figure 2b), indicating that changes in the seasonality of river runoff were the most important driver of the shift in salt import seasonality. In the following section, we will examine a potential driving mechanism. However, as the shift in salt import seasonality is not completely absent in RUNOFF and RUNOFF2, we also need to discuss a possible impact of the other drivers (wind and sea level).

4. Discussion

We analyzed a long hindcast simulation of the Baltic Sea and found that salt import from summer inflows has increased during the model period and is strongly correlated with the annual sub-thermocline temperature

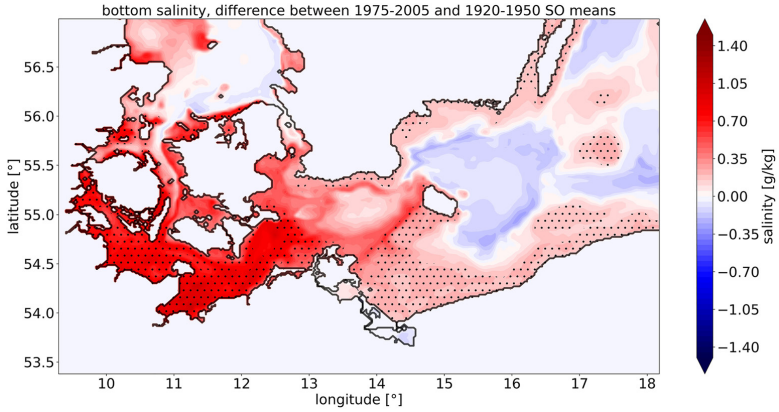

Figure 3. Differences between 1975–2005 and 1920–1950 September– October (SO) means of bottom salinity. Black dots indicate significant changes according to a Student's *t* test with a significance level of 0.95.

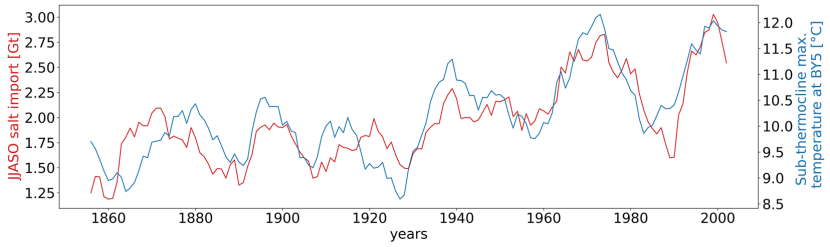

Figure 4. 11-year running means of June– October (JJASO) salt import versus annual temperature maximum below the seasonal thermocline (below 40 m) at station BY5 (Bornholm Basin, for the location see Figure 1).

maximum in the Bornholm Basin. Our sensitivity experiments switched off potential drivers of the observed changes. We found that the variability of the summer inflow time series is most strongly affected in RUNOFF and RUNOFF2, that is, if changes in seasonality of river runoff are ignored.

4.1. Runoff

Concerning accumulated runoff to the Baltic Sea, no significant trend could be found for the 20th century (Meier & Kauker, 2003a). However, there have been changes in seasonality. Meier and Kauker (2003a) have shown that winter and early spring runoff increased significantly since the 1970s, mainly due to river regulation in Sweden and Finland and increased precipitation in winter which is likely related to climate change (Meier et al., 2022). Already Wolf (1972) stated that the seasonality of river runoff affects the probability for highly saline inflows. However, it is not evident why seasonal changes in runoff should lead to seasonal changes in summer inflows since the response scale of Baltic Sea salinity to changes in external forcing is of the order of 30 years (Meier & Kauker, 2003a, 2003b; Winsor et al., 2001).

One mechanism could be a barotropic signal, that is, a change in sea level difference between Baltic Sea and North Sea due to runoff variability. This hypothesis was already raised by Schinke (1996) but he could not prove a causal connection between runoff and saltwater inflow seasonality via the sea level. The sea level in the Baltic Sea exhibits a seasonal cycle with a maximum in late summer or winter and a minimum in spring (Hünicke & Zorita, 2008; Meier et al., 2022; Stramska et al., 2013). According to Hünicke and Zorita (2008), the maximum shifted from late summer to winter during the 20th century, possibly due to changes in precipitation and runoff. Since, for inflows, the sea level gradient in the Baltic Sea entrance area is crucial, we compute the sea level difference between the stations AnholtE and BY2 (for the locations see Figure 1). By comparing 11-year running means of SO sea level difference and salt import, we find that the latter reaches its maximum when the former is minimal (Figure S6 in Supporting Information S1). Changes in sea level difference are only in the range of a few centimeters but in a barotropic inflow situation, even a 1 cm larger sea level difference can lead to a few megatons more salt import if we use Equation 3 in Mohrholz (2018b) for estimating the barotropic volume transport. No comparable correlation is found for JJA.

Finally, we conducted experiment RUNOFF2 with interannual runoff variability but without seasonal changes to get a more profound estimation of the effect of seasonality. As explained in the previous section, the trends in JJA and SO salt import since 1920 are quite close for RUNOFF and RUNOFF2 (Figure 2b). Thus, an impact of runoff seasonality seems possible although the signal is small.

4.2. Wind

Only part of the trend in summer salt import can be explained by the freshwater supply. Hence, wind changes could play a role, too. To present knowledge, there is no systematic overall trend in wind speed over the Baltic Sea (Meier et al., 2022). Coumou et al. (2015) reported a weakening of the atmospheric circulation in summer over mid-latitudes of the northern hemisphere. This could have caused more calm weather periods which are favorable for summer inflows. However, they considered the period 1979–2013 which is rather short and not comparable to our model period.

We analyze the third power of wind speed, which serves as a proxy for the energy input into the ocean by the wind, over the Baltic Sea from HiResAFF forcing between 1920–1950 and 1975–2005. It increased for SO means (Figure S7 in Supporting Information S1 left). Consequently, wind-driven inflows could have intensified. However, the changes are not significant except for a few grid cells. For summer (JJA), we observe decreasing third power of wind speed (Figure S7 in Supporting Information S1 right) between 1920–1950 and 1960–1990 which could have led to more summer inflows. But again, trends are not significant.

The positive trend in summer salt import in WIND is comparable to that in REF (Figure 2b). Still, one has to keep in mind that only the low-frequency variability of wind fields was filtered out in WIND while single inflow events result from variations in wind on a much shorter time scale. It cannot be ruled out that changes in large-scale atmospheric patterns like Scandinavian Blocking occurred and led to changes in high-frequency wind variability but a more profound analysis of atmospheric circulation patterns is beyond the scope of this study.

4.3. Sea Level Rise

Model studies indicate that a higher mean sea level in the North Sea and Baltic Sea will amplify the intensity of saltwater inflows in the future since it enlarges the cross section of the Danish straits (Meier et al., 2017, 2021; Saraiva et al., 2019). As the sea level in the Baltic Sea increased by roughly 20 cm since 1900 (Meier et al., 2022), that effect could have played a role during our model period. Indeed, our sensitivity experiment noSLR shows smaller/more negative trends in salt import compared to REF (Figure 2b). Hordoir et al. (2015) assumed that SLR leads to reduced mixing in the Danish straits and thus to stronger summer inflows. However, Arneborg (2016) questioned their approach and argued that rather the Sound will play a more important role for future saltwater inflows under a rising sea level. Our analysis does not show an impact of the global SLR on the seasonality of inflows since the smaller/more negative trends in noSLR are independent of the season.

4.4. Summary

To summarize the discussion, it is likely that the increase in early autumn (SO) salt import toward the end of the 20th century was mainly of barotropic nature (not baroclinic as commonly assumed), that is, driven by sea level alterations, which were likely caused by changes in runoff seasonality and wind. Concerning the summer (JJA) salt import maximum between 1960 and 1980, the drivers are less clear. Runoff variability and seasonality but also weaker winds could have played a role. Since maxima in JJA and SO salt import do not coincide in time and are perhaps not caused by the same drivers, we cannot exclude the possibility that the trends in JJA and SO salt import are part of multidecadal variations. As mentioned earlier, the main period of multidecadal variability in the Baltic Sea is about 30 years which is shorter than the time scale of the observed changes. However, we know that the Atlantic Multidecadal Variability influences the Baltic Sea water cycle on time scales longer than 60 years (Börgel et al., 2018). A longer modeling period would be necessary to detect more reliable trends.

5. Conclusions

For the first time, we showed a direct link between the exceptional bottom water warming in the Bornholm Basin (western Baltic Sea) and a shift in seasonality of saltwater inflows into the Baltic Sea. While summer and early autumn salt import has increased over the model period, winter salt import decreased. With the help of sensitivity experiments, we were able to attribute part of the changes to a shift in runoff seasonality due to river regulations and climate change. Another driver might be variations of the large-scale atmospheric circulation.

Conflict of Interest

The authors declare no conflicts of interest relevant to this study.

Data Availability Statement

The modeled and observational data necessary to reproduce the figures of this paper and its Supporting Information S1 are publicly available under https://doi.io-warnemuende.de/10.12754/data-2023-0006. The DS1 inflow series prepared by Volker Mohrholz can be downloaded from https://doi.io-warnemuende.de/10.12754/data-

2018-0004 (Mohrholz, 2018a). These datasets and Figure 1 from Radtke et al. (2020) are provided through the Creative Commons (CC) data license of type CC BY 4.0 (https://creativecommons.org/licenses/by/4.0/). The GETM model used for this study is open-source software and available under https://getm.eu/ (IOW, 2023).

Acknowledgments
The research presented in this study is part of the Baltic Earth program (Earth System Science for the Baltic Sea region; see https://www.baltic.earth). Model runs were conducted at the supercomputers of the North German Supercomputing Alliance (HLRN). Data from the long-term monitoring program of the Leibniz Institute for Baltic Sea Research Warnemünde (IOW) were used for model validation. We would like to acknowledge two anonymous reviewers for their constructive and helpful comments. Open Access funding enabled and organized by Projekt DEAL.

References

Almroth-Rosell, E., Wåhlström, I., Hansson, M., Väli, G., Eilola, K., Andersson, P., et al. (2021). A regime shift toward a more anoxic environment in a eutrophic sea in northern Europe. *Frontiers in Marine Science*, *8*, 799936. https://doi.org/10.3389/fmars.2021.799936

Arneborg, L. (2016). Comment on "Influence of sea level rise on the dynamics of salt inflows in the Baltic Sea" by R. Hordoir, L. Axell, U. Löptien, H. Dietze, and I. Kuznetsov. *Journal of Geophysical Research: Oceans*, *121*(3), 2035–2040. https://doi.org/10.1002/2015JC011451

Belkin, I. M. (2009). Rapid warming of large marine ecosystems. *Progress in Oceanography*, *81*(1–4), 207–213. https://doi.org/10.1016/j.pocean.2009.04.011

Börgel, F., Frauen, C., Neumann, T., Schimanke, S., & Meier, H. E. M. (2018). Impact of the Atlantic multidecadal oscillation on Baltic Sea variability. *Geophysical Research Letters*, *45*(18), 9880–9888. https://doi.org/10.1029/2018GL078943

Burchard, H., Bolding, K., Feistel, R., Gräwe, U., Klingbeil, K., MacCready, P., et al. (2018). The Knudsen theorem and the total exchange flow analysis framework applied to the Baltic Sea. *Progress in Oceanography*, *165*, 268–286. https://doi.org/10.1016/j.pocean.2018.04.004

Coumou, D., Lehmann, J., & Beckmann, J. (2015). The weakening summer circulation in the Northern Hemisphere mid-latitudes. *Science*, *348*(6232), 324–327. https://doi.org/10.1126/science.1261768

Dutheil, C., Meier, H. E. M., Gröger, M., & Börgel, F. (2022a). Understanding past and future sea surface temperature trends in the Baltic Sea. *Climate Dynamics*, *58*(11–12), 3021–3039. https://doi.org/10.1007/s00382-021-06084-1

Dutheil, C., Meier, H. E. M., Gröger, M., & Börgel, F. (2022b). Warming of Baltic Sea water masses since 1850. *Climate Dynamics*. https://doi.org/10.1007/s00382-022-06628-z

Elken, J. (Ed.) (1996)., *Deep water overflow, circulation and vertical exange in the Baltic Prober*. Estonian Marine Institute Report Series, 6, Tallinn.

Feistel, R., Nausch, G., & Hagen, E. (2006). Unusual Baltic inflow activity in 2002–2003 and varying deep-water properties. *Oceanologia*, *48*(S), 21–35.

Feistel, R., Nausch, G., Mohrholz, V., Lysiak-Pastuszak, A., Seifert, T., Matthäus, W., et al. (2003). Warm waters of summer 2002 in the deep Baltic Proper. *Oceanologia*, *45*(4), 571–592.

Fischer, H., & Matthäus, W. (1996). The importance of the Drogden sill in the Sound for major Baltic inflows. *Journal of Marine Systems*, *9*(3–4), 137–157. https://doi.org/10.1016/S0924-7963(96)00046-2

Gräwe, U., Klingbeil, K., Kelln, J., & Dangendorf, S. (2019). Decomposing mean sea level rise in a semi-enclosed basin, the Baltic Sea. *Journal of Climate*, *32*(11), 3089–3108. https://doi.org/10.1175/JCLI-D-18-0174.1

Hinrichsen, H.-H., Piatkowski, U., & Jaspers, C. (2022). Sightings of extraordinary marine species in the SW Baltic Sea linked to saline water inflows. *Journal of Sea Research*, *181*, 102175. https://doi.org/10.1016/j.seares.2022.102175

Hofmeister, R., Beckers, J.-M., & Burchard, H. (2011). Realistic modelling of the exceptional inflows into the central Baltic Sea in 2003 using terrain-following coordinates. *Ocean Modelling*, *39*(3–4), 233–247. https://doi.org/10.1016/j.ocemod.2011.04.007

Hordoir, R., Axell, L., Löptien, U., Dietze, H., & Kuznetsov, I. (2015). Influence of sea level rise on the dynamics of salt inflows in the Baltic Sea. *Journal of Geophysical Research: Oceans*, *120*(10), 6653–6668. https://doi.org/10.1002/2014JC010642

Hünicke, B., & Zorita, E. (2008). Trends in the amplitude of Baltic Sea level annual cycle. *Tellus A: Dynamic Meteorology and Oceanography*, *60*(1), 154–164. https://doi.org/10.1111/j.1600-0870.2007.00277.x

ICES. (2023). ICES oceanography [Dataset]. ICES. Retrieved from https://www.ices.dk/data/data-portals/Pages/ocean.aspx

IOW. (2023). *GETM—A 3D hydrodynamic model for coastal oceans*. Leibniz Institute for Baltic Sea Research Warnemünde. Retrieved from https://getm.eu/

IPCC. (2021). *Climate Change 2021: The physical science basis. Contribution of working group I to the sixth assessment report of the intergovernmental panel on climate change*. Cambridge University Press. Retrieved from https://report.ipcc.ch/ar6/wg1/IPCC_AR6_WGI_FullReport.pdf

Kniebusch, M., Meier, H. E. M., Neumann, T., & Börgel, F. (2019). Temperature variability of the Baltic Sea since 1850 and attribution to atmospheric forcing variables. *Journal of Geophysical Research: Oceans*, *124*(6), 4168–4187. https://doi.org/10.1029/2018JC013948

Kniebusch, M., Meier, H. E. M., & Radtke, H. (2019). Changing salinity gradients in the Baltic Sea as a consequence of altered freshwater budgets. *Geophysical Research Letters*, *46*(16), 9739–9747. https://doi.org/10.1029/2019GL083902

Krapf, K., Naumann, M., Dutheil, C., & Meier, H. E. M. (2022). Investigating hypoxic and euxinic area changes based on various datasets from the Baltic Sea. *Frontiers in Marine Science*, *9*, 823476. https://doi.org/10.3389/fmars.2022.823476

Lass, H., & Matthäus, W. (1996). On temporal wind variations forcing salt water inflows into the Baltic Sea. *Tellus A: Dynamic Meteorology and Oceanography*, *48*(5), 663–671. https://doi.org/10.3402/tellusa.v48i5.12163

Laufkötter, C., John, J. G., Stock, C. A., & Dunne, J. P. (2017). Temperature and oxygen dependence of the remineralization of organic matter. *Global Biogeochemical Cycles*, *31*(7), 1038–1050. https://doi.org/10.1002/2017GB005643

Lehmann, A., Myrberg, K., Post, P., Chubarenko, I., Dailidiene, I., Hinrichsen, H.-H., et al. (2022). Salinity dynamics of the Baltic Sea. *Earth System Dynamics*, *13*(1), 373–392. https://doi.org/10.5194/esd-13-373-2022

Liblik, T., & Lips, U. (2019). Stratification has strengthened in the Baltic Sea—An analysis of 35 years of observational data. *Frontiers in Earth Science*, *7*, 174. https://doi.org/10.3389/feart.2019.00174

MacCready, P. (2011). Calculating estuarine exchange flow using isohaline coordinates. *Journal of Physical Oceanography*, *41*(6), 1116–1124. https://doi.org/10.1175/2011JPO4517.1

Matthäus, W., & Franck, H. (1992). Characteristics of major Baltic inflows—A statistical analysis. *Continental Shelf Research*, *12*(12), 1375–1400. https://doi.org/10.1016/0278-4343(92)90060-W

Meier, H. E. M., Dieterich, C., & Gröger, M. (2021). Natural variability is a large source of uncertainty in future projections of hypoxia in the Baltic Sea. *Communications Earth & Environment*, *2*(1), 50. https://doi.org/10.1038/s43247-021-00115-9

Meier, H. E. M., Eilola, K., Almroth-Rosell, E., Schimanke, S., Kniebusch, M., Höglund, A., et al. (2019). Disentangling the impact of nutrient load and climate changes on Baltic Sea hypoxia and eutrophication since 1850. *Climate Dynamics*, *53*(1–2), 1145–1166. https://doi.org/10.1007/s00382-018-4296-y

Meier, H. E. M., Höglund, A., Eilola, K., & Almroth-Rosell, E. (2017). Impact of accelerated future global mean sea level rise on hypoxia in the Baltic Sea. *Climate Dynamics*, *49*(1–2), 163–172. https://doi.org/10.1007/s00382-016-3333-y

Meier, H. E. M., & Kauker, F. (2003a). Modeling decadal variability of the Baltic Sea: 2. Role of freshwater inflow and large-scale atmospheric circulation for salinity. *Journal of Geophysical Research*, *108*(C11), 3368. https://doi.org/10.1029/2003JC001799
Meier, H. E. M., & Kauker, F. (2003b). Sensitivity of the Baltic Sea salinity to the freshwater supply. *Climate Research*, *24*, 231–242. https://doi.org/10.3354/cr024231
Meier, H. E. M., Kniebusch, M., Dieterich, C., Gröger, M., Zorita, E., Elmgren, R., et al. (2022). Climate change in the Baltic Sea region: A summary. *Earth System Dynamics*, *13*(1), 457–593. https://doi.org/10.5194/esd-13-457-2022
Mohrholz, V. (2018a). Baltic saline barotropic inflows (SBI) 1887–2018 [Dataset]. Leibniz Institute for Baltic Sea Research Warnemünde. https://doi.org/10.12754/data-2018-0004
Mohrholz, V. (2018b). Major Baltic inflow statistics—Revised. *Frontiers in Marine Science*, *5*, 384. https://doi.org/10.3389/fmars.2018.00384
Mohrholz, V., Dutz, J., & Kraus, G. (2006). The impact of exceptionally warm summer inflow events on the environmental conditions in the Bornholm Basin. *Journal of Marine Systems*, *60*(3–4), 285–301. https://doi.org/10.1016/j.jmarsys.2005.10.002
Mohrholz, V., Naumann, M., Nausch, G., Krüger, S., & Gräwe, U. (2015). Fresh oxygen for the Baltic Sea—An exceptional saline inflow after a decade of stagnation. *Journal of Marine Systems*, *148*, 152–166. https://doi.org/10.1016/j.jmarsys.2015.03.005
Ni, W., Li, M., Ross, A. C., & Najjar, R. G. (2019). Large projected decline in dissolved oxygen in a eutrophic estuary due to climate change. *Journal of Geophysical Research: Oceans*, *124*(11), 8271–8289. https://doi.org/10.1029/2019JC015274
Radtke, H., Brunnabend, S.-E., Gräwe, U., & Meier, H. E. M. (2020). Investigating interdecadal salinity changes in the Baltic Sea in a 1850–2008 hindcast simulation. *Climate of the Past*, *16*(4), 1617–1642. https://doi.org/10.5194/cp-16-1617-2020
Saraiva, S., Meier, H. E. M., Andersson, H., Höglund, A., Dieterich, C., Gröger, M., et al. (2019). Uncertainties in projections of the Baltic Sea ecosystem driven by an ensemble of global climate models. *Frontiers in Earth Science*, *6*, 244. https://doi.org/10.3389/feart.2018.00244
Schenk, F., & Zorita, E. (2012). Reconstruction of high resolution atmospheric fields for Northern Europe using analog-upscaling. *Climate of the Past*, *8*(5), 1681–1703. https://doi.org/10.5194/cp-8-1681-2012
Schimanke, S., & Meier, H. E. M. (2016). Decadal-to-centennial variability of salinity in the Baltic Sea. *Journal of Climate*, *29*(20), 7173–7188. https://doi.org/10.1175/JCLI-D-15-0443.1
Schinke, H. (1996). Zu den Ursachen von Salzwassereinbrüchen in die Ostsee. *Meereswissenschaftliche Berichte*, *12*.
Stramska, M., Kowalewska-Kalkowska, H., & Świrgoń, M. (2013). Seasonal variability in the Baltic Sea level. *Oceanologia*, *55*(4), 787–807. https://doi.org/10.5697/oc.55-4.787
Tian, R., Cerco, C. F., Bhatt, G., Linker, L. C., & Shenk, G. W. (2022). Mechanisms controlling climate warming impact on the occurrence of hypoxia in Chesapeake Bay. *JAWRA Journal of the American Water Resources Association*, *58*(6), 855–875. https://doi.org/10.1111/1752-1688.12907
Väli, G., Meier, H. E. M., & Elken, J. (2013). Simulated halocline variability in the Baltic Sea and its impact on hypoxia during 1961–2007. *Journal of Geophysical Research: Oceans*, *118*(12), 6982–7000. https://doi.org/10.1002/2013JC009192
Walin, G. (1977). A theoretical framework for the description of estuaries. *Tellus A: Dynamic Meteorology and Oceanography*, *29*(2), 128. https://doi.org/10.3402/tellusa.v29i2.11337
Winsor, P., Rodhe, J., & Omstedt, A. (2001). Baltic Sea ocean climate: An analysis of 100 yr of hydrographic data with focus on the freshwater budget. *Climate Research*, *18*, 5–15. https://doi.org/10.3354/cr018005
Wolf, G. (1972). *Salzwassereinbrüche im Gebiet der westlichen Ostsee* (Vol. 29). Beiträge zur Meereskunde.

Supporting Information for "Changes in seasonality of saltwater inflows caused exceptional warming trends in the western Baltic Sea"

L. Barghorn[1], H. E. M. Meier[1], H. Radtke[1]

[1]Leibniz Institute for Baltic Sea Research Warnemünde, Rostock, Germany

Contents of this file

1. Figures S1 to S7

Figures

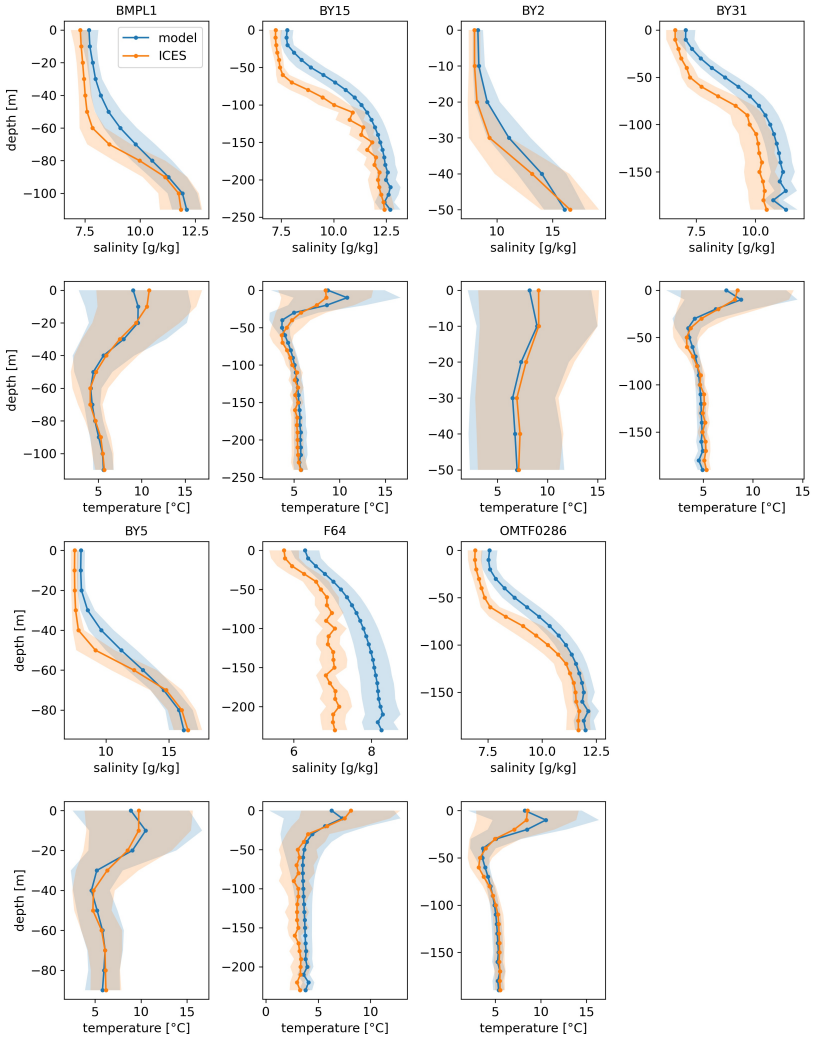

Figure S1. Observed and modeled salinity and temperature profiles averaged over the years 1970-2007 for selected stations. Observational data were taken from the ICES database (ICES, 2023). To increase the amount of observational data, profiles were taken from red rectangles around the stations depicted in Figure 1. Shaded areas indicate +/- one standard deviation.

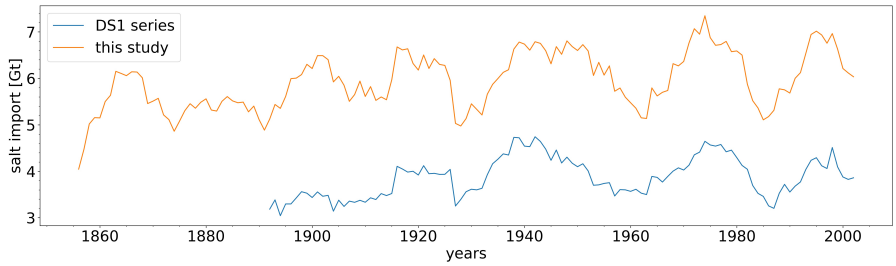

Figure S2. 11-year running means of annual salt import compared for modeled inflows and the DS1 series by Mohrholz (2018). The latter comprises all barotropic inflows which were registered both at Darss Sill and Drogden Sill.

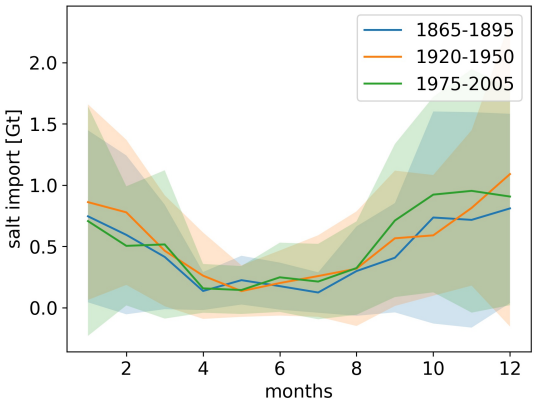

Figure S3. Monthly salt import averaged over three 30-year periods, respectively. Shaded areas depict +/- one standard deviation.

May 24, 2023, 6:59am

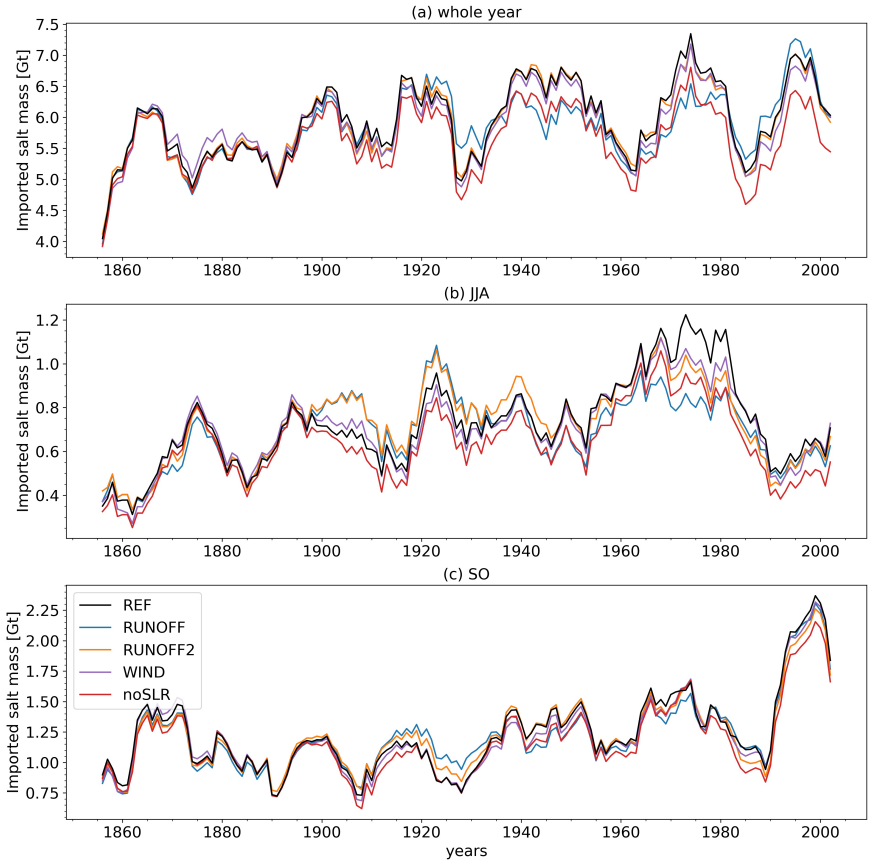

Figure S4. 11-year running means of (a) annual, (b) June - August (JJA) and (c) September - October (SO) salt import for reference simulation REF and sensitivity experiments RUNOFF, RUNOFF2, WIND and noSLR.

May 24, 2023, 6:59am

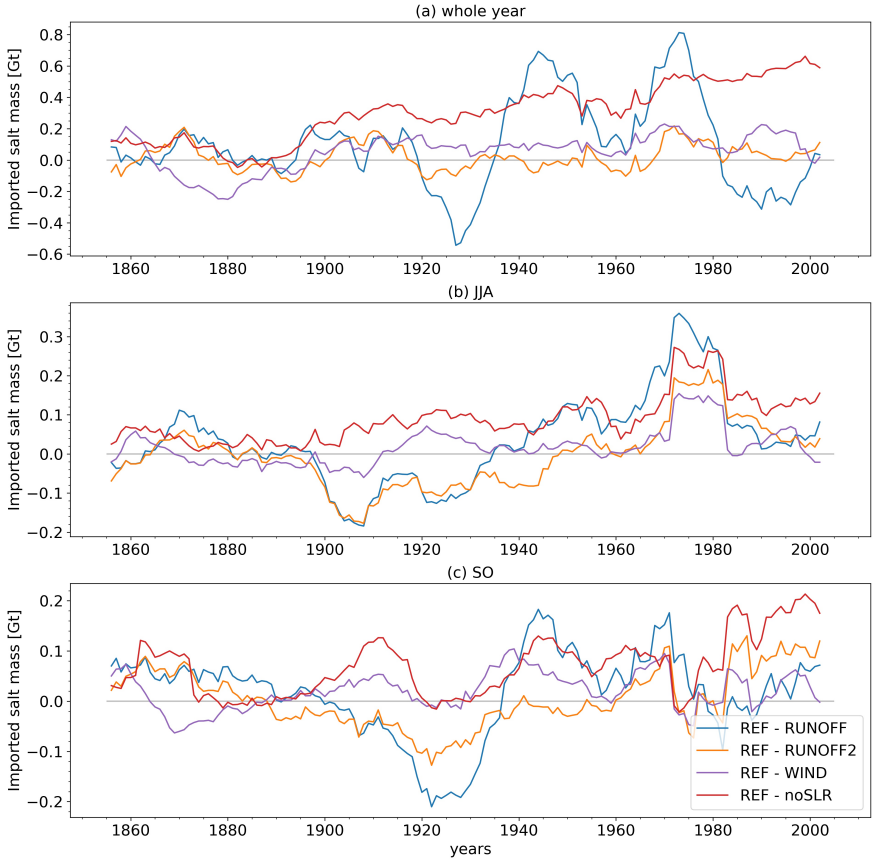

Figure S5. Differences in 11-year running mean salt import per (a) year, (b) June - August (JJA) and (c) September - October (SO) between the reference simulation and sensitivity experiments.

May 24, 2023, 6:59am

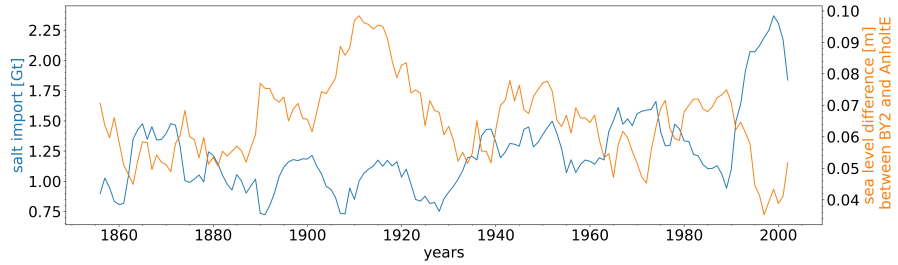

Figure S6. 11-year running means of September - October (SO) salt import and sea level difference between the stations BY2 (Arkona Basin) and AnholtE (Kattegat). For the locations, see Figure 1.

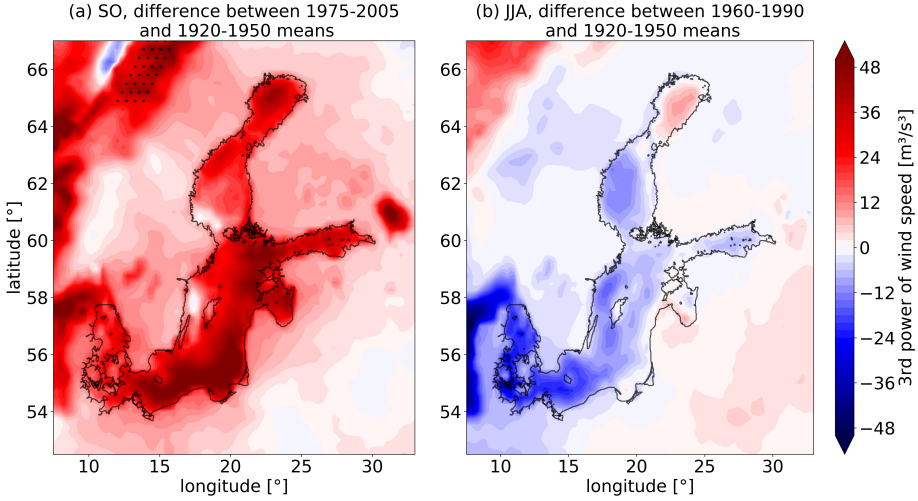

Figure S7. Differences in third power of wind speed from model forcing between 30-year periods with low (1920-1950) and high (1975-2005 for September - October and 1960-1990 for June - August) salt import: (a) for September - October (SO), (b) for June - August (JJA). Black dots indicate where changes are significant according to a Student's t test with a significance level of 0.95. Black lines show coastlines and open boundary in the Kattegat from the model bathymetry (Figure 1).

References

ICES. (2023). *ICES Oceanography [Dataset].* Retrieved from https://www.ices.dk/data/data-portals/Pages/ocean.aspx

Mohrholz, V. (2018). *Baltic saline barotropic inflows (SBI) 1887 - 2018 [Dataset].* Leibniz Institute for Baltic Sea Research Warnemünde. Retrieved from http://doi.io-warnemuende.de/10.12754/data-2018-0004

Climate Dynamics (2025) 63:29
https://doi.org/10.1007/s00382-024-07501-x

ORIGINAL ARTICLE

Warm saltwater inflows strengthen oxygen depletion in the western Baltic Sea

Leonie Barghorn[1] · H. E. Markus Meier[1] · Hagen Radtke[1] · Thomas Neumann[1] · Lev Naumov[1]

Received: 2 April 2024 / Accepted: 18 October 2024

Abstract
Hypoxia is a major environmental threat for coastal seas, including the strongly-stratified Baltic Sea in northern Europe. There, a pronounced increase in nutrient loads since the 1950s led to the development of one of the largest hypoxic areas worldwide. So far, other drives of hypoxia, like the increase in water temperatures due to global warming, have been considered minor compared to eutrophication. We show, by analyzing 159-years long hindcast simulations of three different Baltic Sea models, that exceptional warming trends in deep water layers of the western Baltic Sea deteriorated the local oxygen conditions. The above-average warming is only to a small extent attributed directly to global warming, but mainly to a shift in the seasonality of saltwater inflows from the North Sea towards more warm summer and early autumn inflows. Hence, we identify a so far unknown driver of oxygen depletion in the western Baltic Sea with potentially serious ecological consequences.

Keywords Baltic Sea · Regional climate modeling · Climate change · Salinity dynamics · Hypoxia

1 Introduction

Many coastal systems around the globe are suffering from temporal or permanent oxygen deficiency. Some even developed anoxic zones where no metazoans can survive. Due to its severe impact on ecosystem functioning, hypoxia is considered to be one of the strongest environmental threats to coastal seas worldwide (Diaz and Rosenberg 2008; Vaquer-Sunyer and Duarte 2008; Conley et al. 2009; Fennel and Testa 2019). Oxygen depletion in a water body occurs when the oxygen supply through physical transport is lower than the oxygen consumption in biogeochemical processes like respiration or mineralization of organic matter. Coastal seas are often permanently or seasonally stratified due to freshwater input from rivers. This density stratification hampers the transport of oxygen from the well-ventilated surface layer to the water masses below the pycnocline. At the same time, the supply of organic matter is often high, causing elevated rates of oxygen consumption in the deep water layers and the sediments.

Some coastal systems like the Benguela Current system (Mohrholz et al. 2008) naturally receive a lot of nutrients (nitrogen and phosphorus) through upwelling, causing strong primary production and hence a large supply of organic matter which leads to the formation of oxygen minimum zones (Carr 2002). Other coastal seas, for instance the Chesapeake Bay (Hagy et al. 2004) or the Pearl River Estuary (Dai et al. 2006), saw a strengthening of oxygen depletion during the last decades due to an increased supply of nutrients from anthropogenic sources like fertilizers or wastewater. Rising temperatures because of global warming exacerbate hypoxia, since the oxygen solubility in warmer water is lower and at the same time primary production and oxygen consumption are higher (Meier et al. 2011; Laufkötter et al. 2017; Laurent et al. 2018; Ni et al. 2019; Tian et al. 2022). In some coastal systems, for example the Chesapeake Bay, climate change is also projected to increase the stratification due to changes in winter and spring river runoff, as well as sea level rise, which leads to stronger inflows of saline oceanic waters. This further limits the oxygen supply to the bottom layers (Hong and Shen 2012; Ni et al. 2019).

The Baltic Sea, a semi-enclosed and shallow brackish water basin in northern Europe (Fig. 1), developed one of

✉ Leonie Barghorn
leonie.barghorn@io-warnemuende.de

[1] Department of Physical Oceanography and Instrumentation, Leibniz Institute for Baltic Sea Research Warnemuende, Seestrasse 15, 18119 Rostock, Germany

Published online: 06 December 2024

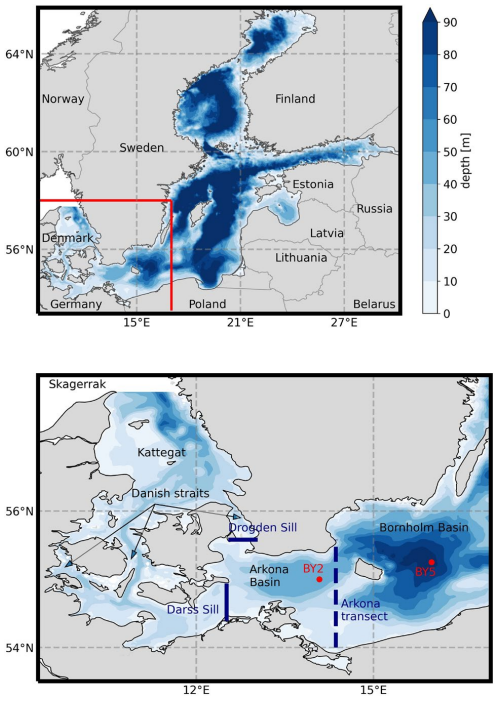

Fig. 1 Model domain and bathymetry of the GETM setup with zoom on the southwestern Baltic Sea. Blue lines denote transects for salt transport calculation. The dashed line indicates the eastern boundary of the Arkona Basin for the salt content calculations (S_{17}). Red dots show stations used for the analysis of deep-water temperatures and oxygen concentrations and the comparison with observational data. Note that depths above 100 m are not resolved by the color scale

the largest hypoxic areas worldwide due to a strong increase in nutrient inputs between the 1950s and 1980s (Gustafsson et al. 2012; Carstensen et al. 2014; Almroth-Rosell et al. 2021; Krapf et al. 2022). Like other coastal seas, the central basins of the Baltic Sea are naturally prone to hypoxia since they are permanently stratified with a pronounced halocline between 50 and 80 m depth (Stigebrandt 1987; Väli et al. 2013). The haline stratification in the Baltic Sea is primarily the result of two drivers: (1) freshwater supply (Winsor et al. 2001; Meier and Kauker 2003a, b), mainly by various rivers from a catchment area about four times as large as the Baltic Sea surface, and (2) the restricted water exchange with the North Sea through the narrow Danish straits with the shallow Drogden Sill (8 m deep) and Darss Sill (19 m deep, see Fig. 1) (Meier et al. 2023; Mohrholz 2018).

The water exchange is characterized by barotropic (wind-driven) or baroclinic (density-gradient-driven) inflows of highly saline water (e. g., Matthäus and Franck 1992; Feistel et al. 2006) which flow eastward along the bottom of the Baltic Sea due to the density gradient between the Danish straits and the central basins. These inflows are the main source of oxygen for the deep basins of the central Baltic Sea and only large so-called Major Baltic Inflows (MBIs) can sporadically ventilate the deepest water layers (Matthäus and Franck 1992). At the same time, the elevated bottom salinity after an MBI leads to a stronger stratification and a shallower halocline, which cause a growth of the hypoxic area in the period following an MBI (Conley et al. 2009; Väli et al. 2013; Almroth-Rosell et al. 2021). In addition, it has been shown that MBIs provide additional organic matter, thereby increasing the oxygen consumption (Meier et al. 2018; Hylén et al. 2021).

Since the 1980s, the nutrient loads in the Baltic Sea have decreased, but so far, the oxygen conditions have not measurably improved and the hypoxic area even reached its largest ever recorded extent in autumn 2018 (Hansson et al. 2019; Almroth-Rosell et al. 2021; Krapf et al. 2022). One reason is a positive feedback mechanism where anoxia stimulates the release of phosphorus from the sediments into the water column. Consequently, nitrogen fixation by cyanobacteria is enhanced, which then causes increased primary production (Vahtera et al. 2007). The impact of climate change on the oxygen conditions in the Baltic Sea is considered to be still small compared to the impact of past elevated nutrient inputs (Meier et al. 2018, 2019) and projections for the coming decades suffer from pronounced uncertainties, especially regarding changes in the water cycle, including the salinity dynamics (Saraiva et al. 2019; Meier et al. 2021). However, several studies have shown that higher bottom temperatures lead to stronger hypoxia, mainly via enhanced mineralization rates and lower oxygen solubility (Krapf et al. 2022; Börgel et al. 2023; Safonova et al. 2024).

An exceptionally high warming trend over the 20th century has been detected in the Bornholm Basin (see location in Fig. 1) (Mohrholz et al. 2006; Kniebusch et al. 2019a; Dutheil et al. 2022). It is almost 100 m deep, the westernmost basin of the central Baltic Sea, and one of the basins that are suffering from hypoxia (Carstensen et al. 2014; Almroth-Rosell et al. 2021; Krapf et al. 2022). A recent study has shown that a major cause of the warming was a shift in the seasonality of saltwater inflows (Barghorn et al. 2023). The main season for large barotropic inflows (MBIs) is between November and January since favorable meteorological conditions, namely a few weeks of easterly winds followed by a few weeks of westerly winds, are most likely to occur then (Matthäus and Franck 1992; Lass and Matthäus 1996; Mohrholz 2018). Smaller barotropic and baroclinic inflows, however, can occur throughout the year and Barghorn et al. (2023) noticed, by analyzing a long hindcast simulation of the Baltic Sea ranging from 1850 to 2008, that summer and early autumn (i. e., June–October)

inflows increased during the model period while winter salt import decreased. Summer and early autumn inflows transport warm surface water from the entrance area of the Baltic Sea to layers in or below the halocline in the central Baltic Sea, especially the Bornholm Basin. The reasons for this shift in inflow seasonality are not yet clear but probably, changes in atmospheric circulation and the seasonality of river runoff played a role.

In this study, the results by Barghorn et al. (2023), which were obtained with the General Estuarine Transport Model (GETM) (IOW 2023b), are revisited and compared to the results from similar hindcast simulations and sensitivity experiments of the Rossby Centre Ocean (RCO) model (Meier et al. 2003) and the Modular Ocean Model (MOM) (Griffies 2004). Other than GETM, these two models were run coupled to biogeochemical models: The Swedish Coastal and Ocean Biogeochemical (SCOBI) model (Eilola et al. 2009) in case of RCO and the Ecological Regional Ocean Model (ERGOM) (Neumann et al. 2022; IOW 2023a) in case of MOM. This allows to analyze the effect of the strong bottom warming on the oxygen conditions in the Bornholm Basin. Barghorn et al. (2023) suggested that the warm inflows might increase the oxygen depletion in the Bornholm Basin due to the above mentioned temperature dependence of dissolved oxygen. In addition, warm inflows are said to be mostly baroclinic (Feistel et al. 2006). This means that the water column in the Danish straits is stratified, while it is well-mixed during barotropic inflows (Wolf 1972; Matthäus and Franck 1992; Feistel et al. 2003). Hence, the ventilation of the highly saline bottom layer during baroclinic inflows might be hampered although most of the oxygen (up to 90%) provided by inflows does not originate from the Danish straits but is entrained on the way to the central Baltic Sea (Neumann et al. 2017). It is commonly assumed that warm inflows ventilate the affected basins at least to some extent, although they transport much less oxygen than MBIs (Feistel et al. 2006; Mohrholz et al. 2006; Neumann et al. 2017; Rak et al. 2020).

2 Methods

2.1 Ocean models

The key model characteristics, which are of importance for this study, are summarized in Table 1. All three models are 3-d ocean models. RCO and MOM are coupled to a Hibler-type sea ice model whereas GETM only includes a thermodynamic sea ice model. For our model runs, RCO and MOM are additionally coupled to biogeochemical models of the NPDZ type; SCOBI (Eilola et al. 2009) in case of RCO and ERGOM (Neumann et al. 2022; IOW 2023a) in case of MOM. All model domains include the whole Baltic Sea but while RCO and GETM have their open boundaries in the Northern Kattegat, as shown in Fig. 1, the model domain of MOM also includes the Skagerrak, where the North Sea starts and the water deepens towards the Norwegian trench. The horizontal resolution is highest for GETM (1 nautical mile), followed by RCO (2 nm) and MOM (3 nm). In the vertical direction, the discretization is quite different for the three models. RCO has 83 layers of 3 m thickness. MOM uses z^* coordinates with layer thicknesses increasing with depth from about 0.5 m at the surface up to 2 m in the deep basins. The exact depths are adjusted with each time step to the sea surface elevation. GETM employs adaptive vertical coordinates (Gräwe et al. 2019) which allow to increase the resolution for instance in regions with complex bathymetry or strong density gradients. The latter is very useful for simulating saltwater inflows (Hofmeister et al. 2011). MOM stores daily 3-d fields of temperature, salinity and oxygen. For RCO, snapshots are taken every other day. GETM writes out the daily salt transport across selected transects (see Figure S1 in the Supplementary information) and daily salinity and temperature values at certain stations, including those in Figure S1. In case of 3-d fields of temperature and salinity, only 5-day means are stored.

Detailed descriptions of the biogeochemical models can be found in Neumann et al. (2022) (ERGOM) and (Eilola

Table 1 Selected characteristics of the model setups used in this study

	GETM	RCO	MOM
Open boundary	Northern Kattegat	Northern Kattegat	Skagerrak
Grid	Arakawa-C	Arakawa-B	Arakawa-B
Horizontal resolution	1 nm	2 nm	3 nm
Vertical resolution	50 layers of adaptive coordinates	83 layers of 3 m thickness	152 layers, thickness increasing towards depth from 0.5 to 2 m
Temporal resolution	Daily for transects and stations 5-daily for 3-d fields	2-daily snapshots	Daily
Biogeochemical model	None	SCOBI	ERGOM

et al. 2009) (SCOBI). Both models apply the Q10 rule (Laufkötter et al. 2017) to describe the temperature sensitivity of mineralization.

2.1.1 Atmospheric forcing, river runoff, and boundary conditions

All three models are forced for the period 1850-2008 by the HiResAFF (High Resolution Atmospheric Forcing Fields) v2 data set which was compiled using the analogue method (Schenk and Zorita 2012). Both GETM and MOM apply a strong wind correction. In case of GETM, the correction is given in Radtke et al. (2020). In MOM, a gust correction following Brasseur (2001) is applied.

The river runoff (provided in monthly resolution) is similar for all models and a compilation of different data as described in Meier et al. (2019).

The lateral boundary conditions of GETM and RCO are described in Meier et al. (2019). At the open boundary of MOM in the Skagerrak, we prescribe climatological data derived from Janssen et al. (1999) for temperature and salinity, and from previous model simulations for the biogeochemical variables. Sea level elevation is estimated from the meteorological forcing by a statistical model.

2.1.2 Initialization

Spin up and initial conditions differ between the models. For GETM, observational data from 1979 are interpolated to the model grid and used as initial conditions (Radtke et al. 2020). The first 30 years of the simulation are considered as a spin up. In case of RCO, the initialization includes 52 years of spin up and is described in Meier et al. (2019). The initial conditions for the MOM runs are found in a 30-year spin up period.

2.1.3 Sensitivity experiments

The main drivers of salinity dynamics in the Baltic Sea are river runoff, wind variations and the global mean sea level rise. To investigate the impact of these drivers on the salt import, sensitivity experiments are analyzed. In a previous study (Barghorn et al. 2023), it was found that summer and early autumn inflows show the strongest change in the experiments with climatological mean runoff, while removing the low-frequency variability in the wind field did not have any effect. When sea level rise was removed, inflows were reduced in all seasons. Here, we compare the experiments with modified runoff and sea level rise of the different models to see whether the findings of Barghorn et al. (2023) are robust. In addition, an RCO experiment with a constant seasonal cycle in atmospheric temperatures is added to disentangle the effects of changing inflow seasonality and increasing air / sea surface temperatures due to global warming on the deep-water temperatures in the Bornholm Basin. The experiments used in this study are listed in Table 2. More detailed descriptions of the GETM sensitivity experiments are found in Barghorn et al. (2023) and in case of RCO for instance in Meier et al. (2019, 2023).

2.2 Observational data

For the evaluation of the model runs, temperature and salinity at selected stations are compared with observational data from the ICES data base (ICES 2023). To increase the data coverage, the observational data are not only taken directly from the stations but from rectangles of $0.4 - 1\,^{\circ}$ size around the stations (see Figure S1 in the supplementary information). For the time series of observed annual bottom and surface salinity, a seasonal bias correction is performed as in Radtke et al. (2020) by applying the General Additive Mixed Model (GAMM) framework (Simpson 2014). Values for the surface salinity time series are taken from the upper 20 m

Table 2 Sensitivity experiments

Model	Experiment	Description
GETM	REF+	Reference simulation with global mean sea level rise
	REF	Reference simulation without sea level rise
	RUNOFF+	Climatological mean runoff repeated for each year, with sea level rise
RCO	REF+	Reference simulation with sea level rise
	REF	Reference simulation without sea level rise
	RUNOFF+	Climatological mean runoff repeated for each year, with sea level rise
	TAIR	Air temperatures and specific humidities of 1904 repeated for each year
		No sea level rise
MOM	REF	Reference simulation without sea level rise
	RUNOFF	Climatological mean runoff, no sea level rise

Note that the labels for the GETM experiments differ from those in Barghorn et al. (2023) to match those of the RCO experiments

while the bottom values include the lowest 10% of the water column, respectively. The quality of the modeled salinity time series is assessed by computing the explained variances as defined in Good and Fletcher (1981) and already applied in Radtke et al. (2020) to GETM. For the validation of the oxygen concentrations in the Bornholm Basin (station BY5; see Fig. 1), values at 80 m depth are used instead of the bottom values, as 80 m is the largest depth with a high coverage of oxygen measurements.

2.3 Quantification of salt import

In Barghorn et al. (2023), saltwater inflows were detected by calculating the salinity-discriminated salt transport over Darss Sill and Drogden Sill transects (see Fig. 1). That method cannot be applied in this study since the temporal resolution of RCO outputs (2-daily snapshots) is too low to capture the highly variable currents over the sills. Therefore, the salt content in water masses with a salinity higher than 17 g/kg in the Arkona Basin (S_{17}) is used as a measure for the salt import. A similar method was successfully applied in Meier and Kauker (2003a) and Dutheil et al. (2022). In contrast to these two publications, no thresholds for a minimum volume or persistence of such a highly saline volume are applied since the focus is not on individual inflows but rather on their multidecadal variability.

The boundaries of the Arkona Basin used for the calculations are the Drogden Sill and Darss Sill in the west and the beginning of the deepening towards the Bornholm Basin in the east (dashed line in Fig. 1). The eastern boundary is necessary because if highly saline water masses enter the Bornholm Basin through the Bornholm Gate, they partly stay there for several months before eventually leaving the basin across the Slupsk Sill further east or diluting by mixing with ambient water masses (e. g., Feistel et al. 2004). Thus, we found that especially after very strong inflows like the one in 1951, the seasonal variations in salt import would not be captured (not shown). In contrast to that, the residence time of inflowing water in the Arkona Basin is usually between a few weeks and 2 months (Gräwe et al. 2015), probably because it is more shallow and only bounded by a shallow sill of about 5 m height in the east (Feistel et al. 2003).

To calculate the salt content of a grid cell based on its salinity, the density of that specific water parcel has to be computed. This is done with the package GSW-Python (TEOS-10 2017) which implements the Thermodynamic Equation of Seawater 2010 (TEOS-10) (JCS 2010). The resulting time series for S_{17} are compared with the salt transport in highly saline water masses (i.e., $S \geq 17$g/kg) over the Darss Sill and Drogden Sill transects obtained with GETM (See Section S2.2 in the supplementary information and Figures S7–S9 therein).

2.4 Correlations

Correlations between two time series are computed as Pearson correlation coefficients. Any long-term linear trends (for instance in the oxygen concentrations) are removed beforehand. In order to determine the degrees of freedom, we analyzed the autocorrelation functions of the respective time series after removing linear trends. We found no significant autocorrelation after year zero for S_{17}, but in case of temperature and oxygen values at station BY5, the time series of annual means or extreme values are significantly autocorrelated at lag-1 (not shown). Hence, for these time series, the number of degrees of freedom is reduced by one.

2.5 Composites

Composite analyses are used to quantify differences between seasons with large and small warm inflows (Sect. 3.4) and between summer and winter seasons with large inflows (Sect. 3.5). In either case, seasons with large inflows are defined as seasons where S_{17} was above the 90th percentile. Correspondingly, seasons with small inflows are defined as seasons where S_{17} was below the 10th percentile. In the composite analyses, all involved time series are linearly detrended. P-values are computed with Mann–Whitney U tests.

2.6 Apparent oxygen utilization

The apparent oxygen utilization (AOU) is defined as the difference between the oxygen saturation concentration at a specific temperature and salinity and the actual oxygen concentration. The oxygen saturation concentration is determined following Garcia and Gordon (1992) with the package GSW-Python (TEOS-10 2017).

2.7 Oxygen budget

The oxygen consumption in the water column and the sediments of the Bornholm Basin is assessed by calculating the oxygen budget following Naumov et al. (2023). They assembled all physical and biochemical sources and sinks of oxygen for MOM/ERGOM in the basin below 70 m. Here, we raise the upper boundary to 60 m to also account for inflows that interleave in or just below the halocline. The terms of the final oxygen budget are split into physical processes (advection and diffusion into and out of the volume), biochemical processes in the water column and biochemical processes in the sediment. The biochemical processes comprise oxygen sources (photosynthesis) and sinks (respiration, mineralization of organic matter, nitrification, coupled nitrification/denitrification, oxidation of reduced material). At the depths considered here, photosynthesis and respiration

by living organisms are negligible, while the biggest oxygen sink is the mineralization of detritus in the sediments (Naumov et al. 2023). In the final budget, source terms are expressed as positive and sink terms as negative oxygen rates. A detailed list of all biochemical processes included in ERGOM is given in Neumann et al. (2022).

3 Results

3.1 Model validation

For validating the models, salinity and temperature profiles as well as time series of bottom and surface salinity are compared to observational data (see supplementary information, Figures S2–S4 and Section 1 therein). The latter were processed following the steps described in Sect. 2.2.

It can be concluded that the models simulate salinities and temperatures well enough for our study at least from 1900 onward (due to the drift in MOM in the first decades). In any case, this study focuses on the period after 1920 due to shortcomings in the river runoff data before that year (Meier et al. 2019; Kniebusch et al. 2019b; Barghorn et al. 2023). Namely, all correlations and trends (if not given differently) were computed from 1920 onward and for MOM, the years before 1920 are not shown in the salinity plots.

Figure 2 shows Taylor diagrams of bottom salinities, bottom temperatures and oxygen concentrations at 80 m at

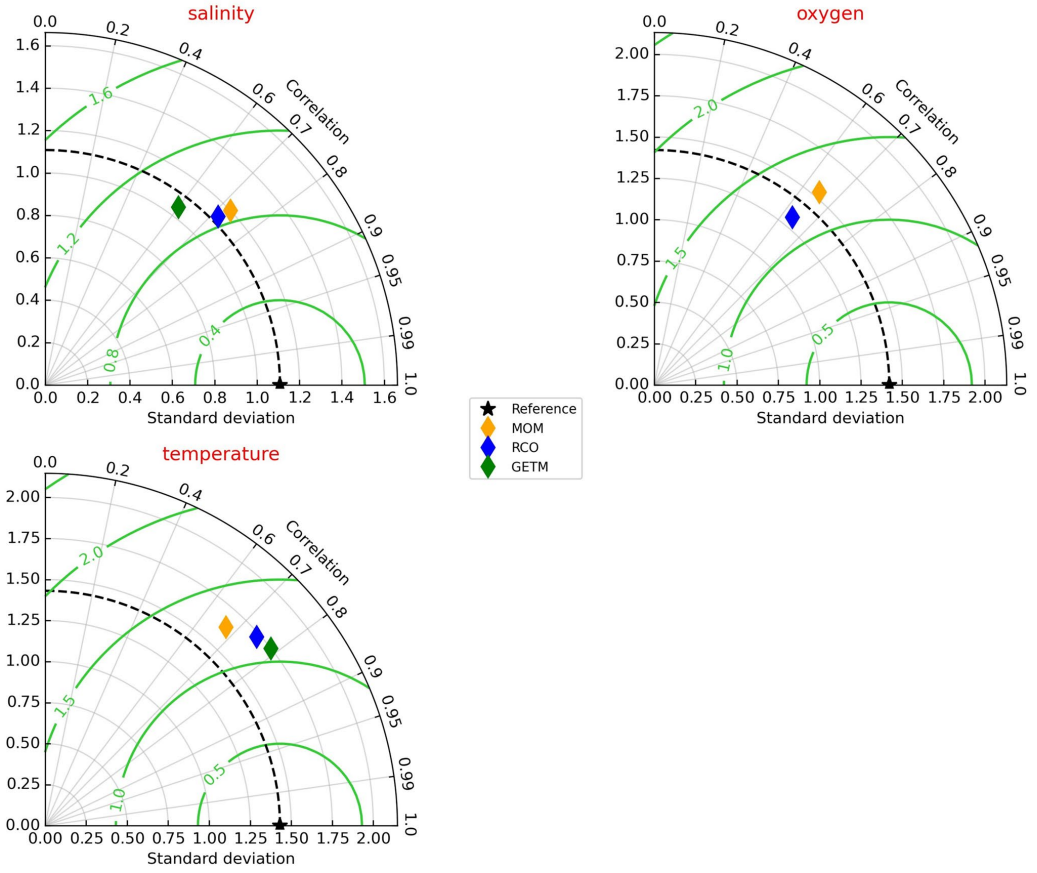

Fig. 2 Taylor diagrams of bottom salinities, bottom temperatures and oxygen concentrations at 80 m at station BY5 (for location see Fig. 1). All coefficients were computed from annual means ranging from 1920 to 2008, leaving out years with gaps in the observations. The reference is the observational data. Green contours display centered root mean square errors of the model data

station BY5 (for location see Fig. 1). All coefficients were computed from annual means ranging from 1920 to 2008. The figure shows that the models agree quite well among each other and have fairly high correlations with and similar standard deviations compared to the observational data. The corresponding time series for temperature and oxygen are depicted in Figure S5 in the supplementary information. One can see that the oxygen concentrations are overestimated in both models, but for both temperatures and oxygen concentrations the long-term trends are comparable to the observations.

3.2 Model comparison

The output of the three different models is compared regarding saltwater inflow variability and seasonality, the dependence of the latter on variations in river runoff and global mean sea level rise, and the correlation between warm inflows and the annual deep-water temperature maximum T_{max} in the Bornholm Basin. The results can be found in Section S2 in the supplementary information (Figures S6-S12) and in Figure S13. All in all, the models yield similar results, namely the increase of summer (June–August; JJA) and early autumn (September–October; SO) inflows over the model period and in particular an increase of early autumn inflows since 1920 (Figures S10, S11, and S13). In addition, summer and early autumn salt import is highly correlated with T_{max} (Figure S12). It is also shown that S_{17} describes the inflow variability very well (Figures S7–S9).

As an example, Fig. 3 displays the main results of the analysis for RCO. The upper panel shows annual and seasonal trends in S_{17} from the reference simulations with (REF+) and without (REF) sea level rise and the experiment RUNOFF+ with climatological mean runoff. It reflects what Barghorn et al. (2023) found for GETM, namely that the trends are less positive / more negative in REF and RUNOFF+. The lower panel shows the June–October (JJASO) mean S_{17} and its correlation with T_{max} at station BY5. As mentioned above, the correlation is quite high, indicating

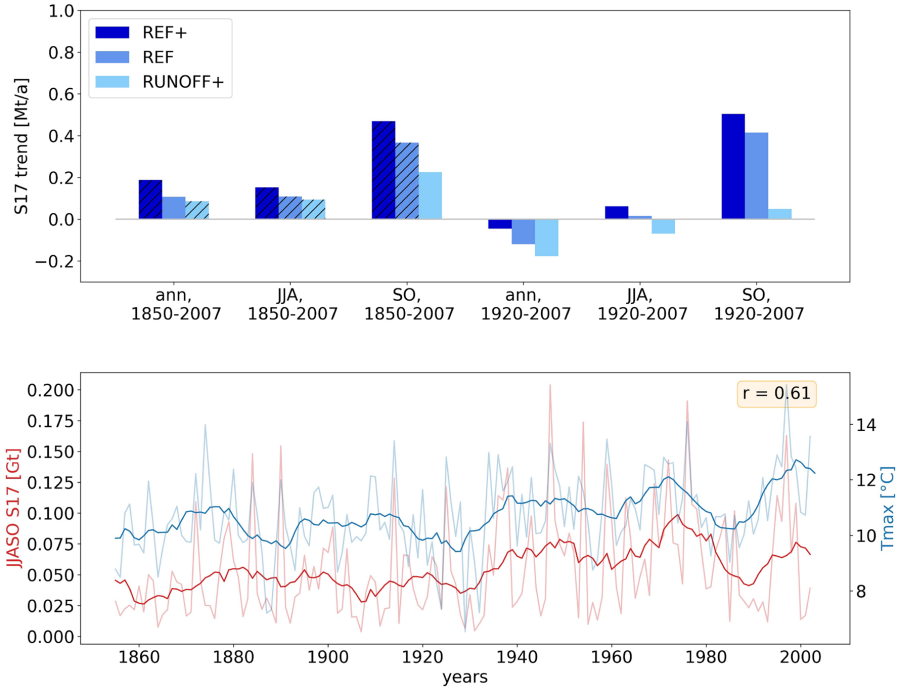

Fig. 3 Results obtained with RCO. Top panel: Annual and seasonal trends in S_{17} from the reference simulations with (REF+) and without (REF) sea level rise and the experiment RUNOFF+ with climatological mean runoff. Hatched bars indicate significant trends with p-values below 0.05. Bottom panel: Annual and smoothed time series of June–October (JJASO) mean S_{17} vs the annual temperature maximum below the seasonal thermocline at station BY5 (T_{max}). The yellow box displays the Pearson correlation coefficient

that warm inflows have an important impact on the deep-water temperatures in the Bornholm Basin.

3.3 Disentangling the drivers of temperature increase in the Bornholm Basin

Despite the relatively high correlation coefficients between June-October (JJASO) means of S_{17} and T_{max} (Figs. 3 and S12), there is still a possibility that the exceptional warming was only to the minor extent caused by a shift in inflow seasonality and is primarily related to the strong surface warming in the western Baltic Sea (Kattegat / Danish straits), as those water masses are the origin of the saltwater inflows. To disentangle the impact of sea surface warming and increase in warm inflows, we analyze the sensitivity experiment TAIR in RCO, where the atmospheric temperatures and specific humidities of 1904 were repeated in each year of the model period. As shown in the upper panel of Fig. 4, the positive trend in T_{max} is less strong than in the reference simulation but still significant. The lower panel shows that (as in the reference simulations) there is a quite high significant correlation of 0.66 between S_{17} for JJASO and T_{max} in TAIR as well. This confirms that the exceptional warming in the deep water layers of the Bornholm Basin was mainly caused by a shift in salt import seasonality.

3.4 Impact of warming on the oxygen content

For RCO and MOM, annual means of oxygen and temperature averaged between 60 m depth and the bottom (approx. 95 m) at station BY5 are compared (see Figure S14 in the supplementary information). The depth range has been chosen as the range below the halocline, where ventilation from above is strongly restricted. One can see that both the original and the smoothed curves are anticorrelated, respectively. The resulting correlation coefficients amount to −0.69 for RCO and −0.79 in case of MOM. Hence, we can assume that the increase in warm inflows intensified hypoxia in the Bornholm Basin.

However, we have to exclude the possibility that an intensified stratification contributed to strengthened bottom hypoxia by hampering the ventilation from above. Monthly trends in stratification (defined here as bottom minus surface density) between 1920 and 2008 are negative for all models and months (not shown), i.e., changes in stratification should rather have improved than worsened the oxygen conditions. Finally, we also compare the deep water temperatures and oxygen concentrations in the Bornholm Basin for the RCO experiments REF (Figure S14) and REF+ (not shown) to check whether the sea level rise had an impact on deep water warming and / or the oxygen conditions. The results are almost identical. This makes sense as sea level rise causes

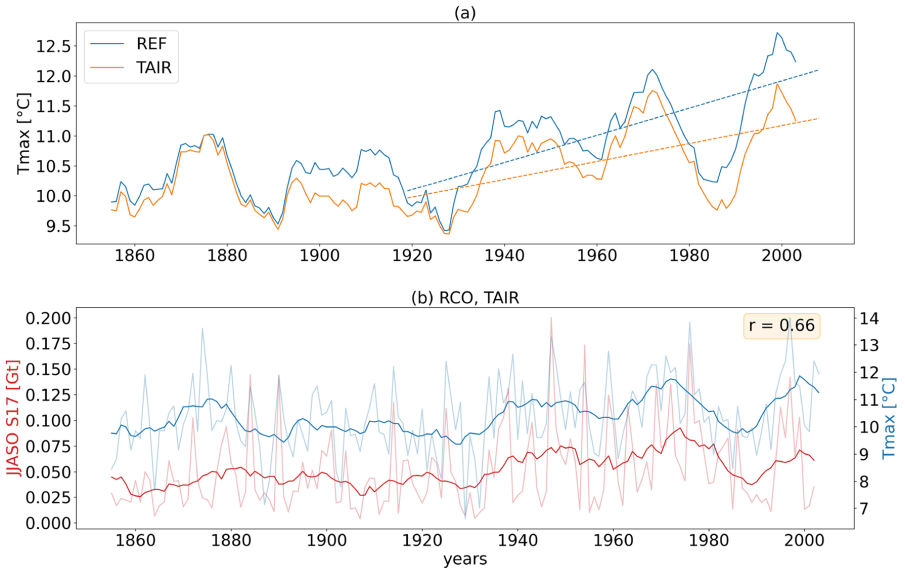

Fig. 4 (a) Smoothed time series of T_{max} for the RCO simulations REF and TAIR. Dashed lines indicate linear trends from 1920 onward. (b) Annual and smoothed time series of JJASO mean S_{17} vs T_{max} for TAIR. The yellow box displays the Pearson correlation coefficient between the two non-smoothed time series from 1920 onward. The p-value is of the order 1e-12

stronger inflows throughout the year, but no change in their seasonality (Barghorn et al. 2023), and consequently also no change in the overall heat transport.

To further prove the suspected connection between the shift in inflow seasonality and deep-water temperatures as well as oxygen conditions in the Bornholm Basin, we compute the differences in the annual mean temperature below 60 m (T_{60}) and the annual minimum of dissolved oxygen ($DO_{\min}$) at station BY5 between years with very high and very low JJASO mean S_{17} (see Sect. 2.5 for the description of the method). The result in Fig. 5 shows that especially in the "lag-1" case, i. e., when T_{60} and $DO_{\min}$ are taken from the year following the extreme event in S_{17}, the differences are substantial. All differences in Fig. 5 are significant with p-values of 0.03 or lower.

3.5 Oxygen dynamics during warm inflows

Two main mechanisms could explain the observed effect of warm inflows on the ventilation of the Bornholm Basin. First of all, the warm inflows themselves could transport less oxygen. Secondly, the higher temperatures in the Bornholm Basin after a warm inflow could lead to a stronger oxygen consumption. We examine these possible reasons with the help of the reference simulation of MOM. First, we compare the mean oxygen concentrations in the highly saline volume in the Arkona Basin for large inflows in June–October (JJASO) with those for large inflows in December–February (DJF). The mean oxygen concentration in large winter inflows is about 1.49 ml/l larger than that in large summer inflows (p-value below 0.001).

To explore, why the oxygen concentrations of warm inflows are lower than those of cold inflows, we compute the *AOU* of both inflow types. For MOM, it is found that *AOU* is higher in June–October than in December–February and there is also a stronger increase over the model period (not shown). However, the *AOU* differences between both seasons are not significant if only the seasons with large inflows (as defined in Sect. 2.5) are compared. Hence, we conclude that the lower oxygen concentrations in warm inflows are mainly related to the lower oxygen solubility and less to the higher oxygen consumption.

For the Bornholm Basin itself, we investigate the daily resolved oxygen content and temperature changes before, during and after the largest warm inflows (as previously defined). The top panel in Fig. 6 exemplary shows the autumn inflow in 1997 (the other inflows are depicted in the supplementary information in Figures S15–S22). Both mean temperatures and oxygen content are computed for the Bornholm Basin below 60 m depth. The correlation between both time series is close to − 1, i. e., the oxygen concent is mainly determined by the temperatures (as previously discussed for the Arkona Basin). Apparently, the inflowing water masses have similar or lower oxygen concentrations as the present water masses in the Bornholm Basin that they replace. This is quite different compared to MBIs like the ones in 2003 or 2014/15 that caused a substantial increase of the oxygen concentrations in the Bornholm Basin (Feistel et al. 2006; Rak et al. 2020).

Apart from the temperature dependence of the oxygen solubility, one also has to consider the temperature dependence of the oxygen consumption. Hence, we calculate oxygen budgets as described in Sect. 2.7. The resulting terms are plotted in the bottom panel of Fig. 6. Positive numbers indicate that oxygen is provided while negative numbers arise when oxygen is consumed. The clearest reaction to the temperature increase can be seen in the sedimentary processes where the oxygen consumption rises simultaneously with the temperature. When comparing both increases for all large warm inflows, a linear relation is found (Fig. 7). The linear trend amounts to 0.37 kt O_2 per day per °C with a p-value of 0.007 if the outlier in the top left corner is omitted. It belongs to the inflow in 1998 which is special in the sense that the ambient temperatures in the Bornholm Basin were

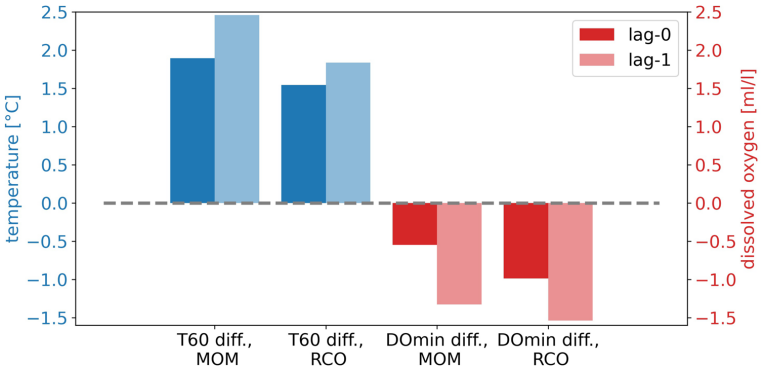

Fig. 5 Differences in the annual mean temperature below 60 m (T_{60}) and the annual oxygen minimum ($DO_{\min}$) at station BY5 between years with very high (≥ 90th percentile) and very low (≤ 10th percentile) JJASO mean S_{17}. "lag-0" means that both S_{17} and T_{60} or $DO_{\min}$ were taken from the same year. In case of "lag-1", T_{60} or $DO_{\min}$ were taken from the following year, respectively

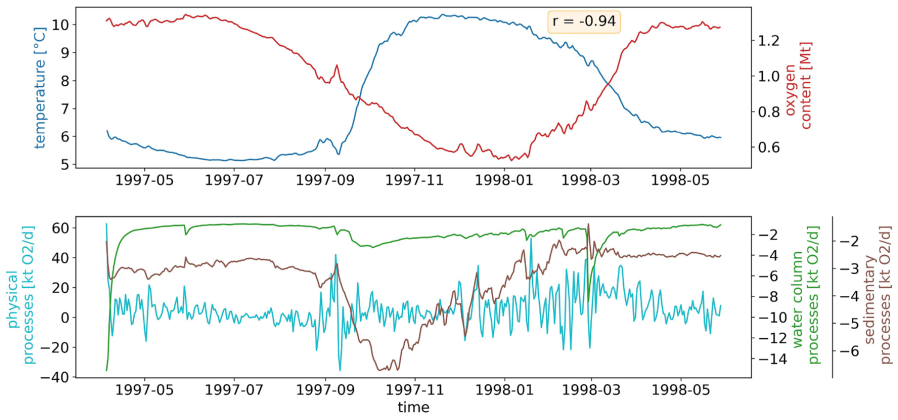

Fig. 6 Top panel: Mean temperature and oxygen content in the Bornholm Basin below 60 m. The yellow box displays the Pearson correlation coefficient between both time series. Bottom panel: Physical, water column and sedimentary processes of the oxygen budget of the Bornholm Basin below 60 m. Both panels show daily means of the MOM/ERGOM reference simulation

still quite high from the 1997 inflow. Hence, the temperature increase in late 1998 was rather small although the inflow was large in terms of S_{17}. A closer look into the individual processes that contribute to the oxygen consumption in the sediments reveals that the latter is strongly dominated by the mineralization of detritus. It should be noted that the connection between temperature and mineralization is exponential according to the Q10 rule implemented in ERGOM (Neumann et al. 2022), but in a limited temperature range, a linear approximation might be reasonable.

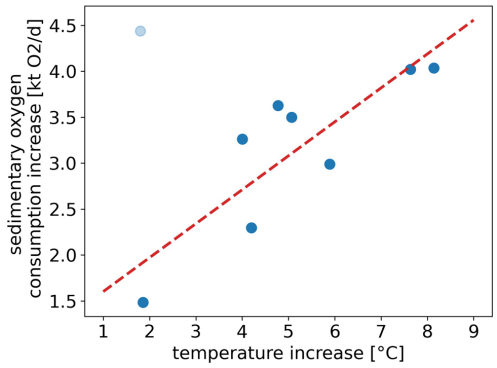

Fig. 7 Increase in sedimentary consumption versus temperature increase during a warm inflow (data from the MOM/ERGOM reference simulation). As for Fig. 5, the largest warm inflows were selected. The red dashed line depicts the linear regression which was calculated without the outlier in light blue in the upper left corner. Both increases were determined by computing the difference between the temperature / sedimentary consumption maximum at the end of the inflow and the "base value" on the first of May of the respective year (well before any inflow started)

To estimate the relative importance of the increase in the sedimentary consumption rate for the oxygen content in the Bornholm Basin, we can compare the trend in Fig. 7 with the corresponding changes in oxygen solubility and *AOU*. The total amount of oxygen that can be dissolved in the Bornholm Basin decreases by 306 kt per °C temperature increase, while *AOU* increases by 164 kt. Note, that *AOU* also incorporates the oxygen consumption that takes place in the inflowing water masses before they reach the Bornholm Basin. As sedimentary oxygen consumption is given as a daily rate, for the comparison with the other changes the timescale is important. Figures 6 and S15–S22 show that it can take many months before the sedimentary oxygen consumption rate turns back to its level before the warm inflow. Thus, the effect of the increased sedimentary oxygen consumption rate accumulates over time. As a simple example, if the rate is increased by 0.37 kt O_2 per day for five months (due to a one degree higher temperature), the total "excess" oxygen consumption already amounts to about 56 kt. Hence, the temperature dependence of the oxygen consumption in the sediments is an important factor.

4 Discussion

In this study, we have assessed the connections between summer inflows, high deep-water temperatures and oxygen depletion in the Bornholm Basin based on data from three Baltic Sea models. As our model validation has shown (Sects. 3.1 and S1 in the supplementary information), the

models reproduce the general features of salinity, temperature and oxygen quite well. However, some biases exist and the bottom values are not easy to reproduce due to their extremely high variability. Hence, in the following we compare our results with previous findings from observational studies.

The connections between summer inflows, high deep-water temperatures and oxygen depletion have been (to a certain extent) discussed based on observational data, for instance in Mohrholz et al. (2006), Rak et al. (2020), and Krapf et al. (2022). However, Mohrholz et al. (2006) and Rak et al. (2020) only studied a very limited number of warm inflow events and Krapf et al. (2022) did not look at inflows. A systematic assessment of the long-term changes as done in this study is not possible with observational data, since a high temporal data coverage in the southwestern Baltic Sea is only available from the 1960s-1970s onward. Thus, many observation-based studies like Liblik and Lips (2019) consider rather short periods starting after 1980. Due to the strong multidecadal variability of the Baltic Sea climate, such periods are too short to yield robust long-term trends. Moreover, the spatial data coverage in the Arkona Basin is not sufficient to get a reasonable measure of S_{17}. However, based on ICES data (ICES 2023) between 1970 and 2009, we observe slightly higher deep-water temperatures (+0.35 °C) and stronger oxygen minima (−0.25 ml/l) at station BY5 in years following high JJASO mean bottom salinities at station BY2 in the Arkona Basin (for the location see Fig. 1).

The ecological impact of the additional decrease in oxygen concentrations due to the warming in the Bornholm Basin is difficult to assess, also, since our study can show the effect of warming on the interannual variability in oxygen but not its effect on the long-term oxygen trend which is dominated by the increasing eutrophication since the 1950s. However, even intermittent hypoxia can severely lower the diversity and abundance of benthic animals, with effects also on higher trophic levels (Conley et al. 2009; Carstensen et al. 2014). For instance, studies show that benthivorous fish like cod change their diet from larger to smaller benthic and more pelagic animals (Conley et al. 2009; Casini et al. 2016; Limburg and Casini 2018). For the eastern Baltic cod, a connection between the expansion of hypoxic areas, changes in the food and spawning ground availability and a decrease in body condition could be found (Casini et al. 2016; Limburg and Casini 2018). The Bornholm Basin is still an important region for the reproduction of the eastern Baltic cod, but also here, a pronounced deterioration in body condition related to the above-mentioned environmental changes could be observed since the end of the 1990s (Eero et al. 2015).

Despite eutrophication being the main driver of oxygen deficiency in the central Baltic Sea (Meier et al. 2019), our study underlines that the effects of rising temperatures on hypoxia should not be neglected, especially, when the general warming due to climate change is intensified by changes in the water cycle, which manifest themselves in the shift in inflow seasonality. In that context, those changes might dampen future positive effects of nutrient input abatement strategies suggested by HELCOM (2013).

Our results are not only important for the Bornholm Basin. As the first deep basin reached by inflows, the Bornholm Basin is particularly affected by them, but the Gdánsk and Eastern Gotland basins further downstream are also reached by at least some warm inflows like the large one in 2002 (Feistel et al. 2004). Dutheil et al. (2022) have shown that also in the Eastern Gotland Basin, deep water layers warmed more strongly than the surface layer. In addition, our study might be of interest for other stratified coastal seas suffering from oxygen depletion and rising water temperatures like the Chesapeake Bay (Ni et al. 2019; Tian et al. 2022).

5 Summary and conclusions

In this study, we assessed the ability of three regional ocean models to reconstruct the multidecadal and seasonal variability of saltwater inflows into the Baltic Sea. Overall, the results of the three models agree well with the findings of other studies based upon observations. We found that the models produce very similar results despite fundamental differences in horizontal, vertical and temporal resolution (the latter with regard to the model output) and different grid types (Figures S6 to S14 in the supplementary information). Primarily, a shift in salt import seasonality towards more summer and early autumn inflows and a strong correlation of these inflows with the deep-water temperatures in the Bornholm Basin were found in all models. Moreover, the fact that the correlation between JJASO means of S_{17} and T_{max} as well as the positive trend in the latter are also visible in the RCO experiment TAIR (see Fig. 4) shows that the strong warming of the deep Bornholm Basin in the last decades was indeed to a large extent caused by the shift in inflow seasonality.

Most importantly, we discovered that years with high JJASO mean S_{17} are followed by years with much higher deep-water temperatures and lower oxygen concentrations compared to years with low JJASO mean S_{17} (Fig. 5). This indicates that the warm water masses, which are transported to the deep layers of the Bornholm Basin by summer and early autumn inflows, enhance oxygen depletion. The oxygen content in the Bornholm Basin before, during, and after warm inflows appeared to be mainly controlled by temperature (Figs. 6, 7, and S15–S22 in the supplementary information), more specifically, by the temperature-dependence of the oxygen solubility and the oxygen consumption in the sediments.

In summary, we found that an increase in warm saltwater inflows in the 20th century led to additional warming in deep

layers of the western Baltic Sea. The warming of the bottom water due to warm saltwater inflows reduced the oxygen content mainly because the oxygen solubility in warm water is lower. This effect might counteract recent efforts to decrease hypoxia in the Baltic Sea by reducing the nutrient input.

Supplementary Information The online version contains supplementary material available at https://doi.org/10.1007/s00382-024-07501-x.

Acknowledgements The research presented in this study is part of the Baltic Earth program (Earth System Science for the Baltic Sea region; see https://www.baltic.earth) and a contribution to the BMBF funded project CoastalFutures (03F0911E). The RCO simulations were performed on the high-performance computing resources operated by the National Supercomputer Centre (NSC) at Linköping University, Sweden. Model runs with GETM and MOM were conducted at the supercomputers of the North German Supercomputing Alliance (HLRN). Data from the long-term monitoring program of the Leibniz Institute for Baltic Sea Research Warnemünde (IOW) was used for model validation. We would like to acknowledge two anonymous reviewers whose constructive comments greatly improved earlier versions of the manuscript.

Author Contributions LB designed the study together with HEMM, performed the REF experiment in GETM, analyzed the model results, validated the models and wrote the paper with the help of all co-authors. HEMM conducted the simulations with RCO, TN the simulations with MOM, and HR REF+ and RUNOFF+ with GETM. HR and LB assembled the observational data for the model validation. LN performed the oxygen budget calculations.

Funding Open Access funding enabled and organized by Projekt DEAL.

Data availability The modeled and observational data necessary to reproduce the figures of this paper and its Supplementary information are publicly available under http://doi.io-warnemuende.de/10.12754/data-2024-0007. These datasets and Figure S1 from Radtke et al. (2020) are provided through the Creative Commons (CC) data license of type CC BY 4.0 (https://creativecommons.org/licenses/by/4.0/).

Code availabilitry The model code of the RCO model is publicly available from the Swedish Meteorological and Hydrological Institute, Norrköping, Sweden (https://www.smhi.se, E-mail: smhi@smhi.se). The GETM model used for this study is open-source software and available under https://getm.eu/ (IOW 2023b). The code of the biogeochemical model ERGOM is available at https://ergom.net/ (IOW 2023a). The ocean model "Modular Ocean Model MOM 5-1" is available from the developers's repository https://github.com/mom-ocean/MOM5 (last access: 19 September 2023).

Declarations

Conflict of interest The authors declare no conflict of interest.

References

Almroth-Rosell E, Wåhlström I, Hansson M et al (2021) A regime shift toward a more anoxic environment in a eutrophic sea in Northern Europe. Front Mar Sci 8:799936. https://doi.org/10.3389/fmars.2021.799936

Barghorn L, Meier HEM, Radtke H (2023) Changes in seasonality of saltwater inflows caused exceptional warming trends in the western Baltic Sea. Geophys Res Lett 50(12):e2023GL103853. https://doi.org/10.1029/2023GL103853

Börgel F, Neumann T, Rooze J et al (2023) Deoxygenation of the Baltic Sea during the last millennium. Front Mar Sci 10:1174039. https://doi.org/10.3389/fmars.2023.1174039

Brasseur O (2001) Development and application of a physical approach to estimating wind gusts. Mon Weather Rev 129(1):5–25. https://doi.org/10.1175/1520-0493(2001)129<0005:DAAOAP>2.0.CO;2

Carr ME (2002) Estimation of potential productivity in Eastern Boundary Currents using remote sensing. Deep-Sea Res II 49:59–80. https://doi.org/10.1016/S0967-0645(01)00094-7

Carstensen J, Conley DJ, Bonsdorff E et al (2014) Hypoxia in the Baltic Sea: biogeochemical cycles, benthic fauna, and management. Ambio 43(1):26–36. https://doi.org/10.1007/s13280-013-0474-7

Casini M, Käll F, Hansson M et al (2016) Hypoxic areas, density-dependence and food limitation drive the body condition of a heavily exploited marine fish predator. R Soc Open Sci 3:160416. https://doi.org/10.1098/rsos.160416

Conley DJ, Björck S, Bonsdorff E et al (2009) Hypoxia-related processes in the Baltic Sea. Environ Sci Technol. https://doi.org/10.1021/es802762a

Dai M, Guo X, Zhai W et al (2006) Oxygen depletion in the upper reach of the Pearl River estuary during a winter drought. Mar Chem 102:159–169. https://doi.org/10.1016/j.marchem.2005.09.020

Diaz RJ, Rosenberg R (2008) Spreading dead zones and consequences for marine ecosystems. Science 321(5891):926–929. https://doi.org/10.1126/science.115640

Dutheil C, Meier HEM, Gröger M et al (2022) Warming of Baltic Sea water masses since 1850. Clim Dyn. https://doi.org/10.1007/s00382-022-06628-z

Eero M, Hjelm J, Behrens J et al (2015) Eastern Baltic cod in distress: biological changes and challenges for stock assessment. ICES J Mar Sci 72:2180–2186. https://doi.org/10.1093/icesjms/fsv109

Eilola K, Meier HM, Almroth E (2009) On the dynamics of oxygen, phosphorus and cyanobacteria in the Baltic Sea; a model study. J Mar Syst 75(1–2):163–184. https://doi.org/10.1016/j.jmarsys.2008.08.009

Feistel R, Nausch G, Mohrholz V et al (2003) Warm waters of summer 2002 in the deep Baltic Proper. Oceanologia 45(4):571–592

Feistel R, Nausch G, Heene T et al (2004) Evidence for a warm water inflow into the Baltic Proper in summer 2003. Oceanologia 46(4):581–198

Feistel R, Nausch G, Hagen E (2006) Unusual Baltic inflow activity in 2002–2003 and varying deep-water properties. Oceanologia 48(S):21–35

Fennel K, Testa JM (2019) Biogeochemical controls on coastal hypoxia. Ann Rev Mar Sci 11:105–30. https://doi.org/10.1146/annurev-marine-010318-095138

Garcia HE, Gordon LI (1992) Oxygen solubility in seawater: better fitting equations. Limnol Oceanogr 37(6):1307–1312. https://doi.org/10.4319/lo.1992.37.6.1307
Good R, Fletcher HJ (1981) Reporting explained variance. J Res Sci Teach 18(1):1–7. https://doi.org/10.1002/tea.3660180102
Gräwe U, Naumann M, Mohrholz V et al (2015) Anatomizing one of the largest saltwater inflows into the Baltic Sea in December 2014. J Geophys Res Oceans 120(11):7676–7697. https://doi.org/10.1002/2015JC011269
Gräwe U, Klingbeil K, Kelln J et al (2019) Decomposing mean sea level rise in a semi-enclosed Basin, the Baltic Sea. J Clim 32(11):3089–3108. https://doi.org/10.1175/JCLI-D-18-0174.1
Griffies SM (2004) Fundamentals of ocean climate models. Princeton Univ. Press, Princeton
Gustafsson BG, Schenk F, Blenckner T et al (2012) Reconstructing the development of Baltic Sea Eutrophication 1850–2006. Ambio 41(6):534–548. https://doi.org/10.1007/s13280-012-0318-x
Hagy JD, Boynton WR, Keefe CW et al (2004) Hypoxia in Chesapeake Bay, 1950–2001: long-term change in relation to nutrient loading and river flow. Estuaries 27(4):634–658. https://doi.org/10.1007/BF02907650
Hansson M, Viktorsson L, Andersson L (2019) Oxygen Survey in the Baltic Sea 2019—Extent of Anoxia and Hypoxia, 1960–2019. Tech. Rep. 67, Swedish Meteorological and Hydrological Institute, Göteborg
HELCOM (2013) HELCOM Copenhagen Ministerial Declaration
Hofmeister R, Beckers JM, Burchard H (2011) Realistic modelling of the exceptional inflows into the central Baltic Sea in 2003 using terrain-following coordinates. Ocean Model 39:233–247. https://doi.org/10.1016/j.ocemod.2011.04.007
Hong B, Shen J (2012) Responses of estuarine salinity and transport processes to potential future sea-level rise in the Chesapeake Bay. Estuar Coast Shelf Sci 104–105:33–45. https://doi.org/10.1016/j.ecss.2012.03.014
Hylén A, van de Velde SJ, Kononets M et al (2021) Deep-water inflow event increases sedimentary phosphorus release on a multi-year scale. Biogeosciences 18(9):2981–3004. https://doi.org/10.5194/bg-18-2981-2021
ICES (2023) ICES Oceanography [Dataset]. https://www.ices.dk/data/data-portals/Pages/ocean.aspx
IOW (2023a) Ecological regional ocean model. https://ergom.net/
IOW (2023b) GETM—a 3D hydrodynamic model for coastal oceans. https://getm.eu/
Janssen F, Schrum C, Backhaus JO (1999) A climatological data set of temperature and salinity for the Baltic Sea and the North Sea. German J Hydrogr 51(Suppl 9):5. https://doi.org/10.1007/BF02933676
JCS (2010) Thermodynamic Equation Of Seawater—2010. https://www.teos-10.org/
Kniebusch M, Meier HEM, Neumann T et al (2019) Temperature variability of the Baltic Sea since 1850 and attribution to atmospheric forcing variables. J Geophys Res Oceans 124(6):4168–4187. https://doi.org/10.1029/2018JC013948
Kniebusch M, Meier HEM, Radtke H (2019) Changing salinity gradients in the Baltic Sea as a consequence of altered freshwater budgets. Geophys Res Lett 46(16):9739–9747. https://doi.org/10.1029/2019GL083902
Krapf K, Naumann M, Dutheil C et al (2022) Investigating hypoxic and euxinic area changes based on various datasets from the Baltic Sea. Front Mar Sci 9:823476. https://doi.org/10.3389/fmars.2022.823476
Lass H, Matthäus W (1996) On temporal wind variations forcing salt water inflows into the Baltic Sea. Tellus A Dyn Meteorol Oceanogr 48(5):663–671. https://doi.org/10.3402/tellusa.v48i5.12163
Laufkötter C, John JG, Stock CA et al (2017) Temperature and oxygen dependence of the remineralization of organic matter. Global Biogeochem Cycles 31(7):1038–1050. https://doi.org/10.1002/2017GB005643
Laurent A, Fennel K, Ko DS et al (2018) Climate change projected to exacerbate impacts of coastal eutrophication in the Northern Gulf of Mexico. J Geophys Res Oceans 123:3408–3426. https://doi.org/10.1002/2017JC013583
Liblik T, Lips U (2019) Stratification has strengthened in the Baltic Sea—an analysis of 35 years of observational data. Front Earth Sci 7:174. https://doi.org/10.3389/feart.2019.00174
Limburg KE, Casini M (2018) Effect of marine hypoxia on Baltic Sea Cod Gadus morhua: evidence from otolith chemical proxies. Front Mar Sci 5:482. https://doi.org/10.3389/fmars.2018.00482
Matthäus W, Franck H (1992) Characteristics of major Baltic inflows—a statistical analysis. Cont Shelf Res 12(12):1375–1400. https://doi.org/10.1016/0278-4343(92)90060-W
Meier HEM, Kauker F (2003) Modeling decadal variability of the Baltic Sea: 2. Role of freshwater inflow and large-scale atmospheric circulation for salinity. J Geophys Res 108(C11):3368. https://doi.org/10.1029/2003JC001799
Meier HEM, Kauker F (2003) Sensitivity of the Baltic Sea salinity to the freshwater supply. Clim Res 24:231–242. https://doi.org/10.3354/cr024231
Meier HEM, Döscher R, Faxén T (2003) A multiprocessor coupled ice-ocean model for the Baltic Sea: application to salt inflow. J Geophys Res 108(C8):3273. https://doi.org/10.1029/2000JC000521
Meier HEM, Andersson HC, Eilola K et al (2011) Hypoxia in future climates: a model ensemble study for the Baltic Sea. Geophys Res Lett 38:L24608. https://doi.org/10.1029/2011GL049929
Meier HEM, Väli G, Naumann M et al (2018) Recently accelerated oxygen consumption rates amplify deoxygenation in the Baltic Sea. J Geophys Res Oceans 123(5):3227–3240. https://doi.org/10.1029/2017JC013686
Meier HEM, Eilola K, Almroth-Rosell E et al (2019) Disentangling the impact of nutrient load and climate changes on Baltic Sea hypoxia and eutrophication since 1850. Clim Dyn 53:1145–1166. https://doi.org/10.1007/s00382-018-4296-y
Meier HEM, Dieterich C, Gröger M (2021) Natural variability is a large source of uncertainty in future projections of hypoxia in the Baltic Sea. Commun Earth Environ 2(1):50. https://doi.org/10.1038/s43247-021-00115-9
Meier HEM, Barghorn L, Börgel F et al (2023) Multidecadal climate variability dominated past trends in the water balance of the Baltic Sea watershed. npj Clim Atmos Sci 6(1):58. https://doi.org/10.1038/s41612-023-00380-9
Mohrholz V (2018) Major Baltic inflow statistics – revised. Front Mar Sci 5:384. https://doi.org/10.3389/fmars.2018.00384
Mohrholz V, Dutz J, Kraus G (2006) The impact of exceptionally warm summer inflow events on the environmental conditions in the Bornholm Basin. J Mar Syst 60:285–301. https://doi.org/10.1016/j.jmarsys.2005.10.002
Mohrholz V, Bartholomae CH, van der Plas AK et al (2008) The seasonal variability of the northern Benguela undercurrent and its relation to the oxygen budget on the shelf. Cont Shelf Res 28:424–441. https://doi.org/10.1016/j.csr.2007.10.001
Naumov L, Neumann T, Radtke H et al (2023) Limited ventilation of the central Baltic Sea due to elevated oxygen consumption. Front Mar Sci 10:1175643. https://doi.org/10.3389/fmars.2023.1175643
Neumann T, Radtke H, Seifert T (2017) On the importance of Major Baltic Inflows for oxygenation of the central Baltic Sea. J Geophys Res Oceans 122(2):1090–1101. https://doi.org/10.1002/2016JC012525
Neumann T, Radtke H, Cahill B et al (2022) Non-Redfieldian carbon model for the Baltic Sea (ERGOM version 1.2)—implementation

and budget estimates. Geosci Model Dev 15(22):8473–8540. https://doi.org/10.5194/gmd-15-8473-2022

Ni W, Li M, Ross AC et al (2019) Large projected decline in dissolved oxygen in a eutrophic estuary due to climate change. J Geophys Res Oceans 124(11):8271–8289. https://doi.org/10.1029/2019JC015274

Radtke H, Brunnabend SE, Gräwe U et al (2020) Investigating interdecadal salinity changes in the Baltic Sea in a 1850–2008 hindcast simulation. Clim Past 16(4):1617–1642. https://doi.org/10.5194/cp-16-1617-2020

Rak D, Walczowski W, Dzierzbicka-Glowacka L et al (2020) Dissolved oxygen variability in the southern Baltic Sea in 2013–2018. Oceanologia 62:525–537. https://doi.org/10.1016/j.oceano.2020.08.005

Safonova K, Meier HEM, Gröger M (2024) Summer heatwaves on the Baltic Sea seabed contribute to oxygen deficiency in shallow areas. Commun Earth Environ. https://doi.org/10.1038/s43247-024-01268-z

Saraiva S, Meier HEM, Andersson H et al (2019) Uncertainties in projections of the Baltic Sea ecosystem driven by an ensemble of global climate models. Front Earth Sci 6:244. https://doi.org/10.3389/feart.2018.00244

Schenk F, Zorita E (2012) Reconstruction of high resolution atmospheric fields for Northern Europe using analog-upscaling. Clim Past 8(5):1681–1703. https://doi.org/10.5194/cp-8-1681-2012

Simpson G (2014) Modelling seasonal data with GAMs. https://www.fromthebottomoftheheap.net/2014/05/09/modelling-seasonal-data-with-gam/

Stigebrandt A (1987) A model for the vertical circulation of the Baltic deep water. J Phys Oceanogr 17(10):1772–1785. https://doi.org/10.1175/1520-0485(1987)017<1772:AMFTVC>2.0.CO;2

TEOS-10 (2017) GSW-Python. https://teos-10.github.io/GSW-Python/

Tian R, Cerco CF, Bhatt G et al (2022) Mechanisms controlling climate warming impact on the occurrence of hypoxia in Chesapeake Bay. JAWRA J Am Water Resour Assoc 58(6):855–875. https://doi.org/10.1111/1752-1688.12907

Vahtera E, Conley DJ, Gustafsson BG et al (2007) Internal ecosystem feedbacks enhance nitrogen-fixing cyanobacteria blooms and complicate management in the Baltic Sea. AMBIO J Hum Environ 36(2):186–194. https://doi.org/10.1579/0044-7447(2007)36[186:IEFENC]2.0.CO;2

Väli G, Meier HEM, Elken J (2013) Simulated halocline variability in the Baltic Sea and its impact on hypoxia during 1961–2007. J Geophys Res Oceans 118(12):6982–7000. https://doi.org/10.1002/2013JC009192

Vaquer-Sunyer R, Duarte CM (2008) Thresholds of hypoxia for marine biodiversity. Biol Sci 105(40):15452–15457. https://doi.org/10.1073/pnas.0803833105

Winsor P, Rodhe J, Omstedt A (2001) Baltic Sea ocean climate: an analysis of 100 yr of hydrographic data with focus on the freshwater budget. Clim Res 18:5–15. https://doi.org/10.3354/cr018005

Wolf G (1972) Salzwassereinbrüche im Gebiet der westlichen Ostsee. Beiträge zur Meereskunde 29

Supplementary information for "Warm saltwater inflows strengthen oxygen depletion in the western Baltic Sea"

Leonie Barghorn[1,*], H. E. Markus Meier[1], H. Radtke[1], T. Neumann[1], L. Naumov[1]

[1]Department of Physical Oceanography and Instrumentation, Leibniz Institute for Baltic Sea Research Warnemuende, Seestrasse 15, 18119 Rostock, Germany
[*]leonie.barghorn@io-warnemuende.de

S1 Detailed model validation

S1.1 Salinity and temperature profiles

Salinity and temperature profiles of the stations shown in Figure S1 averaged over the years 1970-2007 (i.e., a period with good observational data coverage) are depicted in Figure S2. For GETM, modeled and observed profiles are qualitatively similar but the modeled salinities are generally higher and the halocline is shallower in the model. Similar deviations are visible in the MOM data. In contrast to that, the salinities in RCO are closer to the ICES (observational) data and sometimes even lower. At BY5, the station in the Bornholm Basin, which is in the focus of this study, both RCO and MOM show too low bottom salinities. However, in the range of the halocline (roughly between 50 and 60 m at BY5), which is relevant for warm inflows, the models' biases are below one standard deviation of the observational data.

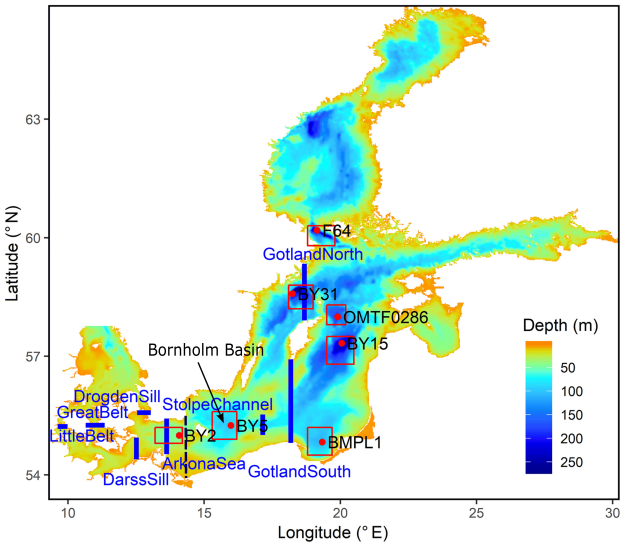

Fig. S1: Model domain and bathymetry of the GETM setup (taken from Radtke et al (2020) and modified). Blue lines denote transects for salt transport calculation. The thin dashed line indicates the eastern boundary of the Arkona Basin for the salt content calculations (S_{17}). Red squares show areas around selected stations from which observational data is taken for the model validation.

S1.2 Time series of bottom and surface salinity

Time series of bottom and surface salinity at the selected stations are shown in Figures S3 and S4. The surface salinity exhibits the same multidecadal variability in all data sets. However, it generally has a positive bias in GETM and a negative bias in RCO. In MOM, there is a drift towards higher salinities during the first about 50-60 years. Afterwards, the salinity is comparable to or even higher than in GETM except for the northernmost station F64.

For the bottom salinity, the model biases are less consistent and the multidecadal variability of the observational data is less well captured by the models. At the most relevant stations for this study, BY2 in the Arkona Basin and BY5 in the Bornholm Basin, the explained variances (ρ^2) between 1970 and 2007 of the different models are between 0.16 (RCO at BY2) and 0.45 (MOM at BY2). An outlier is the negative explained variance of -0.2 for GETM at BY5 which was already discussed in

Radtke et al (2020) (their values are a bit different due to a different time range used for computing the variances). A negative variance arises when the variance of the difference between observations and model is larger than the variance of the observations themselves. In our case, this happened despite a significant correlation of 0.45 between the two time series. However, Radtke et al (2020) found that the explained variance at BY5 is positive at 60 m with 0.34. It seems as if only the values at the very bottom are problematic.

Time series of bottom temperatures and oxygen concentrations at 80 m depth at station BY5 (Figure S5) are discussed in the main text in Section 3.1.

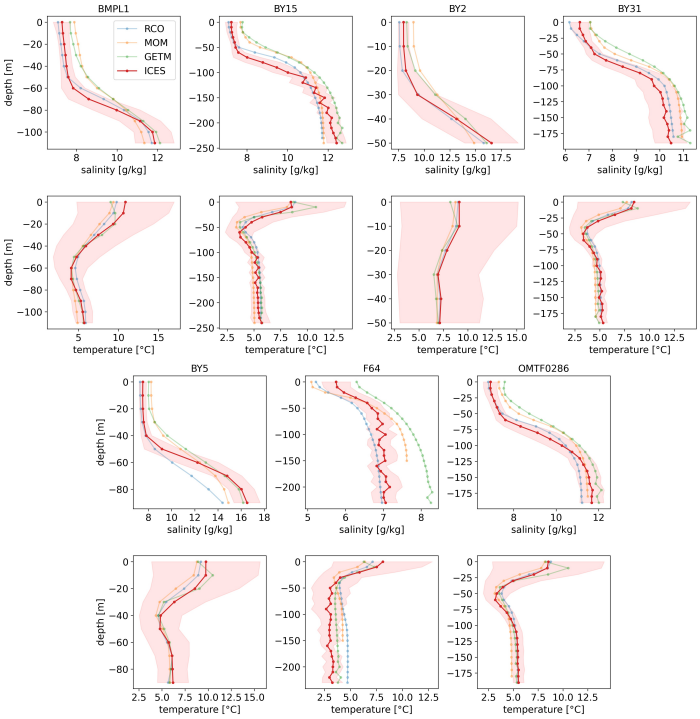

Fig. S2: Salinity and temperature profiles at selected stations (see Figure S1) averaged over the years 1970-2007. Observational data was taken from the ICES data base (ICES, 2023) and assembled over the red rectangles indicated in Figure S1. The model data was taken from the reference simulations. The shaded areas indicate +/− one standard deviation of the ICES data.

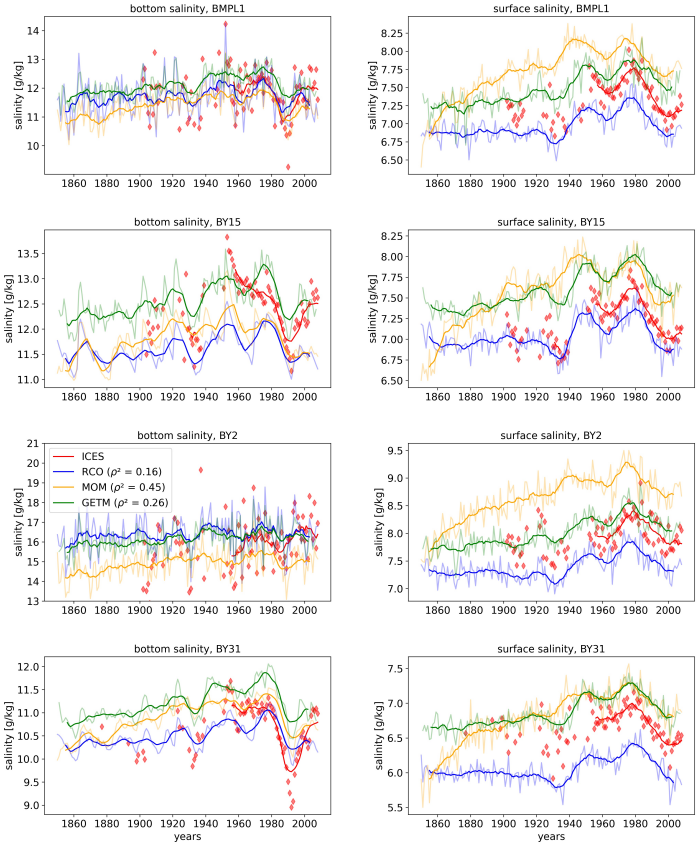

Fig. S3: Time series of annual mean surface and bottom salinities at selected stations (see Figure S1). The ICES data was taken from ICES (2023) and processed as in Radtke et al (2020). The model data was taken from the reference simulations. Bold lines depict 11-year running means. For the bottom salinity at station BY2, explained variances (ρ^2) are displayed.

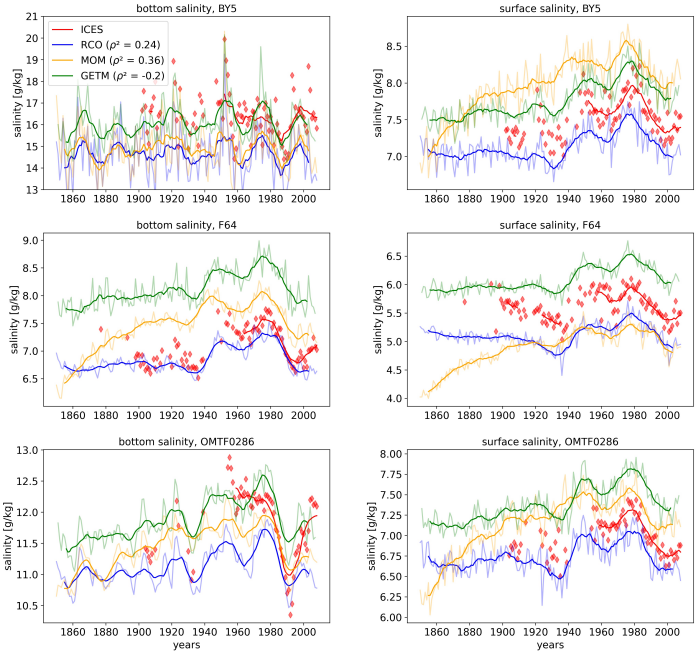

Fig. S4: As Figure S3 for the remaining stations. For the bottom salinity at station BY5, explained variances (ρ^2) are displayed.

S2 Detailed model comparison

S2.1 Variability of salt content in highly saline water masses (S_{17}) in the Arkona Basin

We use the mean daily salt content in grid cells with a minimum salinity of 17 g/kg in the Arkona Basin (S_{17}) as a measure for saltwater inflows. Smoothed time series of annual, summer (June - August; JJA) and early autumn (September / October; SO) means of S_{17} for the reference runs of the three models are depicted in Figure S6. For both annual and seasonal means, the time series of the three models are comparable in

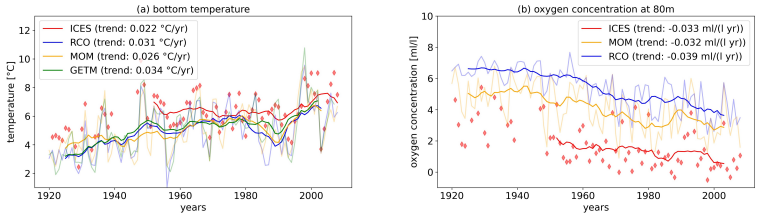

Fig. S5: Time series of bottom temperatures and oxygen concentrations at 80 m depth at station BY5. The ICES data was taken from ICES (2023) and processed as in Radtke et al (2020). The model data was taken from the reference simulations. Bold lines depict 11-year running means. Linear trends over the displayed periods are also given.

magnitude. They also show a similar multidecadal variability, at least in case of annual and SO means, with S_{17} maxima roughly in the 1940s, 1970s, and at the end of the 1990s. Such a multidecadal variability is characteristic for the Baltic Sea water cycle (Winsor et al, 2001; Meier and Kauker, 2003; Mohrholz, 2018; Kniebusch et al, 2019b; Medvedev and Kulikov, 2019; Radtke et al, 2020; Agha Karimi et al, 2021; Stockmayer and Lehmann, 2023; Meier et al, 2023). The time series for JJA look a bit different with only one distinct maximum between 1960 and 1980, which is especially pronounced in the GETM data. To further assess how similar the time series of the different models are to each other, we computed Pearson correlation coefficients between the three time series of each respective season (cf. Section 2.4 in the main text). The coefficients are lowest (but still high) for JJA, ranging from 0.62 to 0.83, and higher for annual and SO means with 0.71 - 0.93 (all p-values are of the order 1e-10 or smaller). Hence, despite fundamental differences in the model setups (see Methods in the main text), the resulting S_{17} time series are reasonably similar.

S2.2 Comparison of S_{17} and saline inflows in GETM

Although S_{17} has been used successfully as a measure for (large) saltwater inflows in earlier studies (Meier and Kauker, 2003; Dutheil et al, 2022), it has so far neither been utilized to study the inflow seasonality, nor to reconstruct the multidecadal variability of inflows of all kinds (small to large, barotropic and baroclinic). Hence, we compare the annual and seasonal time series of S_{17} to the salt import across Darss Sill and Drogden Sill (see Figure S1), to verify whether the former is sufficiently good in reproducing the latter. This is not evident, since the inflowing water can (in extreme cases) need up to 2 months to travel through the Arkona Basin (Gräwe et al, 2015). The results

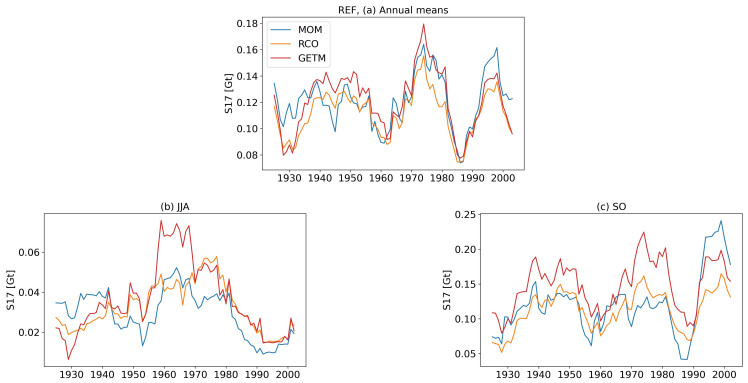

Fig. S6: Time series of annual (a), June - August (JJA, b) and September - October (SO, c) means of S_{17} for the reference simulations (REF) of the three models, smoothed by 11-year running means.

are depicted in Figures S7, S8 and S9. We find that the time series of annual mean S_{17} of all three models fit very well to the salt import in GETM, with correlation coefficients of 0.81 and higher. The strongest deviations are found for JJA means, probably, because summer inflows are in general smaller and thus more difficult to capture. But still, the correlation coefficients amount at least to 0.65 (with p-values of the order of 1e-8 and lower) and the multidecadal variability is captured well by all models. Thus, it can be concluded that S_{17} can successfully reproduce time series of annual and seasonal salt import.

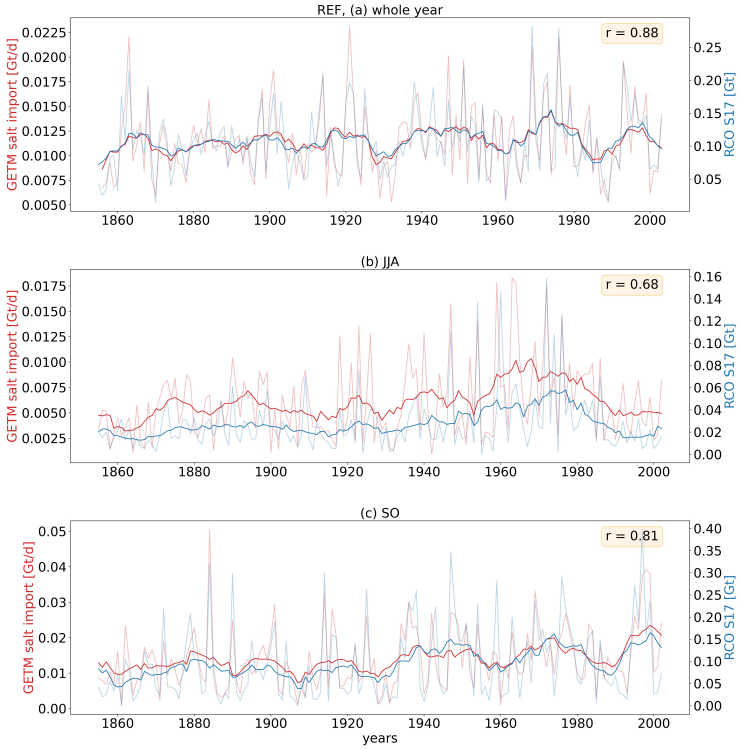

Fig. S7: Annual, June - August (JJA) and September - October (SO) time series of salt import in GETM versus salt content in highly saline water masses in the Arkona Basin (S_{17}) for the reference simulation of RCO. Bold lines indicate 11-year running means. The salt transport was registered at the Darss Sill and Drogden Sill transects (see Figure S1). Yellow boxes display Pearson correlation coefficients between the respective non-smoothed time series from 1920 onward.

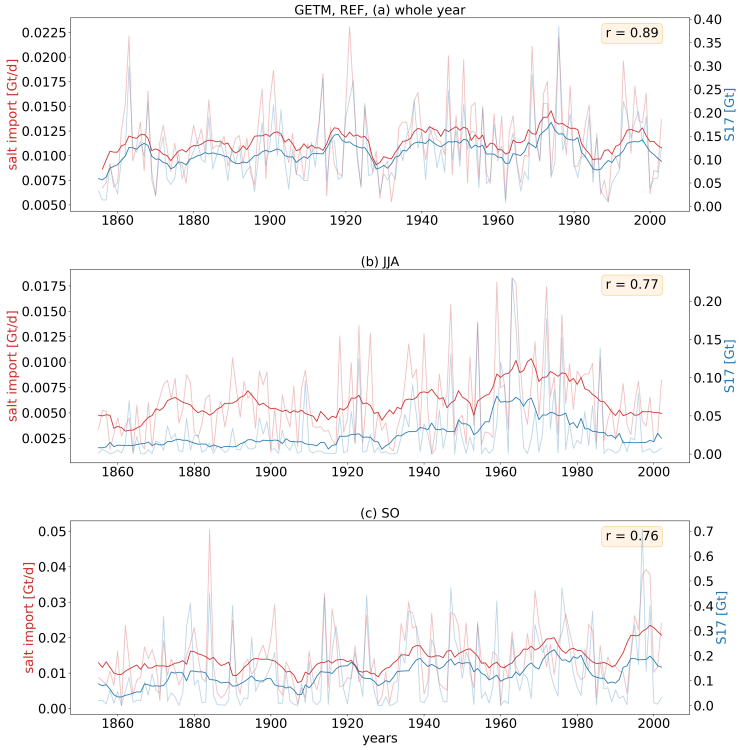

Fig. S8: Same as Figure S7, but for GETM.

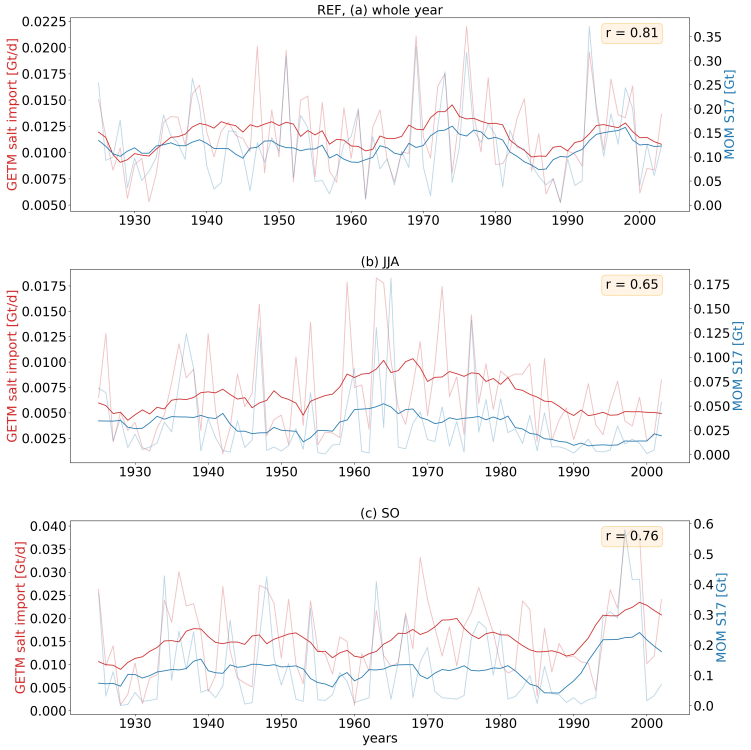

Fig. S9: Same as Figure S7, but for MOM.

S2.3 Trends in S_{17}

Barghorn et al (2023) found that, over the whole model period, both JJA and SO salt import increased significantly, while winter salt import decreased. Since the results before 1920 might suffer from shortcomings in the runoff data (cf Methods in the main text), also trends from 1920 onward were computed. They are more reliable due to the better quality of the runoff data, but, because of the shorter period, might be more affected by the internal multidecadal variability. Hence, both periods were considered. From 1920 onward, a weakly negative trend was found for JJA but a significant positive trend for SO.

The same trends were computed for sensitivity experiments (see Table 2 in the main text) to explore the drivers of the shift in salt import seasonality. In particular, Barghorn et al (2023) looked at the impact of the global mean sea level rise (included in experiments REF+ and RUNOFF+, not included in REF experiments) and that of river runoff (experiment RUNOFF+ works with the climatological mean of runoff and precipitation minus evaporation over the sea, which are repeated for each year of the model period). It was found that the sea level rise increases the salt import independently of the season, which can be explained by the fact that the sea level rise leads to a larger cross section of the Danish straits and consequently to stronger inflows (Hordoir et al, 2015; Arneborg, 2016; Meier et al, 2017, 2021; Saraiva et al, 2019). The experiments with climatological mean runoff exhibit more negative / less positive JJA / SO trends in S_{17} since 1920, while the annual trends are not changed systematically, pointing towards an impact of runoff variability on the inflow seasonality.

As Figure S10 shows, we find similar trends for S_{17} in all three models (unnormalized trends are found in Figure S13). This implies that the significant but rather small signals found by Barghorn et al (2023) are robust and not just a feature in GETM. One exception are the trends in the RUNOFF experiment of MOM that do not show the same systematics as the RUNOFF+ experiments of GETM and RCO. One possible reason could be that the trends are affected by the drift in the first decades of the MOM simulations. Although the curves in Figures S3 and S4 look as if the drift stops at the beginning of the 20th century, this is not completely certain. In addition, the drift might be different in the RUNOFF experiment.

Here, the SO trends for S_{17} since 1920 alone are not significant in any of the experiments. However, to quantify rather the shift in seasonality than the change in a single season, we compute trends for the S_{17} ratio of winter (December - February; DJF) and SO. Figure S11 shows that these trends are significant for REF+ in GETM and both REF and REF+ in RCO (p-values below 0.05).

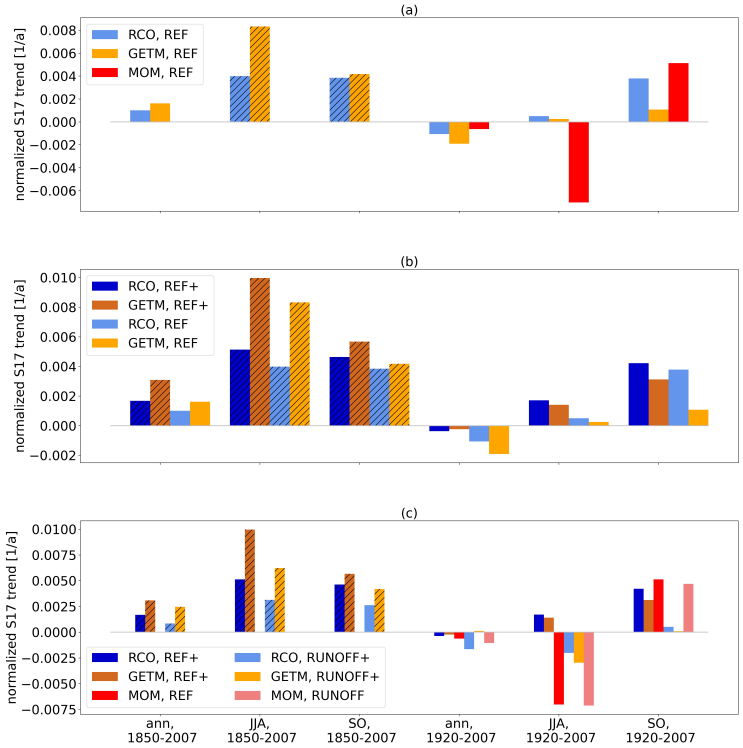

Fig. S10: Annual and seasonal trends in S_{17}, normalized by the respective long-term means. (a) for the reference simulations, (b) comparison of REF and REF+ simulations and (c) comparison of REF+ and RUNOFF+/RUNOFF simulations. Hatched bars indicate significant trends (p-values below 0.05).

S2.4 Temperature trends in the Bornholm Basin and correlation with S_{17}

The initial motivation to study the seasonality of salt import was the assumption that an increase in warm summer and early autumn inflows led to the exceptional warming in the Bornholm Basin (Mohrholz et al, 2006; Meier et al, 2006; Kniebusch et al, 2019a; Dutheil et al, 2022). Barghorn et al (2023) found a significant correlation between

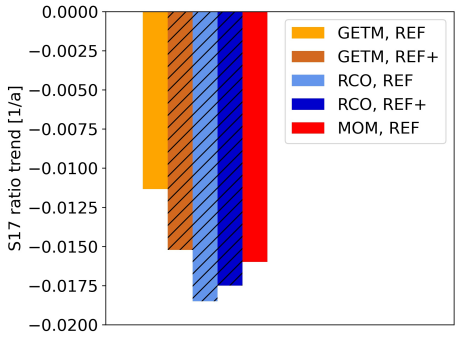

Fig. S11: Trends of the ratio between December - February (DJF) and September - October (SO) means of S_{17} over the period 1920 - 2007 in REF and REF+ simulations. Hatched bars indicate significant trends (p-values below 0.05).

the summer and early autumn (June - October; JJASO) salt import and the annual temperature maximum below the seasonal thermocline ($T_{\max}$) at station BY5 in the Bornholm Basin (see Figure S1). The thermocline was used as an upper boundary for the calculation of $T_{\max}$ since the exact height where warm inflows interleave may vary. As shown in Figure S12, similarly high correlation coefficients are found for S_{17} and $T_{\max}$ in all three models.

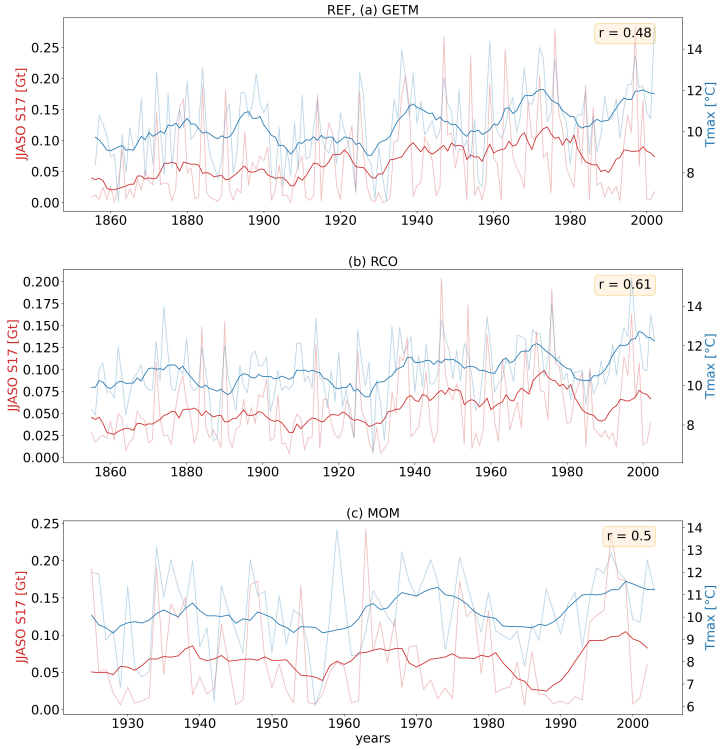

Fig. S12: Annual and smoothed time series of June - October (JJASO) mean S_{17} vs the annual temperature maximum below the seasonal thermocline at station BY5 ($T_{\max}$) for the reference simulations of GETM (a), RCO (b), and MOM (c). Yellow boxes display Pearson correlation coefficients between the respective non-smoothed time series from 1920 onward. P-values are of the order 1e-6 or smaller.

S3 Additional figures

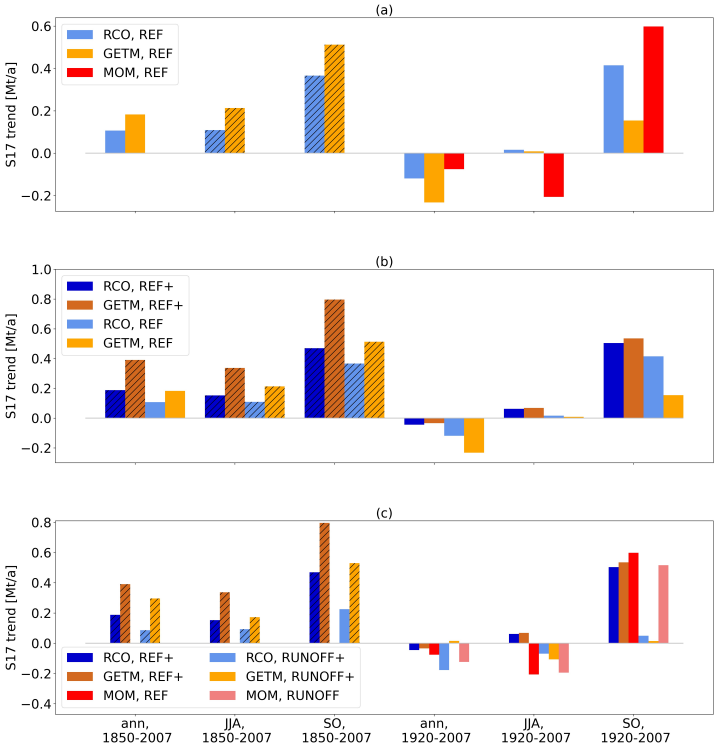

Fig. S13: Annual and seasonal trends in S_{17}. (a) for the reference simulations, (b) comparison of REF and REF+ simulations and (c) comparison of REF+ and RUNOFF+/RUNOFF simulations. Hatched bars indicate significant trends (p-values below 0.05). Normalized trends can be found in Figure S10.

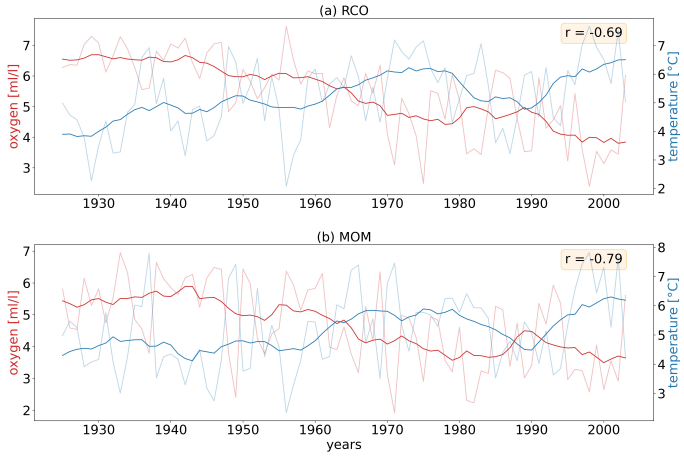

Fig. S14: Annual and smoothed time series of the oxygen content vs the temperature averaged between 60 m depth and the bottom at station BY5, for the reference simulations of RCO (a) and MOM (b). Yellow boxes display Pearson correlation coefficients between the respective non-smoothed and detrended time series from 1920 onward. P-values are of the order 1e-13 or smaller.

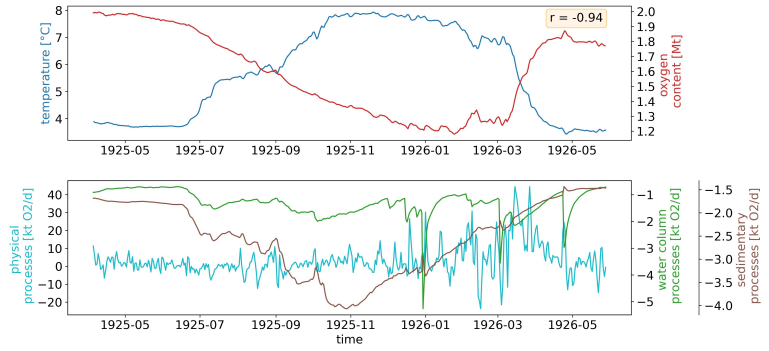

Fig. S15: Top panel: Mean temperature and oxygen content in the Bornholm Basin below 60 m. The yellow box displays the Pearson correlation coefficient between both time series. Bottom panel: Physical, water column and sedimentary processes of the oxygen budget of the Bornholm Basin below 60 m. Both panels show daily means.

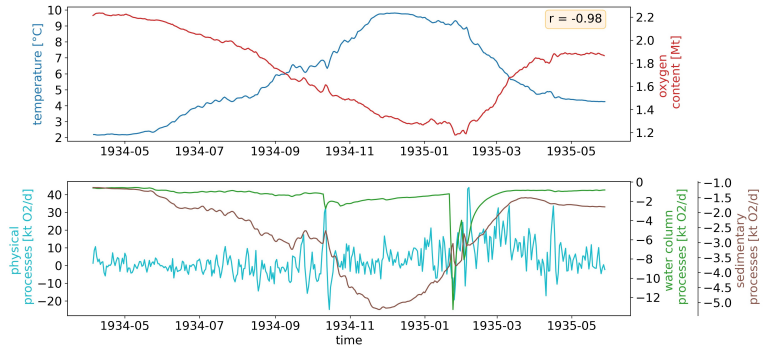

Fig. S16: As Figure S15, but for 1934/35.

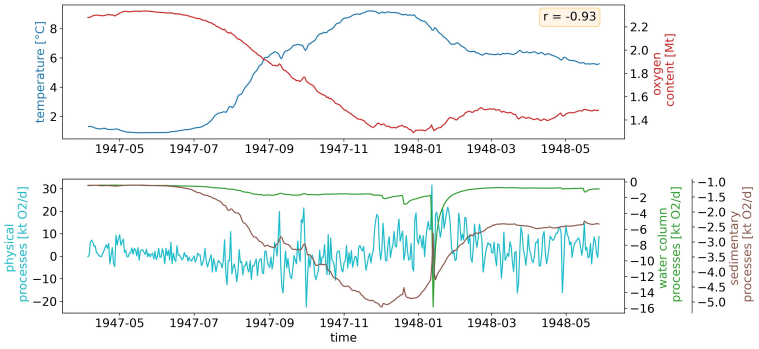

Fig. S17: As Figure S15, but for 1947/48.

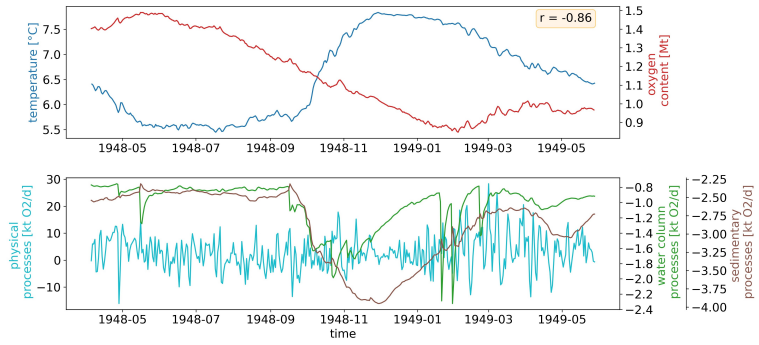

Fig. S18: As Figure S15, but for 1948/49.

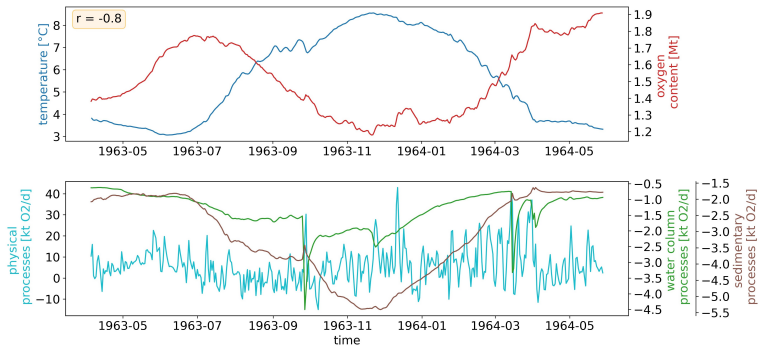

Fig. S19: As Figure S15, but for 1963/64.

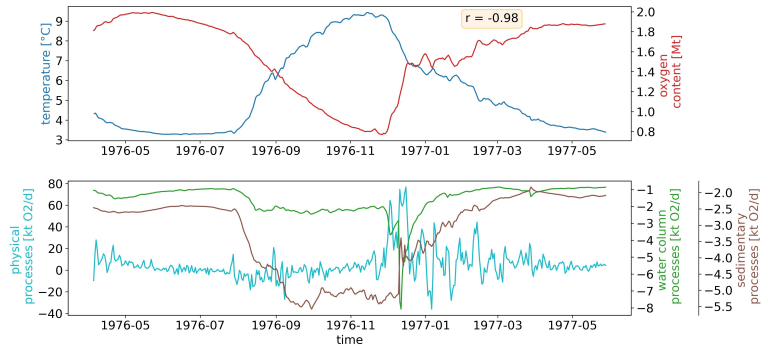

Fig. S20: As Figure S15, but for 1976/77.

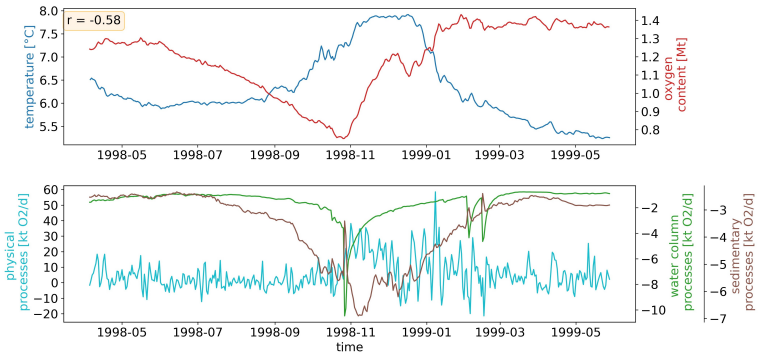

Fig. S21: As Figure S15, but for 1998/99.

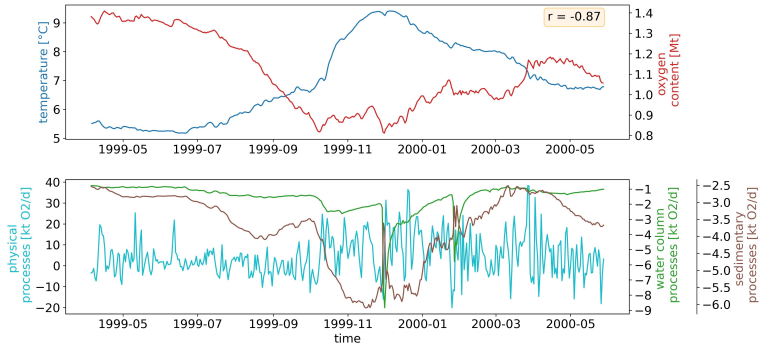

Fig. S22: As Figure S15, but for 1999/2000.

References

Agha Karimi A, Bagherbandi M, Horemuz M (2021) Multidecadal Sea Level Variability in the Baltic Sea and Its Impact on Acceleration Estimations. Frontiers in Marine Science 8:702512. https://doi.org/10.3389/fmars.2021.702512, URL https://www.frontiersin.org/articles/10.3389/fmars.2021.702512/full

Arneborg L (2016) Comment on "Influence of sea level rise on the dynamics of salt inflows in the Baltic Sea" by R. Hordoir, L. Axell, U. Löptien, H. Dietze, and I. Kuznetsov. Journal of Geophysical Research: Oceans 121(3):2035–2040. https://doi.org/10.1002/2015JC011451

Barghorn L, Meier HEM, Radtke H (2023) Changes in Seasonality of Saltwater Inflows Caused Exceptional Warming Trends in the Western Baltic Sea. Geophysical Research Letters 50(12):e2023GL103853. https://doi.org/10.1029/2023GL103853

Dutheil C, Meier HEM, Gröger M, et al (2022) Warming of Baltic Sea water masses since 1850. Climate Dynamics https://doi.org/10.1007/s00382-022-06628-z

Gräwe U, Naumann M, Mohrholz V, et al (2015) Anatomizing one of the largest saltwater inflows into the Baltic Sea in December 2014. Journal of Geophysical Research: Oceans 120(11):7676–7697. https://doi.org/10.1002/2015JC011269

Hordoir R, Axell L, Löptien U, et al (2015) Influence of sea level rise on the dynamics of salt inflows in the Baltic Sea. Journal of Geophysical Research: Oceans 120(10):6653–6668. https://doi.org/10.1002/2014JC010642

ICES (2023) ICES Oceanography [Dataset]. URL https://www.ices.dk/data/data-portals/Pages/ocean.aspx

Kniebusch M, Meier HEM, Neumann T, et al (2019a) Temperature Variability of the Baltic Sea Since 1850 and Attribution to Atmospheric Forcing Variables. Journal of Geophysical Research: Oceans 124(6):4168–4187. https://doi.org/10.1029/2018JC013948

Kniebusch M, Meier HEM, Radtke H (2019b) Changing Salinity Gradients in the Baltic Sea As a Consequence of Altered Freshwater Budgets. Geophysical Research Letters 46(16):9739–9747. https://doi.org/10.1029/2019GL083902

Medvedev I, Kulikov E (2019) Low-Frequency Baltic Sea Level Spectrum. Frontiers in Earth Science 7:284. https://doi.org/10.3389/feart.2019.00284, URL https://www.frontiersin.org/article/10.3389/feart.2019.00284/full

Meier HEM, Kauker F (2003) Modeling decadal variability of the Baltic Sea: 2. Role of freshwater inflow and large-scale atmospheric circulation for salinity. Journal of Geophysical Research 108(C11):3368. https://doi.org/10.1029/2003JC001799

Meier HEM, Feistel R, Piechura J, et al (2006) Ventilation of the Baltic Sea deep water: A brief review of present knowledge from observations and models. Oceanologia (48):133–164

Meier HEM, Höglund A, Eilola K, et al (2017) Impact of accelerated future global mean sea level rise on hypoxia in the Baltic Sea. Climate Dynamics 49:163–172. https://doi.org/10.1007/s00382-016-3333-y

Meier HEM, Dieterich C, Gröger M (2021) Natural variability is a large source of uncertainty in future projections of hypoxia in the Baltic Sea. Communications Earth & Environment 2(1):50. https://doi.org/10.1038/s43247-021-00115-9

Meier HEM, Barghorn L, Börgel F, et al (2023) Multidecadal climate variability dominated past trends in the water balance of the Baltic Sea watershed. npj Climate and Atmospheric Science 6(1):58. https://doi.org/10.1038/s41612-023-00380-9

Mohrholz V (2018) Baltic saline barotropic inflows (SBI) 1887 - 2018 [Dataset]. URL http://doi.io-warnemuende.de/10.12754/data-2018-0004

Mohrholz V, Dutz J, Kraus G (2006) The impact of exceptionally warm summer inflow events on the environmental conditions in the Bornholm Basin. Journal of Marine Systems 60:285–301. https://doi.org/10.1016/j.jmarsys.2005.10.002

Radtke H, Brunnabend SE, Gräwe U, et al (2020) Investigating interdecadal salinity changes in the Baltic Sea in a 1850–2008 hindcast simulation. Climate of the Past 16(4):1617–1642. https://doi.org/10.5194/cp-16-1617-2020

Saraiva S, Meier HEM, Andersson H, et al (2019) Uncertainties in Projections of the Baltic Sea Ecosystem Driven by an Ensemble of Global Climate Models. Frontiers in Earth Science 6:244. https://doi.org/10.3389/feart.2018.00244

Stockmayer V, Lehmann A (2023) Variations of temperature, salinity and oxygen of the Baltic Sea for the period 1950 to 2020. Oceanologia 65(3):466–483. https://doi.org/10.1016/j.oceano.2023.02.002

Winsor P, Rodhe J, Omstedt A (2001) Baltic Sea ocean climate: an analysis of 100 yr of hydrographic data with focus on the freshwater budget. Climate Research 18:5–15. https://doi.org/10.3354/cr018005

npj | climate and atmospheric science

www.nature.com/npjclimatsci

ARTICLE OPEN

Multidecadal climate variability dominated past trends in the water balance of the Baltic Sea watershed

H. E. Markus Meier[1,2✉], Leonie Barghorn[1], Florian Börgel[1], Matthias Gröger[1], Lev Naumov[1] and Hagen Radtke[1]

The Baltic Sea watershed includes the territories of 14 countries in Northern, Central, and Eastern Europe. Long-term observations have shown that the climate in this area is characterised by a pronounced multidecadal variability, with a period of about 30 years, but its origin is thus far unknown. We propose that the observed ~30-year fluctuations in Baltic Sea salinity are caused by the Atlantic Multidecadal Variability and the North Atlantic Oscillation, which together modulate precipitation over the watershed and hence the river discharge into the Baltic Sea. The return of a large portion of the outflowing brackish Baltic Sea water with the inflowing salt water, due to mixing at the entrance area results in a positive feedback mechanism that amplifies the multidecadal variations in salinity. The strength of this self-amplification is considerable since atmospheric forcing has nearly the same periodicity as the response time of the freshwater content to external freshwater inputs.

npj Climate and Atmospheric Science (2023)6:58 ; https://doi.org/10.1038/s41612-023-00380-9

INTRODUCTION

The footprint of anthropogenic warming has been detected in many variables of the energy cycle, even at a regional scale[1]. In Northern Europe, the warming associated with climate change significantly affects the cryosphere (snow, sea ice, lake ice, river ice and glaciers), whereas systematic changes in water cycle variables (precipitation, evaporation, river discharge, ocean salinity) are less obvious[1]. In the early 1990s, the global water and energy exchanges (GEWEX) project, as part of the World Climate Research Programme, recognised the Baltic Sea catchment area as one of the regions on Earth where changes in the water cycle could be quantified[2]. This region was singled out because the salinity of the semi-enclosed Baltic Sea depends on the freshwater supply (Supplementary Fig. 1a) from a catchment area that is about four times as large as the Baltic Sea surface (Fig. 1). As the salinity of the Baltic Sea and water exchange between the Baltic Sea and the adjacent North Sea (the latter estimated from sea level records within and outside the Baltic Sea) have been monitored since the 19th century (Supplementary Fig. 2), the Baltic Sea region is well-suited to studies of the regional water cycle, using salinity as a proxy for changes in precipitation and evaporation in the entire catchment area[2–4].

Rather than a systematic trend, the mean salinity of the Baltic Sea is characterised by a pronounced low-frequency variability with a period of about 30 years, at least since 1920 (Supplementary Fig. 3). This variability has been documented in long-term observations[5–8] and historical, model-based reconstructions[8–11]. A similar multidecadal variability describes the total river discharge from the Baltic Sea catchment area[9] (see also Supplementary Fig. 4), individual river flows[12], barotropic saltwater inflows across the sills located in the Baltic Sea entrance area[13] (see also Supplementary Fig. 5), water temperature[14], sea level[15], and atmospheric variables such as precipitation and the winds over the Baltic Sea region[9]. Centennial changes have been determined as well, including a positive trend along the north-south gradient of sea surface salinity (SSS) for the period 1900–2008[8]. However, neither the trends in mean salinity[6–9] nor those at selected monitoring stations[16] were statistically significant.

Recent studies suggest that the Atlantic Multidecadal Variability (AMV) contributes to the observed low-frequency variability of the Baltic Sea basin[17,18] and other regions in the Northern Hemisphere, such as the Arctic Ocean[19]. The AMV is defined as the low-frequency variability, with alternating anomalous warm and cold states, that characterises the annual mean, spatially averaged sea surface temperature (SST) in the North Atlantic[20]. For the period 950–1800, Börgel et al.[18] traced the AMV signal determined in a regionalised paleoclimate simulation of the last millennium[21] to the Baltic Sea region. The AMV, with a currently observed period of 60–90 years[22–24], likely affected the water temperature in the Baltic Sea and partly explained the stronger increase in the mean SST of the Baltic Sea[14] than of other coastal seas worldwide[25] as determined since the 1980s.

In mid and high northern latitudes, the most prominent pattern of climate variability is the North Atlantic Oscillation (NAO), which strongly influences the weather over northeastern North America, Greenland, and Europe during winter at time scales of about 4–10 years[26] and controls the strength and direction of westerly winds across the North Atlantic region. The NAO index is defined as the difference in atmospheric pressure at sea level between the Icelandic Low and the Azores High. Several studies have shown a mutual causal influence of the AMV and NAO[27–32]. For example, Börgel et al.[17] found that the AMV causes changes in the zonal position of the NAO's centres of action over time. During a positive AMV, the Icelandic Low moves further towards North America, and the Azores High further toward Europe, with the opposite occurring during a negative AMV[17]. As a consequence of the shifting centres of action, the correlations between the NAO and variables characterising the Northern European climate, such as water temperature, sea ice, and river discharge, vary in time[17].

In this study, with the aid of historical, model-based ocean reconstructions and sensitivity experiments, we provide an explanation for the origin and mechanisms of the low-frequency variability in Baltic Sea salinity and in other variables that show a

[1]Department of Physical Oceanography and Instrumentation, Leibniz Institute for Baltic Sea Research Warnemünde, 18119 Rostock, Germany. [2]Department of Research and Development, Swedish Meteorological and Hydrological Institute, 60176 Norrköping, Sweden. ✉email: markus.meier@io-warnemuende.de

Published in partnership with CECCR at King Abdulaziz University

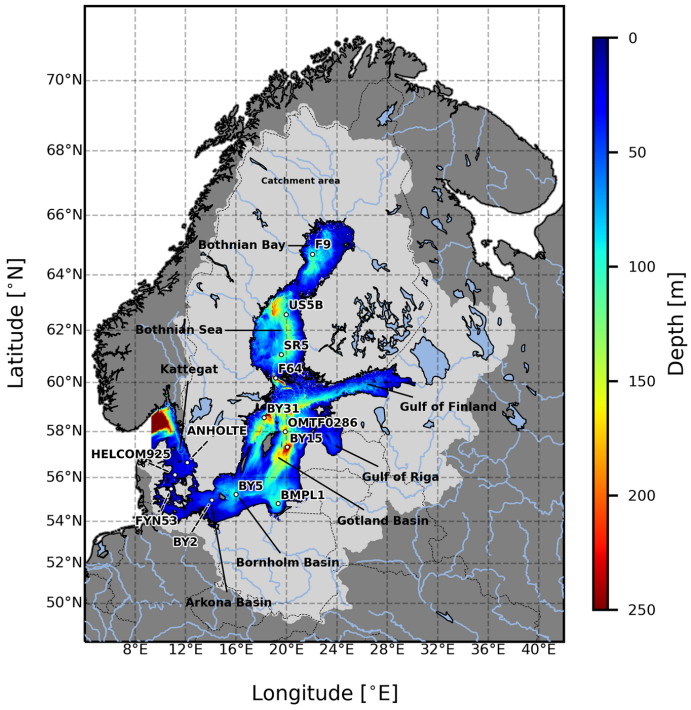

Fig. 1 Baltic Sea bathymetry. Water depth (in m)[60] and the locations of the long-term monitoring stations are shown. The domain of the Baltic Sea model is limited, with open boundaries in the northern Kattegat. The main sub-basin of the central Baltic Sea is the Gotland Basin.

Table 1. Numerical experiments.

	Experiment	Description	Relative sea level rise	Average salinity 1900–2005
1	REF+	Reference run with a sea level rise	1 mm year^{-1} [40]	7.72 g kg^{-1}
2	REF	Reference	0	7.60 g kg^{-1}
3	RUNOFF+	Climatological mean river discharge and constant net precipitation of 2364 m^3 s^{-1} [62], sea level rise is considered	1 mm year^{-1} [40]	7.61 g kg^{-1}
4	RUNOFF	As RUNOFF+ but without sea level rise	0	7.49 g kg^{-1}
5	WIND	As RUNOFF but with the repeated wind of the year 1904	0	5.82 g kg^{-1} (7.49 g kg^{-1} with drift correction)

period of about 30 years. For the period 1850–2008, five numerical simulations were performed, including a reference run (REF+), a sensitivity experiment that included the climatological mean freshwater supply (RUNOFF+), and both runs in which the global sea level rise (SLR) was excluded (REF and RUNOFF). Finally, a sensitivity experiment (WIND) was carried out that was identical to RUNOFF but with repeated wind fields for the year 1904 (Table 1).

We argue that the AMV is the pacemaker of the variability of the moisture transport from the North Atlantic to Northern Europe, as it periodically shifts the centres of action of the NAO with a current period of about 60 years. Hence, Northern Europe is alternately under the stronger and weaker influence of the milder, wetter North Atlantic climate. As the NAO and AMV influence Northern Europe, the combination of their respective patterns affects the annual mean precipitation over the Baltic Sea catchment area, river discharge, and the sea level in the Baltic Sea for a period of about 30 years. Consequently, salinity in the Baltic Sea oscillates with the same periodicity due to direct dilution. However, the latter oscillation is considerably amplified because, in addition to dilution, saltwater inflows are less (more) saline during decades with increasing (decreasing) accumulated freshwater input. Due to this self-amplification, by monitoring Baltic Sea salinity, large-scale changes in the Northern Hemisphere water cycle can be detected, thereby furthering the aims of the global GEWEX project.

Our findings are also significant with respect to ecosystem functions and structure. Changes in salinity significantly affect the marine ecosystem because many species are adapted to specific salinity ranges, including the freshwater to marine conditions of the Baltic Sea[33–35]. This study traces the origin of natural variations in salinity on multidecadal time scales. With our results, the trends caused by climate change could be separated from natural variations. Although this goal has not yet been fully achieved, decadal climate predictions for salinity may soon become possible. Such predictions could aid sustainable ecosystem

management, including the planning of fishing quotas. For instance, the reduction in weight of 3-year-old central Baltic Sea herring (*Clupea harengus*) from the late 1970s until today has been attributed to the declining salinity resulting from the multidecadal variability, which has also led to a reduction of fish catches and thus an estimated economic loss of roughly €100 million[36]. If the decline in salinity in this or other cases had been known in time, fisheries management could have reacted to the changed environmental conditions for the fish and adjusted catch quotas, and possibly an economic loss could have been avoided.

RESULTS

The origin of the low-frequency variability in the Baltic Sea

During periods with a positive winter NAO index, the winter climate over Northern Europe is warmer and wetter, and the volume of river flow from the Baltic Sea catchment area is larger compared to the long-term mean (Fig. 2). Due to the lateral displacement of the centres of action of the NAO, in particular the Icelandic Low, the AMV affects both the location of the storm track over Northern Europe and the winter NAO index in the period band of >60 years (Fig. 3). Although this power band lies just outside the cone of influence of the wavelet power spectrum of the NAO, due to the relatively short time series since 1825[37] (not shown), we argue that the combination of the zonal displacement of the NAO centres and the AMV is largely responsible for the multidecadal variability of the atmospheric flow over Northern Europe. Moreover, as the temperature fluctuations related to AMV variability and the movement of the NAO centres of action have the same periodicity, the resulting signal contains the square of the AMV harmonic with a period of about 30 years. Otherwise, the impact of the interference on the NAO is relatively small (Fig. 3). Thus, the dominating wavelet power of the NAO is situated within a period band of 4–10 years and within an AMV period band of >60 years, as expected (Fig. 3). Our hypothesis, that the AMV accounts for the 30-year climate variability over Northern Europe, is supported by the relatively high wavelet coherence of the squared AMV and the winter mean zonal wind over the central Baltic Sea in that period band (not shown). However, a confirmation of our hypothesis is difficult as the observed and reconstructed time series are relatively short compared to the dominating long-time scales of the AMV. A more detailed analysis of regional climate variability, for instance, in paleoclimate simulations and their dependencies on the AMV remains for future research.

Winter precipitation over Northern Europe, mainly explained by the advection of humid air masses from the Atlantic, therefore has a pronounced low-frequency variability of about 30 years, the phase of which corresponds well with the atmospheric flow field

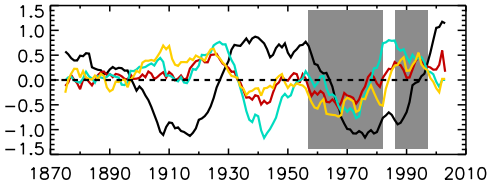

Fig. 2 Atlantic Multidecadal Variability (AMV) index, North Atlantic Oscillation (NAO) index, precipitation averaged over the Baltic Sea catchment area, and total river discharge. Low-pass filtered AMV (black)[59], precipitation[52] (red), river discharge[10] (cyan), and the winter (December through February) NAO index[37] (orange), with a cut-off frequency of 12 years. All records were normalised by their standard deviations. Selected recent periods with predominantly low (1957–1982) and high (1986–1997) NAO indices are shown as grey-shaded areas.

over the region (Fig. 2). A calculation of the Pearson correlation coefficients between the low-pass filtered precipitation or river discharge and the winter NAO index with a cut-off period of 12 years (shown in Fig. 3) yielded a value of 0.76 or 0.58. Moreover, the correlation between precipitation and river discharge was similarly high (0.79), in accordance with an earlier study[38]. Hence, river discharge is subject to multidecadal variations within the same period of about 30 years and with an amplitude of about 7% of the total mean river discharge of about 14,000 $m^3 s^{-1}$ (Supplementary Figs. 1 and 4).

In the following, we analyse a set of sensitivity studies aimed at disentangling the contributions of the different physical drivers to the low-frequency variability of the Baltic Sea's salinity. In general, salinity in estuaries is controlled by the freshwater supply from rivers of the catchment area and precipitation minus evaporation over the sea, saltwater inflows from the open ocean, and mixing by tides and wind fields.

In the Baltic Sea, the large annual freshwater supply, comprising about 2.3% of the sea's total volume, causes a large horizontal gradient in salinity of about 20 g kg^{-1} between the entrance area and the eastern- and northern-most parts of the Baltic Sea. To examine the impact of multidecadal freshwater input variations on salinity, we performed a sensitivity experiment (RUNOFF+) based on the climatological mean freshwater input (Table 1). As the Baltic Sea is semi-enclosed, with limited water exchange with the world ocean through narrow and shallow straits (Fig. 1), wind-driven large saltwater inflows, so-called major Baltic inflows (MBIs), occur only sporadically, but they are essential for the ventilation of Baltic Sea's deep water[13]. The intensity of saltwater inflows will probably increase as the global sea level rises because, in a first approximation, the transport is proportional to the cross-section at the sills[39]. Using the sensitivity experiments REF and RUNOFF without the global SLR, we investigated whether the SLR is responsible for the observed trends in the recent evolution of salinity. As the zonal west wind may hamper the outflow of brackish water from the Baltic Sea and thus limit the inflow of saltwater, an additional experiment with a constant wind was performed (WIND). Unlike in many other estuaries, in the Baltic Sea, the tides are small and low-frequency wind-induced mixing does not affect the temporal evolution of the mean salinity[11].

Impact of the freshwater supply on salinity

In the two model simulations with and without SLR (REF+ and REF), the mean salinity during 1900–2005 was 7.72 and 7.60 g kg^{-1}, respectively (Table 1). The analysis was limited to the period 1900–2005 because the reconstructed river discharge before 1900 is less reliable. The difference in mean salinity reflects the effect of the SLR relative to the sea bottom on the overall salinity in the Baltic Sea. Similar values were obtained in the two sensitivity experiments focusing on climatological freshwater input with and without SLR (RUNOFF+ and RUNOFF). The applied SLR of 1 mm $year^{-1}$ or 10.6 cm during 1900–2005 relative to the sea bottom at the sills in the Baltic Sea entrance area[40] corresponded to a salinity increase of 0.12 g kg^{-1} or +1.13 g kg^{-1} m^{-1}, which was somewhat smaller than the value obtained in a study by Meier et al.[39], in which the average salinity change per SLR was +1.41 g kg^{-1} m^{-1}. The difference can be explained by the temporal evolution of the SLR, i.e., a linear vs. step-function-like increase, as in Meier et al.[39], and the different study periods.

The results of the sensitivity experiment RUNOFF+ suggested that the interannual variations in the total freshwater supply alone explained about 52% of the Baltic Sea's interannual mean salinity variations determined in REF+ for periods >12 years (Fig. 4). The standard deviations in RUNOFF+ amounted to 0.1 g kg^{-1}, compared with 0.2 g kg^{-1} in REF+.

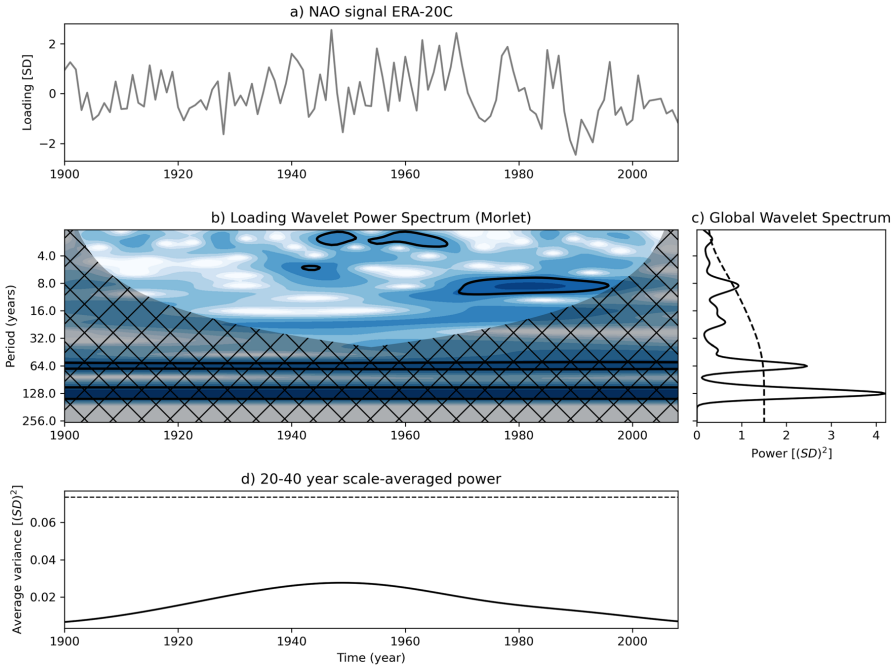

Fig. 3 Spectrum of the winter North Atlantic Oscillation (NAO) index 1900–2010. a Time series of the principal component of the first orthogonal function, **b** wavelet power, **c** power averaged over time and **d** wavelet power averaged for a period band of 20–40 years as a function of time. The black contour lines in the wavelet power spectrum show a 95% significance level[61]. The winter (December to February) NAO index was calculated from the reanalysis data ERA20C[58].

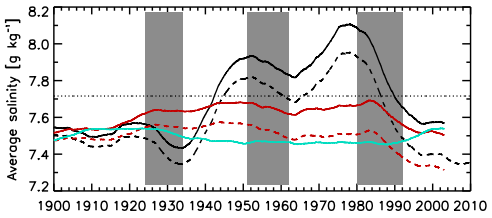

Fig. 4 Mean salinity of the Baltic Sea. Low-pass filtered, spatially averaged salinity with a cut-off period of 12 years in five numerical experiments: the reference simulation (REF+, black line), the reference simulation without a sea level rise (REF, black dashed line), and the sensitivity experiments with a climatological mean river discharge and constant net precipitation with (RUNOFF+, red line) and without (RUNOFF, red dashed line) a sea level rise and with constant wind from 1904 (WIND, cyan line). As the salinity of the WIND simulation drifted during the simulation because the wind during 1904 was not representative of the mixing input during the entire period, a drift following an e-function with an e-folding time scale of 25 years was subtracted, and the curve was shifted by a constant offset to the start value of RUNOFF in 1900. Periods with a decreasing mean salinity and a preceding local maximum in the freshwater supply (1924–1934, 1951–1962, 1980–1992) are shown as grey-shaded areas. The periods in between (1935–1950 and 1963–1979) are characterised by an increasing mean salinity and a preceding local minimum in the freshwater supply.

Impact of the freshwater supply on saltwater inflows

As data on MBIs[13] and river discharge show a significant wavelet coherence at the period of about 30 years, with river discharge preceding saltwater inflows by about 20 years (Supplementary Fig. 6), we examined whether the freshwater supply to the Baltic Sea has a causal influence on MBIs and found that the intensity of MBIs is modulated by the accumulated freshwater supply (Fig. 5). During periods with anomalously high (low) freshwater content in the Baltic Sea, the salinity of the MBIs decreases (increases), as indicated by the difference in the inflow volume with a salinity > 17 g kg^{-1} (V_{17}) between REF+ and RUNOFF+. Although changes in V_{17} are <3 km^3, or about 20% (Fig. 5), the accumulated salt transport on a decadal time scale has a significant impact on the Baltic Sea's salt content. As in the reconstructed MBIs[13] shown in Supplementary Fig. 5, a period of about 30 years is discernible (Fig. 5).

Our model results thus indicate a positive feedback mechanism amplifying the multidecadal oscillations in the mean salinity of the Baltic Sea. As described in the study by Mohrholz[13], barotropic salt transports can be approximated by the product of the inflow volume and the vertically averaged salinity in the Baltic Sea entrance area (S_B) after the so-called Kattegat–Skagerrak salinity front, separating saline North Sea and brackish Baltic Sea outflow waters[41], has reached the sills (Fig. 1). S_B depends on the surface layer salinity, which at a multidecadal time scale is a function of the mean salinity of the Baltic Sea. As volume transports during saltwater inflows only show small differences in their intensities

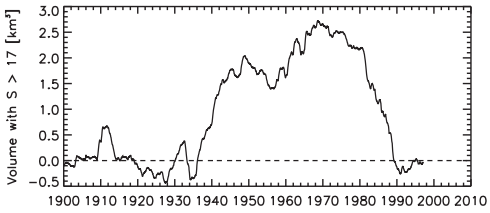

Fig. 5 Changes in saltwater inflow volume caused by low-frequency freshwater inputs. The differences in the low-pass filtered inflowing volume, with salinity > 17 g kg^{-1} and a cut-off period of 12 years, between the sensitivity experiments REF+ and RUNOFF+ are shown. The dashed line indicates zero.

with a negligible effect on mean salinity (see next sub-section), the multidecadal variations in MBIs can be explained by S_B alone. During periods characterised by an anomalously high freshwater content in the Baltic Sea, the S_B in the MBIs is, on average, smaller than during periods with an anomalously low freshwater content. Hence, the net salt import is reduced. As proof of this relationship, we calculated the surface and bottom salinity differences between REF+ and RUNOFF+ averaged during periods of decreasing mean salinity preceded by a local maximum in the freshwater supply for the years 1924–1934, 1951–1962, and 1980–1992 (Fig. 4). During these periods, the SSS in the Kattegat and the inflowing bottom salinity in the entrance area (Belt Sea) and Arkona Basin (for the location, see Fig. 1) were smaller in REF+ than in RUNOFF+ (Fig. 6a, b). Conversely, during periods with increasing mean salinity with a preceding, local minimum in freshwater supply, i.e., in 1935–1950 and 1963–1979, the SSS in the Kattegat and the inflowing bottom salinity in the entrance area (Belt Sea) and Arkona Basin were higher in REF+ than in RUNOFF+ (Fig. 6c, d). The results for V_{17} confirmed that saltwater transports related to MBIs increase (decrease) during periods of increasing (decreasing) mean salinity (Fig. 5).

Impact of wind anomalies on salinity

The results of our sensitivity experiment (WIND) suggested that the effects of the low-frequency variations of the wind on the mean salinity of the Baltic Sea (Fig. 4, blue curve) and the saltwater inflow volume V_{17} (not shown) are small. In the WIND, in addition to the constant freshwater supply, the wind fields of the year 1904 were repeated annually.

The period 1983–1992, during which there was no MBI, was an exception to the overall conclusion that wind plays only a minor role in the multidecadal salinity fluctuations[13]. During this so-called stagnation period, both the anomalously large freshwater surplus and the absence of wind patterns causing saltwater inflows resulted in a decline in the mean salinity (Fig. 4). Such stagnation periods are not unusual[21]. An analysis of paleoclimate simulations showed that periods of decreasing salinity over 10 years occur approximately once per century as part of the natural variability.

The winter mean SSS and the bottom salinity differences in RUNOFF+ between 1986–1997 and 1957–1982 are shown in Fig. 6e, f. These two periods were characterised by predominantly positive (1986–1997) and negative (1957–1982) NAO indices (Fig. 2). The SSS in the Kattegat and entrance area (Belt Sea) during 1986–1997 was higher than during 1957–1982 because of the higher sea level in the Kattegat. As a west wind hampers the outflow of surface layer water and consequently the saltwater inflow in the bottom layer at any north-south section within the Baltic Sea, the bottom salinity in the central Baltic Sea (Gotland Basin) was lower during 1986–1997 than during 1957–1982. An important role in the bottom salinity in the Gotland Basin is played by the Słupsk Channel, which connects the western (Bornholm Basin) and central Baltic Sea. In the sensitivity experiment WIND, the bottom salinity difference in the central Baltic Sea between 1986–1997 and 1957–1982 was positive because of the absence of the hampering effect of the west wind (not shown).

Impact of the sea level in the Kattegat on salinity

The sea level in the Kattegat at the open boundary of the model domain correlated well with the daily variations of the meridional sea level pressure difference over the North Sea[42,43], which may suggest an effect on saltwater inflow at multidecadal time scales. However, the results of the sensitivity experiment WIND, with constant external forcing except for the varying sea level at the open boundary in the Kattegat, indicated only a small impact of low-frequency variations in the sea level of the Kattegat on the mean salinity.

DISCUSSION

Our model simulations for the past >100 years suggest that multidecadal variations in the freshwater supply roughly explain 52% of the multidecadal variations in the mean salinity of the Baltic Sea, in agreement with previous studies[9,11]. According to Radtke et al.'s analytical approach[11], only about 27% of the variations can be explained by a 'direct dilution' effect. Hence, we conclude that most of the remainder of the 52% can be accounted for by a positive feedback mechanism operating between the accumulated freshwater supply and saltwater inflows into the Baltic Sea. During periods of enhanced freshwater supply, (1) the salinity in the surface layer decreases, (2) the location of the Kattegat–Skagerrak front moves northward, and (3) the salinity at the sills decreases. Consequently, inflow events are less saline and thereby amplify the freshening of the water body during phases of enhanced freshwater supply. As the turnover period of the freshwater content, i.e., the time scale of the internal response to external freshwater variations, roughly matches the period of external forcing in the multidecadal power band[44], this coincidence results in a considerable amplification of the salinity oscillations with a periodicity of about 30 years.

Based on Fig. 6, we estimate a peak-to-peak salinity difference—both at the sea surface and bottom and due to the moving Kattegat–Skagerrak front—of about 0.5 g kg^{-1} between selected decades with anomalous high and low freshwater input. This salinity difference would be roughly 2.5% of the salinity of 20 g kg^{-1} in the Baltic Sea entrance area. As the mean salinity varies by ~7–8% peak-to-peak (Fig. 4), at least about one-third of these variations can be roughly explained by the self-amplification effect, over and above the direct dilution effect[11]. Hence, these two processes, dilution and amplification, explain most of the signal.

Due to the self-amplification mechanism and the unique setting of the Baltic Sea, systematic changes in its water balance, e.g., those resulting from an intensified hydrological cycle of Northern Europe or the changes in large-scale atmospheric circulation patterns caused by global warming[45], might be detected earlier in the Baltic Sea than elsewhere in the Northern Hemisphere.

Our sensitivity experiments allowed us to distinguish between the influences of the low-frequency oscillations in the freshwater supply, wind forcing, and the water level in the Kattegat on the salinity of the Baltic Sea. The results suggest a dominant effect of freshwater variations via direct dilution and the above-described feedback mechanism. The remaining low-frequency variability can be explained by the timing of saltwater inflows and, in particular, the absence of these events during stagnation periods. The direct impact of the multidecadal wind variability on transport in the sea redistributes the salinity within the Baltic Sea via Ekman dynamics[46], but the impact on the mean salinity variations is only minor.

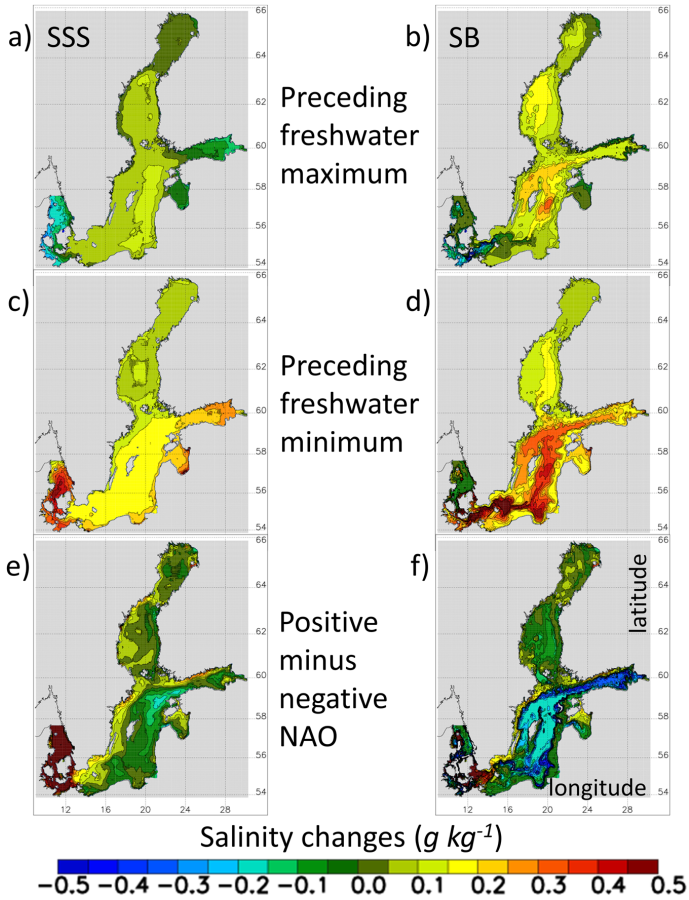

Fig. 6 Differences in sea surface and bottom salinities (in g kg^{-1}) caused by river discharge and west wind anomalies. a, **b** Differences in the autumn and winter mean (September to February), sea surface salinity (SSS) (**a**), and bottom salinity (SB) (**b**) between REF+ and RUNOFF+ averaged during 1924–1934, 1951–1962 and 1980–1992, i.e., periods with a decreasing mean salinity (Fig. 4) and with a preceding, local maximum in the freshwater supply (Fig. 2). **c**, **d** Same as (**a**) and (**b**) but showing the averaged salinity difference during 1935–1950 and 1963–1979 with increasing mean salinity (Fig. 4) and a preceding local minimum in the freshwater supply (Fig. 2). **e**, **f** Differences in the winter SSS (**e**) and bottom salinity (**f**) according to RUNOFF+ between 1986–1997 (a period with predominantly positive NAO indices, i.e., wet and with a low salinity) and 1957–1982 (a period with predominantly negative NAO indices, i.e., dry and with a high salinity).

The in situ observations of the national monitoring programme in the Baltic Sea for the period 1982–2016 showed a decrease in upper layer salinity of −0.005, to −0.014 g kg^{-1} year^{-1}, and an increase in the sub-halocline deep layer salinity of +0.02 to +0.04 g kg^{-1} year^{-1}, thereby strengthening the stratification[47]. Vertical stratification is controlled by saltwater inflows and vertical diffusion across the halocline. Hence, saltwater intrusions into the central Baltic Sea result in a sawtooth-like temporal progression of the unfiltered stratification record (not shown). In the absence of large saltwater inflows and the presence of an anomalously high freshwater supply, stratification decreased during the stagnation period 1980–1992. In 1993, it dramatically increased again. Hence, the temporal sequence of saltwater inflows, rather than the freshwater supply, mainly explains the trends since 1980 observed by Liblik and Lips[47]. Although the freshwater supply largely controls multidecadal variations in mean salinity (Supplementary Fig. 3), which is mainly controlled by the SSS, the effect of multidecadal freshwater input variations on the changes in stratification is smaller than the effect of MBIs over time scales >4 years (Supplementary Fig. 7). An accumulation of power within the 20- to the 40-year period band was not statistically significant (Supplementary Fig. 8).

METHODS

A detailed description of the Baltic Sea model setup was presented in a previous study[10]. Here we provide a summary of the physical module.

Model description

The Rossby Centre Ocean model, a three-dimensional ocean circulation model coupled to a Hibler-type, multi-category sea-ice model, was used[48–51]. Subgrid-scale mixing in the ocean was

parameterised using a state-of-the-art k–ε turbulence closure scheme with flux boundary conditions. A flux-corrected, monotonicity-preserving transport scheme, without explicit horizontal diffusion, was embedded in the model. The model domain comprised the Baltic Sea and the Kattegat, with lateral open boundaries in the northern Kattegat (Fig. 1). The horizontal resolution was 3.7 km, and the vertical resolution was 3 m.

Atmospheric forcing

Regionalised reanalysis data for 1958–2007, historical station data of daily sea level pressure, and monthly air temperature observations were used in the reconstruction of multivariate 3-h, high-resolution atmospheric forcing fields (HiResAFF) for the period 1850–2008, based on the analogue method[52]. The latter searches for the atmospheric surface fields that are most similar to the historical observations in a library of predictands from the calibration period 1958–2007. The predictands or analogues are multivariate atmospheric forcing fields of 2 m air temperature, 2 m specific humidity, 10 m wind, precipitation, total cloud cover, and mean sea level pressure recorded in the Rossby Centre Atmosphere Ocean model[53], with a horizontal resolution of 0.25° × 0.25° (~25 km) interpolated onto a regular geographical grid.

River discharge

Monthly mean river flows were calculated from several merged data sets (Supplementary Fig. 1). Since the inter-annual variability of the reconstructed river discharge was significantly underestimated before but not after 1900 (Supplementary Fig. 1), the analysis was limited to the period 1900–2008.

Lateral boundary data

Daily mean sea level elevations at the lateral boundary were calculated from the reconstructed meridional sea level pressure gradient across the North Sea[42]. Gustafsson et al.[43] calculated the correlations of the various frequency bands using empirical orthogonal functions (EOFs) to avoid underestimating extremes. The mean value of the time series was subtracted and replaced at the lateral boundary by the mean sea level in the Nordic Height System 1960[54]. A linearly rising mean sea level of 1 mm year^{-1} relative to the sea bottom at the sills in the entrance area was implemented by continuously deepening the water depth at all grid points[40,55]. A spatially differing land uplift with greater rates in the north than in the south was not considered. In the case of inflow, temperature and salinity were nudged towards the observed climatological seasonal mean profiles for 1980–2005 located north of the lateral boundary in Kattegat.

Initial conditions

After a spin-up simulation for 1850–1902 utilising the reconstructed forcing described above, the physical variables calculated for the end of the spin-up simulation on January 1, 1903, were used as the initial conditions for January 1, 1850.

Experimental strategy

A 159-year reference simulation for 1850–2008 was performed using the forcing data described above (henceforth referred to as REF+). In addition to REF+, four sensitivity experiments were carried out with the same experimental setup as in REF+ but with modified forcing data to identify the main drivers of the multidecadal variability (Table 1). The sensitivity experiments REF, RUNOFF and WIND have previously been analysed[8,10]. In REF+ and RUNOFF+, the global eustatic sea level rise was considered.

The RUNOFF+ and RUNOFF sensitivity experiments with climatological mean freshwater input were conducted to investigate the effects of interannual to multiannual variations in river discharge on the salinity of the Baltic Sea. In the WIND experiment, in addition to the freshwater input, interannual variations in atmospheric forcing were also neglected by repeating the 1904 atmospheric forcing for all years. The results of this sensitivity experiment show the effect of the low-frequency variations of the wind field on salinity. As 1904 does not contain an MBI event, the salinity decreases with an e-folding time scale of 25 years. Conversely, the atmospheric forcing with a year with MBI would result in a drift to higher salinity. However, regardless of the chosen sensitivity experiment, the influence of the multidecadal variations in the wind field on the salinity can be studied after subtracting the drift.

Previous studies concluded that ice cover in the Baltic Sea in the 20th century had no influence on salinity[9]. Therefore, this effect was not analysed here.

Evaluation of saltwater inflows

Sporadic events of large saltwater inflows, so-called MBIs, are essential for the ventilation of the Baltic Sea's deep water[13]. Simulated MBIs, calculated from the inflowing volume with salinity > 17 g kg^{-1} (V_{17}), were close to the MBIs calculated from the observations of Mohrholz[13]. The largest inflow on record was in 1951. Three out of the four largest MBIs, i.e. those in 1921, 1951, and 2014, were also identified as record events in the simulation when the reference run was prolonged[56]. Only the MBI in 1898 was not reproduced, probably due to the inaccurate data used as forcing in our simulation or in the reconstruction of the MBIs[13]. Furthermore, a distinct stagnation period from 1983 to 1992 was identified in our simulation, as was also observed. This analysis demonstrated that our modelled MBIs sufficiently well reproduced the observed MBIs.

Evaluation of salinity at selected stations

Supplementary Fig. 2 shows the simulated and observed sea surface and bottom salinities at selected monitoring stations with relatively long records of observations (Fig. 1). At stations located within the Baltic Sea, the model accurately reproduced the pronounced multidecadal variability of about 30 years, both at the sea surface and the sea bottom (Supplementary Fig. 2, see also Fig. 4 and Supplementary Fig. 3). However, there was less agreement between the model's results and observations at the three available stations located in the entrance area, i.e., the Kattegat and the Great Belt. This was in part due to the sparse measurements in this area and to the difficulty of adequately evaluating the model in this highly dynamic transition area between the North Sea and the Baltic Sea. Furthermore, at some stations located in the central Baltic Sea (e.g., BY15, OMTF0286, BY31), there was also less agreement between the model's results for bottom salinity and observations during about 1950–1970. Probably the simulated intensity of the large MBI in 1951 is underestimated. Please note that long-term reconstructed atmospheric fields have been used as forcing data whose quality is less good than that of reanalysis data or observations. If high-quality atmospheric forcing data are used, the RCO model can reproduce saltwater inflows well[57].

For further results of the model evaluation, the reader is referred to Meier et al.[10].

Observational datasets

The winter (December to February) NAO index was derived from long-term observations of the difference in sea level pressure between Reykjavik, Iceland, and Gibraltar, Spain (available from the Climatic Research Unit, University of East Anglia; https://crudata.uea.ac.uk/cru/data/nao/nao.dat)[37] and from an EOF analysis of the reanalysis data ERA20C[58]. Despite differences in the resulting records, the conclusions of this study do not depend on

the method used to calculate the NAO index. The annual mean AMV index was calculated from SST anomalies recorded in the HadISST dataset[59] averaged over the North Atlantic between 0 and 70°N latitude. Precipitation data from the HiResAFF dataset[52] were averaged over the Baltic Sea catchment area between 9.6°E and 32°E and between 52.4°N and 67.4°N. The simulated salinity was evaluated using observations from the International Council for the Exploration of the Sea (ICES) at https://www.ices.dk/data/data-portals/Pages/ocean.aspx. These measurements were post-processed to fill gaps, following the method of Radtke et al.[11].

DATA AVAILABILITY

The observational and model data analysed in this study and displayed in the figures are publicly available from the Leibniz Institute for Baltic Sea Research Warnemünde (IOW) at the doi server https://doi.io-warnemuende.de/10.12754/data-2023-0001. Water depth data compiled by Seifert and Kayser[60] and saltwater inflow data DS5 calculated by Mohrholz[13] are publicly available from https://www.io-warnemuende.de/topography-of-the-baltic-sea.html and https://www.io-warnemuende.de/major-baltic-inflow-statistics-7274.html (http://doi.io-warnemuende.de/10.12754/data-2018-0004), respectively. These datasets are provided through the Creative Commons (CC) data license of type CC BY 4.0 (https://creativecommons.org/licences/by/4.0/).

CODE AVAILABILITY

The model code of the ocean model used for the historical simulations is publicly available from the Swedish Meteorological and Hydrological Institute, Norrköping, Sweden (https://www.smhi.se, E-mail: smhi@smhi.se).

Received: 4 November 2022; Accepted: 16 May 2023;
Published online: 05 June 2023

REFERENCES

1. Meier, H. E. M. et al. Climate change in the Baltic Sea region: a summary. *Earth Syst. Dynam.* **13**, 457–593 (2022).
2. Reckermann, M. et al. BALTEX—an interdisciplinary research network for the Baltic Sea region. *Environ. Res. Lett.* **6**, 045205 (2011).
3. Meier, H. E. M., Rutgersson, A. & Reckermann, M. An Earth System Science Program for the Baltic Sea region. *Eos* https://doi.org/10.1002/2014EO130001 (2014).
4. Lehmann, A. et al. Salinity dynamics of the Baltic Sea. *Earth Syst. Dynam.* **13**, 373–392 (2022).
5. Samuelsson, M. Interannual salinity variations in the Baltic Sea during the period 1954–1990. *Cont. Shelf Res.* **16**, 1463–1477 (1996).
6. Winsor, P., Rodhe, J. & Omstedt, A. Erratum: Baltic Sea ocean climate: an analysis of 100 yr of hydrographical data with focus on the freshwater budget. *Clim. Res.* **25**, 183 (2003).
7. Winsor, P., Rodhe, J. & Omstedt, A. Baltic Sea ocean climate: an analysis of 100 yr of hydrographic data with focus on the freshwater budget. *Clim. Res.* **18**, 5–15 (2001).
8. Kniebusch, M., Meier, H. E. M. & Radtke, H. Changing salinity gradients in the Baltic Sea as a consequence of altered freshwater budgets. *Geophys. Res. Lett.* **46**, 9739–9747 (2019).
9. Meier, H. E. M. & Kauker, F. Modeling decadal variability of the Baltic Sea: 2. Role of freshwater inflow and large-scale atmospheric circulation for salinity. *J. Geophys. Res.* **108**, 3368 (2003).
10. Meier, H. E. M. et al. Disentangling the impact of nutrient load and climate changes on Baltic Sea hypoxia and eutrophication since 1850. *Clim. Dyn.* **53**, 1145–1166 (2019).
11. Radtke, H., Brunnabend, S. E., Gräwe, U. & Meier, H. E. M. Investigating interdecadal salinity changes in the Baltic Sea in a 1850–2008 hindcast simulation. *Climate* **16**, 1617–1642 (2020).
12. Gailiušis, B., Kriaučiūnienė, J., Jakimavičius, D. & Šarauskienė, D. The variability of long-term runoff series in the Baltic Sea drainage basin. *Baltica* **24**, 45–54 (2011).
13. Mohrholz, V. Major Baltic inflow statistics—revised. *Front. Mar. Sci.* **5**, 384 (2018).
14. Kniebusch, M., Meier, H. E. M., Neumann, T. & Börgel, F. Temperature Variability of the Baltic Sea Since 1850 and Attribution to Atmospheric Forcing Variables. *J. Geophys. Res.* **124**, 4168–4187 (2019).
15. Medvedev, I. & Kulikov, E. Low-frequency Baltic Sea level spectrum. *Front. Earth Sci.* **7**, 284 (2019).
16. Fonselius, S. & Valderrama, J. One hundred years of hydrographic measurements in the Baltic Sea. *J. Sea Res.* **49**, 229–241 (2003).
17. Börgel, F., Frauen, C., Neumann, T. & Meier, H. E. M. The Atlantic Multidecadal Oscillation controls the impact of the North Atlantic Oscillation on North European climate. *Environ. Res. Lett.* **15**, 104025 (2020).
18. Börgel, F., Frauen, C., Neumann, T., Schimanke, S. & Meier, H. E. M. Impact of the Atlantic Multidecadal Oscillation on Baltic Sea Variability. *Geophys. Res. Lett.* **45**, 9880–9888 (2018).
19. Cai, Q., Beletsky, D., Wang, J. & Lei, R. Interannual and decadal variability of Arctic Summer Sea Ice associated with atmospheric teleconnection patterns during 1850–2017. *J. Clim.* **34**, 9931–9955 (2021).
20. Enfield, D. B., Mestas-Nuñez, A. M. & Trimble, P. J. The Atlantic Multidecadal Oscillation and its relation to rainfall and river flows in the continental U.S. *Geophys. Res. Lett.* **28**, 2077–2080 (2001).
21. Schimanke, S. & Meier, H. E. M. Decadal-to-centennial variability of salinity in the Baltic Sea. *J. Clim.* **29**, 7173–7188 (2016).
22. Knight, J. R., Folland, C. K. & Scaife, A. A. Climate impacts of the Atlantic Multidecadal Oscillation. *Geophys. Res. Lett.* **33**, L17706 (2006).
23. Schlesinger, M. E. & Ramankutty, N. An oscillation in the global climate system of period 65–70 years. *Nature* **367**, 723–726 (1994).
24. Sutton, R. T. & Hodson, D. L. R. Atlantic ocean forcing of North American and European summer climate. *Science* **309**, 115–118 (2005).
25. Belkin, I. M. Rapid warming of large marine ecosystems. *Prog. Oceanogr.* **81**, 207–213 (2009).
26. Hurrell, J. W. Decadal trends in the North Atlantic Oscillation: regional temperatures and precipitation. *Science* **269**, 676–679 (1995).
27. Peings, Y. & Magnusdottir, G. Forcing of the wintertime atmospheric circulation by the multidecadal fluctuations of the North Atlantic Ocean. *Environ. Res. Lett.* **9**, 034018 (2014).
28. Gastineau, G. & Frankignoul, C. Influence of the North Atlantic SST variability on the atmospheric circulation during the twentieth century. *J. Clim.* **28**, 1396–1416 (2015).
29. Delworth, T. L. et al. The central role of ocean dynamics in connecting the North Atlantic oscillation to the extratropical component of the Atlantic multidecadal oscillation. *J. Clim.* **30**, 3789–3805 (2017).
30. Delworth, T. L. & Zeng, F. The impact of the North Atlantic oscillation on climate through its influence on the Atlantic Meridional overturning circulation. *J. Clim.* **29**, 941–962 (2016).
31. Wills, R. C. J., White, R. H. & Levine, X. J. Northern hemisphere stationary waves in a changing climate. *Curr. Clim. Chang. Rep.* **5**, 372–389 (2019).
32. Sun, C., Li, J. & Jin, F.-F. A delayed oscillator model for the quasi-periodic multidecadal variability of the NAO. *Clim. Dyn.* **45**, 2083–2099 (2015).
33. Remane, A. Die Brackwasserfauna: mit besonderer Berücksichtigung der Ostsee. *Zool. Anz.* **Suppl. 7**, 34–74 (1934).
34. Vuorinen, I. et al. Scenario simulations of future salinity and ecological consequences in the Baltic Sea and adjacent North Sea areas–implications for environmental monitoring. *Ecol. Indic.* **50**, 196–205 (2015).
35. Holopainen, R. et al. Impacts of changing climate on the non-indigenous invertebrates in the northern Baltic Sea by end of the twenty-first century. *Biol. Invasions* **18**, 3015–3032 (2016).
36. Dippner, J. W., Fründt, B. & Hammer, C. Lake or Sea? The Unknown Future of Central Baltic Sea Herring. *Front. Ecol. Evol.* **7**, 143 (2019).
37. Jones, P. D., Jonsson, T. & Wheeler, D. Extension to the North Atlantic oscillation using early instrumental pressure observations from Gibraltar and south-west Iceland. *Int. J. Climatol.* **17**, 1433–1450 (1997).
38. Kauker, F. & Meier, H. E. M. Modeling decadal variability of the Baltic Sea: 1. Reconstructing atmospheric surface data for the period 1902-1998. *J. Geophys. Res.* **108**, 3268 (2003).
39. Meier, H. E. M., Höglund, A., Eilola, K. & Almroth-Rosell, E. Impact of accelerated future global mean sea level rise on hypoxia in the Baltic Sea. *Clim. Dyn.* **49**, 163–172 (2017).
40. Madsen, K. S., Høyer, J. L., Suursaar, Ü., She, J. & Knudsen, P. Sea level trends and variability of the Baltic Sea From 2D statistical reconstruction and altimetry. *Front. Earth Sci.* **7**, 243 (2019).
41. Rodhe, J. & Winsor, P. On the influence of the freshwater supply on the Baltic Sea mean salinity. *Tellus A* **54**, 175–186 (2002).
42. Gustafsson, B. G. & Andersson, H. C. Modeling the exchange of the Baltic Sea from the meridional atmospheric pressure difference across the North Sea. *J. Geophys. Res.* **106**, 19731–19744 (2001).
43. Gustafsson, B. G. et al. Reconstructing the development of Baltic Sea eutrophication 1850-2006. *Ambio* **41**, 534–548 (2012).
44. Döös, K., Meier, H. E. M. & Döscher, R. The Baltic haline conveyor belt or the overturning circulation and mixing in the Baltic. *Ambio* **33**, 261–266 (2004).

45. Busuioc, A., Chen, D. & Hellström, C. Temporal and spatial variability of precipitation in Sweden and its link with the large-scale atmospheric circulation. *Tellus A* **53**, 348–367 (2001).
46. Krauss, W. & Brügge, B. Wind-produced water exchange between the Deep Basins of the Baltic Sea. *J. Phys. Oceanogr.* **21**, 373–384 (1991).
47. Liblik, T. & Lips, U. Stratification has strengthened in the Baltic Sea—an analysis of 35 years of observational data. *Front. Earth Sci.* **7**, 174 (2019).
48. Meier, H. E. M., Döscher, R. & Faxén, T. A multiprocessor coupled ice-ocean model for the Baltic Sea: application to salt inflow. *J. Geophys. Res.* **108**, 3273 (2003).
49. Meier, H. E. M. Modeling the pathways and ages of inflowing salt-and freshwater in the Baltic Sea. *Estuar. Coast. Shelf Sci.* **74**, 610–627 (2007).
50. Meier, H. E. M. On the parameterization of mixing in three-dimensional Baltic Sea models. *J. Geophys. Res.* **106**, 30997–31016 (2001).
51. Mårtensson, S., Meier, H. E. M., Pemberton, P. & Haapala, J. Ridged sea ice characteristics in the Arctic from a coupled multicategory sea ice model. *J. Geophys. Res.* **117**, C00D15 (2012).
52. Schenk, F. & Zorita, E. Reconstruction of high resolution atmospheric fields for Northern Europe using analog-upscaling. *Climate* **8**, 1681–1703 (2012).
53. Döscher, R. et al. The development of the regional coupled ocean-atmosphere model RCAO. *Boreal Environ. Res.* **7**, 183–192 (2002).
54. Ekman, M. & Mäkinen, J. Mean sea surface topography in the Baltic Sea and its transition area to the North Sea: a geodetic solution and comparisons with oceanographic models. *J. Geophys. Res.* **101**, 11993–11999 (1996).
55. Meier, H. E. M., Dieterich, C. & Gröger, M. Natural variability is a large source of uncertainty in future projections of hypoxia in the Baltic Sea. *Commun. Earth Environ.* **2**, 50 (2021).
56. Meier, H. E. M., Väli, G., Naumann, M., Eilola, K. & Frauen, C. Recently accelerated oxygen consumption rates amplify deoxygenation in the Baltic Sea. *J. Geophys. Res.* **123**, 3227–3240 (2018).
57. Meier, H. E. M., Döscher, R., Broman, B. & Piechura, J. The major Baltic inflow in January 2003 and preconditioning by smaller inflows in summer-autumn 2002: a model study. *Oceanologia* **46**, 557–579 (2004).
58. Poli, P. et al. ERA-20C: an atmospheric reanalysis of the twentieth century. *J. Clim.* **29**, 4083–4097 (2016).
59. Rayner, N. A. et al. Global analyses of sea surface temperature, sea ice, and night marine air temperature since the late nineteenth century. *J. Geophys. Res.* **108**, 4407 (2003).
60. Seifert, T. & Kayser, B. A high resolution spherical grid topography of the Baltic Sea. *Issue 9 of Meereswissenschaftliche Berichte* (Institut fur Ostseeforschung, Warnemünde 77–88 (Marine Science Report, Baltic Sea Research Institute, 1995).
61. Grinsted, A., Moore, J. C. & Jevrejeva, S. Application of the cross wavelet transform and wavelet coherence to geophysical time series. *Nonlinear Proc. Geophys.* **11**, 561–566 (2004).
62. Meier, H. E. M. & Döscher, R. Simulated water and heat cycles of the Baltic Sea using a 3D coupled atmosphere-ice-ocean model. *Boreal Environ. Res.* **7**, 327–334 (2002).

ACKNOWLEDGEMENTS

The research presented in this study is part of the Baltic Earth programme (Earth System Science for the Baltic Sea region, see http://www.baltic.earth) and was funded by the Swedish Research Council for Environment, Agricultural Sciences and Spatial Planning (Formas) through the ClimeMarine project within the framework of the National Research Programme for Climate (grant No. 2017-01949). Data from the IOW's long-term monitoring programme were used.

AUTHOR CONTRIBUTIONS

H.E.M.M. designed the research, performed the sensitivity simulations, analysed the model results and wrote the paper with the help of all co-authors: L.B., F.B., M.G., L.N. and H.R. L.B. and F.B. performed the wavelet analyses and L.N. analysed the model results vs. observations. H.R. prepared the salinity observations and analysis tools.

FUNDING

Open Access funding enabled and organized by Projekt DEAL.

COMPETING INTERESTS

The authors declare no competing interests.

ADDITIONAL INFORMATION

Supplementary information The online version contains supplementary material available at https://doi.org/10.1038/s41612-023-00380-9.

Correspondence and requests for materials should be addressed to H. E. Markus Meier.

Reprints and permission information is available at http://www.nature.com/reprints

Publisher's note Springer Nature remains neutral with regard to jurisdictional claims in published maps and institutional affiliations.

Multidecadal climate variability dominated past trends in the water balance of the Baltic Sea catchment area

H. E. Markus Meier[1,2,*], Leonie Barghorn[1], Florian Börgel[1], Matthias Gröger[1], Lev Naumov[1], and Hagen Radtke[1]

[1]Department of Physical Oceanography and Instrumentation, Leibniz Institute for Baltic Sea Research Warnemünde, 18119 Rostock, Germany.

[2]Department of Research and Development, Swedish Meteorological and Hydrological Institute, 60176 Norrköping, Sweden.

*e-mail: markus.meier@io-warnemuende.de

Corresponding author:

H. E. Markus Meier

Department of Physical Oceanography and Instrumentation

Leibniz Institute for Baltic Sea Research Warnemünde

Seestrasse 15

18119 Rostock

Germany

Tel.: +49 381 5197 150

E-mail: markus.meier@io-warnemuende.de

Supplementary Information

This Supplementary Information consists of Supplementary Figures 1–8.

Supplementary Figures

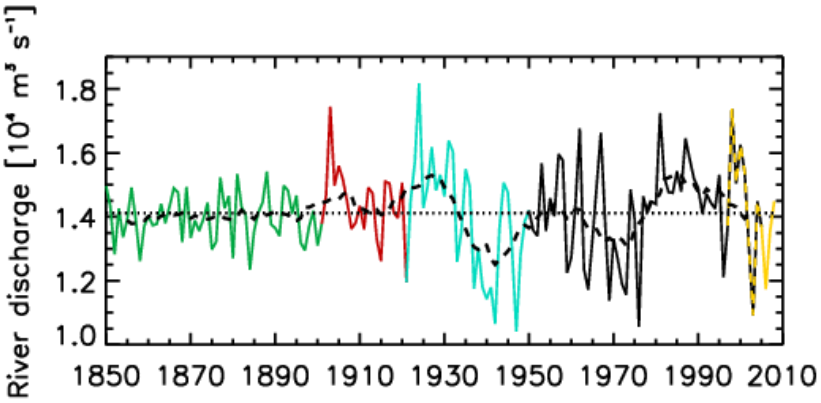

Supplementary Fig. 1 Reconstructed total river discharge to the Baltic Sea 1850-2008. Annual (solid line) and low-pass filtered (dashed line) river discharge reconstructed from various datasets (indicated by different colors) with a cut-off period of 12 years by Meier et al. (2019). The long-term mean (1850-2008) river runoff to the Baltic Sea (dotted line) amounts to 14,100 $m^3 s^{-1}$. (Source: Meier et al., 2019; their Fig. 3 published open access under the terms of the Creative Commons Attribution 4.0 International licence)

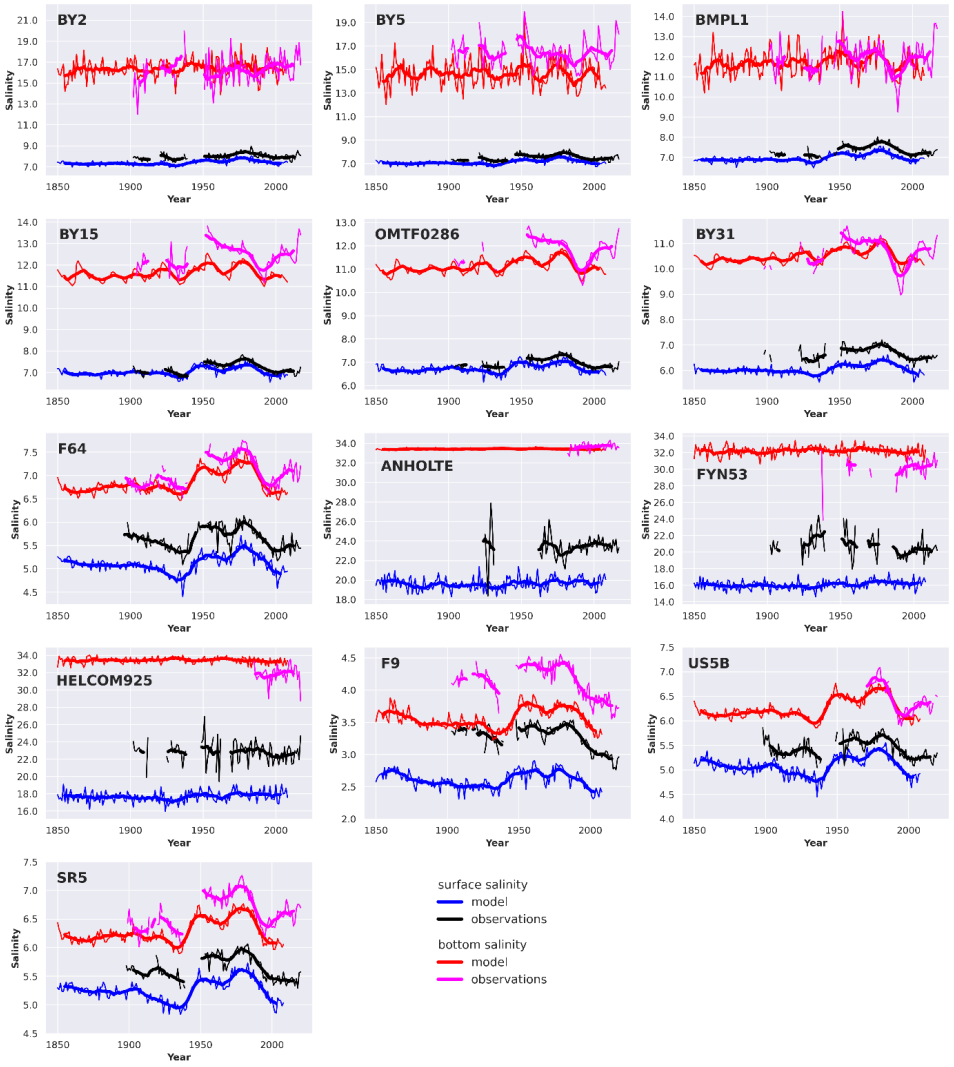

Supplementary Fig. 2 Simulated and observed sea surface and bottom salinities at various monitoring stations. Salinities in g kg^{-1}. Following Radtke et al. (2020), measurements are post-processed to fill gaps. Thin lines: annual averages. Thick lines: 11-year running mean. In Fig. 1, the locations of the long-term monitoring stations are shown.

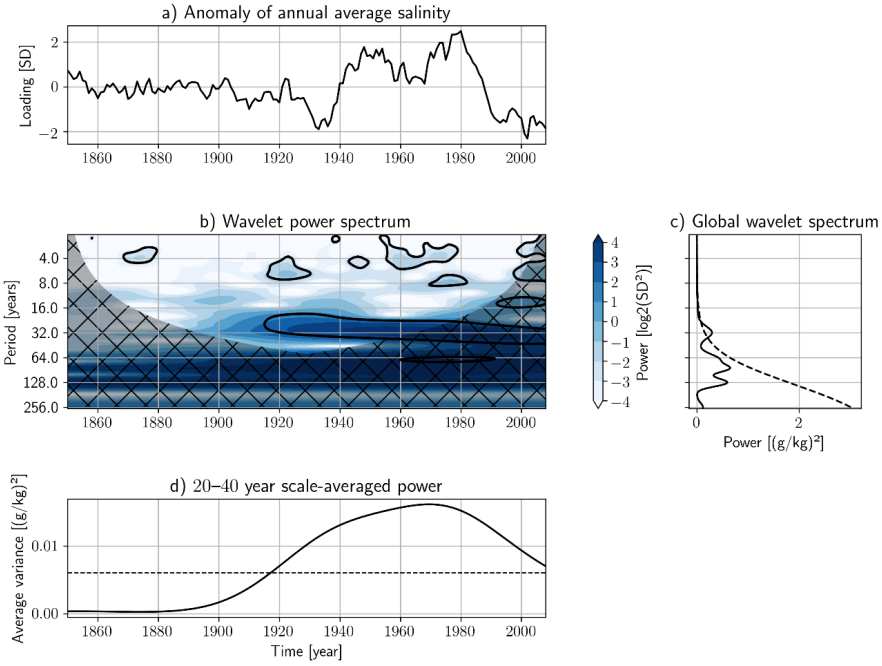

Supplementary Fig. 3 Spectrum of annual mean salinity averaged over the Baltic Sea 1850-2008. Shown are results of the reference simulation REF+. a) Time series, b) wavelet power, c) power averaged over time and d) wavelet power averaged for the period band between 20 and 40 years as a function of time. The black contour lines in the wavelet power spectrum show the 95% significance level (Grinsted et al., 2004).

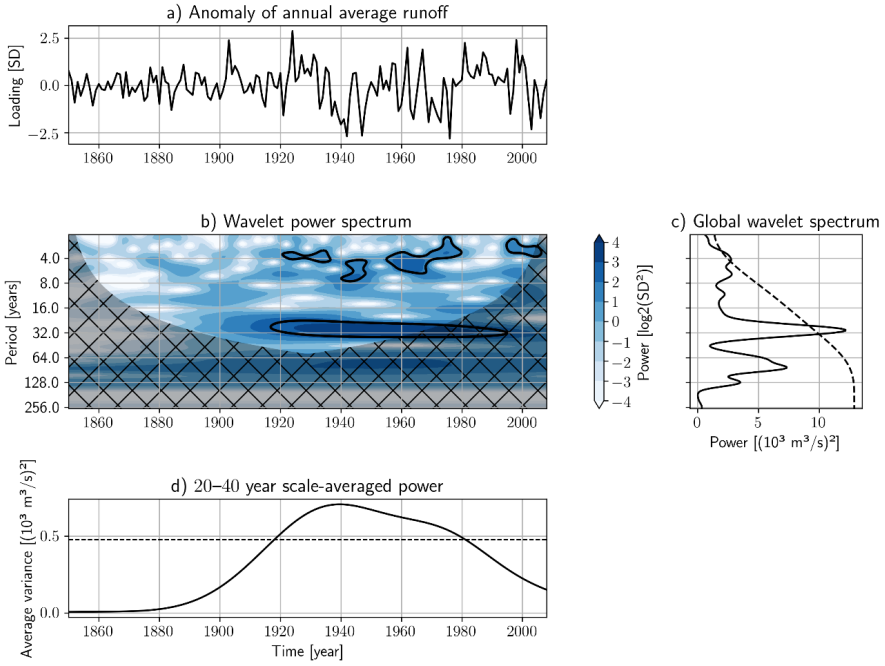

Supplementary Fig. 4 Spectrum of the annual river discharge to the Baltic Sea 1850-2008. a) Time series, b) wavelet power, c) power averaged over time and d) wavelet power averaged for the period band between 20 and 40 years as a function of time. The black contour lines in the wavelet power spectrum show the 95% significance level (Grinsted et al., 2004). (Data source: Meier et al., 2019)

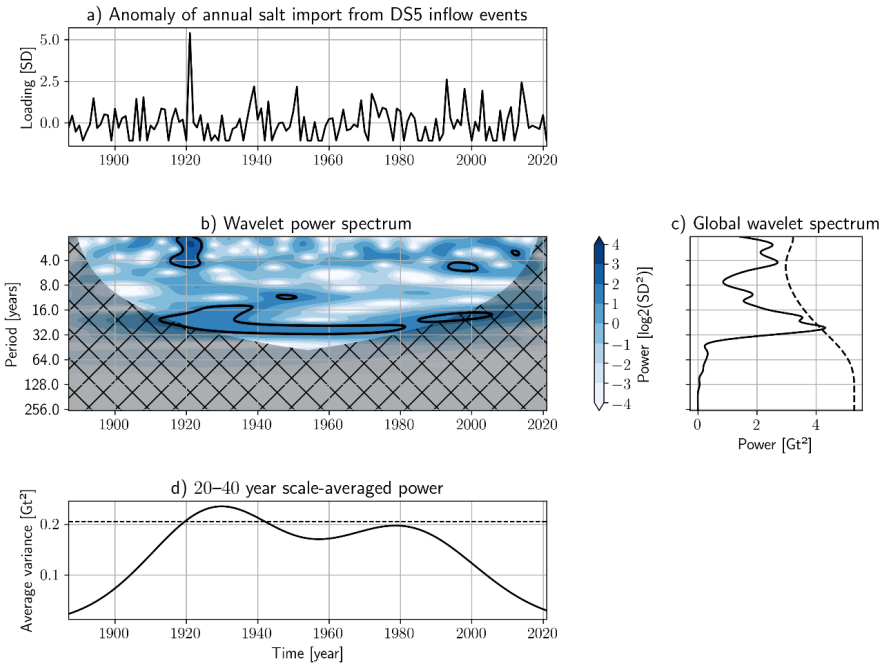

Supplementary Fig. 5 Spectrum of the annual mean salt import from reconstructed Major Baltic Inflows (so-called DS5 events) 1887-2021. a) Time series, b) wavelet power, c) power averaged over time and d) wavelet power averaged for the period band between 20 and 40 years as a function of time. The black contour lines in the wavelet power spectrum show the 95% significance level (Grinsted et al., 2004). (Data source: Mohrholz, 2018)

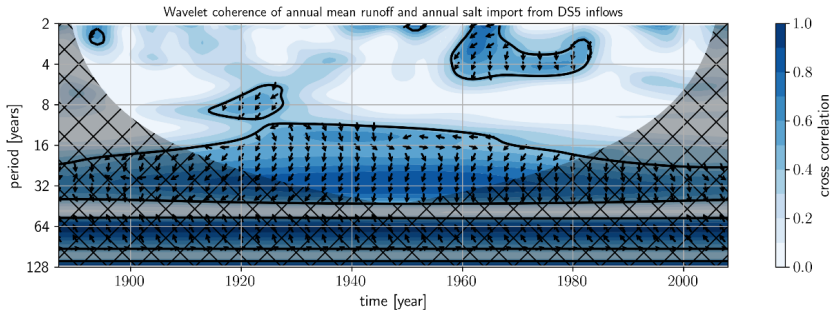

Supplementary Fig. 6 Wavelet coherence between the annual mean river discharge and the annual mean salt import from DS5 inflow events 1887-2008. The black contour lines show the 95% significance level (Grinsted et al., 2004). The arrows in the significant regions indicate the phase relationship between the signals: pointing right (left) in phase (antiphase), and river discharge leading (lagging) the salt import straight down (up). (Data source: Mohrholz, 2018; Meier et al., 2019)

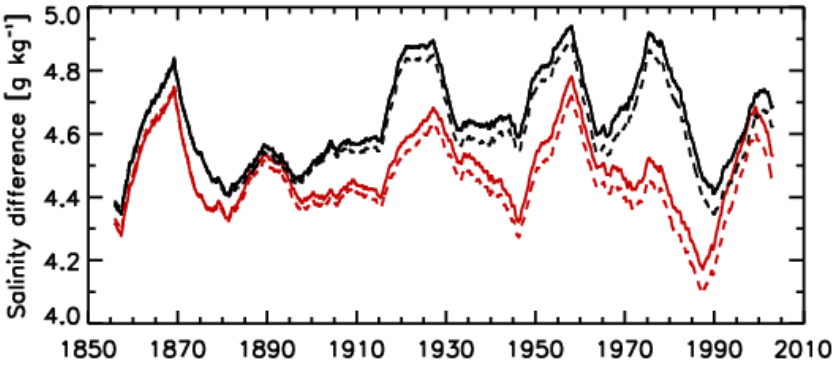

Supplementary Fig. 7 Stratification in the central Baltic Sea. Low-pass filtered salinity difference (in g kg^{-1}) between sea surface and bottom salinity at Gotland Deep (BY15) with a cut-off period of 12 years. For the location of the monitoring station BY15 see Fig. 1. The curves show the numerical experiments REF+ (black solid line), REF (black dashed line), RUNOFF+ (red solid line) and RUNOFF (red dashed line).

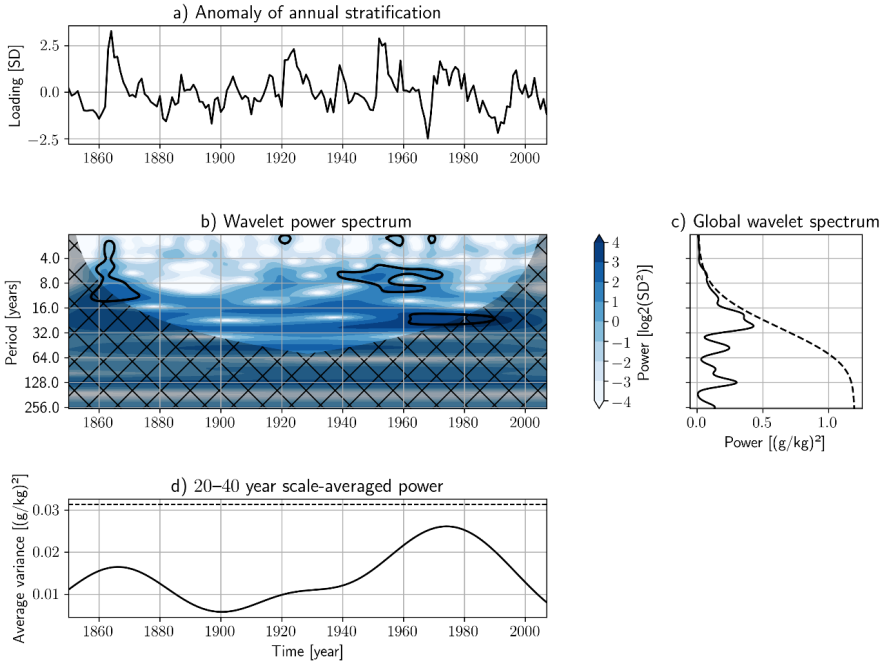

Supplementary Fig. 8 Spectrum of annual mean stratification in the central Baltic Sea 1850-2008. Shown is the salinity difference (in g kg^{-1}) between sea surface and bottom salinity at Gotland Deep (BY15) in the numerical experiment REF+. a) Time series, b) wavelet power, c) power averaged over time and d) wavelet power averaged for the period band between 20 and 40 years as a function of time. The black contour lines in the wavelet power spectrum show the 95% significance level (Grinsted et al., 2004).

References

Grinsted, A., Moore, J. C., & Jevrejeva, S. Application of the cross wavelet transform and wavelet coherence to geophysical time series. *Nonlinear Proc. Geoph.*, **11**(5/6), 561-566 (2004).

Meier, H. E. M., et al. Disentangling the impact of nutrient load and climate changes on Baltic Sea hypoxia and eutrophication since 1850. *Clim. Dyn.,* **53**(1), 1145-1166 (2019).

Mohrholz, V. Major Baltic inflow statistics–revised. *Front. Mar. Sci.*, **5**, 384 (2018).

Radtke, H., Brunnabend, S. E., Gräwe, U., & Meier, H. E. M. Investigating interdecadal salinity changes in the Baltic Sea in a 1850–2008 hindcast simulation. *Clim. Past*, **16**(4), 1617-1642 (2020).

Atlantic Multidecadal Variability control on European seas is mainly externally forced

Barghorn, L., Börgel, F., Gröger, M., and Meier, H. E. M.

Department of Physical Oceanography and Instrumentation, Leibniz Institute for Baltic Sea Research Warnemuende, Seestrasse 15, Rostock, 18119, Germany

E-mail: leonie.barghorn@io-warnemuende.de

Abstract. The semi-enclosed European seas (Baltic Sea, North Sea, Mediterranean Sea, and Black Sea) have been among the fastest warming seas worldwide during the last decades. Projections of future temperature trends can provide essential information for decision makers, but they are subject to a number of uncertainties. One important source of uncertainty is the rather high internal climate variability in that region. Separating internal variability and forced trends is therefore paramount. Particularly powerful tools for this separation are Single-Model Initial-condition Large Ensembles (SMILEs). In such ensembles, the same model is run multiple times with similar forcing but varying initial conditions, resulting in different realizations of internal variability. This study employs two SMILEs to decompose European sea surface temperatures (SSTs) into forced trends and internal variability and to investigate whether and how the latter is affected by the Atlantic Multidecadal Variability (AMV) in the historical period and different future emission scenarios. It is shown that on a decadal scale, the effect of the AMV on the European SSTs will stay important, especially in lower emission scenarios. However, on longer time scales, forced trends will be much higher and in all but the lowest emission scenario considered, more than 2 °C warming compared to 1950 are very likely to be reached until the end of the century in all semi-enclosed European seas.

Keywords: regional climate change, climate variability, Atlantic Multidecadal Variability
Submitted to: *Environ. Res. Lett.*

1. Introduction

Global warming has been advancing rapidly since the beginning of the industrial era, causing rising water temperatures almost everywhere around the globe [29]. Of special concern are the changes in so-called large marine ecosystems (LMEs). These coastal areas are hotspots of marine biomass production and may account for about 80 % of the annual worldwide fish catch, while they are also most affected by multiple stressors [28]. The European seas North Sea, Baltic Sea, Mediterranean Sea, and Black Sea are

examples for such LMEs and have been among the fastest warming coastal seas during the last decades [3, 35, 28, 56] with sea surface temperature (SST) trends reaching up to 0.65 °C per decade during the last 42 years in the Black Sea [56]. As the rising temperatures may strongly affect the marine ecosystems and surrounding coastal regions, for instance through strengthening heatwaves [56, 22], it is crucial to assess which range of temperature trends and variability might occur in the future. This is particularly important when considering low emission scenarios in which forced trends are presumably weaker and natural fluctuation become more significant.

For the Baltic Sea, it has been suggested that the intensified warming after 1980 partly resulted from a phase switch of the Atlantic Multidecadal Variability (AMV) from a cold to a warm state [32]. The AMV summarizes multidecadal fluctuations that are observed in the North Atlantic SSTs. It usually fluctuates on time scales larger than 50 years, but the exact period length has varied in the past [33, 7, 4]. Several studies have shown that the North Atlantic SSTs, and the AMV in particular, affect the European climate [19, 7, 10, 6, 47, 9, 34, 8, 41]. For the Baltic Sea, [32] discovered that its low-pass filtered SSTs were highly correlated with the AMV throughout the 20th century. [8] made use of a low frequency component analysis [61] to define a monthly resolved AMV index based on temperature reanalysis data and found that the impact of the AMV on the Baltic SSTs is significant during the winter months. For the Mediterranean Sea, an impact of the AMV on the SST variability was reported as well [39, 52, 46, 62].

The origin of the AMV is still debated. Many studies describe it as a mode of internal variability that is strongly linked to the Atlantic Meridional Overturning Circulation (AMOC) [64] and the dynamical coupling of ocean and atmosphere [33, 59]. Others claim that the AMV is not primarily a mode of internal variability of the ocean, but driven by external natural and/or anthropogenic forcing [42, 38, 37]. Recently, [48] and [49] have made an attempt to reconcile these two theories by splitting the AMV into an internal and an externally forced part. This can be realized by working with a so-called Single-Model Initial-condition Large Ensemble (SMILE) [60, 17, 44]. As all members in such an ensemble are initialized from a different state of an undisturbed preindustrial control run, they evolve in various realizations of internal variability. If the ensemble is large enough, those variations will cancel out when computing the ensemble average and one will be left with externally forced variability. Hence, the multidecadal variability in the North Atlantic retrieved from the ensemble mean SSTs may be summarized as the externally forced AMV. Similarly, the internal AMV can be determined for each ensemble member from its SSTs minus the ensemble mean SSTs. It should be mentioned that the name "forced AMV" might not be ideal, as the corresponding SST patterns are not limited to the North Atlantic but instead resemble a global SST pattern [48, 49].

In this study, we use CMIP6 simulations covering the historical period (1850-2014) and four emission scenarios (2015-2100) from a 50-members ensemble of the Max Planck

Institute Earth System Model [44] plus one emission scenario from a 100-members ensemble of the Community Earth System Model [50] to analyze future trends and changes of variability in European SSTs and how they relate to forced and internal components of the AMV. By carefully separating those different contributions to the future development of European SSTs, we aim to provide a range of possible outcomes of future regional climate change which is of high importance for adaptation strategies and risk management [15].

2. Data and methods

2.1. Data

2.1.1. MPI-ESM grand ensemble The CMIP6 [20] forced MPI grand ensemble (MPI-GE CMIP6) consists of 50 realizations of the historical period (1850-2014) plus five emission scenarios corresponding to the shared socioeconomic pathways (SSPs) 1-1.9 (not used in this study), 1-2.6, 2-4.5, 3-7.0, and 5-8.5 which were performed with the low resolution MPI-ESM version 1.2 (MPI-ESM-1-2-LR, from now on MPI-ESM) [40, 44]. All 50 members were initialized from a different state of a millennium-long preindustrial simulation in order to cover the whole phase space of the climate system. The MPI-ESM resolves the ocean on a GR 15 grid with about 1.5 ° horizontal resolution and 40 vertical levels. The GR 15 grid has two poles placed over southern Greenland and Antarctica [31] which leads to rather high resolutions in the North Atlantic. The atmosphere is resolved with about 1.8 °. For the analysis, all variables are interpolated on a 1 ° latitude-longitude grid.
The MPI ensemble was chosen due to its high number of members and emission scenarios. In addition, it has an average climate sensitivity [44] and its increase of global mean temperatures during the last decades matches the trend in reanalysis data quite well [51]. It has been shown that the North Atlantic Current in the MPI-ESM is too zonal, which also affects storm pathways towards Europe [43]. Nevertheless, the MPI-ESM is one of the models with a relatively realistic representation of AMOC and AMV [43, 59, 38, 17, 48, 45, 63, 11] although the amplitude of AMV variability is underestimated as in most CMIP6 models [5]. The high-resolution version of MPI-ESM-1-2 (which does not differ substantially from the low-resolution version) has also been found to be one of the CMIP6 models best suited for studies on European climate [45].

2.1.2. CESM2 grand ensemble To address the robustness of the MPI-ESM results, we compare them to similar results from a CMIP6 forced 100-member large ensemble of the Community Earth System Model version 2 (CESM2) [50]. It covers the historical period plus the high-emission scenario SSP370. CESM2 [12] resolves the atmosphere with 0.9 ° in latitude and 1.25 ° in longitude. The resolution of the ocean component is 1.125 ° in zonal direction and up to 0.25 ° in meridional direction where the resolution

increases towards lower latitudes [50]. Again, the SSTs are interpolated onto a 1° latitude-longitude grid before the analysis.

The members were initialized from a preindustrial control simulation [50]. Like MPI-ESM, CESM2 and its precessor CESM1 have been used for several studies of climate variability in the North Atlantic region and shown good performance [16, 17, 11, 24] although CESM also underestimates the AMV variability [5]. A few differences between the two models might be noteworthy in the light of the following analysis: by comparing CMIP6 preindustrial control simulations, [9] found that the AMV in CESM2 has maximum power at lower frequencies than in MPI-ESM. In addition, the equilibrium climate senstivity but also aerosol-mediated cooling effects are much stronger in CESM2 [58], implying that it reacts more strongly to external forcing.

2.2. AMV definition

Data processing and AMV calculation closely follow the methods of [17] and [49]. Two 140 years long time windows (1880-2020 and 1950-2090) are chosen for the analysis, the latter one corresponding to that used in [17]. Both time windows, especially the second one, mix parts of the historical period and the scenarios. However, shorter periods have shown not to capture the internal variability to a sufficient extent. Annual mean SST anomalies (SSTAs) are computed and smoothed by Butterworth lowpass filters with a cutoff of 10 years.

The total AMV is the sum of its internal and forced components:

$$\text{totalAMV} = \text{iAMV} + \text{fAMV}. \tag{1}$$

The total AMV results from the SSTAs of each member, the internal AMV (iAMV) from SSTAs of each member minus ensemble mean SSTAs (i. e., iSSTAs), and the forced AMV (fAMV) from ensemble mean SSTAs (fSSTAs). The AMV indices and corresponding SST patterns are retrieved with the residual method described in [17, 49], as it has been shown that this method can effectively separate internal variability and forced trends. It works as follows:

(i) Global mean SSTAs (GSSTAs) at each time step are computed via area-weighted average between 60° S and 60° N.

(ii) The local SSTAs are regressed onto the GSSTAs.

(iii) The residual temperature anomalies (SSTAres), where local and global long-term trends are removed, are retrieved by subtracting the regression pattern scaled by the GSSTA at each time step from the local SSTAs.

(iv) The AMV index is determined by computing the area-weighted average of the residual SSTAs in the North Atlantic (latitudes between 0° N and 60° N and longitudes between 80° W and 0° W, see red box in Figure 1).

(v) The corresponding AMV pattern is derived by regressing the SSTAres onto the AMV index. To make the different patterns comparable in terms of magnitude, they are scaled with the temporal standard deviations of the respective AMV indices.

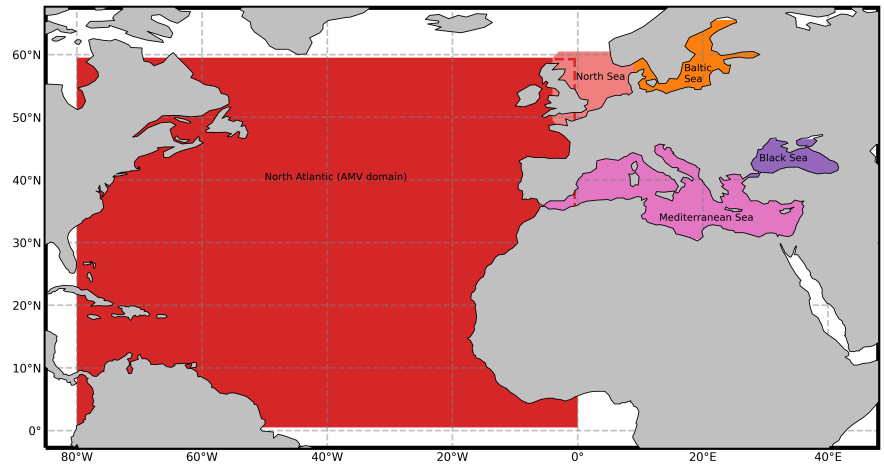

Figure 1. AMV domain and semi-enclosed European seas.

3. Results

The results section is organized as follows: We start by presenting historical and future developments of the SSTs of the European seas. Then, the different AMV patterns are displayed. Finally, the links between the local SSTs and the AMVs are explored.

3.1. SST trends and variability in the European seas

Figure 2 shows trends of area-weighted averaged SSTs in the historical period (1880-2020) and the SSP scenarios (1950-2090) for the four European seas as defined in Figure 1. Boxplots are used to visualize the spread among the ensemble members. All seas are warming and the trends increase with increasing scenario. Across all scenarios, the Baltic Sea is expected to experience the strongest warming and to exhibit the greatest ensemble spread. Even in SSP126, a minimum warming of more than 2 °C is very likely in the Baltic Sea as indicated by the low end of the whisker. Both the North Sea and the Mediterranean Sea are characterized by smaller trends and smaller ensemble spreads, but a warming of 2 °C or more is also likely to occur in SSP245 or higher. The Black Sea shows the second largest trends. In line with the previous results, the Baltic Sea SSTs exhibit the highest internal variability, followed by the North Sea and Black Sea. This can be deduced from Figure 3 which displays ensemble standard deviations of the basin-averaged SSTs. They fluctuate on interannual to multidecadal time scales and decrease slightly over large parts of the period except for the Mediterranean Sea where the variability seems to stay rather constant.

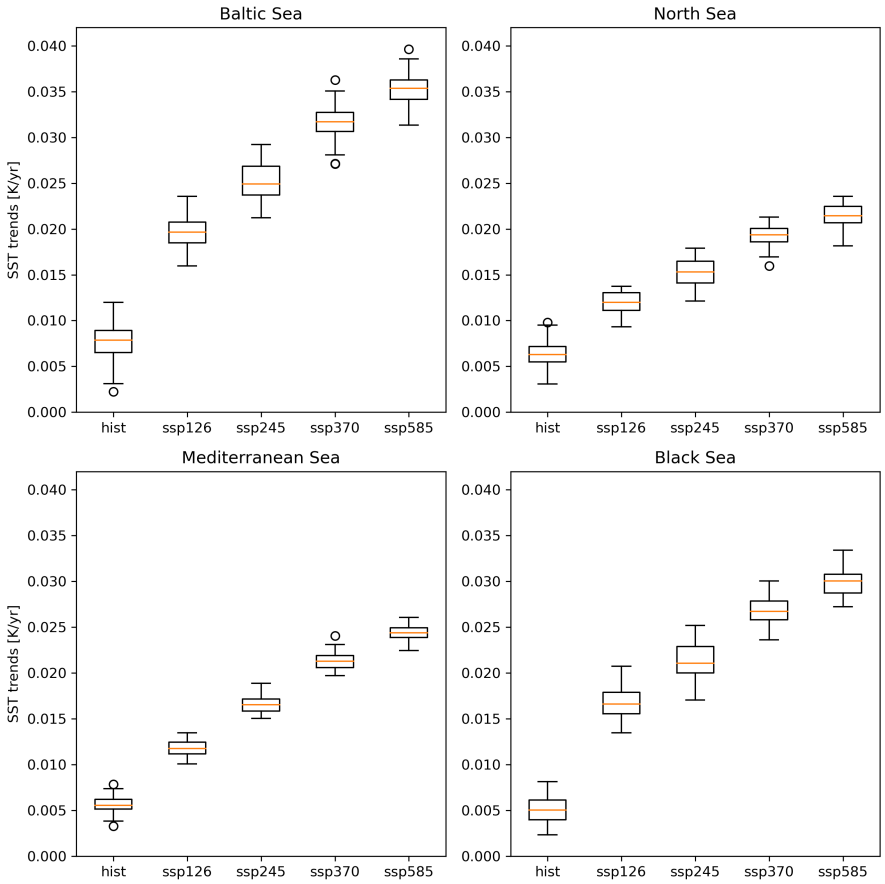

Figure 2. Trends of area-weighted basin averaged SSTs over the historical period (1880-2020) and the SSP scenarios (1950-2090) in the MPI-ESM ensemble. Orange lines in the box plots indicate the respective ensemble median.

3.2. AMV patterns and variability

Figure 4 shows the total AMV, iAMV, and fAMV patterns in the historical period and the four scenarios, plus the forced regional trends which were computed for each grid point as the difference between the local and the globally averaged trend in ensemble mean SSTs. The patterns of the total AMV are very similar to those of the iAMV. In addition, the latter appear to be quite constant throughout the scenarios. This implies that the mechanism driving the iAMV is not much affected by anthropogenic climate change which agrees with [17] and [48]. Similar to [49], we find that the iAMV is coupled to the internal component of the AMOC (iAMOC) which we compute as the maximum

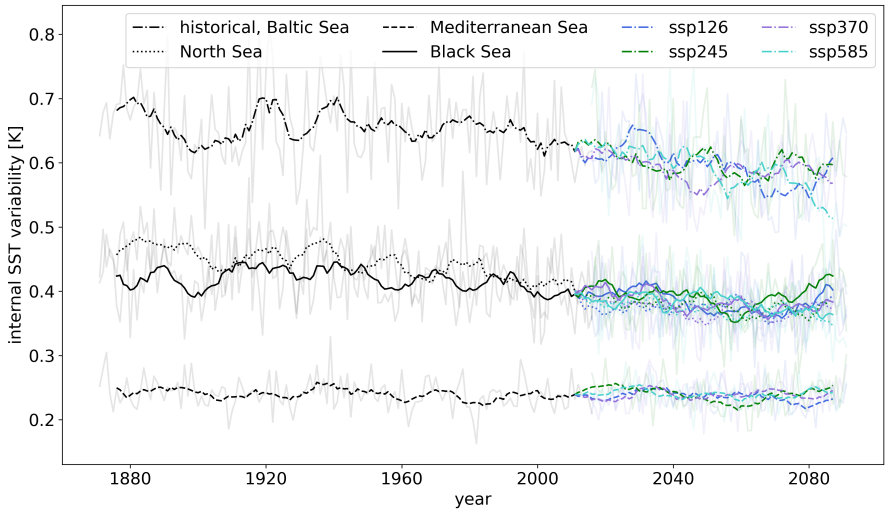

Figure 3. Ensemble standard deviations of area-weighted basin averaged SSTs. Bold lines depict 10-year running means.

of the ocean meridional overturning mass streamfunction, provided in the model output, in the North Atlantic above 20 °N and below 500 m depth. The connection manifests in a peak in iAMV - iAMOC cross correlations (Figure S1 in the Supplementary Information) around lag-0, with a slight skew towards a leading iAMOC. In Europe, the iAMV pattern gets weaker with increasing distance from the Atlantic.

The fAMV patterns exhibit strong positive SSTs along the coasts in the subpolar North Atlantic and east of Greenland. Slightly negative SSTs are found in the central North Atlantic whereby their positions are not constant across the scenarios and they do not exist in the historical period. East and south of the negative SSTs is again a branch of slight positive anomalies. In Europe, strong positive SSTs which increase with the scenarios prevail mainly in the Baltic Sea and also in the North Sea and the Black Sea. Especially in the high emission scenarios, the fAMV patterns bear a certain similarity to the forced regional trends. This makes sense, as the fAMV is thought to be the reaction of the ocean to temporal variations in the external forcing (e. g., aerosols or greenhouse gasses) [48, 49]. It should be pointed out that the strongest regression slopes of the fAMV are not found in the North Atlantic, i. e., the region defining the classical AMV.

In Figure S2 in the Supplementary information, 60-year running variances of the fAMV and iAMV (for the latter, ensemble means of the individual variances) are displayed. Windows of 60 years length are chosen here and also in the following section for the running correlations to always include at least one full AMV cycle. The results for

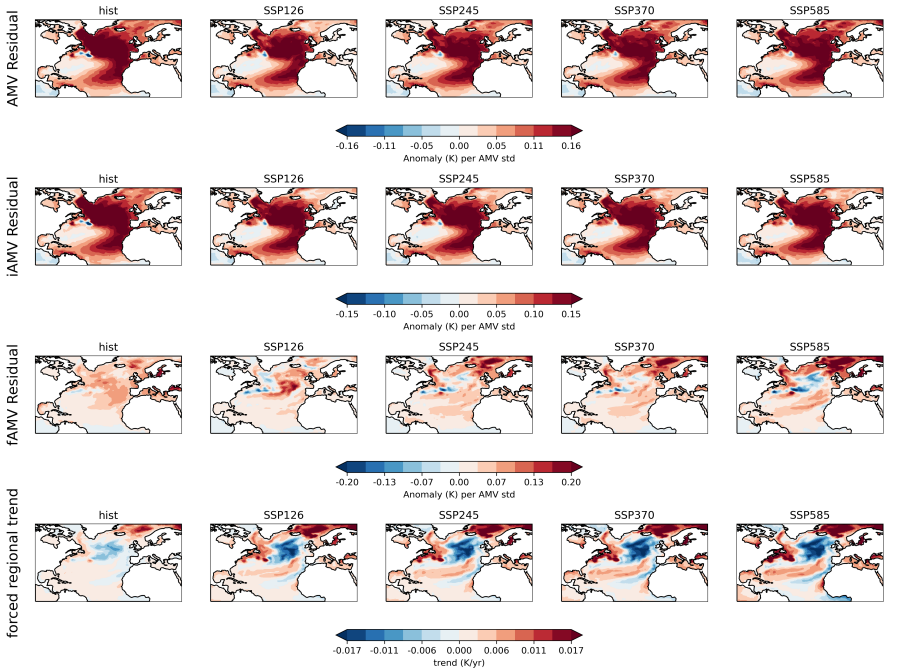

Figure 4. Standardized AMV, iAMV, and fAMV patterns plus forced local trends in the MPI-ESM ensemble.

iAMV and fAMV are quite different. The fAMV variances exhibit strong multidecadal variations with maxima around 1950 and 2000 during the historical period, and an overall decrease in the 21st century. In contrast, the iAMV variances fluctuate on shorter time scales and show an overall decreasing trend. In terms of absolute values, the iAMV variances are about one magnitude larger than the fAMV variances. However, the magnitudes of the patterns shown in Figure 4 indicate that both AMV components are important, albeit in different regions.

3.3. AMV impact on European SSTs

To account for a lagged response between the AMV and the European SSTs, we compute cross correlations between the iAMV / fAMV and local iSSTAres / fSSTAres which are depicted in Figure 5. The fAMV is highly correlated with the local fSSTAres for all scenarios and seas at lag-0. The curves are mostly not symmetric but slightly skewed towards negative lags, indicating that the fAMV rather leads the local fSSTAres. There is no systematic change in the maximum correlations with increasing scenarios. The results support the suspicion that the fAMV is rather a global than a North Atlantic phenomenon with a common origin in fluctuations of the external forcing that affect

both the North Atlantic (i. e., the AMV) and the European SSTs.

The correlations for the iAMV differ between the seas. In case of the Black Sea, the ensemble means of the cross correlations are close to zero everywhere. Both the Mediterranean Sea and the North Sea show maximum correlations of 0.25 or more at lag-0. While the curves are quite symmetric for the former, they are slightly skewed towards positive lags for the latter. In case of the Baltic Sea, the maximum correlations are smaller and not at lag-0, but lag-7. A possible explanation for the observed lag could include the North Atlantic Oscillation (NAO). The NAO is commonly defined as the first EOF of the sea level pressure anomaly over the North Atlantic and considered the most important mode of atmospheric variability in that region [25]. It is known to have an important influence on the European climate, especially in winter [25]. During a positive NAO phase, the pressure difference between the Icelandic Low and the Azores High is larger than average, causing stronger westerlies that advect warm and moist air towards Europe [25]. According to various studies [26, 13, 14, 59, 9], the NAO is an important driver of the AMOC and the AMV. Although the NAO is mainly known to fluctuate on time scales below 10 years [25, 41], it also exhibits significant wavelet power at periods of around 60 years like the AMV [41]. [6] have shown that the AMV mainly influences the zonal positions of the NAO's centers of action which leads to changes in the Atlantic storm tracks.

To explore the iAMV-NAO connection in our data, we plot the iAMV regression patterns of iSSTAres, residual internal 2m air temperature anomalies (iSATAres), and residual internal geopotential height anomalies at 1000 hPa (iZGAres; as a measure of sea level pressure) 7 years before an iAMV maximum (see Figure 6). The sea level pressure pattern clearly resembles that of an NAO+ phase and both SST and SAT show the corresponding temperature patterns [2, 59, 54, 23] with positive anomalies in the gulf stream region, the Norwegian and Greenland seas, and the Baltic Sea and horseshoe-shaped negative anomalies in the subpolar and the low latitude North Atlantic. [59] reported lags between 2 and 15 years between the SST patterns in Figure 6 and an AMV maximum which agrees with our results. Contrary to the situation in the Baltic Sea, lag-0 maxima for the North Sea and Mediterranean Sea could indicate that their SSTs are more directly affected by changes in the North Atlantic SSTs. [62] found the maximum correlation between the AMV and Mediterranean SSTs at a small lag of 2 years and for the North Sea, our result is in line with [27, 56]. As mentioned above, the North Sea also shows some correlation at small positive lags like the Baltic Sea. However, they might be less important due to the direct connection of the North Sea to the Atlantic. In addition, the Baltic Sea has a rather shallow mixed layer of 50-70 meters depth above a permanent halocline [57] which likely makes it more sensitive to meteorological forcing.

The 60-year running iSSTAres-iAMV correlations in Figure 7 are relatively constant over time. In contrast, the 60-year running fSSTAres-fAMV correlations are close to

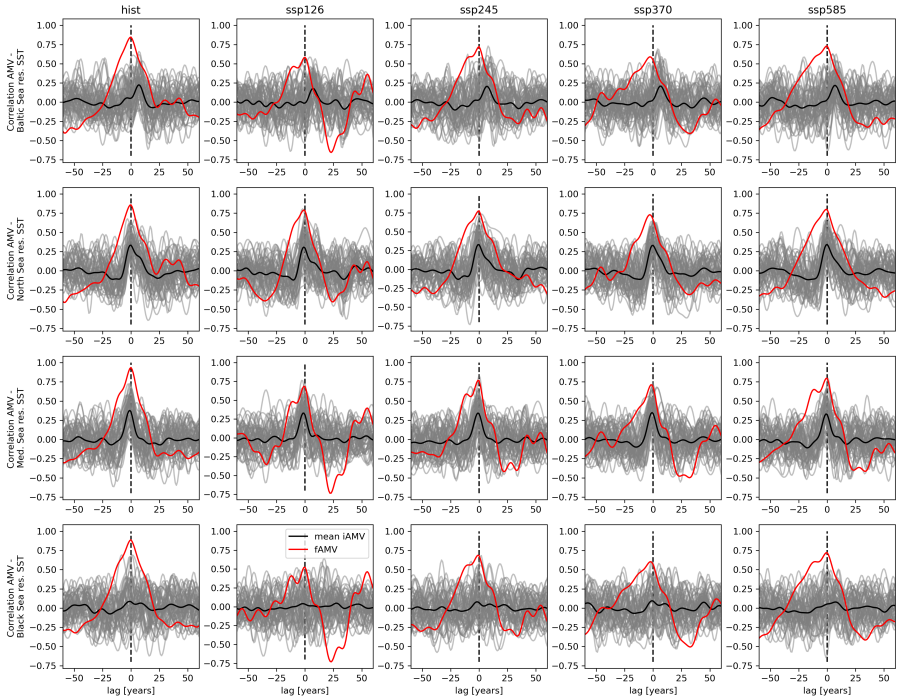

Figure 5. iAMVs-iSSTAres (grey lines) and fAMV-fSSTAres (red lines) for the historical period (1880-2020) and the SSP scenarios (1950-2090) in the MPI-ESM ensemble. Black lines denote the ensemble means of the iAMV-iSSTAres cross correlations. Positive lags indicate leading local SSTs and negative lags leading AMVs.

one throughout most of the 20th century and show a strong decrease at the beginning of the 21st century until about 2035, where some curves (especially in the Baltic Sea and Black Sea) reach quite high negative values. Afterwards, most of the curves increase again. The quite dramatic change of the fSSTAres-fAMV correlations at the beginning of the 21st century is remarkable. It might be related to the fact that the external forcing in the scenarios is quite different from that in the historical period. For instance, the radiative forcing by anthropogenic aerosols changes rather abruptly at the beginning of the scenarios (see [36], their Figure 3). In addition, the variability of biomass burning emissions in CMIP6 is strongly enhanced between 1997 and 2014; the period where satellite data were available [21].

3.4. Comparison with CESM2

Selected results obtained with CESM2 are shown in Section 2 in the supplementary information. One can see that although the fAMV and iAMV variances are quite

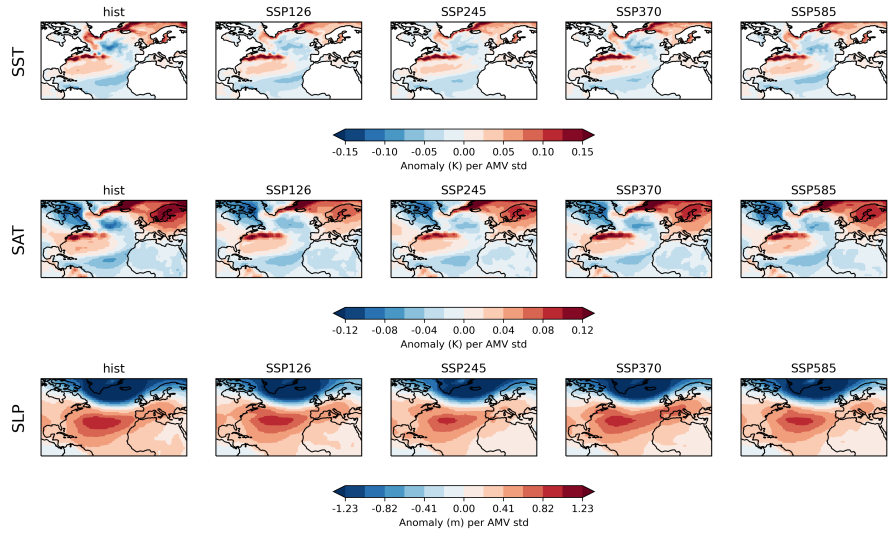

Figure 6. iSSTAres, iSATAres, and iSLPAres regression patterns onto the iAMV 7 years before an iAMV maximum for the historical period (1880-2020) and the SSP scenarios (1950-2090) in the MPI-ESM ensemble. SLP is expressed as the geopotential height anomaly at 1000 hPa.

different, likely reflecting the model-specific reactions to changes in the external forcing, the relations between the AMV components and European SSTs are very similar.

3.5. Relative importance of AMV and forced trends for the European seas

As a synthesis of the results presented so far, we compare the impact of the AMVs and forced trends over time in the different basins. For that purpose, we compute the area-weighted basin averages of the iAMV and fAMV patterns presented in Figure 4 (but not the standardized patterns, i.e., not scaled by the respective AMV standard deviations). Next, the pattern averages are multiplied with the respective AMV indices to produce time series of the local AMV impact. Finally, running decadal trends of these "local" iAMVs and fAMVs are calculated and compared to running decadal forced local trends based on the ensemble mean area-weighted basin averaged SSTs. A comparable strategy was applied for instance in [30] for temperature trends in East Asia. One should note that the the trends resulting from the "local" fAMVs (i. e., specific fluctuations of the ensemble mean SSTs) are expected to also appear in the forced trends since the latter comprise all fluctuations of ensemble mean SSTs.

The results are depicted in Figure 8. In case of the local iAMV trends, the spread between the 10th and the 90th percentiles among the ensemble members are given. It

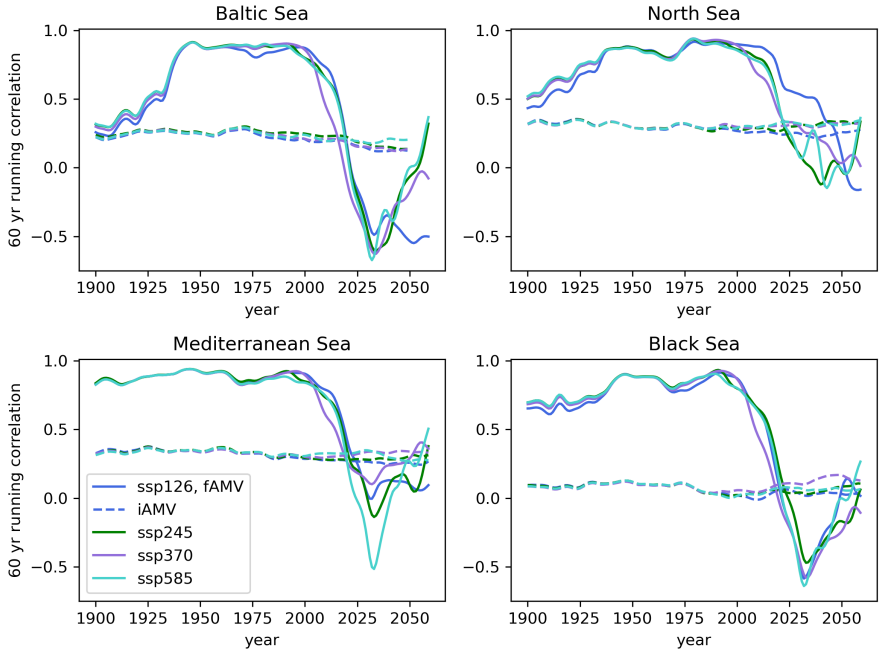

Figure 7. Centered 60-year running correlations between fAMVs and local fSSTAres and between iAMVs and local iSSTAres (dashed lines) in the MPI-ESM ensemble. For the latter, ensemble means of the individual correlations are given. In case of the iAMV-iSSTAres correlations in the Baltic Sea, a lag of 7 years was implemented according to the outcome of the cross correlations in Figure 5.

should be mentioned that the iAMV and fAMV patterns were computed for the whole 140 years periods. Therefore, the fAMV trends in the historical parts of the SSP period are different in magnitude for the different scenarios. As explained in Section 2.2, the periods could not be split into smaller parts as the AMV patterns would not have been captured sufficiently. The figure shows that in the high emission scenarios SSP370 and SSP585, the forced trends are almost always out of range of the local AMV trends. In the lower scenarios, this is only partly the case as the forced trends rather decrease after the global maximum around the 1990s which was likely caused by a fast decrease in European aerosol emissions that had damped the warming trends in the previous decades, in particular in Eastern Europe [55, 1]. Increased warming in the northern hemisphere due to higher biomass burning variability between 1997 and 2014 might also have contributed to the forced trends [21]. It is interesting that the range of iAMV trends is quite high even for the Baltic Sea where the ensemble mean iAMV pattern is rather weak. This underlines the pronounced internal variability where some ensemble members show a very strong iAMV impact in the Baltic Sea. All in all, the local effects

Figure 8. Running decadal trends of "local" fAMV and iAMV (for the latter, the spans between the 10th and the 90th percentiles among the ensemble members are given) and running decadal forced local trends, all for the historical period (1880-2020) and the SSP scenarios (1950-2090) in the MPI-ESM ensemble.

of the AMV (internal or external) will continue to play an important role for the SST variability on decadal to multidecadal time scales, especially in the low emission scenarios. It is also noteworthy that the decadal forced and fAMV trends seem to be quite in phase until about 1970 and rather out of phase afterwards. The former is logical given that the local fAMV trends are part of the forced trends, but the latter is not easily explainable.

4. Discussion

In our study, we analyze the historical and future impact of the AMV on the SSTs of European seas in an MPI-ESM SMILE. By decomposing the AMV in its internal and forced parts, we find that the latter seems to have a stronger connection with the European seas, especially the Baltic Sea and the Black Sea. For the Baltic Sea, this is remarkable as it changes the perspective on earlier studies like those by [32] and [8]. In both studies, single modeled or observational time series were used which means they could not distinguish between iAMV and fAMV, but only consider the total AMV. They concluded from their analyses that the internal multidecadal variability of the North Atlantic affected the Baltic SSTs during the historical period. However, this

conclusion now has to be questioned as our results imply that they might have rather seen the impact of the fAMV, i.e., an externally forced phenomenon that is not particularly characteristic for the North Atlantic. This also applies to publications showing a connection between the AMV and the Mediterranean Sea [39, 52, 46, 62].

While our results are mainly based on regressions and correlations, and cannot provide a mechanistic explanation, they are in agreement with previous studies [6, 9, 8]. However, in their work they where not able to distinguish between iAMV and fAMV. We can also only speculate on the origin of the fAMV and on what causes the tremendous changes in the running fSSTAres-fAMV correlations at the beginning of the 21st century. The underlying causes could be identified by conducting experiments with SMILEs separately for the different kinds of anthropogenic and natural forcing. This is currently accomplished in the Large Ensemble Single Forcing Model Intercomparison Project [53].

Another possible drawback of our study is the fact that the European seas are not well resolved in the global models. Although both MPI-ESM and CESM have only modest SST biases in the European seas (with the exception of the Black Sea in case of MPI-ESM) [43, 12], this does not ensure that the multidecadal SST variabilities are captured. In that context, running regional models with downscaled CMIP6 forcing could be a great step forward.

The two SMILEs considered in this study (the MPI-GE and the CESM2-GE) show partly differing results, for instance concerning the development of the fAMV and iAMV variances in the scenario SSP370. Nevertheless, they agree to a large extent in their fSSTAres-fAMV and iSSTAres-iAMV cross-correlations. This indicates that the described impacts of iAMV and fAMV on the European SSTs are not just a feature of one particular ocean model.

To conclude, our study underlines the importance of a proper distinction between internal and forced modes of variability - not only the AMV, but any mode of climate variability around the globe. In addition, this work is (to our knowledge) the first to compare the SST variability of the semi-enclosed European seas and how they are affected by the North Atlantic. Earlier publications usually focused on atmospheric parameters of European climate like air temperature or precipitation [47, 9, 18]. Finally, our work provides a range of possible future regional SST trends and variations and thus contains important information for decision makers.

Acknowledgements

The research presented in this study is part of the Baltic Earth program (Earth System Science for the Baltic Sea region; see https://www.baltic.earth) and a contribution to the BMBF funded project CoastalFutures (03F0911E). We thank the Max Planck

Institute for Meteorology (for the MPI-GE) and the US CLIVAR Working Group on Large Ensembles (for the CESM2-GE). In addition, we would like to thank Leonard Borchert, Sebastian Brune, and Clara Deser for their constructive feedback.

Data availability

CMIP6 model results are available from the Earth System Grid Federation MetaGrid database (https://esgf-node.llnl.gov/search/cmip6/, latest access: 2024-10-09).

References

[1] A. Barkhordarian, H. Von Storch, E. Zorita, and J. J. Gómez-Navarro. An attempt to deconstruct recent climate change in the Baltic Sea basin. *Journal of Geophysical Research: Atmospheres*, 121(22), November 2016.

[2] Nicolas Barrier, Christophe Cassou, Julie Deshayes, and Anne-Marie Treguier. Response of North Atlantic Ocean Circulation to Atmospheric Weather Regimes. *Journal of Physical Oceanography*, 44(1):179–201, January 2014.

[3] Igor M. Belkin. Rapid warming of Large Marine Ecosystems. *Progress in Oceanography*, 81(1-4):207–213, 2009.

[4] Alessio Bellucci, Denis Mattei, Paolo Ruggieri, and Luca Famooss Paolini. Intermittent Behavior in the AMOC-AMV Relationship. *Geophysical Research Letters*, 49:e2022GL098771, 2022.

[5] Rémy Bonnet, Christine M. McKenna, and Amanda C. Maycock. Model spread in multidecadal North Atlantic Oscillation variability connected to stratosphere–troposphere coupling. *Weather and Climate Dynamics*, 5:913–926, 2024.

[6] Florian Börgel, Claudia Frauen, Thomas Neumann, and H. E. Markus Meier. The Atlantic Multidecadal Oscillation controls the impact of the North Atlantic Oscillation on North European climate. *Environmental Research Letters*, 15(10):104025, September 2020.

[7] Florian Börgel, Claudia Frauen, Thomas Neumann, Semjon Schimanke, and H. E. Markus Meier. Impact of the Atlantic Multidecadal Oscillation on Baltic Sea Variability. *Geophysical Research Letters*, 45(18):9880–9888, 2018.

[8] Florian Börgel, Matthias Gröger, H. E. Markus Meier, Cyril Dutheil, Hagen Radtke, and Leonard Borchert. The impact of Atlantic Multidecadal Variability on Baltic Sea temperatures is limited to winter. *npj Climate and Atmospheric Science*, 6(64), 2023.

[9] Florian Börgel, H. E. Markus Meier, Matthias Gröger, Monika Rhein, Cyril Dutheil, and Jan Moritz Kaiser. Atlantic multidecadal variability and the implications for North European precipitation. *Environmental Research Letters*, 17(4):044040, 2022.

[10] L. Caesar, S. Rahmstorf, A. Robinson, G. Feulner, and V. Saba. Observed fingerprint of a weakening Atlantic Ocean overturning circulation. *Nature*, 556:191–196, 2018.

[11] Jacob Coburn and Sara C. Pryor. Evolution of the Internal Climate Modes under Future Warming. *Journal of Climate*, 36(2):511–529, 2023.

[12] G. Danabasoglu, J.-F. Lamarque, J. Bacmeister, D. A. Bailey, A. K. DuVivier, J. Edwards, L. K. Emmons, J. Fasullo, R. Garcia, A. Gettelman, C. Hannay, M. M. Holland, W. G. Large, P. H. Lauritzen, D. M. Lawrence, J. T. M. Lenaerts, K. Lindsay, W. H. Lipscomb, M. J. Mills, R. Neale, K. W. Oleson, B. Otto-Bliesner, A. S. Phillips, W. Sacks, S. Tilmes, L. Van Kampenhout, M. Vertenstein, A. Bertini, J. Dennis, C. Deser, C. Fischer, B. Fox-Kemper, J. E. Kay, D. Kinnison, P. J. Kushner, V. E. Larson, M. C. Long, S. Mickelson, J. K. Moore, E. Nienhouse, L. Polvani, P. J. Rasch, and W. G. Strand. The Community Earth System Model Version 2 (CESM2). *Journal of Advances in Modeling Earth Systems*, 12(2):e2019MS001916, February 2020.

[13] Thomas L. Delworth, Fanrong Zeng, Gabriel A. Vecchi, Xiaosong Yang, Liping Zhang, and Rong Zhang. The North Atlantic Oscillation as a driver of rapid climate change in the Northern Hemisphere. *Nature Geoscience*, 9:509–512, 2016.

[14] Thomas L. Delworth, Fanrong Zeng, Liping Zhang, Rong Zhang, Gabriel A. Vecchi, and Xiaosong Yang. The Central Role of Ocean Dynamics in Connecting the North Atlantic Oscillation to the Extratropical Component of the Atlantic Multidecadal Oscillation. *Journal of Climate*, 30(10):3789–3805, 2017.

[15] Clara Deser. "Certain Uncertainty: The Role of Internal Climate Variability in Projections of Regional Climate Change and Risk Management". *Earth's Future*, 8(12):e2020EF001854, December 2020.

[16] Clara Deser, James W. Hurrell, and Adam S. Phillips. The role of the North Atlantic Oscillation in European climate projections. *Climate Dynamics*, 49:3141–3157, 2017.

[17] Clara Deser and Adam S. Phillips. Defining the Internal Component of Atlantic Multidecadal Variability in a Changing Climate. *Geophysical Research Letters*, 48:e2021GL095023, 2021.

[18] Clara Deser and Adam S. Phillips. A range of outcomes: the combined effects of internal variability and anthropogenic forcing on regional climate trends over Europe. *Nonlinear Processes in Geophysics*, 30:63–84, 2023.

[19] Aurélie Duchez, Eleanor Frajka-Williams, Simon A. Josey, Dafydd G. Evans, Jeremy P. Grist, Robert Marsh, Gerard D. McCarthy, Bablu Sinha, David I. Berry, and Joël J.-M. Hirschi. Drivers of exceptionally cold North Atlantic Ocean temperatures and their link to the 2015 European heat wave. *Environmental Research Letters*, 11:074004, 2016.

[20] Veronika Eyring, Sandrine Bony, Gerald A. Meehl, Catherine A. Senior, Bjorn Stevens, Ronald J. Stouffer, and Karl E. Taylor. Overview of the Coupled Model Intercomparison Project Phase 6 (CMIP6) experimental design and organization. *Geoscientific Model Development*, 9:1937–1958, 2016.

[21] J. T. Fasullo, Jean-Francois Lamarque, Cecile Hannay, Nan Rosenbloom, Simone Tilmes, Patricia DeRepentigny, Alexandra Jahn, and Clara Deser. Spurious Late Historical-Era Warming in CESM2 Driven by Prescribed Biomass Burning Emissions. *Geophysical Research Letters*, 49(2):e2021GL097420, January 2022.

[22] Matthias Gröger, Florian Börgel, Sven Karsten, H.E. Markus Meier, Kseniia Safonova, Cyril Dutheil, Aurore Receveur, and Patrick Polte. Future climate change and marine heatwaves - Projected impact on key habitats for herring reproduction. *Science of The Total Environment*, 951:175756, November 2024.

[23] Matthias Gröger, Cyril Dutheil, Florian Börgel, and Markus H. E. Meier. Drivers of marine heatwaves in a stratified marginal sea. *Climate Dynamics*, 62(5):3231–3243, May 2024.

[24] Qinxue Gu, Melissa Gervais, Gokhan Danabasoglu, Who M. Kim, Frederic Castruccio, Elizabeth Maroon, and Shang-Ping Xie. Wide range of possible trajectories of North Atlantic climate in a warming world. *Nature Communications*, 15:4221, 2024.

[25] J. W. Hurrell. Decadal trends in the North Atlantic Oscillation: regional temperatures and precipitation. *Science*, 269(5224):676–679, 1995.

[26] James W. Hurrell and Clara Deser. North Atlantic climate variability: The role of the North Atlantic Oscillation. *Journal of Marine Systems*, 79(3-4):231–244, February 2010.

[27] John Huthnance, Ralf Weisse, Thomas Wahl, Helmuth Thomas, Julie Pietrzak, Alejandro Jose Souza, Sytze Van Heteren, Natalija Schmelzer, Justus Van Beusekom, Franciscus Colijn, Ivan Haigh, Solfrid Hjøllo, Jürgen Holfort, Elizabeth C. Kent, Wilfried Kühn, Peter Loewe, Ina Lorkowski, Kjell Arne Mork, Johannes Pätsch, Markus Quante, Lesley Salt, John Siddorn, Tim Smyth, Andreas Sterl, and Philip Woodworth. Recent Change—North Sea. In Markus Quante and Franciscus Colijn, editors, *North Sea Region Climate Change Assessment*, pages 85–136. Springer International Publishing, Cham, 2016. Series Title: Regional Climate Studies.

[28] IOC-UNESCO and UNEP. Large Marine Ecosystems: Status and Trends. Technical report, United Nations Environment Programme (UNEP), Nairobi, 2016.

[29] IPCC. *Climate Change 2021: The Physical Science Basis. Contribution of Working Group I to the Sixth Assessment Report of the Intergovernmental Panel on Climate Change*. Cambridge University Press, Cambridge, United Kingdom and New York, NY, USA, 2021.

[30] Dajeong Jeong, Changhyun Yoo, and Sang-Wook Yeh. Contributions of external forcing and internal variability to the multidecadal warming rate of East Asia in the present and future climate. *npj Climate and Atmospheric Science*, 7(1):22, January 2024.

[31] J. H. Jungclaus, N. Fischer, H. Haak, K. Lohmann, J. Marotzke, D. Matei, U. Mikolajewicz, D. Notz, and J. S. von Storch. Characteristics of the ocean simulations in the Max Planck Institute Ocean Model (MPIOM) the ocean component of the MPI-Earth system model. *Journal of Advances in Modeling Earth Systems*, 5:422–446, 2013.

[32] Madline Kniebusch, H. E. M. Meier, Thomas Neumann, and Florian Börgel. Temperature Variability of the Baltic Sea Since 1850 and Attribution to Atmospheric Forcing Variables. *Journal of Geophysical Research: Oceans*, 124(6):4168–4187, 2019.

[33] Mads Faurschou Knudsen, Marit-Solveig Seidenkrantz, Bo Holm Jacobsen, and Antoon Kuijpers. Tracking the Atlantic Multidecadal Oscillation through the last 8,000 years. *Nature Communications*, 2(178), 2011.

[34] Julian Krüger, Joakim Kjellsson, Robin Pilch Kedzierski, and Martin Claus. Connecting North Atlantic SST Variability to European Heat Events over the Past Decades. *Tellus A: Dynamic Meteorology and Oceanography*, 75(1):358–374, 2023.

[35] Fernando P. Lima and David S. Wethey. Three decades of high-resolution coastal sea surface temperatures reveal more than warming. *Nature Communications*, 3:704, 2012.

[36] Marianne T. Lund, Gunnar Myhre, and Bjørn H. Samset. Anthropogenic aerosol forcing under the Shared Socioeconomic Pathways. *Atmospheric Chemistry and Physics*, 19:13827–13839, 2019.

[37] Michael E. Mann, Byron A. Steinman, Daniel J. Brouillette, and Sonya K. Miller. Multidecadal climate oscillations during the past millennium driven by volcanic forcing. *Science*, 371:1014–1019, 2021.

[38] Michael E. Mann, Byron A. Steinman, and Sonya K. Miller. Absence of internal multidecadal and interdecadal oscillations in climate model simulations. *Nature Communications*, 11(49), 2020.

[39] Salvatore Marullo, Vincenzo Artale, and Rosalia Santoleri. The SST Multidecadal Variability in the Atlantic–Mediterranean Region and Its Relation to AMO. *Journal of Climate*, 24(16):4385–4401, 2011.

[40] Thorsten Mauritsen, Jürgen Bader, Tobias Becker, Jörg Behrens, Matthias Bittner, Renate Brokopf, Victor Brovkin, Martin Claussen, Traute Crueger, Monika Esch, Irina Fast, Stephanie Fiedler, Dagmar Fläschner, Veronika Gayler, Marco Giorgetta, Daniel S. Goll, Helmuth Haak, Stefan Hagemann, Christopher Hedemann, Cathy Hohenegger, Tatiana Ilyina, Thomas Jahns, Diego Jimenéz-de-la Cuesta, Johann Jungclaus, Thomas Kleinen, Silvia Kloster, Daniela Kracher, Stefan Kinne, Deike Kleberg, Gitta Lasslop, L. Kornblueh, Jochem Marotzke, Daniela Matei, Katharina Meraner, Uwe Mikolajewicz, Kameswarrao Modali, Benjamin Möbis, Wolfgang Am. Müller, Julia E. M. S. Nabel, Christine C. W. Nam, Dirk Notz, Sarah-Sylvia Nyawira, Hanna Paulsen, Karsten Peters, Robert Pincus, Holger Pohlmann, Julia Pongratz, Max Popp, Thomas Jürgen Raddatz, Sebastian Rast, Rene Redler, Christian H. Reick, Tim Rohrschneider, Vera Schemann, Hauke Schmidt, Reiner Schnur, Uwe Schulzweida, Katharina D. Six, Lukas Stein, Irene Stemmler, Bjorn Stevens, Jin-Song von Storch, Fangxing Tian, Aiko Voigt, Philipp Vrese, Karl-Hermann Wieners, Stiig Wilkenskjeld, Alexander Winkler, and Erich Roeckner. Developments in the MPI-M Earth System Model version 1.2 (MPI-ESM1.2) and Its Response to Increasing CO2. *Journal of Advances in Modeling Earth Systems*, 11:998–1038, 2019.

[41] H. E. Markus Meier, Leonie Barghorn, Florian Börgel, Matthias Gröger, Lev Naumov, and Hagen Radtke. Multidecadal climate variability dominated past trends in the water balance of the Baltic Sea watershed. *npj Climate and Atmospheric Science*, 6(1):58, 2023.

[42] Lisa N. Murphy, Katinka Bellomo, Mark Cane, and Amy Clement. The role of historical forcings

in simulating the observed Atlantic multidecadal oscillation. *Geophysical Research Letters*, 44:2472–2480, 2017.

[43] W. A. Müller, J. H. Jungclaus, T. Mauritsen, J. Baehr, M. Bittner, R. Budich, F. Bunzel, M. Esch, R. Ghosh, H. Haak, T. Ilyina, T. Kleine, L. Kornblueh, H. Li, K. Modali, D. Notz, H. Pohlmann, E. Roeckner, I. Stemmler, F. Tian, and J. Marotzke. A Higher-resolution Version of the Max Planck Institute Earth System Model (MPI-ESM1.2-HR). *Journal of Advances in Modeling Earth Systems*, 10:1383–1413, 2018.

[44] Dirk Olonschek, Laura Suarez-Gutierrez, Sebastian Milisnki, Goratz Beobide-Arsuaga, Johanna Baehr, Friederike Fröb, Tatiana Ilyina, Christopher Kadow, Daniel Krieger, Hongmei Li, Jochem Marotzke, Étienne Plésiat, Martin Schupfner, Fabian Wachsmann, Lara Wallberg, Karl-Hermann Wieners, and Sebastian Brune. The New Max Planck Institute Grand Ensemble With CMIP6 Forcing and High-Frequency Model Output. *Journal of Advances in Modeling Earth Systems*, 15:e2023MS003790, 2023.

[45] Tamzin E. Palmer, Carol F. McSweeney, Ben B. B. Booth, Matthew D. K. Priestley, Paolo Davini, Lukas Brunner, Leonard Borchert, and Matthew B. Menary. Performance-based sub-selection of CMIP6 models for impact assessments in Europe. *Earth System Dynamics*, 14:457–483, 2023.

[46] Andrea Pisano, Salvatore Marullo, Vincenzo Artale, Federico Falcini, Chunxue Yang, Francesca Elisa Leonelli, Rosalia Santoleri, and Bruno Buongiorno Nardelli. New Evidence of Mediterranean Climate Change and Variability from Sea Surface Temperature Observations. *Remote Sensing*, 12(1):132, January 2020.

[47] Said Qasmi, Christophe Cassou, and Julien Boé. Teleconnection Processes Linking the Intensity of the Atlantic Multidecadal Variability to the Climate Impacts over Europe in Boreal Winter. *Journal of Climate*, 33(7):2681–2700, 2020.

[48] Minhua Qin, Aiguo Dai, and Wenjian Hua. Influence of Anthropogenic Warming on the Atlantic Multidecadal Variability and Its Impact on Global Climate in the Twenty-First Century in the MPI-GE Simulations. *Journal of Climate*, 35(9):2805–2821, 2022.

[49] Jon Robson, Rowan Sutton, Matthew B. Menary, and Michael W. K. Lai. Contrasting internally and externally generated Atlantic Multidecadal Variability and the role for AMOC in CMIP6 historical simulations. *Philosophical Transactions A*, 381:20220194, 2023.

[50] Keith B. Rodgers, Sun-Seon Lee, Nan Rosenbloom, Axel Timmermann, Gokhan Danabasoglu, Clara Deser, Jim Edwards, Ji-Eun Kim, Isla R. Simpson, Karl Stein, Malte F. Stuecker, Ryohei Yamaguchi, Tamás Bódai, Eui-Seok Chung, Lei Huang, Who M. Kim, Jean-François Lamarque, Danica L. Lombardozzi, William R. Wieder, and Stephen G. Yeager. Ubiquity of human-induced changes in climate variability. *Earth System Dynamics*, 12(4):1393–1411, December 2021.

[51] Dominik L. Schumacher, Jitendra Singh, Mathias Hauser, Erich M. Fischer, Martin Wild, and Sonia I. Seneviratne. Exacerbated summer European warming not capturedby climatemodelsneglecting long-term aerosol changes. *Communications Earth & Environment*, 5(182), 2024.

[52] Nikolaus Skliris, Sarantis Sofianos, Athanasios Gkanasos, Anneta Mantziafou, Vasilis Vervatis, Panagiotis Axaopoulos, and Alex Lascaratos. Decadal scale variability of sea surface temperature in the Mediterranean Sea in relation to atmospheric variability. *Ocean Dynamics*, 62:13–30, 2012.

[53] Doug M. Smith, Nathan P. Gillett, Isla R. Simpson, Panos J. Athanasiadis, Johanna Baehr, Ingo Bethke, Tarkan A. Bilge, Rémy Bonnet, Olivier Boucher, Kirsten L. Findell, Guillaume Gastineau, Silvio Gualdi, Leon Hermanson, L. Ruby Leung, Juliette Mignot, Wolfgang A. Müller, Scott Osprey, Odd Helge Otterå, Geeta G. Persad, Adam A. Scaife, Gavin A. Schmidt, Hideo Shiogama, Rowan T. Sutton, Didier Swingedouw, Shuting Yang, Tianjun Zhou, and Tilo Ziehn. Attribution of multi-annual to decadal changes in the climate system: The Large Ensemble Single Forcing Model Intercomparison Project (LESFMIP). *Frontiers in Climate*, 4:955414, September 2022.

[54] Lingfeng Tao, Jiabei Fang, Xiu-Qun Yang, Xuguang Sun, Danping Cai, and Yu Wang. Role of

North Atlantic Tripole SST in Mid-Winter Reversal of NAO. *Geophysical Research Letters*, 50(15):e2023GL103502, August 2023.

[55] Robert Vautard, Pascal Yiou, and Geert Jan Van Oldenborgh. Decline of fog, mist and haze in Europe over the past 30 years. *Nature Geoscience*, 2(2):115–119, February 2009.

[56] Karina Von Schuckmann, Lorena Moreira, Mathilde Cancet, Flora Gues, Emmanuelle Autret, Ali Aydogdu, Lluis Castrillo, Daniele Ciani, Andrea Cipollone, Emanuela Clementi, Gianpiero Cossarini, Alvaro De Pascual-Collar, Vincenzo De Toma, Marion Gehlen, Rianne Giesen, Marie Drevillon, Claudia Fanelli, Kevin Hodges, Simon Jandt-Scheelke, Eric Jansen, Melanie Juza, Ioanna Karagali, Priidik Lagemaa, Vidar Lien, Leonardo Lima, Vladyslav Lyubartsev, Ilja Maljutenko, Simona Masina, Ronan McAdam, Pietro Miraglio, Helen Morrison, Tabea Rebekka Panteleit, Andrea Pisano, Marie-Isabelle Pujol, Urmas Raudsepp, Roshin Raj, Ad Stoffelen, Simon Van Gennip, Pierre Veillard, and Chunxue Yang. The state of the ocean in the northeastern Atlantic and adjacent seas. *State of the Planet*, 4-osr8:1–32, September 2024.

[57] Germo Väli, H. E. Markus Meier, and Jüri Elken. Simulated halocline variability in the Baltic Sea and its impact on hypoxia during 1961-2007. *Journal of Geophysical Research: Oceans*, 118(12):6982–7000, 2013.

[58] Chenggong Wang, Brian J. Soden, Wenchang Yang, and Gabriel A. Vecchi. Compensation Between Cloud Feedback and Aerosol- Cloud Interaction in CMIP6 Models. *Geophysical Research Letters*, 48:e2020GL091024, 2021.

[59] Robert C. J. Wills, Kyle C. Armour, David S. Battisti, and Dennis L. Hartmann. Ocean–Atmosphere Dynamical Coupling Fundamental to the Atlantic Multidecadal Oscillation. *Journal of Climate*, 32(1):251–272, 2019.

[60] Robert C. J. Wills, David S. Battisti, and Kyle C. Armour. Pattern Recognition Methods to Separate Forced Responses from Internal Variability in Climate Model Ensembles and Observations. *Journal of Climate*, 33(20):8693–8719, 2020.

[61] Robert C. J. Wills, Tapio Schneider, John M. Wallace, David S. Battisti, and Dennis L. Hartmann. Disentangling Global Warming, Multidecadal Variability, and El Niño in Pacific Temperatures. *Geophysical Research Letters*, 45:2487–2496, 2018.

[62] Xiaoqin Yan and Youmin Tang. Multidecadal Variability in Mediterranean Sea Surface Temperature and Its Sources. *Geophysical Research Letters*, 48(11):e2020GL091814, June 2021.

[63] Davide Zanchettin, Shih-Wei Fang, Myriam Khodri, Nour-Eddine Omrani, Sara Rubinetti, Angelo Rubino, Claudia Timmreck, and Johann H. Jungclaus. Thermohaline patterns of intrinsic Atlantic Multidecadal Variability in MPI-ESM-LR. *Climate Dynamics*, 61:2371–2393, 2023.

[64] Rong Zhang, Rowan Sutton, Gokhan Danabasoglu, Young-Oh Kwon, Robert Marsh, Stephen G. Yeager, Daniel E. Amrhein, and Christopher M. Little. A Review of the Role of the Atlantic Meridional Overturning Circulation in Atlantic Multidecadal Variability and Associated Climate Impacts. *Reviews of Geophysics*, 57:316–375, 2019.

Supplementary information for "Atlantic Multidecadal Variability control on European seas is mainly externally forced"

Barghorn, L., Börgel, F., Gröger, M., and Meier, H. E. M.

Department of Physical Oceanography and Instrumentation, Leibniz Institute for Baltic Sea Research Warnemuende, Seestrasse 15, Rostock, 18119, Germany

E-mail: leonie.barghorn@io-warnemuende.de

1. Additional figures

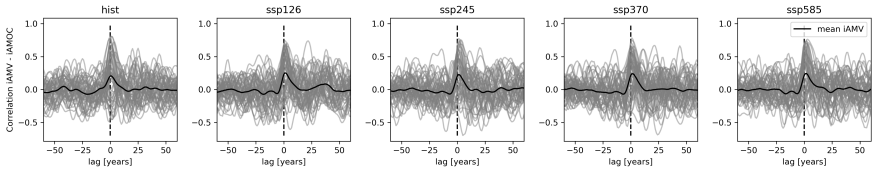

Figure S1: Cross-correlations between iAMV and iAMOC for the historical period (1880-2020) and the SSP scenarios (1950-2090) in the MPI-ESM ensemble. Black lines denote the ensemble means of the iAMV-iAMOC cross-correlations. Positive lags indicate leading iAMOC and negative lags leading iAMV. The AMOC is computed as the maximum of the ocean meridional overturning mass streamfunction in the North Atlantic above 20 °N and below 500 m depth.

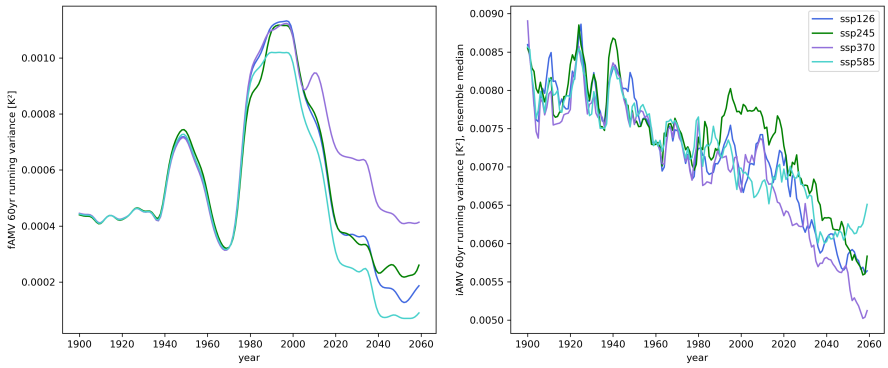

Figure S2: Centered 60-year running variances of the fAMV (left) and the iAMV (right; ensemble mean variances) in the MPI-ESM ensemble.

2. Results obtained with CESM2

Figure S3 is the CESM equivalent for Figure 4 in the main text. One can observe that the iAMV patterns of CESM are overall comparable to those of MPI-ESM. The fAMV patterns of the historical period and SSP370 differ quite strongly, mainly in the subpolar gyre and west of Europe. In addition, the fAMV patterns seem to be more pronounced in CESM since they are strongly reflected in the total AMV patterns and the fAMV running variance (Figure S4) is up to one order of magnitude larger than those of MPI-ESM. A possible reason could be that both models respond differently to external forcings like aerosols [5]. In that context, it is noteworthy that both fAMV and iAMV running variances (the latter in Figure S5) are qualitatively comparable for the historical period, but not for SSP370. There, variances decrease in case of MPI-ESM, but increase in case of CESM. Again, this might indicate that both models respond differently to the external forcing which intensifies in the high emission scenario SSP370. In addition, the CESM ensemble consist of 50 members driven with the original CMIP6 aerosol forcing and 50 members where discontinuities in the biomass burning emissions in 1997 and 2014 [2] were removed by smoothing the time series [4]. Such a method was not applied in case of the MPI ensemble. It is not clear what could be the reason behind the increasing iAMV variance. One should also note that the forced regional trends of both models are quite different. In particular, the CESM trends show a very pronounced warming hole in the subpolar gyre region (also seen in [3]).

The SSTAres-AMV cross-correlations of CESM are displayed in Figure S6. They are largely similar to those of MPI-ESM (Figure 5 in the main text) although the iSSTAres-iAMV peaks appear to be a bit broader. Two things are remarkable: Firstly, the peak for the Baltic Sea has a small positive lag in the historical period (as for MPI-ESM), but not in the scenario. Secondly, the fSSTAres-fAMV peaks

are consistently broader in the scenario. The broader peaks could in general imply that the dominant frequencies in the time series of CESM are lower (which would be in accordance with the results from the wavelet analysis in [1]).

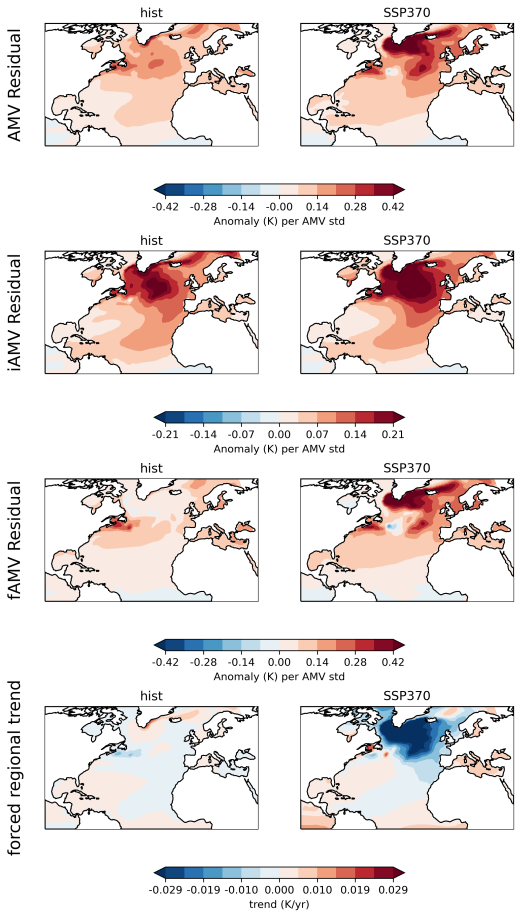

Figure S3: Standardized AMV, iAMV, and fAMV patterns plus forced local trends for the historical period (1880-2020) and the SSP scenarios (1950-2090) in the CESM ensemble.

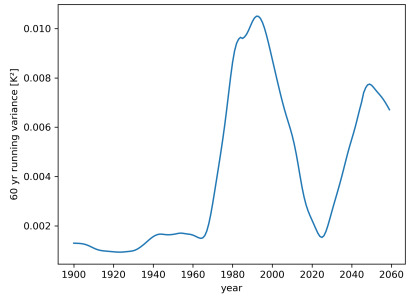

Figure S4: Centered 60-year running variances of the fAMV in the CESM ensemble.

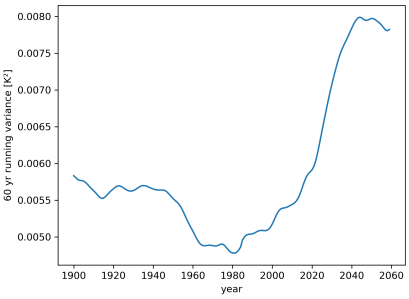

Figure S5: Centered 60-year running variances of the iAMV (ensemble mean variances) in the CESM ensemble.

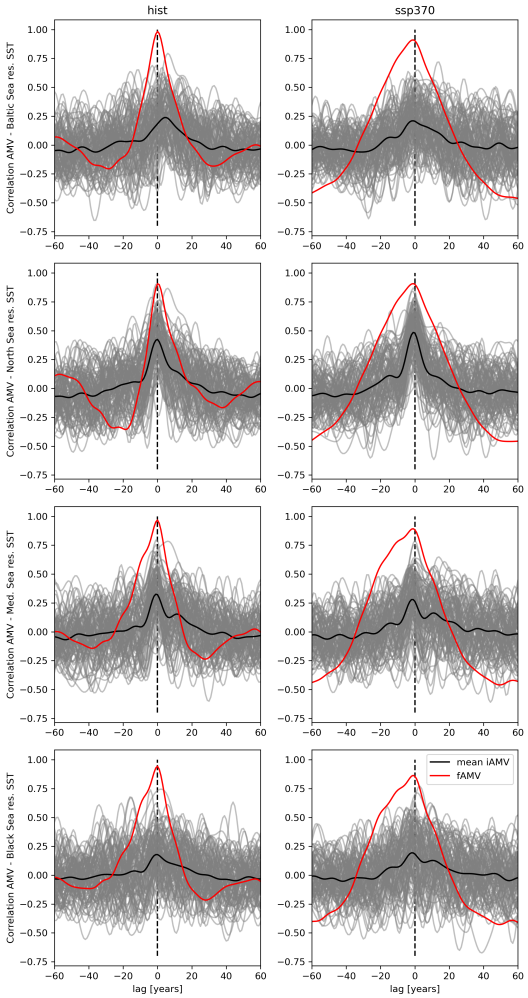

Figure S6: iAMV-iSSTAres (grey lines) and fAMV-fSSTAres (red lines) cross correlations for the historical period (1880-2020) and SSP370 (1950-2090) in the CESM ensemble. Black lines denote the ensemble means of the iAMV-iSSTAres cross-correlations. Positive lags indicate leading local SSTs and negative lags leading AMV.

References

[1] Florian Börgel, H. E. Markus Meier, Matthias Gröger, Monika Rhein, Cyril Dutheil, and Jan Moritz Kaiser. Atlantic multidecadal variability and the implications for North European precipitation. *Environmental Research Letters*, 17(4):044040, 2022.

[2] J. T. Fasullo, Jean-Francois Lamarque, Cecile Hannay, Nan Rosenbloom, Simone Tilmes, Patricia DeRepentigny, Alexandra Jahn, and Clara Deser. Spurious Late Historical-Era

Warming in CESM2 Driven by Prescribed Biomass Burning Emissions. *Geophysical Research Letters*, 49(2):e2021GL097420, January 2022.

[3] Qinxue Gu, Melissa Gervais, Gokhan Danabasoglu, Who M. Kim, Frederic Castruccio, Elizabeth Maroon, and Shang-Ping Xie. Wide range of possible trajectories of North Atlantic climate in a warming world. *Nature Communications*, 15:4221, 2024.

[4] Keith B. Rodgers, Sun-Seon Lee, Nan Rosenbloom, Axel Timmermann, Gokhan Danabasoglu, Clara Deser, Jim Edwards, Ji-Eun Kim, Isla R. Simpson, Karl Stein, Malte F. Stuecker, Ryohei Yamaguchi, Tamás Bódai, Eui-Seok Chung, Lei Huang, Who M. Kim, Jean-François Lamarque, Danica L. Lombardozzi, William R. Wieder, and Stephen G. Yeager. Ubiquity of human-induced changes in climate variability. *Earth System Dynamics*, 12(4):1393–1411, December 2021.

[5] Chenggong Wang, Brian J. Soden, Wenchang Yang, and Gabriel A. Vecchi. Compensation Between Cloud Feedback and Aerosol- Cloud Interaction in CMIP6 Models. *Geophysical Research Letters*, 48:e2020GL091024, 2021.